

# VU Research Portal

## The estrogen receptor, environmental estrogens and the role of cytochrome P450 in bioactivation

van Lipzig, M.M.H.

2011

### **document version**

Publisher's PDF, also known as Version of record

[Link to publication in VU Research Portal](#)

### **citation for published version (APA)**

van Lipzig, M. M. H. (2011). *The estrogen receptor, environmental estrogens and the role of cytochrome P450 in bioactivation*. [PhD-Thesis - Research and graduation internal, Vrije Universiteit Amsterdam].

### **General rights**

Copyright and moral rights for the publications made accessible in the public portal are retained by the authors and/or other copyright owners and it is a condition of accessing publications that users recognise and abide by the legal requirements associated with these rights.

- Users may download and print one copy of any publication from the public portal for the purpose of private study or research.
- You may not further distribute the material or use it for any profit-making activity or commercial gain
- You may freely distribute the URL identifying the publication in the public portal

### **Take down policy**

If you believe that this document breaches copyright please contact us providing details, and we will remove access to the work immediately and investigate your claim.

### **E-mail address:**

[vuresearchportal.ub@vu.nl](mailto:vuresearchportal.ub@vu.nl)

**The estrogen receptor,  
environmental estrogens and the role of  
cytochrome P450 in bioactivation**

**Marola M.H. van Lipzig  
2011**

The printing of this thesis was kindly supported by TNO Quality of Life, Zeist.  
Printed by GVO drukkers & vormgevers bv. | Pons & Looien, Ede.

ISBN 978-90-6464-459-7

Cover: artistic impression of the endogenous estrogen 17 $\beta$ -estradiol.  
Design © by Marola van Lipzig (2011)

VRIJE UNIVERSITEIT

**THE ESTROGEN RECEPTOR, ENVIRONMENTAL ESTROGENS  
AND THE ROLE OF CYTOCHROME P450 IN BIOACTIVATION**

ACADEMISCH PROEFSCHRIFT

ter verkrijging van de graad Doctor aan  
de Vrije Universiteit Amsterdam,  
op gezag van de rector magnificus  
prof.dr. L.M. Bouter,  
in het openbaar te verdedigen  
ten overstaan van de promotiecommissie  
van de faculteit der Exacte Wetenschappen  
op donderdag 17 maart 2011 om 13.45 uur  
in de aula van de universiteit,  
De Boelelaan 1105

door  
Marola Maria Henriëtte van Lipzig  
geboren te Delft

promotor:  
copromotor:

prof. dr. N.P.E. Vermeulen  
dr. J.H.N. Meerman

*Voor mijn ouders.*

commissie:           prof. Dr. R. Leurs  
                              prof. Dr. A.J. Murk  
                              dr. J.N.M. Commandeur  
                              dr. ir. J. Legler

The investigations described in this thesis were carried out in the Leiden Amsterdam Center for Drug Research (LACDR), Division of Molecular Toxicology, Department of Chemistry and Pharmaceutical Sciences, Faculty of Sciences, Vrije Universiteit, De Boelelaan 1083, 1081 HV Amsterdam, The Netherlands.

# Contents

<b>Chapter 1</b>	General introduction
<b>Chapter 2</b>	Formation of estrogenic metabolites of benzo[ <i>a</i> ]pyrene and chrysene by cytochrome P450 activity and their combined and supra-maximal estrogenic activity
<b>Chapter 3</b>	Bioactivation of dibrominated biphenyls to estrogenic metabolites by cytochrome P450 activity
<b>Chapter 4</b>	Prediction of ligand binding affinity and orientation of (xeno)estrogens to the estrogen receptor by molecular dynamics simulations and the linear interaction energy method
<b>Chapter 5</b>	Prediction of binding affinity of halogenated biphenyls to the estrogen receptor by molecular dynamics simulations and the linear interaction energy method
<b>Chapter 6</b>	The chemical interaction between the estrogen receptor and monohydroxybenzo[ <i>a</i> ]pyrene derivatives studied by fluorescence line-narrowing spectroscopy
<b>Chapter 7</b>	Conclusions and perspectives, epilogue

## Abbreviations

## References

## Nederlandse Samenvatting

## Nawoord

## Publications

## Curriculum vitae



# Chapter 1

## General Introduction

The estrogen receptor, environmental estrogens and the  
role of cytochrome P450 in bioactivation



## 1 Summary

The research described in this thesis concerns the biotransformation and the bioactivation of environmental contaminants into estrogenic compounds, thereby adding possible endocrine disruption to their hazardous properties. Endocrine disrupting compounds (EDC) have shown to adversely affect animals and wildlife via many different mechanisms (reviewed for estrogen-receptor mediated effects in **Chapter 1**). Human exposure to estrogenic compounds and its impact on human health, however, remains disputed due to the low levels present in the environment. Usually, there is a large difference between high exposures generally used in laboratory experiments or with dramatic environmental incidents, *versus* the relatively low levels found in the 'ordinary' environment. In order to understand health risks of estrogenic endocrine disruptors, as much information as possible regarding their biological activity is needed, i.e., their extent of exposure and mechanisms of action via pathways involved in hormone action and homeostasis, including the biological activities of possible metabolites.

In this thesis, we focused on the biotransformation of environmental contaminants, such as polycyclic aromatic hydrocarbons (PAH) (**Chapter 2**) and polyhalogenated biphenyls (PHB), by cytochrome P450 enzymes (CYP) into compounds with increased estrogenic activities. Metabolites formed *in vitro* have been identified and tested for estrogen-receptor affinity and activation. In some cases we also tested metabolites for inhibition of estrogen sulfotransferase (**Chapter 3**), because estrogen sulfotransferase (hEST) is involved in regulation of estrogen activity and homeostasis.

Many metabolites were found and several exhibited estrogenic activity via either of the two pathways. The affinities of some of the metabolites were in the same range as the endogenous ER-ligand estradiol. Furthermore, the combined estrogenic effects of the metabolites were found to be significant. This indicates the importance of considering biological activities of metabolites of environmental contaminants, especially with respect to low-dose exposures.

In addition to *in vitro* experiments, metabolites of PAH and halogenated biphenyls have been implemented in an *in silico* estrogen receptor  $\alpha$  (ER $\alpha$ ) protein model based on the crystal structure of the ligand binding domain, for the accurate prediction of binding affinity and orientation of estrogenic compounds. The *in silico* model was based on the linear interaction energy (LIE) approach, and has good predictive value, which was tested on a large set of known environmental estrogens (**Chapter 4**). Subsequently, the *in silico* model was applied to predict estrogen receptor binding affinities of halogenated biphenyls metabolites (**Chapter 5**) with unknown affinity.

---

In order to verify the binding orientation of two hydroxylated metabolites of benzo[a]pyrene (BAP) to the ER $\alpha$ , fluorescence line-narrowing (FLN) spectroscopy was used. The favoured binding orientation as detected by FLN spectroscopy supported the *in silico* predictions and substantiated the predictive value of the LIE model (**Chapter 6**).

At the end of the thesis, it is concluded that an underestimation of the overall risk of exposure to estrogens may well result when assessing the contribution of the parent compounds individually only, and experimental or computational studies should be included to elucidate whether compounds can be bioactivated into more estrogenic metabolites (**Chapter 7**).

## 2 Rationale

At the time the project started (1998), bioactivation of environmental contaminants with respect to *increased* estrogenicity was not commonly taken into account in the evaluation of adverse biological properties of substances. The main aim of this thesis was therefore to investigate whether bioactivation of xenobiotics would lead to the formation of more estrogenic metabolites. We focused on the bioactivation of hydrophobic PHBs and PAHs by CYP enzymes and their ER $\alpha$  binding properties. PAHs and PHB are well-known pollutants, which accumulate in lipophilic environment. Subsequently, after e.g. consumption of fish or water from polluted sites, they are extensively biotransformed by the mammalian CYP enzyme family. Metabolism mostly yields hydroxylated products, many of which are hard to isolate or identify. For that reason, we used the -at that time recently- published crystal structure of the ER $\alpha$  ligand binding domain to develop an *in silico* model for the prediction of ER $\alpha$  binding affinity. The challenge was to train and test the computational model with steroids, phytoestrogens, a wide variety of structurally diverse (xeno)estrogens and a subset of identified and unknown PAH and PHB metabolites, in order to obtain a model with reliable predictive value regarding binding affinity as well as preferred binding orientation.

### 3 Endocrine disruption

Endocrine-disrupting chemicals (EDCs) are compounds that modulate the endocrine system and potentially induce adverse health effects in exposed humans and wildlife. When the research described in this thesis started and later, a wide variety of structurally diverse environmental compounds had already been identified as endocrine disrupting chemicals when the work for this thesis started<sup>[1-5]</sup>. Among these compounds are natural steroid hormones, pharmaceuticals, phytochemicals, and industrial chemicals including pesticides, PHBs and PAHs.

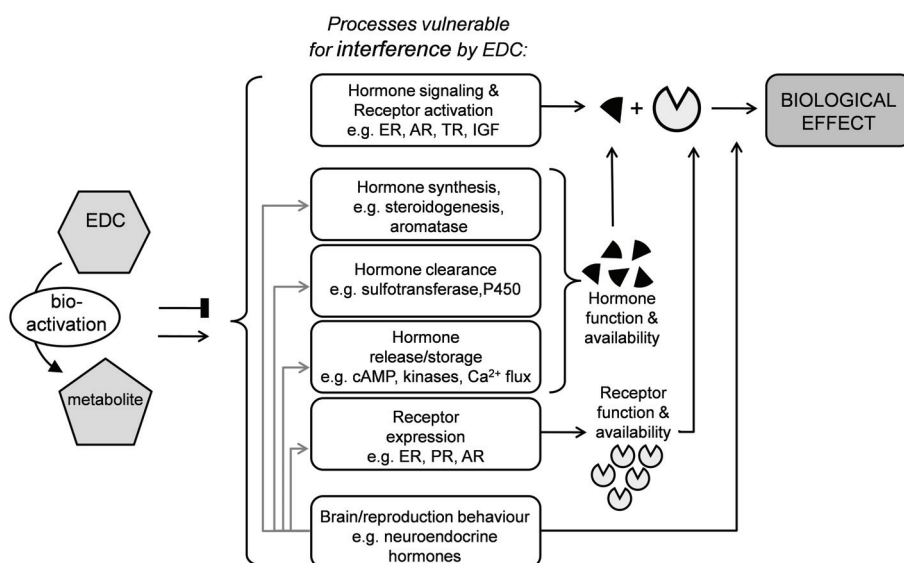


**Figure 1:** Schematic view of possible pathways of endocrine disruption. By definition: “Endocrine disruptors interfere with the synthesis, secretion, transport, binding, action, or elimination of natural hormones in the body that are responsible for the maintenance of homeostasis (normal cell metabolism), reproduction, development, and/or behavior”. As can be seen in the figure, the EDC may itself, or after bioactivation, directly or indirectly interfere, by stimulation or inhibition, with hormone signaling and all processes that affect normal hormone signaling.

Key: EDC = endocrine disrupting compound, ER = estrogen receptor, AR = Androgen receptor, TR = Thyroid receptor, PR = progesterone receptor, IGF = insulin growth factor, P450 = cytochrome P450, cAMP = cyclic AMP.

**Table 1** *Types of endocrine disrupting compounds with some examples.*

Types of Endocrine disruptors		
Natural compounds	Anthropogenic compounds	
	Pharmaceuticals	Chemicals
estrogens	oral contraceptives	pesticides, insecticides
estradiol	estradiol	DDT, DDE, atrazine,
estriol	ethinylestradiol	tributyl tin, toxaphene,
progestogens	diethylstilbestrol	methoxychlor,
progesterone	hormone therapy	vinclozolin
androgens	tamoxifen	industrial chemicals
testosterone	psychotherapeutics	polychlorinated
dehydro-	benzodiazepines	biphenyls (PCB), dioxins,
epiandrosterone	anti inflammatory	TCDD, polyaromatic
thyroids	diclofenac	hydrocabons (PAH),
corticoids	ibuprofene	dibenzofurans,
phytoestrogens	antibiotics	perchlorates
flavonoids		plastics, plasticizers
isoflavonoids		alkylphenols, phthalates,
genistein		bisphenol A
daidzein		ordinary house hold products
plant sterols		nonyl phenol
resveratrol		polybrominated
		diphenyl ethers
		heavy metals
		lead, mercury, cadmium

These compounds have the potential to mimic endogenous hormones and disrupt the endocrine and reproductive system of exposed animals<sup>[6-8]</sup>, see Figure 1 for possible targets and pathways.

Many reports have been issued, suggesting links between human and wildlife exposure to endocrine toxic chemicals and increasing rates of hormone dependent cancers (breast and prostate), reproductive disorders such as developmental effects of the male reproductive tract, falling sperm counts, early menarche and endometriosis. Some well-known examples such as DES-induced cervical cancer in daughters of DES-exposed women<sup>[9]</sup>, the human TCDD exposure incident in Seveso, Italy (1976), which induced long-term effects such as spontaneous abortion, cytogenetic abnormalities, congenital malformation,

impaired liver function and lipid metabolism, as well as neurologic and immunologic impairment<sup>[10]</sup>. The same spill was also associated with an increased breast cancer incidence after dioxin exposure, which had been measured in the women's serum, just after exposure<sup>[11]</sup>. Human exposure to PCBs occurred after consumption of fish from the Great Lakes and contaminated rice in Yu Shu, Japan and Yu Chang, Taiwan, and resulted in irregular menstrual cycles and altered immune responses<sup>[12]</sup>. Direct feminization of men and reduced sex drive and fertility has been observed in men working in plastic factories who experienced exposure to very high levels of the xenoestrogen bisphenol A (BPA)<sup>[13]</sup>. In Table 1, different types of compounds described as (suspected) endocrine disruptors are summarised. A complete overview of proven or suspected endocrine disrupting properties, where identified, and their mechanism of action, is presented at [www.le.ac.uk](http://www.le.ac.uk)<sup>[14]</sup>.

## 4 Environmental estrogens

Environmental contaminants may disrupt endocrine signaling and homeostasis through many pathways, e.g. by activating or inhibiting hormone receptors or disturbing regular hormone bioavailability. In this thesis, the focus is on the estrogen receptor, probably the most studied target in the field of endocrine disruption. Natural estrogens are steroid hormones, produced by female gonads (ovaries) and affect behavior and cause characteristic physiological changes in females. Studies on the uterine action of 17 $\beta$ -estradiol, led to the conclusion that the biological effects of estrogens occur through the activation of the estrogen receptor (ER)<sup>[15]</sup>. However, it has become clear that a large variety of other natural and man-made compounds can bind to and subsequently activate the ER. Humans and animals have unintentionally been exposed to environmental estrogens, due to environmental spills or accidents with chemical compounds, and several well-known environmental estrogens were revealed from these incidents, see Figure 2 and the text below for several examples.

### 4.1 Notorious players

The number of studies of actual observed endocrine disruption in humans is relatively small when compared to the abundance of studies with suspected endocrine disrupting chemicals in animals and in laboratory settings. Below is a list of the most striking chemical-induced endocrine disrupting incidents in humans. These incidents have initially made scientists and nowadays also consumers aware of the importance of taking into account the possible hormone activity of compounds.

---

## DES

One of the most notorious environmental EDC is diethylstilbestrol (DES), a very potent synthetic estrogen. DES was commonly given to pregnant women in the United States, Europe, and Australia from 1948-1971 to prevent miscarriage during pregnancy. Daughters born to women who took DES developed structural abnormalities in their vagina, cervix, or uterus, and many suffered from irregular menstruation and difficulties in pregnancy such as infertility, miscarriage, ectopic pregnancy, and giving birth prematurely. Only limited number of studies focused on 'DES sons'. Recent studies show no increase in infertility even among those with genital malformation. There have been effects reported for sons of mothers who took DES (DES-grandsons); some men developed testicular abnormalities<sup>[16]</sup>.

## PCBs

Another class of well-known contaminants affecting normal hormone homeostasis are the polychlorinated biphenyls, PCBs. PCBs are used for a variety of industrial purposes, they are very persistent and, therefore, have been a widespread threat for wildlife and human health. During the 1960s, mink that were fed fish from Lake Michigan branches that were contaminated with polychlorinated biphenyls (PCBs). The exposed mink suffered from severe effects including high mortality rates and serious reproductive failure<sup>[17,18]</sup>. Two episodes of human PCB poisoning due to contamination of rice bran oil with PCBs made news headlines in the 1960s and 1970s. These events took place in Japan in 1968 (Yusho) and in Taiwan in 1979 (Yu-Cheng). Many people consumed oil contaminated with PCBs and high levels of thermal degradation products of PCBs, and became seriously ill. Victims of the poisoning experienced symptoms such as chloracne, nausea and liver disorders. Children of women who were pregnant at the time of the poisonings showed behavioral and cognitive problems, developmental and growth delays, and reduced penile length in boys<sup>[19]</sup>. PCBs are metabolised and hydroxylated biphenyls are formed. These have been detected in the serum of pregnant women<sup>[20]</sup>, and correlate to developmental problems *in utero*<sup>[21]</sup>. Substantial amounts of polybrominated biphenyl (PBB) congeners, have been produced as flame retardants and also the brominated biphenyls possess the potency to interfere with estrogen function<sup>[22,23]</sup> and their presence in serum of pregnant women has been correlated to longer time to pregnancy<sup>[24]</sup>. Recently, the polybrominated diphenylethers (PBDE) have gained attention because they also interfere with androgen function in addition to their (anti)estrogenic properties.

### *Dioxin(s)*

Dioxins belong to the polychlorinated dibenzodioxins and occur as by-products in the manufacturing of organochlorides, such as PVC (polyvinyl chloride). They have also been used as herbicides, e.g. during the Vietnam War. In 1976 an explosion at the ICMESA chemical manufacturing plant in Seveso, Italy, released approximately 30 kg of dioxin into the environment<sup>[25]</sup>. The release of dioxin occurred in the densely populated area, which resulted in the highest known residential exposure to the most toxic dioxin, 2,3,7,8-tetrachlorodibenzo-p-dioxin (TCDD). The major adverse health outcome was chloracne, but some exposed residents also had abnormal liver function and higher frequency of abnormal nerve function<sup>[10]</sup>.

### *DDT*

Later, in the 1980s, Lake Apopka, one of Florida's largest lakes, became polluted with contaminants from several sources, among them the pesticide dichlorodiphenyl-trichloroethane (DDT), and its metabolites. A combination of agricultural run-off, city sewage and a pesticide spill from a chemical company has resulted in several adverse health effects in wildlife, most notably in its population of alligators. Female alligators had plasma estradiol concentrations that were twice the normal level and had abnormal ovarian morphology and male alligators developed abnormal reproductive organs, such as very small phalli and even ovaries<sup>[26]</sup>. Exposure to DDT and its metabolite DDE had a striking impact on the ability of alligators in Lake Apopka to reproduce.

Bald eagles consumed prey which had high levels of DDT concentrated in their fatty tissues; this resulted in eggs with thin shells that cracked fairly easily during incubation. Consequently, there was a significant decline in the population of bald eagles in the United States. Since the ban of DDT in the 1970s, the bald eagle population has been increasing.

### *Bisphenol A*

Bisphenol A, commonly abbreviated as BPA, an organic compound with two functional phenol groups and is used as a bifunctional building block of several important plastics and plastic additives, and has been suspected of being hazardous to humans since the 1930s.

BPA has received a lot of attention during the last decade, especially concerns about the use of BPA in consumer products were regularly reported in the news media in 2008. Several governments issued reports questioning its safety, prompting retailers to remove products containing it from their shelves. The United States Food and Drug Administration

---

(FDA) raised concerns in a report in 2010, regarding exposure of fetuses, infants, and young children to BPA. BPA exhibits estrogenic receptor affinity and estrogenic activity *in vitro* and *in vivo* in rodent models disrupts reproduction has a carcinogenic effect. Furthermore, it may cause sexual dysfunction in BPA exposed men<sup>[13]</sup>, may increase obesity as perinatal BPA exposure adversely affects adult body weight and adiposity<sup>[27]</sup>. BPA also binds to the thyroid receptor and may cause disruption of thyroid signaling<sup>[28]</sup>.

#### 4.2 Other classes of endocrine disruptors

Also, many compounds have been recognized as endocrine disruptors, because they caused adverse health effects in animals in the wild, e.g. due to spills. In addition, these compounds have been tested in many animal studies and these should be considered as possible endocrine disruptors as well. Below are a few examples of classes of compounds well-known for their possible hormone-interfering properties.

##### *Pesticides*

Pesticides are intended to repel or kill organisms, and they include insecticides, acaricides, fungicides, herbicides, rodenticides, avicides, larvicides, and germicides<sup>[29]</sup>. Pesticides are widely used on pets, furniture or as insect repellent, and applied in house, but also in public places like schools, hospitals, etc. Remarkably, it was shown that in humans, dietary exposure predominates, at least for certain pesticides, such as malathion<sup>[30]</sup>. Pesticide degradation is lower indoors than outdoors, and pesticides accumulate on toys, carpets, and dust, sources that can become major routes of exposure for infants and toddlers<sup>[29,31]</sup>. Pesticides are structurally very diverse, ranging from inorganic substances to organometallic compounds. The organochlorines form the major class of pesticides, and they include the aforementioned DDT, dieldrin, kepone (chlordecone), atrazine, methoxychlor and chlordane, which all have been identified as endocrine disruptors since they may interfere with regular estrogen or androgen function. Health effect studies for these compounds suggest neurotoxicity, effects on developing reproductive system, effects on lactation, and cancers, including breast cancer<sup>[32-35]</sup>. Although the use of most these compounds is banned, exposure still occurs since they are generally very persistent and still present in the environment. Furthermore, for example atrazine is still used in large amounts, despite the use restriction. Some approved pesticides also appear to also have effects on the endocrine system, for example various pyrethroids have been demonstrated to have weak anti-androgenic, anti-estrogenic, or estrogenic activity; and chlorpyrifos has been shown to affect thyroid hormones in animal and human studies<sup>[36-39]</sup>, and to affect infant development in human health studies<sup>[40]</sup>.

### *Plasticizers*

Plasticizers are used in many products (bottles, gels, paints, to increase their flexibility, transparency, durability, and to prolong a products life. Most commonly used are the phthalates, and many have been shown to exert endocrine disrupting properties. The most widely-used phthalates are the di-2-ethyl hexyl phthalate (DEHP), the diisodecyl phthalate (DIDP), and the diisononyl phthalate (DINP). DEHP is the dominant plasticizer used in PVC due to its low cost. Also, they are used in a variety of cosmetic products, toys including teething rings, medical products (I.V. and dialysis bags) and all kinds of materials used in food packaging and processing, which explains the major exposure route for humans: diet<sup>[41]</sup>. Due to their application purposes, indoor exposure concentrations are generally higher than outdoor concentrations. Phthalate metabolites have been detected in virtually all human urine samples tested, indicating widespread exposure<sup>[42]</sup>. Some phthalates have been shown to interfere with androgen function. In animal studies, effects on the developing male reproductive tract and reduced fertility have been reported<sup>[43]</sup>. In humans, maternal levels of urinary phthalate metabolites was associated with irregular reproductive tract development in male offspring<sup>[44]</sup>. Animal studies suggest that current exposure levels in the general population are below levels of health concern, however, a studies in humans with typical levels of exposure have demonstrated adverse health effects.

### *Alkylphenols*

Alkylphenols are used in high production volumes as surfactants and for detergents, and disinfectants and building block chemicals for example fuels, polymers, fragrances, thermoplastic elastomers and antioxidants. They are widespread and important indoor air contaminants (reviewed in<sup>[41]</sup>. Alkylphenols are present in wastewater and aquatic environments and during biodegradation, more persistent alkylphenols are formed, such as nonylphenols, which accumulate in sewage and rivers. 4-Nonylphenol and 4-octylphenol have been shown to be estrogenic<sup>[45]</sup>.

#### *4.3 Dealing with low concentration and ubiquitous exposure*

Although the potency of EDCs is widely recognized, it is still questioned whether EDCs have the potential to interfere with the endocrine system of humans and wildlife at naturally occurring concentrations. Are EDCs really a risk to humans? Although the hormonal potencies of many xenoestrogens is much lower than of endogenous estrogens, *in vitro* studies in yeast and human breast cancer cells showed that the estrogenicity of mixtures of xenoestrogens is significant, even when their individual concentrations are

---

below threshold levels (See Chapter 2<sup>[46]</sup> and references<sup>[47,48]</sup>). Moreover, at present, no ecosystem has been left untouched. No human has been born since the middle of the 20<sup>th</sup> century without some exposure, already before birth, to anthropogenic hormonally-active compounds, and this may lead to unwanted enhancement of the effects of endogenous estrogens<sup>[49]</sup>.

Many studies have been performed on the subject of endocrine disruption, and they proved to be very useful in understanding potential mechanisms (receptors, enzymes) of disruption of developmental biology of humans, but more importantly, they demonstrate that low dose exposure (specifically prenatal) at environmental levels can adversely affect regular reproductive development<sup>[34,50-52]</sup>. Moreover, in recent years, the non-reproductive effects of EDCs have gained attention, such as an increase in cancer susceptibility in humans<sup>[34]</sup>.

In addition to investigating properties of individual chemicals, the effects of low concentrations and exposure to mixtures of EDCs have become more important. A very basic rule in toxicology is: 'the dose makes the poison'. Any compound is toxic, if it is concentrated enough. In other words, compounds are considered not toxic, when the concentration is below a threshold. In the field of endocrine disruption, the *low dose debate* discusses whether the concentrations EDCs humans are exposed to, in daily life, are sufficient to induce adverse health effects, especially since it has been shown that in unborn children are much more vulnerable to low concentrations of EDC than adults. Furthermore, it has been shown that mixtures of low concentrations of EDC can exert significant effects where the effects of individual compounds would be considered harmless, and most humans are exposed to numerous chemicals simultaneously during a lifetime.

In relation to this thesis it is important to stress that most studies focus on the endocrine disrupting properties of the parent environmental contaminant, and do not take into account the possible adverse effects that metabolites of environmental contaminants might induce<sup>[22,53-55]</sup>.

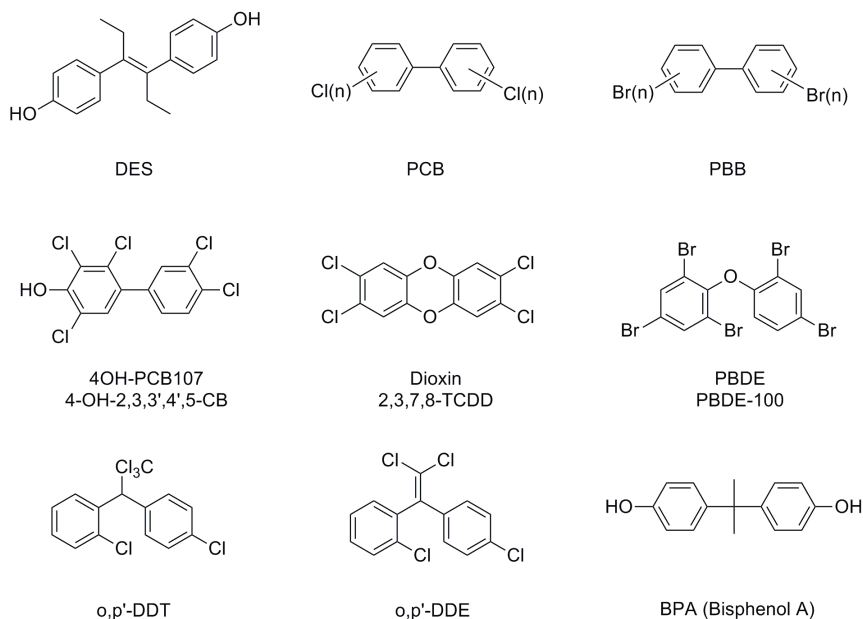


**Figure 2: Notorious xenoestrogens:** **DES** (diethylstilbestrol, synthetic estrogen), general structure of **PCB** (polychlorinated biphenyl) and **PBB** (polybrominated biphenyl), hydroxylated PCB: **4-hydroxy-PCB107**, **Dioxin**, e.g. 2,3,7,8- tetrachloordibenzo-p-dioxine, most toxic dioxin known), **PBDE** (polybrominated diphenyl ether), e.g. PBDE-100, **o,p'-DDT** (dichlorodiphenyltrichloroethane, insecticide) and its biologically active metabolite **o,p'-DDE**, **BPA** (bisphenol A, used in plastics household products).

#### 4.4 Endocrine disruption, beyond reproduction

As estrogens and the estrogen receptor are critical in the development and maintenance of the reproductive systems in humans and wildlife, it seems logical to assume that exogenous estrogenic compounds primarily affect the reproductive organs of exposed individuals. If exposure is sufficiently high and population-wide, this may have important effects on the reproduction of humans and animals. However, hormones such as estrogen play important roles in many other biological processes as well, thus it is crucial that endocrine disruption and interference with these non-reproductive systems is also investigated. Current opinions in research are not unanimous where risks are concerned.

##### Cancer risks

Any hormone-dependent cancer is susceptible to the effects of exogenous hormonally active compounds in principle. The relationship between estrogen and its receptors in the development of cancer, especially breast cancer, has been known for years. The estrogen

---

mediated carcinogenic process is complicated and the effects of estrogens have shown to be cell type/tissue dependent. Genetic factors, timing and dosage of exposure and condition at the time of exposure all play a role in the susceptibility of individuals. Whether environmental estrogens play a crucial role in the development of cancer, is yet to be elucidated<sup>[56]</sup>. Furthermore, treatment of estrogen-dependent cancers by hormone replacement therapy (HRT) may also be hampered by exogenous compounds<sup>[57]</sup>. In addition, many environmental contaminants are known to alter endogenous enzyme activities, such as CYPs, which are involved in the metabolism and disposition of natural estrogens. CYP1A1 and CYP1B1 catalyze the hydroxylation of the A-ring of E2 to form the catechols 2- or 4-hydroxy-E2, which may lead to an increased breast cancer risk factor since a high 4-OH-E2:2-OH-E2 ratio has been suggested as a marker for breast neoplasm<sup>[58]</sup>.

### *Obesity*

In recent times, also adipose tissue is considered as active endocrine organ that participates in the regulation of appetite and the metabolic integration between organs and inflammatory responses. Several studies have shown that a variety of environmental endocrine disrupting chemicals can influence adipogenesis and obesity. Compounds disrupting these processes are called *obesogens*. Studies in humans and rodents identified weight gain as a significant change following prenatal and neonatal DES exposure, and perinatal exposure of rodents to Bisphenol A in drinking water<sup>[51,59]</sup>. However, the results of research trying to link obesity to environmental estrogen exposure are conflicting. For example, soy-based infant formula containing genistein, has been associated with adult obesity<sup>[60,61]</sup>. In contrast, genistein and daidzein intake has been associated with *decreased* obesity in postmenopausal women and ovariectomized rodents<sup>[62-65]</sup>. The adverse effects of obesogens appear to be dependent on several factors, such as the period in development in which exposure takes place, and the dose.

### *Brain and behaviour*

In the last decennium, work has suggested that EDCs may affect the development of the brain, behaviour and memory functions. E.g. PCBs cause developmental neurotoxicity in man via disruption of normal thyroid function<sup>[66,67]</sup>. It has been shown in rodent models for reproductive behaviour, that early exposure to low doses of PCBs (prenatal) or the phytoestrogen coumestrol (neonatal) adversely affect sexual performance and reduce reproductive success in exposed animals<sup>[52,68]</sup>.

#### 4.5 Estrogenic metabolites of environmental contaminants

Initially, research focused on the endocrine disrupting properties of un-metabolised (parent) compounds such as polycyclic aromatic compounds (PAH) and polyhalogenated biphenyls (PHB), although it was already known for a long time that these compounds are extensively metabolised by living organisms. For instance, it is widely accepted that carcinogenic PAHs and PHBs are metabolised (bio-activated) to chemically reactive intermediates that may react covalently with DNA and other macromolecules<sup>[69-71]</sup>. Bio-activation mainly occurs via CYP enzymes and epoxide hydrolases<sup>[72]</sup>. CYP enzymes are present in every cell and are responsible for metabolizing endogenous compounds such as steroids and exogenous compounds (xenobiotics), e.g., pesticides, pollutants, natural products and drugs. Actually, almost any moderately to highly hydrophobic organic compound is likely to be a substrate for a CYP.

CYP-mediated metabolism of PAHs and PHBs yields primarily mono- and di-hydroxy metabolites and dihydrodiols. The parent compounds have shown to be estrogenic in mammalian cells *in vitro*<sup>[53,73-75]</sup>, and *in vivo*<sup>[1,76,77]</sup>. However, they show no or very low affinity for the ER, whereas their hydroxylated metabolites show significantly higher ER binding affinities, as we and others have shown<sup>[22,46,53,54,74,78]</sup>. From these studies, it became clear that neglecting metabolism and estrogenicity of metabolites may lead to significant underestimation of possible adverse effects. In 2006, the OECD issued a review paper on the use and justification of incorporation of *in vitro* metabolism studies in endocrine disruptors<sup>[79]</sup>. Although in other areas of toxicity testing, such as genotoxicity, *in vitro* assays routinely take into account possible biotransformation of xenobiotics, in the field of endocrine disruption, the motivation to include metabolism studies or metabolites in testing for endocrine disruption properties of compounds is growing, and our studies contribute to the awareness of endocrine disrupting metabolites. Ever since the research performed for this thesis has been published, several studies have followed investigating the EDC metabolism into active metabolites as well as exploring the parent EDC<sup>[80-85]</sup>. Examining the metabolism of compounds into more hormonally active compounds should be an integral part of endocrine disruption testing.

#### 4.6 The role of Cytochrome P450 (CYP) in endocrine disruption

Information on the metabolism of xenobiotic substances is important in the evaluation of its toxicological potency. Metabolism mainly occurs in the liver, however, may occur in practically all cell types, and can be divided in phase I metabolism and phase II metabolism. Phase I metabolism involves mixed function oxidase activities of the cytochrome P450 (CYP) enzymes, generally yielding more soluble compounds to facilitate elimination by Phase II metabolism enzymes, which catalyze the conjugation of the

metabolites, generated by phase I metabolism. Environmental contaminants often are persistent, lipophilic compounds, and excellent substrates for CYP enzymes. Many isoenzymes of the CYP family have been characterized. CYP1A1 and CYP1A2 are mainly involved in metabolism of (planar) PAHs, PCBs, dioxins and aromatic amines. The former is primarily expressed in extrahepatic tissue, such as lung, brain, GI (gastrointestinal) tract, lymphocytes, heart and breast, whereas the latter is only found in liver. CYP1A1 is also one of the major enzymes participating in endogenous estrogen hydroxylation. Compounds such as PAHs and PCBs or cigarette smoke can induce CYP1A1 enzyme activity via activation of the aryl hydrocarbon receptor (AhR). The AhR is a ligand-inducible transcription factor that regulates gene expression of several CYPs. Significant data suggest that the ER is also an important mediator of AhR activity, and cross-talk between the ER and the AhR has been observed, however, the exact mechanism remains unclear. It has been shown that E2 regulates AhR expression levels and its inducibility<sup>[86]</sup>.

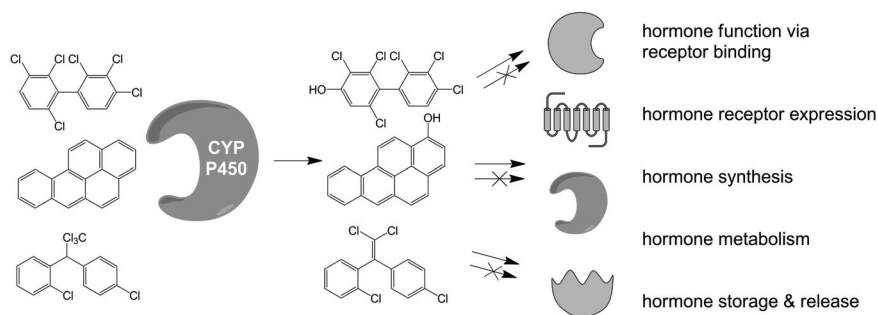


**Figure 3:** Illustration of CYP-mediated biotransformation of environmental contaminants into endocrine disrupting compounds.

Many CYPs have been suggested to play a key role in increased risk factors in breast cancer, among which CYP1A1, 1A2, 1B1, 3A4 and 3A5. In addition to enzyme expression and induction or inhibition of enzyme activity, CYP polymorphisms also seem to play a role in the susceptibility to breast cancer initiation or progression, as was demonstrated for CYP1A1, CYP1A2 and CYP1B1 polymorphisms<sup>[87-89]</sup>. Considering the fact that many cells and tissues used for screening of estrogenic activity, e.g. T47D and MCF-7 cells and rodent uterus, are metabolically active and express many different xenobiotics metabolizing enzymes such as CYPs, it is very possible that the observed estrogenic effects of certain persistent environmental chemicals in cells *in vitro* and also in whole animals are the result of the formation of estrogenic metabolites by these enzymes. For example, the

synthetic organochlorine methoxychlor (used as insecticide) has estrogenic activity *in vivo*, while it is inactive *in vitro*<sup>[90]</sup>. Several CYP enzymes are involved in the metabolism of methoxychlor, and the formed HPTE and other hydroxylated metabolites have been shown to be estrogenic *in vitro*<sup>[24,90]</sup>. In addition, methoxychlor metabolites, including HPTE (2,2-bis-(*p*-hydroxyphenyl)-1,1,1-trichloroethane), also exhibit agonist and antagonist affinities for the AR and may interfere with thyroid hormone function. Another example is the industrial PCB-mixture Aroclor-1254, which exhibited increased estrogenic activity in an MCF-7 cell proliferation assay after co-incubation of the cells with the metabolizing rat liver S9 fraction<sup>[53]</sup>. PCBs are converted by different CYP enzymes. Tamoxifen is a good CYP substrate, and its conversion to e.g. 4-OH-tamoxifen is required for its therapeutic use against breast cancer.

#### *CYP in endogenous hormone metabolism*

Apart from a role in the metabolism and generation of estrogenic metabolites of PAHs, PCBs and PBBs, CYP enzymes also are involved in the biosynthesis of natural estrogens through the synthesis of steroids from cholesterol via a series of reactions, which involve various CYP enzymes<sup>[91]</sup>. The CYP enzymes have gained interest as molecular targets of EDCs, since they produce highly potent endogenous steroid hormones<sup>[92]</sup>. Many CYP isoforms exist, of which 2C11, 2A1, 2B1, 3A1 and 2C19 catalyze essential stages in steroidogenesis; CYP 2C19 is also called 'aromatase' and controls the formation of androgens into aromatic estrogens. Induction of aromatase by the herbicide atrazine has been shown in several *in vitro* systems. Aromatase inhibitors such as Arimidex (chemical name: anastrozole), Aromasin (chemical name: exemestane), and Femara (chemical name: letrozole) on the other hand are currently in use for the treatment of (ER-positive) breast cancer, based on their antagonizing effects on estrogen expression. Also other CYP enzymes may be important targets of EDCs. Environmental contaminants such as DDT and its analogues are known CYP2B and CYP2C inducers. Prenatal or neonatal exposure to these compounds may lead to increased risk of breast and vaginal tumors in humans, due to induced expression of CYP2B and CYP2C enzymes during foetal development<sup>[93,94]</sup>.

**Table 2:** Overview of CYP activities, arranged by family and function.

Family	Function	Isoforms
CYP1	drug and steroid (especially estrogen) metabolism	CYP1A1, CYP1A2, CYP1B1
CYP2	xenobiotics drug and steroid metabolism xenobiotics	CYP2A6, CYP2A7, CYP2A13, CYP2B6, CYP2C8, CYP2C9, CYP2C18, CYP2C19, CYP2D6, CYP2E1, CYP2F1, CYP2J2, CYP2R1, CYP2S1, CYP2U1, CYP2W1
CYP3	drug and steroid (including testosterone) metabolism xenobiotics	CYP3A4, CYP3A5, CYP3A7, CYP3A43
CYP4	arachidonic acid or fatty acid metabolism	CYP4A11, CYP4A22, CYP4B1, CYP4F2, CYP4F3, CYP4F8, CYP4F11, CYP4F12, CYP4F22, CYP4V2, CYP4X1, CYP4Z1
CYP5	thromboxane A2 synthase	CYP5A1
CYP7	bile acid biosynthesis 7-alpha hydroxylase of steroid nucleus	CYP7A1, CYP7B1
CYP8	varied	CYP8A1 (prostaglandin synthase), CYP8B1 (bile acid biosynthesis)
CYP11	steroid biosynthesis	CYP11A1, CYP11B1, CYP11B2
CYP17	steroid biosynthesis, 17-alpha hydroxylase	CYP17A1
CYP19	steroid biosynthesis: aromatase synthesizes estrogen	CYP19A1
CYP20	unknown function	CYP20A1
CYP21	steroid biosynthesis	CYP21A2
CYP24	vitamin D degradation	CYP24A1
CYP26	retinoic acid hydroxylase	CYP26A1, CYP26B1, CYP26C1
CYP27	varied, vitamins	CYP27A1 (bile acid biosynthesis), CYP27B1 (vitamin D3 1-alpha hydroxylase, activates vitamin D3), CYP27C1 (unknown function)
CYP39	7-alpha hydroxylation of 24-hydroxycholesterol	CYP39A1
CYP46	cholesterol 24-hydroxylase	CYP46A1
CYP51	cholesterol biosynthesis	CYP51A1 (lanosterol 14-alpha demethylase)

#### 4.7 Sulfotransferases

Interference of environmental compounds with another class of estrogen metabolizing enzymes, the sulfotransferases, has been the subject of several studies in recent

years<sup>[95,96]</sup>. Sulfotransferases are cytosolic phase II biotransformation enzymes, that play an important role in the inactivation of estrogens. They are responsible for maintaining the balance between sulfation and desulfation of estrogens<sup>[97,98]</sup>. Estrogen sulfate is pharmacologically inactive, and it is the major kind of steroid in plasma. Free estrogen is released at the target tissue by sulfatases. Formation of estrogen sulfates is controlled by sulfotransferase enzymes (SULT isoforms). The major form involved in estrogen sulfonation is SULT1E1, which can be inhibited by a variety of compounds, such as several flavonoids. SULT1A1 has a higher  $K_m$  for estrogens but will sulfonate them at physiological levels while also accepting a wide range of phenolic compounds as substrates. Hence, inhibition of SULT enzymes could lead to a lower concentration of circulating estrogen sulfates, or higher levels of intercellular estrogens. Inhibition of sulfotransferases has been shown to elicit significant undesirable effects on regular estradiol homeostasis and estrogen bioavailability<sup>[96,99]</sup>. Hydroxylated PCB metabolites were shown to be very potent (nanomolar) inhibitors of human estrogen sulfotransferase (hEST)<sup>[99]</sup>, displaying higher hEST binding affinities than ER binding affinities<sup>[100,101]</sup>. They are expressed throughout the whole body, however highly expressed in mammary tissues. Sulfation of estrogens yields hydrophilic molecules, which are unable to bind to the ER. Ergo, by inhibiting the sulfation of e.g. endogenous E2, the hydroxylated PCBs may increase E2 bio-availability in target tissues, thereby exerting an indirect estrogenic effect<sup>[99]</sup>.

## 5 Estrogens and the estrogen receptor

Estrogens play a crucial role in the development, growth and maintenance of a diverse range of tissues, and in the regulation of sexual and reproductive organs and behavior<sup>[2]</sup>. Estrogens act via binding to estrogen receptors (ER). The classical intracellular ER is a nuclear receptor with DNA-binding transcriptional activity, and two isoforms exist, ER $\alpha$  and ER $\beta$ , that are differentially expressed in various tissues. A membrane-coupled estrogen receptor (GPR30) has also been identified. There are multiple pathways through which ERs induce their biological responses.

Below, the different mechanisms of estrogen-receptor mediated activity are explained, and illustrated in Figure 4.

### 5.1 *Classical mechanism of action; genomic ERE-mediated transcription*

In view of this thesis, the function and physical properties of the classical nuclear ER are described in more detail. Figures 5 and 6 illustrate the domain structure of nuclear ERs and general organization.

---

The classical genomic pathway is the most studied ER-mediated signaling pathway. Estrogens bind to the ER, which induces a conformational change, enabling receptor dimerisation and translocation to the nucleus. In the nucleus, the liganded receptor recruits co-activator proteins to form a functional ER complex, which binds to estrogen response elements (ERE) in the DNA, and gene transcription and transactivation can take place. ER target genes which have full or half ERE sites include pS2, cathepsin D, EGR3 and others.

The ER has different phosphorylation sites, and is targeted by kinases, including MAPK and PI3K/Akt. Several phosphorylation sites are located at the activation function 1 (AF-1) region of ERs, in the A/B domain. The phosphorylated ER forms a more stable transcription complex with the co-activators and upregulates the transcription activity of ER.

By recruitment of specific co-regulatory proteins, such as SRC-1, AIB1 and p300/CBP, the complex either stimulates (co-activators) or inhibits (co-repressor) transcription. The final direction (stimulation or repression) is determined by gene, cell, and signaling context<sup>[102-105]</sup>. The interactions of co-regulators with ERs can be controlled at several levels, such as coregulator expression, posttranslational modifications, and ligand binding. For many coregulators there is evidence for genome-wide competition for their recruitment to other nuclear receptors and DNA-binding factors, which is an important factor that determines gene expression.

Two isoforms of the cytosolic form of ER have been identified as yet. The initially cloned ER<sup>[106]</sup> became known as ER $\alpha$  when the other ER subtype was characterized as ER $\beta$  by Kuiper *et al* in 1996<sup>[107]</sup>. Both ERs bind the endogenous estrogen, 17 $\beta$ -estradiol (E2) with very high affinities (pmol range), show different tissue expression and distinct responses to various agonist and antagonists<sup>[108,109]</sup>. Activated ER $\alpha$  induces proliferation in uterus, mammary glands and the immune system and is associated with hormone-dependent cancers, such as breast, endometrial, prostate and ovarian and thyroid cancers. In contrast, ER $\beta$  has inhibitory effects on cancer development, it may have chemoprotective and pro-apoptotic function, or even therapeutic effects in cancer. Both ER isoforms readily form homodimers, but ER $\alpha$  and ER $\beta$  also form functional heterodimers *in vitro* and *in vivo*, and if both isoforms are expressed, the heterodimers predominate and efficiently transactivate reporter genes<sup>[110,111]</sup>. ER $\alpha$  and ER $\beta$  both bind AP1 sites, however ER $\alpha$  induces transcriptional activation, whereas ER $\beta$  is inhibitory. Although ER $\alpha$  and ER $\beta$  show similar potency in reporter gene transactivation and appear to bind to similar target sequences, co-expression of ER $\alpha$  and ER $\beta$  resulted in dramatic alterations in transcriptional profiles in breast cancer cell lines<sup>[112]</sup>, supporting the fact that the two receptors aim at different targets. Among the explanations why ER $\beta$  has different

properties than ER $\alpha$  and co-expression of ER $\alpha$  and ER $\beta$  results in differential expression may be the recent finding that ER $\beta$  regulates three distinct classes of genes and that the unliganded form of ER $\beta$  regulated more genes than the liganded form<sup>[113]</sup>.

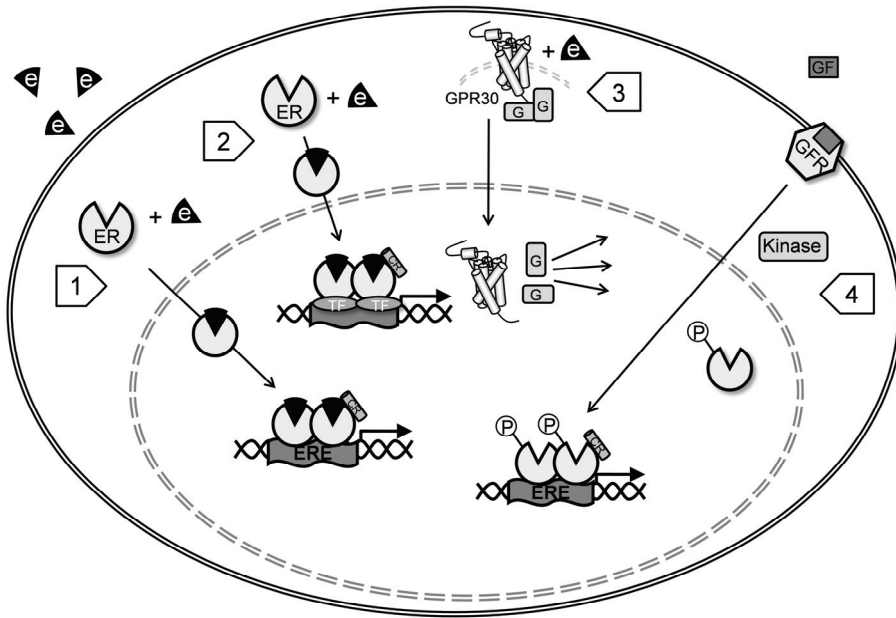


**Figure 4:** Different estrogen receptor (ER) mediated signaling:

- 1: Ligand-dependent ERE-mediated estrogen signaling (genomic, direct): 'Classical' ligand-induced ER $\alpha$  or ER $\beta$  dimerization and subsequent binding to specific estrogen response element (ERE) in the DNA leads to transcriptional activity. Co-regulator (CR) molecules regulate the activity of the transcriptional complexes.
- 2: Ligand-dependent, non-ERE-mediated estrogen signaling (genomic, indirect): Ligand-induced ER dimers (ER $\alpha$  or ER $\beta$ ) interact with other transcription factors, such as activator protein (AP)-1, NF- $\kappa$ B and Sp1, forming complexes that bind to non-ERE containing target genes and stimulate transcription. Co-regulator (CR) molecules regulate the activity of the transcriptional complexes.
- 3: Ligand-dependent, non-genomic, rapid estrogen signaling: ERs and membrane-bound GPR30 localized at or near the cell membrane mediate rapid estrogen responses by activating the phosphatidylinositol-3/Akt (PI3K/Akt) and/or protein kinase C/mitogen activated protein kinase (PKC/MAPK) signal transduction pathways.
- 4: Ligand-independent estrogen receptor activation: ERE-mediated transcription may be induced by in growth factor (GF) activated receptor tyrosine kinases that can phosphorylate the ER through activated MAPK and/or PI3K/Akt pathways. The phosphorylated ER can induce ligand-independent transactivation.

Key: ER = estrogen receptor, e = estrogen, GPR30 = membrane bound ER, TF = transcription factor, ERE = estrogen response element, CR = coregulator, GF = growth factor, GFR = growth factor receptor, P = phosphate.

---

### 5.2 Genomic non-ERE mediated transcription

Estrogen binding to the receptor may also induce transcription of non-ERE controlled DNA binding sites, by binding to other transcription factors, e.g. SP1, AP1 and NF- $\kappa$ B<sup>[114-116]</sup>. ER acts as a co-activator via protein-protein interactions, and genes activated via this way include ovalbumin, IGF-1, collagenase, VEGF, c-Myc, cyclin D1, c-fos, NF- $\kappa$ B, and the LDL receptor<sup>[117,118]</sup>.

### 5.3 Non-genomic actions of estrogens, rapid estrogen action

Nuclear ER-mediated transcriptional mechanisms take time (minutes to hours), and cannot explain the observed rapid estrogen-induced effects which occur within seconds to minutes after activation. These effects take place outside the nucleus and are initiated from the membrane<sup>[119,120]</sup>. ERs that may be responsible for the 'extra-nuclear' effects may either be the 'classical' nuclear ER $\alpha$  or ER $\beta$ , or membrane bound ERs (mER). So far, only one mER has been molecularly characterized: GPR30 or GPER (G-coupled estrogen receptor)<sup>[121,122]</sup>. Upon binding of estradiol to GPR30 (with affinity compared to nuclear ERs<sup>[121]</sup>), rapid estrogen-induced membrane mediated transactivation is induced. There exist some controversies concerning GPR30 localization and whether or not the receptor is estrogen responsive (reviewed in Langer *et al.*<sup>[123-126]</sup>). Although most GPCRs are expressed in the plasma membrane, several studies with GPR30 show that membrane bound ER localizes in the endoplasmic membrane<sup>[125]</sup>. Yet, also evidence is available on expression in the plasma membrane<sup>[121,127]</sup>.

Non-genomic effects of endocrine disrupting chemicals have gained attention<sup>[92,128,129]</sup>, and studies have revealed that EDCs receptors also bind to GPR30. Next to estradiol and other natural estrogenic ligands, GPR30 binds o,p'-DDE with the same affinity as ER $\alpha$  does in breast cancer cells, and also shows high binding affinity for genistein, whereas other EDCs, such as diethylestilbestrol (DES), did not significantly bind<sup>[122]</sup>.

### 5.4 Ligand-independent activation of the ER

Sufficient studies have demonstrated ligand-independent activation of the ER. Ligand-independent activation is entirely dependent on the cellular context of the ER, i.e. the presence of regulatory proteins. Many regulatory proteins have been shown to associate with the ER. For example, EGF (epidermal growth factor) or IGF-I (insulin-like growth factor) can activate the ER in the absence of a ligand<sup>[130-132]</sup>. Similarly, PPAR binding protein (PBP), a component of the thyroid hormone receptor associated proteins, which are involved in transcription, functions as an ER $\alpha$  co-activator, and also interacts with ER $\alpha$  in a ligand-independent manner. As a matter of fact, also ligand-activated ER needs to

interact with a complex of co-regulatory proteins to form a macromolecular complex to activate downstream signalling pathways<sup>[133]</sup>. As a result of binding of (partial) agonists and antagonists, different structural rearrangements of ERs are formed. These structural rearrangements are essential for transcriptional regulation, since the exposed surface of the receptor controls the recruitment of specific co-activators and other co-regulatory proteins<sup>[134,135]</sup>, which determines the actual response of the activated ER. In general, this functionality is controlled by the ligand-dependent AF-2 function. However, it has been demonstrated that if the AF-1 domain is combined with the DBD, even in the absence of the LBD, it can act constitutively, i.e. ligand-independently, to activate transcription from genes containing the appropriate response element in the promoter<sup>[136,137]</sup>. Still, the full transcriptional activation by ER $\alpha$  and ER $\beta$  requires functional synergy with the AF-2 domain<sup>[138]</sup>.

## 6 In focus: physical properties of the classical estrogen receptor

In the current thesis, the focus is on (environmental) estrogens in relation to the classical nuclear estrogen receptor  $\alpha$ . Characterization of non-genomic or membrane bound estrogen receptors has gained interest recently, however, a extensive description of the structure and function of other estrogen-sensitive receptors is beyond the scope of this introduction chapter, and we refer to recent literature for detailed information on mechanism of action of those receptors<sup>[121,122,126,139-141]</sup>.

### 6.1 General organization of the ER

The classical ER is a member of the nuclear receptor (NR) superfamily, and functions as transcription factor to modulate gene expression in a ligand-dependent manner<sup>[142]</sup>. Nuclear receptors are a large family of structurally related ligand-inducible DNA-binding transcription factors, including steroid receptors (SRs) such as the androgen (AR) and progesterone receptors (PR), thyroid/retinoids receptors (TR, RARs and RXRs) and vitamin D receptors. These receptors share a common modular structure, however, they all are activated by very distinct lipophilic small molecules (ligands) such as estrogens, glucocorticoids, progesterone, retinoids, and fatty acid derivatives. The shared structural organization of NRs comprises six functional regions (A-F) showing different sequence conservation (Figure 5). The N-terminal A/B domain is not well conserved among NRs. The steroid receptors (NR which bind steroid hormones) are characterized by large A/B domains. In ER $\alpha$  it contains the ligand-*independent* transactivation function AF-1, which is lacking in ER $\beta$ . The N-terminal domains of ER $\alpha$  and ER $\beta$  only show 20% homology and

have very different lengths ( $ER\alpha < ER\beta$ ). No clear secondary structural information on this region has yet been gained. The highly conserved C-region contains the DNA-binding domain (DBD) and the conserved E-region contains the ligand-binding domain (LBD), which holds the ligand-dependent transactivation function AF-2. Both the DBD and the LBD have been studied intensively, and widespread structural data have become available in the last decades. The regions D and F are not conserved and are variable in size, D may be a linker between the DBD and the LBD, and F is a C-terminal extension region of the LBD.

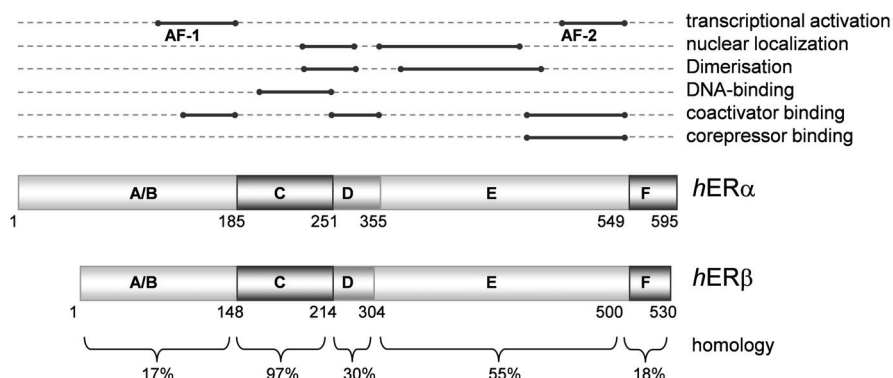


**Figure 5:** Graphical representation of the functional domains of the  $ER\alpha$  and  $ER\beta$ . The homology of the receptors per functional region is provided in %.

General function per domain: A/B: Transcriptional activity (AF-1 and AF-2)  
C: DNA binding domain (DBD)  
D: Hinge region (nuclear translocation)  
E: Ligand binding domain (LBD)  
F: Agonist/antagonist distinction

## 6.2 Tertiary structure of the ER

The ER LBD is arranged in an antiparallel  $\alpha$ -helical 'sandwich' fold, a universal fold within the receptor superfamily, as was first described for the human RXRa apolipoprotein LBD<sup>[143]</sup>. The ER LBD contains 11  $\alpha$ -helices (H1-H12) organized in a three-layered sandwich structure with H4, H5, H6, H8 and H9 flanked on one side by H1 and H3, and on the other side by H7, H10, and H11 (Figure 6).

The binding of an agonist induces a dramatic conformational change in the ER that produces realignment of H12 over the ligand binding pocket<sup>[134,144]</sup> so H12 functions as a closing lid. A subsequent feature of ligand burial by H12 realignment is the exposure of a surface where co-regulatory proteins (i.e. co-activators or co-repressors) can bind.

There, the ER interacts with consensus LXXLL sequences (L, leucine; X, any amino acid) which exist in many different co-activator/co-repressor proteins.

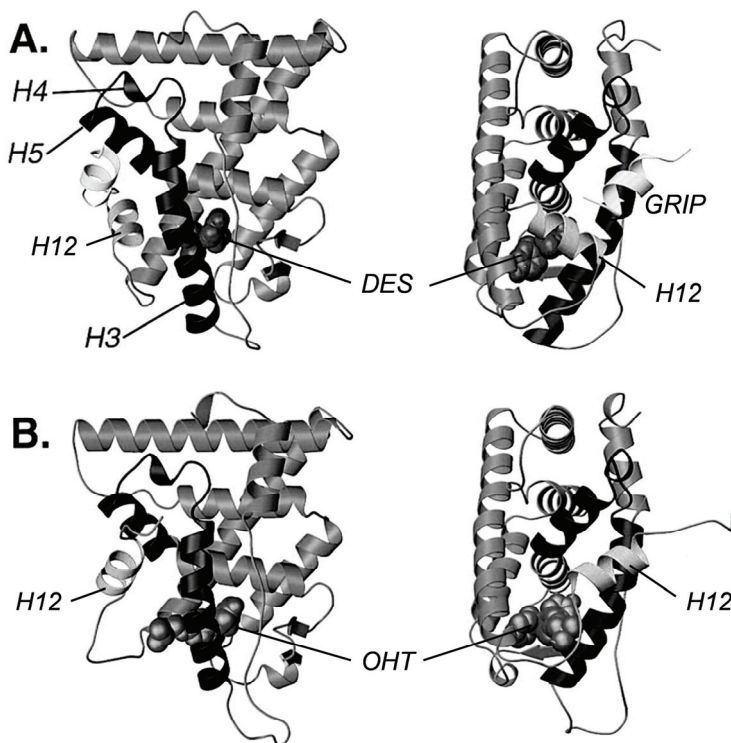
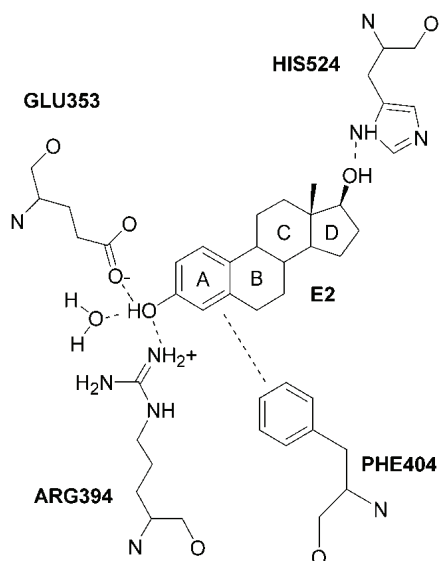


**Figure 6:** Graphical view/3D structure of liganded and unliganded ER. The ER is a 12-helical folded cytosolic receptor with a buried lipophilic binding cavity. Upon binding, Helix 12 rearranges, allowing dimerization, and coregulators (e.g. GRIP) to bind and form transactive (agonist) or non-transactive (antagonist) complexes. Shown is ER $\alpha$  bound to DES (agonist) vs. Hydroxy-tamoxifene (antagonist), showing different alignment of Helix 12. Reprinted from Shiau et al., (1998), *Cell*, 95(7), with permission from Elsevier.

### 6.3 Activation by agonists

From the crystal structures of ligand-bound ER $\alpha$ , for example with E2, DES, Genistein or other compounds<sup>[134,144-146]</sup> and from extensive structure activity research<sup>[147-149]</sup>, it is known that the ER $\alpha$  binding site is a narrow cavity that preferably hosts the binding of lipophilic compounds, equipped with a phenol that can interact by hydrogen bonding with the residues Glu353 and Arg394, and water molecules stabilizing these interactions. The phenolic moiety is an almost absolute requisite feature of an estrogen, and it is held in place by Phe404 in the ER $\alpha$ . At a distance of ideally 10-12 Å another hydrogen bond interaction with the amino residue His524 greatly enhances estrogen binding. The binding of the natural ligand E2 in the ER $\alpha$  is illustrated in Figure 7.

Even though the molecular structure of E2 is well-matched by the ER binding cavity, there are relatively large unoccupied hydrophobic cavities above and below the steroid skeleton. In fact, the binding cavity is nearly twice the volume of E2. Therefore, the ER allows binding of rather large lipophilic substituents, such as in the case of DES (**2** in Figure



8). The two ethyl groups contribute significantly to the high affinity for the ER. Also chlorine and bromine atoms are well tolerated, e.g. as is observed for the extremely high affinity of 11- $\beta$ -chloromethyl-E2 (**3** in Figure 8)<sup>[150]</sup>. The addition of this particular substituent resulted in a 10-30 fold higher affinity for the ER $\alpha$  than E2. Some unusual estrogenic compounds have been identified, one of them being the insecticide chlordecone (Kepone, **4** in Figure 8), which has no structural resemblance to typical estrogens such as E2 and DES, however, the ER $\alpha$  hosts ten chlorine atoms arranged in a cube-like structure.

**Figure 7:** Graphical view of binding of 17 $\beta$ -estradiol to the ER $\alpha$  by hydrogen bonding with Glu535 and Arg394, and His524. Phe404 interacts by perpendicular pi-pi stacking.

The different structural rearrangements of ERs which are formed upon binding of (partial) agonists and antagonists, are essential for the transcriptional regulation by ERs, since the exposed surface of the receptor controls the recruitment of specific co-activators and other co-regulatory proteins<sup>[134,135]</sup>, which determines the actual response of the activated ER. In general, this functionality is controlled by the ligand-dependent AF-2 function of the ER. However, it has been demonstrated that if the AF-1 domain is combined with the DBD, even in the absence of the LBD, it can act constitutively, i.e. ligand-independently, to activate transcription from genes containing the appropriate response element in the promoter<sup>[136,137]</sup>. Still, the full transcriptional activation by ER $\alpha$  and ER $\beta$  requires functional synergy with the ligand-dependent AF-2 domain<sup>[138]</sup>.

## 6.4 Antiestrogens and antagonists

'Classical' anti-estrogens, i.e. full ER antagonists with a bulky side-chain, such as ICI 164,384 (**10** in Figure 8), bind to the cavity of the ER, similarly to E2 and DES, however, their bulky side chain obstructs realignment of H12 (see Figure 6). The 'closed' position of H12, as observed in the E2-bound ER $\alpha$  complex, represents the most favourable geometry for co-activator binding<sup>[151]</sup>. Bulky side chain antiestrogens such as ICI164,384 and raloxifene (**11** in Figure 8) and prevent co-regulator binding, hampering transactivation and signal transduction<sup>[134]</sup>.

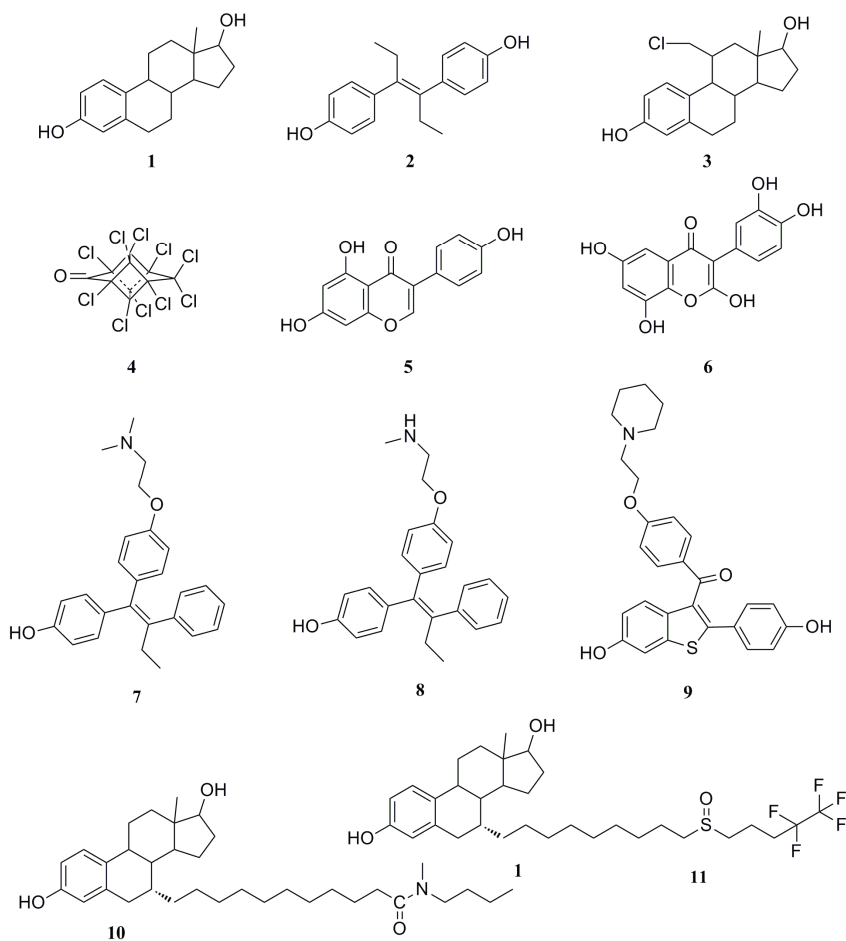


**Figure 8:** Molecular structures of ER binding compounds: the ER $\alpha$  agonists E2 (**1**), DES (**2**), 11- $\beta$ -chloromethyl-E2 (**3**), Kepone (**4**) and partial agonists genistein (**5**) and quercetin (**6**), 4-OH-tamoxifene (**7**), endoxifen (**8**) and antagonist ICI164,384 (**10**), raloxifene (**9**) and ICI182,780 (Faslodex or fulvestrant) (**11**).

---

Actually, the term ‘anti-estrogen’ has become inadequate, because it has been shown that ER-mediated anti-estrogenicity is not only the result of the molecular descriptors of the compound itself, it is the combined result of a specific ER conformation induced by ligand binding together with the cellular context (i.e. the expression of co-regulatory proteins) where binding occurs. In brief, some compounds can induce estrogenic (agonist) responses in a certain cellular environment, and antiestrogenic (antagonist) effects in another. This selectiveness will be explained below. By preventing the formation of an active conformation of the ER, *pure* antagonists impair the recruitment of co-activators, in a ligand-dependent manner<sup>[142,152,153]</sup>. ER isoform selectivity also determines whether a compound is an estrogen or an antiestrogen.

### 6.5 Partial agonists

Partial agonists are defined as compounds that induce a *sub-optimal* functional response at maximal receptor occupancy, when compared to the maximal response, induced by a reference compound (in this case E2) at maximal receptor occupancy. As a consequence, partial agonism is always a *relative* characteristic of functionality, and is dependent on the receptor, the reference compound and the assay system (or tissue) used. Genistein, a plant flavonoid (**5** in Figure 4), for example, is a full agonist for ER $\alpha$  and a partial agonist for ER $\beta$ <sup>[108,145]</sup>. Crystallography showed that genistein bound to ER $\beta$  induces a sub-optimal realignment of H12. In this case, realignment of H12 adopts an antagonist-like orientation, similar -but not equal- to raloxifen-bound ER $\beta$ , while a functional (agonist-like) response is obtained. The realignment of H12 is incomplete, and the co-activator binding site is not (yet) completely revealed after binding of genistein. Consequently, co-activators have to compete with H12 first, to displace H12, before binding and transactivation can take place<sup>[145, Pike, 2000]</sup>. It was shown that quercetin (**6** in Figure 8), another soy-derived flavonoid with moderate ER $\alpha$  binding affinity, was a partial ER $\alpha$  agonist, in an *in vitro* cell-based assay. Quercetin itself only induced half-maximal receptor activation, and moreover, it inhibited other estrogens agonistic effects, indicating that it binds to the ligand binding site of the ER $\alpha$ . No structural explanation was given for these observations<sup>[154]</sup>, however, the structural resemblance with genistein is very high, indicating a similar way of selective ligand-induced receptor activation is very plausible.

Estrogenic flavonoids such as genistein have been studied for their supposedly beneficial health effects in relation to e.g. cancer incidence (reviewed in<sup>[155]</sup>). Flavonoids like genistein have powerful antioxidant properties, and may be able to prevent cell damage caused by free radicals. Similarly to E2, flavonoids bind to both ER $\alpha$  and ER $\beta$ , and have been shown to prevent bone loss in postmenopausal women, and contribute to the lower incidence of

cardiovascular disease in Asian countries and in vegetarians<sup>[156-158]</sup>. In contrast to E2, they inhibit the proliferation of cancer cells like some anti-estrogens<sup>[159-161]</sup>. These observations indicate that genistein and other flavonoids may fully (or partially) agonise or block the ER, and this can be explained by the fact that ER $\alpha$  and ER $\beta$  are differentially expressed and show differed ligand specificities. Compounds, like genistein, that display such tissue-specific properties, are called *selective estrogen receptor modulators* (SERMs, see paragraph below).

Phytoestrogens exhibit various biological activities. It was demonstrated in women in asian countries, that higher serum and urine genistein concentrations (due to dietary soy intake) correlated with lower breast cancer risks<sup>[162]</sup>. Although these data suggest that long-life consumption of soy-derived phytoestrogens is beneficial, it should be questioned whether dietary intake of phytoestrogens via e.g. food supplements should be encouraged. Due to their ER-agonist properties, the intake of high doses of concentrated genistein or daidzein may aid to the onset of tumor development<sup>[155]</sup>.

In addition to stimulation of the ER-dependent cell-signaling pathways, some phytoestrogens are known to inhibit certain other cell-signalling pathways. For example, genistein is an inhibitor of protein tyrosine kinase<sup>[163,164]</sup>. Activated kinases may phosphorylate and activate ERs. Apigenin and quercetin are inhibitors of the phosphatidylinositol kinase (PI3K) pathway and thereby block cell signaling<sup>[165]</sup>. Phytoestrogens may thus activate ER-dependent cell signaling, and simultaneously inhibit signal transduction of growth factors involved in stimulation of ER-mediated cell-signaling (see Figure 9).

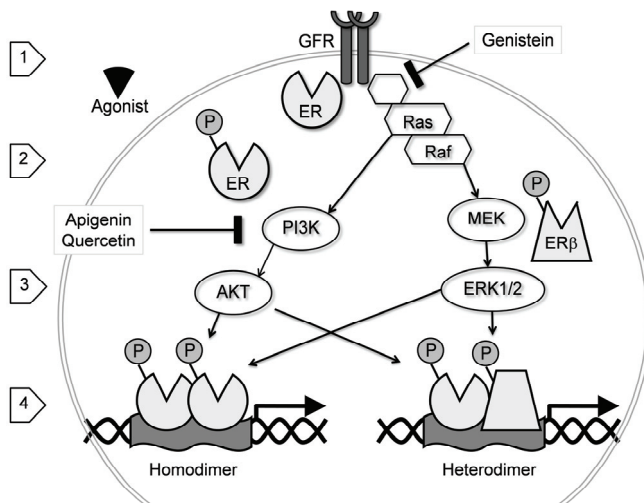


**Figure 9:** Possible phytoestrogen action on ER-mediated signaling. Growth factors activate cell-signaling pathways (ERK1/2, PI3K/AKT) and membrane-associated ERs, through the GFR. Subsequently, the activated kinases phosphorylate and activate cytosolic ER. Phytoestrogen may inhibit these pathways: e.g. genistein is a potent tyrosine kinase inhibitor and inhibits signal transduction of growth factors, and apigenin and quercetin inhibit PI3K and further inhibits cell signaling. Modified from<sup>[166]</sup>.

## 6.6 Selective estrogen receptor modulators; SERMs

SERMs are defined as estrogen receptor ligands that function as ER *agonists* in some tissues and ER *antagonists* in others. Estrogens are widely used clinically to control reproduction and for hormone therapy in women. Anti-estrogens are used to treat breast cancer in women. Given the implicated risk factor of estrogen treatment in reproduction, breast and uterine cancer, and unwanted side effects of anti-estrogen treatment, e.g. osteoporoses, there is a great need for drugs with tissue-selective properties. ER $\alpha$  and ER $\beta$  are differentially distributed in various estrogen target tissues. The binding cavities of ER $\alpha$  and ER $\beta$  actually only differ by a small variation in volume and by two amino acids, and despite this great similarity, the two receptors show differences in ligand binding specificity. Tamoxifen was the first compound identified as a SERM. Tamoxifen is currently used as treatment of ER-positive breast cancer<sup>[167]</sup> and is extensively metabolised, e.g., 4-hydroxytamoxifen has been identified as a metabolite with antagonistic activity (See structure 6 in Figure 8). It probably is further metabolised and recently N-desmethyl-4-hydroxytamoxifen (Endoxifen, 8 in Figure 8) has been acknowledged as the primary metabolite responsible for therapeutic activity of tamoxifen in ER-positive breast cancer<sup>[168]</sup>. 4-Hydroxytamoxifen has ER agonist activity in the liver and the uterus (endometrial), and is suggested to be linked to the initiation of hepatocellular carcinoma

and endometrial cancer, respectively. Although these observations point to undesirable side effects, they were important milestones in understanding ER pharmacology and SERMs<sup>[167]</sup>.

Raloxifene another potent SERM, displays a very different biological profile from tamoxifen, while tamoxifen acts as a partial agonist in uterine tissue and as a potent antagonist in breast tissue, raloxifene acts as an antagonist in both tissue types<sup>[169]</sup>. As explained earlier, these tissue-dependent properties of the SERMs are controlled by different expression and concentrations of coregulator proteins<sup>[133,169,170]</sup>. Next to the cellular context, the charge-neutralizing bridge between the bulky-chain of compounds such as lasofoxifene, with Asp351 in the ER was shown to play a role in the preferred recruitment of these coregulators as well<sup>[146]</sup>, which emphasizes the importance of elucidating structural characteristics of binding of any (anti)estrogen in order to explain observed effects.

### 6.7 Selective Estrogen Receptor Down-regulators; SERD

In addition to existing SERMs, there is a need for ER ligands which would not cause endocrine resistance in breast cancer. The search for such compounds led to the discovery of the selective estrogen receptor down-regulators, SERDs. Some currently identified SERDs, such as fulvestrant (**11** in Figure 8) and ICI164,384 (**10** in Figure 8) have a more antagonistic profile than SERMs and are capable of inhibiting the growth of certain tamoxifen-resistant breast cancer cells *in vivo*<sup>[171]</sup> and *in vitro*<sup>[172]</sup>. SERDs are mechanistically distinct from SERMs, and when they bind to the ER $\alpha$ , no transactivation takes place, irrespective of the cofactors/repressors which are expressed in the tissue. Due their long bulky side chains at the 7 $\alpha$  and 11 $\beta$  positions, receptor dimerization is sterically hindered and it has been proposed this distortion of the conformation of the ER ligand binding domain exposes hydrophobic surfaces, which promotes accelerated degradation of the ER protein<sup>[173]</sup>. Although the difference between SERMs and SERDs appears to be crucial in the lead optimization and development of candidate therapeutics in cancer treatment, the current thesis will not further focus on this item, for a review of SERDs properties and potentials, see<sup>[174,175]</sup>.

## 7 Accurate risk assessment

At present it is known that EDCs may affect almost every ecosystem, wildlife or animal studied. Whether humans are at risk still remains rather unclear. There are many epidemiological studies indicating that anthropological activities affect human health and

---

induce ecological imbalances. Although causal relationships are often hard to establish, compounds that can affect any species can potentially affect humans as well. However, questions remain at what concentrations and what are the effects of low-dose exposure?

Bio-activation of PAHs<sup>[53]</sup>, PHBs<sup>[78]</sup> and other contaminants such as DDT and methoxychlor<sup>[176,177]</sup> leads to the formation of more estrogenic metabolites, therefore research focusing on the risk of estrogenic pollutants should also include metabolism studies. Exposure to potential endocrine disrupting compounds also involves exposure to their metabolites. The potency of many of these compounds may be significantly increased after biotransformation, and the risks from exposure to these chemicals should not be neglected.

Furthermore, one has to realize that humans and wildlife are never exclusively exposed to one single compound. Possible EDC are formed from components in diet, used as pharmaceuticals, occur as environmental pollutants or are processed in general applications (bottles, plastics, biocides, etc.). Science has long been neglecting that daily exposure to chemicals concerns multiple compounds and thus mixture exposure. Over 95% of the resources in toxicology research concentrate on studying single chemicals<sup>[178]</sup>. It is also still largely unknown what the real effects of mixtures of different EDCs and whether or not their effects are synergistic, the effects of combinations of EDCs, e.g. affecting different endocrine systems in one organism, and the effects of the production of (more potent) metabolites of EDCs. Rajapakse *et al.* showed that the combined effect of 11 xenoestrogens, present at a level well below their no-observed-effect concentration (NOEC), led to a dramatic enhancement of E2 action. Hence, while the risk from exposure to individual weak estrogenic compounds seems insignificant, combined they may very well disrupt hormone regulation in humans and wildlife<sup>[47]</sup> and should therefore be included in investigating the endocrine disruption of xenoestrogens. In our laboratory, we have also shown that mixtures of estrogens act in an additive fashion, and together they produced distinct estrogenic responses in binding assays as well as an *in vitro* reporter gene assay, whereas when administered individually, they did not induce a noticeable response<sup>[46]</sup>. This has since been studied by several groups as well, indicating these effects should really be taken into account when judging the hazardous properties of compounds<sup>[81,154,179-181]</sup>.

In addition to the study of so-called cocktail mixtures of EDC, whether consisting of different parent compounds or EDC metabolites, there is growing interest in the overlap of effects EDCs induce in different endocrine systems as well<sup>[182]</sup>. This however, was beyond the scope of this thesis.

Taken together, in spite of evidence in animals and in *in vitro* experiments that exposure to environmental contaminants leads to endocrine disruption, it is still largely unclear whether EDCs are a relevant threat to humans. Low exposure concentrations of humans remains the most important issue of discussion. Many EDCs are known to be metabolised into one or even more (active) metabolites. Furthermore, the aspect of combined exposure to mixtures of possible EDCs should be taken into account. *Ergo*, it is of great importance to know the individual biological activities of EDCs, as well as the activity of the metabolite(s) formed, and finally, the hazards of combined exposure.

### *In vitro and in vivo testing for estrogenic activity*

There are many ways to test the estrogenic properties of putative estrogens *in vitro*, and these can be divided in three categories: *competitive ER binding assays*, *cell proliferation assays* and *reporter gene assays*. Competitive binding assays with radiolabeled ligands can be performed to measure ER binding affinity using ER from different sources<sup>[183]</sup>, such as from uterus (e.g. sheep, rat, rabbit, mouse), cancer cell lines (e.g. human MCF-7) and recombinant human ER. These assays provide accurate ligand binding affinities, however do not discriminate between (partial) agonist or antagonists or SERMs. To reveal these properties, cell proliferation assays (e.g. E-SCREEN<sup>[45]</sup>) can be used to measure the increase of cell number after exposure to estrogens with agonistic activity. Estrogens induce cell proliferation by activation of the ER in ER-positive cells (from breast tissue e.g.), hence increase in cell number after estrogen exposure is a direct measure for estrogenicity. With some modifications, such assays may also be used to test for antagonistic activity.

Finally, reporter-gene assays (e.g. ER-Calux<sup>®</sup><sup>[184]</sup>, YES-screen<sup>[185]</sup>) can be used to investigate ER-mediated transcriptional and translational activity of compounds, and such assays may also discriminate between agonists and antagonists. Recently, more sophisticated *in vitro* systems have been developed, e.g. the conformation-specific peptide recognition system. In this *in vitro* system, each conformation of the ER-LBD is recognized by a unique combination of peptides, defining a specific peptide recognition pattern. This enables investigators to discriminate between the conformational states of the ER-LBD, induced by binding of an (anta)gonist or a partial (anta)gonist<sup>[186,187]</sup>. A FRET-based assay has been developed by the group of Michalides, that can discriminate between the agonist and antagonist conformation of ligand-bound ER $\alpha$ <sup>[188]</sup>.

Several *in vivo* assays are available as well, such as the classical rodent uterine wet weight assay<sup>[76]</sup>, and the more recent vitellogenin induction assays<sup>[189]</sup> in rainbow trout and reporter-gene assays using transgenic zebra fish<sup>[190]</sup>. There are always shortcomings using model systems for the assessment of estrogenic activity of compounds. As mentioned

---

before, the combined exposure of different compounds and the metabolic activation including the production of estrogenic metabolites are generally not considered, and the outcome of the assay may easily be ascribed to the parent compound(s) administered. Furthermore, it remains unknown what metabolites could be formed, and in most cases it is impossible to isolate and identify these metabolites.

*In silico testing for estrogenic activity: need for computational models*

In light of the above, it is of great value to develop reliable methods to *predict* ER $\alpha$  binding affinity of compounds of which active metabolites are unknown or impossible to isolate, e.g. by the use of computer models. For the ER, many approaches have been used to calculate ligand binding affinities, ranging from ligand-based comparative molecular field analysis (CoMFA) studies using ligand-descriptors<sup>[191]</sup>, to protein-based methods using empirical scoring functions<sup>[192]</sup>, docking studies<sup>[193-195]</sup> and molecular dynamics simulations (MD), using free energy perturbation methods (FEP)<sup>[149,196-198]</sup>. At present, computational models involving ER are widely used in lead discovery finding the perfect compound, such as a SERM or a SERBA, and they have already proven to serve well<sup>[148,198,199]</sup>. As yet, all compounds still have to be tested for efficacy in experimental *in vitro* or *in vivo* systems.

*In silico* calculation of ligand binding affinities may provide accurate information on ligand binding, however, also unknown ligands or ligands hard to obtain can be easily included. The linear interaction energy (LIE) approximation is a method for the precise estimation of binding affinities. The method uses molecular dynamics (MD) simulations of bound receptor-ligand complexes, and was first described and further extended by Åqvist *et al.*<sup>[200-203]</sup> and successfully used in predictive computational studies<sup>[149,204,205]</sup>. From the MD simulations, binding free energies can be obtained assuming a linear response for electrostatic interactions and an empirical expression for non-polar contributions. The most important advantages are that only (convergent) averages of the interaction energies between the ligand and its surroundings need to be evaluated, thus thermal averaging over different conformations is carried out by MD. The method is based on estimating *absolute* binding energies, and faster than rigorous FEP calculations. The LIE approach determines the difference in binding between the ligand solvated in water and ligand bound to a (solvated) protein, therefore MD simulations of those two states are carried out. The van der Waals and electrostatic contributions to the binding affinity are considered separately, allowing semi-empirical correction for overestimating polar interactions over non-polar interactions. Although widely used scoring functions are generally faster than MD, the LIE methods proves to be much more accurate in predicting absolute binding affinities.

Our believe is, that in the near future, computer models for prediction of binding affinity, binding orientation and complex molecular processes such as metabolism will be sophisticated enough to compete with experimental and biochemical methods. Especially computationally integrating metabolism and efficacy modeling should be within reach shortly. Computational (bio)chemistry will become more and more important in the research to accurately assess the biomolecular properties and subsequent risks for human and wildlife of environmental compounds, (future) medicines, dietary products, etcetera.

## 8 Aim of the thesis

When starting the research in 1998 which is described in this thesis, the role of bioactivation of environmental contaminants was not adequately acknowledged yet. Most compounds were considered to be possible endocrine disruptors, based on the properties of the parent compound. Therefore, the main aim of this thesis set out then, was to investigate whether bioactivation of known environmental contaminants, would lead to the formation of more estrogenic metabolites or not. We focused on the bioactivation of hydrophobic PCBs and PAHs by CYP enzymes. These compounds are known to be extensively metabolised by CYP enzymes, resulting in the formation of more hydrophilic compounds. The combination of hydrophobic aromatic molecules, equipped with hydroxyl groups were considered then to be good candidates for ER ligand affinity. Since the un-metabolised PCB and PAH molecules are not known as potent ER activators or inhibitors, and exposure to these compounds was shown to have great impact on endocrine systems after e.g. environmental spills or incidents, we then felt the need to investigate whether their metabolites could be responsible for the observed effects. We focused on the *in vitro* formation and identification of hydroxylated metabolites by CYPs,, and on their ER affinities and estrogenic activities *in vitro*, as well as sulfotransferase inhibition capacity. We investigated individual PCBs and PAHs as well as mixtures of their metabolites. Situations such as unintentional exposures of humans to environmental contaminants like pesticides, PCBs, dioxins etc. by spills *in vivo*, do not lead to extensive metabolite identification, let alone offer adequate insight in the possible endocrine disrupting burden caused by the formation of the metabolites. Metabolites were generally formed in low concentrations, were difficult to synthesize and were therefore not available for *in vitro* testing either. Because our initial *in vitro* data suggested that we should focus on biological activities of metabolites as well, we employed *in silico* modeling strategies to build a computational model for the accurate prediction of ligand binding affinities and preferred orientations of ligand binding to the ER $\alpha$ . We optimised the crystal structure

---

(published in 1997) and used it with the linear interaction energy (LIE) approach, based on molecular dynamics (MD) simulations of receptor-ligand and water-ligand complexes.

It is generally accepted that high levels of exposure to EDCs damage endocrine systems in animals and humans, and scientific debates now concentrate on whether there is a risk to the general population of humans and animals exposed to the low levels of endocrine disrupting compounds. An often neglected but nevertheless important aspect in this debate should be the contribution of bioactivated contaminants with high(er) endocrine disrupting potency, the exposure to mixtures (for example due to metabolism) and the cumulative exposure, since these may contribute significantly during prenatal phases of animals and humans development. In the studies conducted and described in the current thesis, clarifying steps have been undertaken and discussed, to support the hypothesis that bioactivation of environmental contaminants and mixture capacity should be considered in order to avoid underestimation of the danger of endocrine disruption by environmental contaminants.

## Chapter 2

Formation of estrogenic metabolites of benzo[*a*]pyrene and chrysene by cytochrome P450 activity and their combined and supra-maximal estrogenic activity

Marola M.H.van Lipzig, Nico P.E. Vermeulen, Renato Gusinu, Juliette Legler, Heinz Frank, Albrecht Seidel and John H.N. Meerman.

Environmental Toxicology and Pharmacology, 2005 (19), 41-55.

---

## ABSTRACT

Metabolism of polycyclic aromatic hydrocarbons (PAHs) has been studied intensively, and potential metabolites with estrogenic activity have been identified previously. However, little attention has been paid to the metabolic pathways in mammals and to the combined effect of individual metabolites. Several hydroxylated metabolites of benzo[*a*]pyrene (BaP) and chrysene (CHN) were formed by rat liver microsomal cytochrome P450 (CYP) activity, some of which possess estrogenic activity. All mono- and several dihydroxylated metabolites of BaP and CHN were tested for ER affinity and estrogenic activity in a proliferation assay (E-screen) and in a reporter-gene assay (ER-Calux). Twelve estrogenic metabolites were identified with EC<sub>50</sub> values ranging from 40 nM to 0.15 mM. The combined effect of a mixture of seven PAH-metabolites was also studied in the ER binding assay. At concentrations that show little activity themselves, their joint action clearly exhibited significant estrogenic activity.

BaP itself exhibited estrogenicity in the ER-Calux assay due to bio-activation into estrogenic metabolites, probably via aryl hydrocarbon receptor (AhR) induced CYP activity. Furthermore, 2-hydroxy-CHN (2-OH-CHN) induced supra-maximal (400 %) estrogenic effects in the ER-Calux assay. This effect was entirely ER-mediated, since the response was completely blocked with the ER-antagonist ICI182,780. We showed that 2-OH-CHN increased ER-concentration, using ELISA techniques, which may explain the observed supra-maximal effects. Co-treatment with the AhR-antagonist 3',4'-dimethoxyflavone (DMF) enhanced ER-signalling, possibly via blockage of AhR-ER inhibitory cross-talk.

## 1 Introduction

Exposure to environmental estrogens has been proposed to be a risk factor for disruption of reproductive development and tumorigenesis of humans and wildlife<sup>[4]</sup>. Estrogens play a crucial role in the development, growth and regulation of sexual and reproductive organs and behaviour<sup>[2]</sup>. Estrogens act via binding to estrogen receptors (ER), members of the nuclear receptor superfamily, that function as transcription factor to modulate gene expression in a ligand-dependent manner<sup>[142]</sup>. In the nucleus, binding of ligands induces a conformational change of the ER, enabling the receptor to dimerise. The dimer binds to the palindrome estrogen response elements (ERE) in DNA, where it enhances gene transcription leading to e.g. protein synthesis and cell proliferation<sup>[134]</sup>. Two ER isoforms have been identified, ER $\alpha$  and ER $\beta$ , that show different tissue expression and distinct ligand binding properties<sup>[109]</sup>.

Exposure to xenobiotics that interfere with the endogenous hormone balance, for example by binding to the ER, may lead to endocrine disruption<sup>[206]</sup>. In recent years, a wide variety of structurally diverse environmental compounds have been identified as endocrine disruptors. Among these compounds are natural steroid hormones, pharmaceuticals, industrial chemicals including polychlorinated biphenyls (PCBs), pesticides and polycyclic aromatic hydrocarbons (PAHs). PAHs are one of the largest classes of chemicals present in the environment<sup>[207]</sup>. They have been considered a health risk for wild life and humans for a long time<sup>[208]</sup>. Human exposure to PAHs occurs via food intake, smoking, and by occupational exposure<sup>[209]</sup>. The carcinogenic properties of PAHs have been extensively studied<sup>[69-71]</sup> and it is now widely accepted that PAHs are metabolised to intermediates that may react covalently with DNA and other macromolecules. In order to exert their carcinogenic properties, metabolism to reactive intermediates, also called 'bio-activation', must be catalyzed by cytochrome P450 (CYP) enzymes and epoxide hydrolases<sup>[72]</sup>.

Hormone-responsive tissues are known to be very susceptible to tumour formation. Therefore, hormonal carcinogenesis has already been studied for many decades. Although it is generally believed that the carcinogenicity of hormones is based upon tumour promoting activity, the exact mechanisms are still not completely elucidated. In addition, estrogens like 17 $\alpha$ -ethinylestradiol fail to induce mammary cancers in rodents<sup>[210]</sup> and they even may be anti-carcinogenic in some animal models<sup>[211]</sup>, while other estrogens, like E2 and diethylstilbestrol, induce tumours and clearly have genotoxic effects<sup>[212]</sup>. This suggests that solely tumour promoting activity may not be sufficient for tumour formation

by estrogens. Furthermore, the 3,9-dihydroxy metabolites of the rat mammary genotoxic carcinogen 7,12-dimethylbenz[*a*]anthracene (DMBA) and benz[*a*]anthracene (BA), have affinity for the estrogen receptor and are weakly estrogenic in a rat bioassay<sup>[213]</sup>. This might be related to the fact that DMBA is one of the most specific and potent carcinogens for the mammary gland in rodents. Furthermore, mammary tumours induced by benzo[*a*]pyrene (BaP) and other PAHs are predominantly estrogen-dependent<sup>[69,214,215]</sup> and exposure of rats to PAHs induces a complete estrus in these animals<sup>[216,217]</sup>.

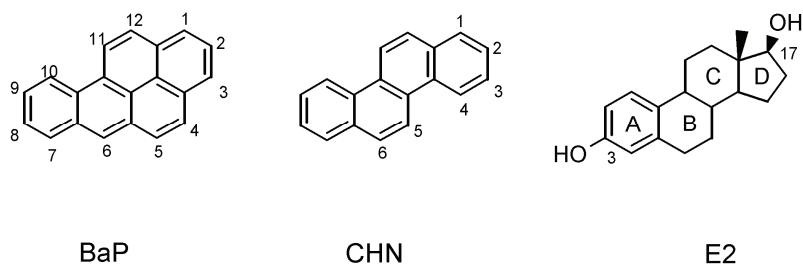


**Figure 1:** The molecular structures of parent compounds benzo[*a*]pyrene (BaP), chrysene (CHN) and 17 $\beta$ -estradiol (E2). The numbers indicate the positions of the hydroxyl group substituents.

The structural resemblance of BaP (Figure 1) and steroid hormones such as 17 $\beta$ -estradiol (E2, Figure 1) has been the objective of several studies<sup>[209,216,218]</sup>. BaP showed estrogenic activity in several cellular systems *in vitro*,<sup>[53,219,220]</sup> but no ER-affinity of BaP was found in radioligand binding assays. Most assays utilize cultured, ER-expressing breast cancer cells (e.g. MCF-7 cells or T47D cells), which are metabolically highly active, and express both phase I (e.g. cytochromes P450) and phase II (e.g. glucuronyltransferases, sulfotransferases) metabolism enzymes<sup>[221-223]</sup>. Therefore, the estrogenic properties of BaP might be due to metabolism into estrogenic metabolites. Recently, 3-hydroxy-BaP (3-OH-BaP) and 9-hydroxy-BaP (9-OH-BaP) have been identified as having low affinity for ER $\alpha$  and ER $\beta$ <sup>[53]</sup>. Furthermore, Hirose *et al.* reported that mono-hydroxylated BaP metabolites in general showed higher affinity for the ER $\beta$  than for ER $\alpha$ <sup>[220]</sup>, but in this particular study no EC<sub>50</sub> values were reported. In their yeast gene expression system, none of the metabolites showed estrogenicity for ER $\alpha$ , however, 1-, 2-, 3- and 9-OH-BaP induced estrogenic activity via ER $\beta$ , and anti-estrogenic activity for ER $\beta$  was observed for 8-OH-BaP<sup>[220]</sup>. In yet another study, 1-, 3-, 7- and 9-OH-BaP bound to both ER $\alpha$  and ER $\beta$  in binding experiments and activated ER $\alpha$  and ER $\beta$ -signaling in a reporter-gene assay, however, these metabolites failed to induce estrogenic effects *in vivo* in mice<sup>[54]</sup>.

CHN (Figure 1) is another environmentally important PAH and a major component of coal tar and a common atmospheric pollutant<sup>[224]</sup>. It occurs at about the same level as BaP in

products of incomplete combustion, automobile exhaust and cigarette smoke. Hydroxylated CHN metabolites have been found in mammalian cell culture<sup>[225]</sup> and in fish<sup>[226]</sup>, and although CHN is known not to act as a complete carcinogen, it was found that dihydrodiol-metabolites of CHN have tumorigenic activities<sup>[227]</sup>. Some hydroxylated CHN metabolites have also been tested for estrogenic activity. The 2-OH-CHN showed binding affinity for ER $\alpha$  and ER $\beta$ , and were weakly estrogenic in transfected human-ER $\alpha$  and mouse-ER $\beta$  cells<sup>[219]</sup>. 6-hydroxy-CHN was found to be anti-estrogenic in a reporter-gene assay<sup>[228]</sup>.

Besides binding to the ER, PAHs such as BaP, DMBA and BA are known to be potent agonists of the aryl hydrocarbon receptor (AhR) and may be anti-estrogenic by down-regulation of nuclear ER levels and ER-signaling<sup>[229,230]</sup>. BaP and CHN have been reported to displace [<sup>3</sup>H]-E2 in a whole cell assay under conditions that permit metabolism, however, they were both anti-estrogenic in a post-confluent growth assay<sup>[231]</sup>. Furthermore, as stated above, some PAH metabolites are estrogenic in binding assays and reporter-gene assays, but fail to induce estrogenic effects *in vivo*.

Thus, there still exists contradiction and unresolved questions in respect to the estrogenic, non-estrogenic or anti-estrogenic activities of hydroxylated BaP- and CHN-metabolites.

In the present study, we have investigated the formation of estrogenic metabolites of BaP and CHN by rat liver microsomal cytochrome P450s. Furthermore, we tested eighteen individual mono- and three dihydroxylated metabolites of BaP and CHN for affinity for the ER in a radioligand binding assay. The combined estrogenic effect of a mixture of seven different mono-hydroxylated metabolites was also determined in the ER binding assay and a clear joint effect was observed. Metabolites were also tested for estrogenic activity in a cell proliferation assay (E-screen) and in a reporter-gene assay (ER-Calux) using stably transfected ER-positive T47D cells which revealed, among others, that several BaP and CHN metabolites induced 'supra-maximal' effects (effects greater than estradiol itself).

## 2 Methods

### 2.1 Chemicals

17 $\beta$ -Estradiol (E2), benzo[*a*]pyrene (BaP), chrysene (CHN), activated charcoal, sulforhodamine B (SRB) were purchased from Sigma Chemical co., St. Louis, U.S.A. [<sup>3</sup>H]-E2 was obtained from Amersham (Buckinghamshire, UK). 3',4'-dimethoxyflavone (DMF) was obtained from Idofine Chemical Co. Inc. (New Jersey, U.S.A.). ICI182,780 was kindly provided by Dr. A. Wakeling (AstraZeneca, Macclesfield, UK). Pure hydroxy-BaPs and

---

*trans*-7,8-dihydroxy-7,8-dihydrobenzo[*a*]pyrene (7,8-OH-H<sub>2</sub>BaP) were obtained from the Chemical Carcinogen Reference Standard Repository of the National Cancer Institute (Kansas, U.S.A.). Pure hydroxy-CHNs were kindly provided by Dr. Albrecht Seidel (Grosshansdorf, Germany). Dextran (MW 60.000-90.000) was obtained from Duchefa, Haarlem, The Netherlands. Mouse monoclonal anti-human ER $\alpha$  was obtained from Santa Cruz (California, U.S.A.), goat anti-mouse IgG-HRP conjugate was purchased from BioRad Laboratories Inc. (Hercules, U.S.A.). All other chemicals were of analytical grade and purchased from Sigma-Aldrich Co. (St Louis, U.S.A.).

## 2.2 *Microsomal incubations of BaP and CHN for generation of metabolites*

Metabolite mixtures of BaP and CHN were generated using  $\beta$ -naphthoflavone (BNF)-induced rat liver microsomes. Microsomes were prepared from BNF-treated male Wistar rats as described before<sup>[232]</sup>. Incubations (10 ml total volume) were performed in 100 mM K<sub>2</sub>HPO<sub>4</sub>/KH<sub>2</sub>PO<sub>4</sub> buffer (pH 7.4), containing 5 mM MgCl<sub>2</sub>, 250  $\mu$ M BaP or CHN, and ca. 1 mg/ml microsomal protein and reaction was started by addition of NADPH (final concentration 1 mM). After 45 minutes of incubation at 37°C, reactions were terminated by the addition of 10% HClO<sub>4</sub> (10% v/v) and samples were kept on ice. Complete incubation mixtures were extracted by 10 ml isopropyl ether and evaporated under a stream of nitrogen. Samples were redissolved in 250  $\mu$ l DMSO to perform analysis and bioassays, and stored at -20°C with 0.5 mg/ml vitamin C to avoid further oxidation. Controls comprised of incubations without PAH, incubations without NADPH and incubations immediately terminated after the start of the reactions.

## 2.3 *HPLC*

Redissolved extracts (50  $\mu$ l) from microsomal incubations of BAP and CHN and all individual hydroxylated metabolites were analysed by high performance liquid chromatography (HPLC, pumps 303 and 305, manometer 805, dynamic mixer 811C and auto-injector 232 Bio, manufactured by Gilson, Middleton, U.S.A.) using a reversed phase C18-column (ChromSpher 5  $\mu$ M, 100 x 3 mm, Chrompack, The Netherlands) and a gradient elution with solvent A (10% acetonitrile, 1% acetic acid) and solvent B (90% acetonitrile, 1% acetic acid). The gradient programme was as follows: isocratic elution at 100%A / 0% B from 0 to 2 minutes, gradient elution to 0% A/100% B from 2 to 25 minutes, isocratic elution at 0% A/100% B from 25 to 30 minutes, gradient elution back to 100% A/0% B from 30 to 40 minutes and isocratic elution at 100%A/0% B from 40 to 45 minutes. The flow rate of the mobile phase was 0.6 ml/min. Compounds were detected at a wavelength of 254 nm (uv/vis photospectrometer type 1575 manufactured by Jasco Ltd, UK).

## 2.4 Cell Culture

*Wild type T47D cells.* The T47D human breast adenocarcinoma cell line was kindly provided by Dr. B. van der Burg (Hubrecht Laboratory, Netherlands Institute for Developmental Biology, Utrecht, The Netherlands). The cells were maintained in 75 cm<sup>2</sup> flasks (Costar Corning, New York, U.S.A.) in a 1:1 mixture of Dulbecco's modified Eagle medium (DMEM) and Ham's F12 medium (D/F+, Gibco, Rockville, U.S.A.), supplemented with L-glutamine, 0.1 mM non-essential amino acids (NEA, Gibco), 7.5% heat inactivated foetal bovine serum (FBS, Biowhittaker, Walkersville, U.S.A.) and penicillin (50 U/ml)-streptomycin mix (50 µg/ml) (Biowhittaker). T47D cells were cultured at 37°C, 5% CO<sub>2</sub>.

*Stably transfected T47D.Luc cells.* Stably transfected T47D.Luc cells were obtained from BioDetection systems b.v. (BDS), Amsterdam, The Netherlands. The T47D.Luc cells were maintained for passage number 10 to 25 in 75 cm<sup>2</sup> flasks in a 1:1 mixture of DMEM and Ham's F12 medium (D/F+, Gibco, Rockville, U.S.A.), supplemented with 0.1 mM NEA and 7.5% heat inactivated FBS. T47D cells were cultured at 37°C, 7.5% CO<sub>2</sub>.

## 2.5 Assays

*Competitive ligand binding assay.* Competitive binding assays were performed as described before<sup>[185]</sup>. Briefly, affinity for the ER was determined using cytosol from homogenised fresh sheep uterus, disposed of adherent fat and connective tissue. A mixture of 3 nM [<sup>3</sup>H]-E2, uterine cytosolic protein (final concentration was between 0.5-1 mg/ml depending on the uterus batch) and competing ligand in a total volume of 325 µl in TEA-buffer (10 mM TEA, 15 µM EDTA, pH 7.4) was incubated for 3 hours at 4°C. Subsequently, 300 µl of a 0.8%-0.08% charcoal-dextran slurry in TEA-buffer was added to remove unbound radioligand, and the mixture was incubated for 10 minutes at 4°C. Mixtures were centrifuged at 10.000 x g in an Eppendorf centrifuge for 10 minutes at 4°C, and aliquots from the supernatant were analysed for receptor-bound [<sup>3</sup>H]-E2 in 4 ml scintillation liquid (HiSafe 3, Perkin Elmer, Wellesley, U.S.A.) in a 1900 Tricarb scintillation counter (Packard Instruments, Perkin Elmer, Wellesley, U.S.A.). Each experiment, a complete E2 concentration curve was included in duplicate and used to determine 0% and 100% displacement. Concentration of DMSO in the assay was always 3%, and this concentration did not alter the binding characteristics of the ER for E2. Experiments were performed at least three times on separate days. The ligand binding affinities (K<sub>d</sub>) were calculated with Graphpad Prism 3.0 (GraphPad Software Inc., 2000, San Diego, CA). The combined effect of a mixture of 7 hydroxylated PAH metabolites was tested in the ER binding assay. Concentrations of the individual compounds were based on their individual EC<sub>50</sub> values in the binding assay, according to the concept of concentration addition, as described by Backhaus *et al.*<sup>[233]</sup> and Altenburger *et al.*<sup>[234]</sup>.

---

*Cell proliferation assay (modified E-screen).* The original E-screen assay was described before by Soto *et al.*<sup>[45]</sup> and optimised in our laboratory for use with T47D cells. Wild type T47D cells were plated at a density of 50.000 cells/ml in 250 µl/well in 48-well plates (Costar) and allowed to attach overnight. Medium was discarded the following day and changed to assay medium, i.e. phenol red-free 1:1 mixture of DMEM and Ham's F12 medium (D/F-, Gibco), supplemented with 0.1 mM NEA, penicillin (50 U/ml)-streptomycin mix (50 µg/ml) and 5% charcoal-dextran stripped FBS (CDFBS). CDFBS was prepared by two successive treatments of heat inactivated FBS with a 0.5%-0.05% charcoal-dextran mixture at 37°C for 1.5 hours, as described by Soto *et al.*<sup>[45]</sup>. The stripped serum was ultra-centrifuged at 100.000g for 1 hour and filter sterilised through 0.22 µm Millex®-GP filters (Millipore, Bedford, U.S.A.) and kept at -20°C until use. Cells were maintained in 5% CDFBS in D/F- for 48 hours. Then medium was changed to fresh 5% CDFBS in D/F- containing the test compounds (DMSO < 0.1%). Cells were exposed in triplicate and allowed to proliferate for 5 days. An E2 standard curve was included in triplicate in each experiment, and control and E2 calibration points were included in triplicate on every plate within the same experiment. After 5 days, cells were fixed and stained using the Sulforhodamine B assay, as described below. For each compound, experiments were performed at least on three different days.

*Sulforhodamine B assay.* Cell number was determined using the colorimetric sulforhodamine B (SRB) assay<sup>[235]</sup>. Cells were fixed in 48-well plates by gently adding 75 µl of a 50% trichloroacetic acid (TCA) solution directly to the assay medium in each well. Plates were left at 4°C for 1 hour, then washed five times with tap water and air-dried. 150 µl 0.4% (w/v) SRB in 1% acetic acid was added to each well, and the plates were left at room temperature for 30 minutes. SRB solution was discarded and plates were washed five times with 1% acetic acid and air-dried again. Bound SRB was solubilised with 250 µl 10 mM unbuffered Tris solution (pH >10) on a plate shaker for ten minutes. Absorbance was measured at 530 nm on a Wallac Victor2 plate reader (Perkin Elmer, Wellesley, U.S.A.). The SRB assay was calibrated with plates with known cell densities per well (determined by microscopic counting). SRB values were corrected for background measurements.

*ER-Calux luciferase assay.* ER-Calux assay was performed as described before<sup>[184]</sup>. Briefly, cells were plated at a density of 50.000 cells/ml in 100 µl assay medium per well in 96-well plates (Nunclo<sup>®</sup>, Nunc) and allowed to attach overnight. ER-Calux assay medium contained D/F- (Gibco), supplemented with 0.1 mM NEA and 5% CDFBS. Medium was renewed the following day and cells were left in the incubator for another 48 hours.

Subsequently, cells were exposed to various compounds in triplicate in fresh assay medium. Control incubations and an E2 standard curve were included in triplicate on every plate. DMSO concentration was 0.1% (v/v) in all incubations. After cells were incubated for 6 hours, medium was removed. Cells were lysed by addition of 30  $\mu$ l/well Triton-lysis buffer (1% Triton X-100, 25 mM Tris, 2 mM DTT, 2 mM CDTA and 10% glycerol, pH 7.8) and were gently shaken for 10 minutes at room temperature. Lysed cells were placed in -20°C and kept until measurement of luciferase activity. Luciferase measurement was performed with an Anthos Lucy 2 luminometer. A 100  $\mu$ l-aliquot of a solution containing 20 mM tricine, 1.07 mM magnesium hydroxide carbonate, 2.67 mM magnesium sulphate, 0.10 mM EDTA, 270  $\mu$ M co-enzyme A, 470  $\mu$ M luciferine and 530  $\mu$ M ATP, pH 7.8, was added to each well and conversion of substrate was measured immediately. To avoid bias by scattering, the luminescence was extinguished by addition of 0.2 N NaOH before the next sample was measured. Experiments were performed at least three times on different occasions. EC<sub>50</sub> values were calculated using Graphpad Prism 3.0.

*ELISA for determination of ER $\alpha$  expression.* T47D.Luc cells were treated similarly as described in the ER-Calux assay. Cells were seeded in 96-well plates (Nunc<sup>®</sup>, Nunc) in assay-medium (100.000 cells/ml in 100  $\mu$ l/well) and allowed to attach for 48 hours. Medium was changed and cells were left for 48 hours before exposure. After 6 hours exposure to various compounds in triplicate in fresh assay medium, medium was aspirated and cells were washed with 0.05 M tris-buffered 0.15 M saline (TBS, pH 7.5). Cells were fixated in 4% paraformaldehyde for 30 minutes at room temperature, permeabilised with 0.5% Igepal CA-630 in TBS for 30 minutes at room temperature, and subsequently blocked with blocking buffer (1% fat free milk in 0.1M NaHCO<sub>3</sub>, pH 8.6) overnight at 4°C. Cells were incubated with the primary antibody, mouse monoclonal anti-human ER $\alpha$ , in 0.1% BSA in TBS, overnight at 4°C on a shaker. The next day, cells were incubated with the secondary antibody, goat anti-mouse IgG-HRP conjugate, for 2 hours at room temperature on a shaker. Staining of the cells was achieved by adding 75  $\mu$ l/well of a ready-to-use liquid peroxidase substrate solution, containing 3,3',5,5'-tetramethylbenzidine (TMB, Sigma). After approximately 10 minutes the colour reaction was stopped by adding 50  $\mu$ l 0.5 M H<sub>2</sub>SO<sub>4</sub> per well. Aliquots were transferred to a new 96-well plate and absorbance was measured at 450 nm.

## 2.6 Statistical analysis.

All data were analysed with Graphpad Prism 3.0. Statistical analysis was carried out by Student's *t*-test. P-values < 0.05 were considered to indicate a significant difference.

### 3 Results

#### 3.1 Competitive ligand binding assay

EC<sub>50</sub> values for binding to the ER of metabolite mixtures of BaP and CHN and their individual hydroxylated metabolites were determined by radioligand receptor binding assays, using ER from sheep uterus cytosol and radiolabeled estradiol.

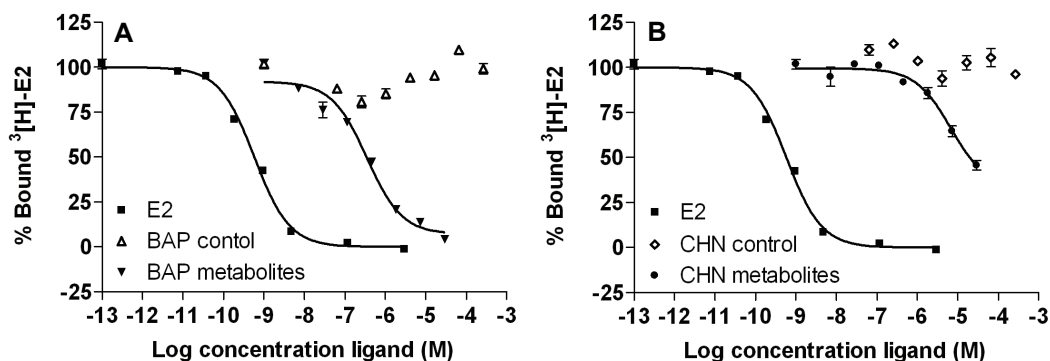


**Figure 2:** Displacement of [<sup>3</sup>H]-E2 from ER from sheep uterus cytosol by unlabeled E2 (■), control incubations (open symbols), and by 45 minutes incubations of 250 μM BaP (in **A**) and 250 μM CHN (in **B**) with BNF-induced microsomes (closed symbols). Concentration E2 is shown in M. The concentrations of CHN, BaP (t=0) and their metabolite mixtures (t=45) are based on the initial concentration of the parent compound in the incubation, after extraction and resolution, in M. Shown is a typical experiment of three independent experiments. Each point represents the mean of duplicate incubations. The bars indicate the higher and lower values.

Test concentrations up to 30 mM of PAH metabolites were used to obtain complete sigmoidal competition curves for EC<sub>50</sub> calculation. E2 displaced radiolabeled E2 with an EC<sub>50</sub> value of 0.4 ± 0.05 nM (mean ± SEM; n= 10). Non-metabolised BaP and CHN did not compete with radiolabeled estradiol for binding to the ER (Table 1).

Metabolite mixtures isolated from rat liver microsomal incubations of BaP and CHN (with NADPH) showed more affinity for the ER than the respective parent compounds or the control incubations (Figure 2), suggesting that BaP- and CHN-metabolites, formed by P450 enzyme activity, have a higher affinity for the ER than BaP and CHN themselves. The HPLC-diagrams in Figures 3A and 3B show that significant amounts of metabolites are present in

extracts from incubations with rat liver microsomes. Based on the retention times of individual hydroxylated reference metabolites, some metabolites *viz.*, 3-OH-BaP, 7,8-dihydroxy-BaP, 1-OH-CHN, 3-OH-CHN and 1,2-dihydroxy-CHN could be identified (Figure 3), but no complete analysis was performed on the extracts.

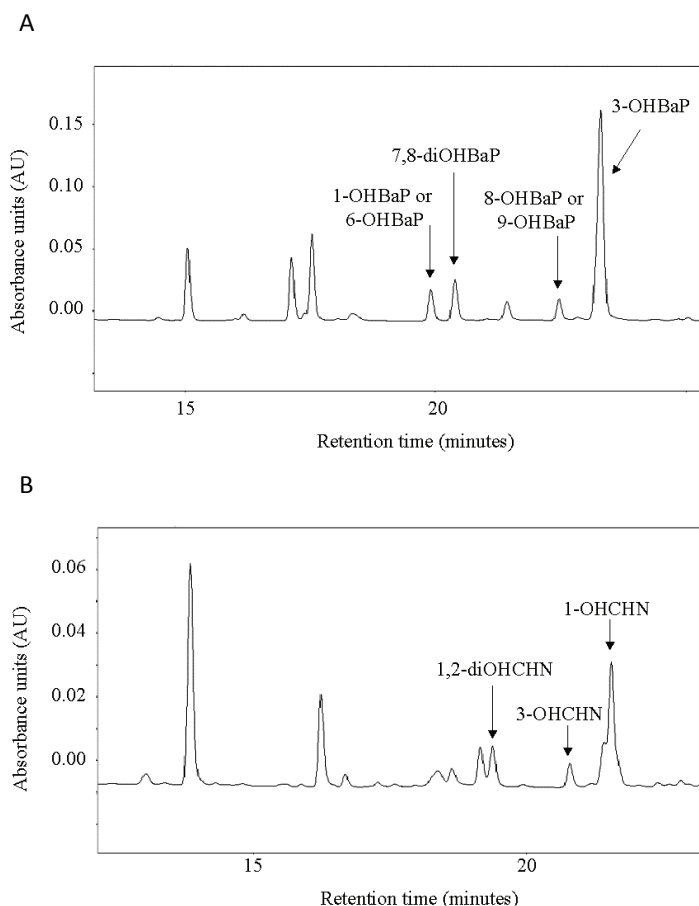


**Figure 3:** Representative HPLC-chromatogram of diisopropyl extracts after 0 ( $t = 0$ , bottom trace) and 45 minutes ( $t = 45$ , upper trace) of BNF-induced rat liver microsomal incubation of 250  $\mu\text{M}$  BaP (in **A**, above) and 250  $\mu\text{M}$  CHN (in **B**, below). The chromatograms of  $t = 0$  minutes (bottom trace) have been lowered 0.01 absorption units, for better visualization. Incubations without NADPH showed similar chromatograms as  $t=0$  minutes (not shown). Designated metabolites were identified based on the retention times of individual hydroxylated reference metabolites and control (0 minutes) incubations.

**Table 1**

Compound	Binding Affinity		E-screen		ER-Calux	
	EC <sub>50</sub> (M)	SEM (M)	EC <sub>50</sub> (M)	SEM(M)	EC <sub>50</sub> (M)	SEM (M)
E2	3.95 *10 <sup>-10</sup>	0.5 *10 <sup>-10</sup>	1.08 *10 <sup>-11</sup>	0.4 *10 <sup>-11</sup>	1.03 *10 <sup>-11</sup>	0.1 *10 <sup>-11</sup>
BaP	n.a.		tox		9.21*10 <sup>-6</sup>	3.3 *10 <sup>-6</sup>
1-OH-BaP	1.62 *10 <sup>-5</sup>	0.4 *10 <sup>-5</sup>	n.a.		n.a.	
2-OH-BaP	3.40 *10 <sup>-6</sup>	0.5 *10 <sup>-6</sup>	E <sub>max</sub> 10% at 3 *10 <sup>-7</sup>		2.10 *10 <sup>-6</sup>	0.7 *10 <sup>-6</sup>
3-OH-BaP	1.08 *10 <sup>-6</sup>	0.5 *10 <sup>-6</sup>	E <sub>max</sub> 40% at 3 *10 <sup>-6</sup>		2.09 *10 <sup>-7</sup>	0.7 *10 <sup>-7</sup>
4-OH-BaP	n.a.		tox		n.a.	
5-OH-BaP	n.a.		n.a.		n.a.	
6-OH-BaP	n.a.		tox		n.a.	
7-OH-BaP	5.25 *10 <sup>-5</sup>	0.2 *10 <sup>-5</sup>	n.a.		3.25 *10 <sup>-6</sup>	0.9 *10 <sup>-6</sup>
8-OH-BaP	1.86 *10 <sup>-6</sup>	0.3 *10 <sup>-6</sup>	E <sub>max</sub> 30% at 3 *10 <sup>-6</sup>		2.62 *10 <sup>-7</sup>	0.6 *10 <sup>-7</sup>
9-OH-BaP	1.01 *10 <sup>-5</sup>	0.2 *10 <sup>-5</sup>	E <sub>max</sub> 40% at 9 *10 <sup>-7</sup>		4.71*10 <sup>-8</sup>	1.6 *10 <sup>-8</sup>
10-OH-BaP	1.48 *10 <sup>-4</sup>	0.4 *10 <sup>-4</sup>	n.a.		n.a.	
11-OH-BaP	n.a.		tox		n.a.	
12-OH-BaP	n.a.		tox		n.a.	
7,8-OH-BaP	1.44 *10 <sup>-5</sup>	0.8 *10 <sup>-5</sup>	tox		n.a.	
7,8-OH-H <sub>2</sub> BaP	n.a.		tox		n.a.	
CHN	n.a.		n.a.		n.a.	
1-OH-CHN	2.64 *10 <sup>-5</sup>	2.4 *10 <sup>-5</sup>	n.a.		1.72 *10 <sup>-6</sup>	0.2 *10 <sup>-6</sup>
2-OH-CHN	6.27 *10 <sup>-7</sup>	3.1 *10 <sup>-7</sup>	1.17 *10 <sup>-6</sup>	0.4 *10 <sup>-6</sup>	3.15 *10 <sup>-7</sup>	0.9 *10 <sup>-7</sup>
3-OH-CHN	4.02 *10 <sup>-6</sup>	1.3 *10 <sup>-6</sup>	4.92 *10 <sup>-6</sup>	1.5 *10 <sup>-6</sup>	1.10 *10 <sup>-6</sup>	0.1 *10 <sup>-6</sup>
4-OH-CHN	n.a.		n.a.		n.a.	
5-OH-CHN	n.a.		n.a.		n.a.	
6-OH-CHN	n.a.		n.a.		n.a.	
1,2-OH-CHN	8.77 *10 <sup>-7</sup>	0.8 *10 <sup>-7</sup>	n.a.		n.a.	

*n.a.* = no affinity or no activity

*tox* = toxic for cells

*E<sub>max</sub>* = maximal effect in %, compared to 1 nM E2

**Table 1:** ER binding affinity and estrogenic activities of BaP, CHN and hydroxylated metabolites. EC<sub>50</sub> values in mol/L (M) for BaP, CHN and their hydroxylated metabolites in the ER binding assay, the E-screen and the ER-Calux assay. Mean EC<sub>50</sub> values are based on at least three independent measurements ± standard error of the mean (SEM). Compounds showing no affinity (*n.a.*) in the ER binding assay, did not show any effect at the highest concentration tested, i.e. 30 mM. Compounds showing no activity (*n.a.*) in the E-screen assay or the ER-Calux assay, did not show any effect at the highest concentration tested, i.e. 10 μM. Specific details concerning toxicity (*tox*) are described in the Results section. For several hydroxylated BaP-metabolites, maximal effects (*E<sub>max</sub>*) were observed in the E-screen at the given concentrations (expressed as % of the maximal effect of E2). Higher concentrations of these compounds resulted in toxicity and lower effects.

No ER affinity was found for 4-OH-BaP, 5-OH-BaP, 6-OH-BaP, 11-OH-BaP, 12-OH-BaP and trans-7,8-OH-H<sub>2</sub>BaP (Table 1). The other BaP metabolites competed with radiolabeled E2 for binding to the ER with EC<sub>50</sub> values ranging from  $1.5 \times 10^{-4}$  M to  $1.1 \times 10^{-6}$  M, in the following order of affinity: 3-OH-BaP > 8-OH-BaP > 2-OH-BaP > 9-OH-BaP > 7,8-OH-BaP > 1-OH-BaP > 7-OH-BaP > 10-OH-BaP. EC<sub>50</sub> values were calculated from at least three separate experiments, and are summarised in Table 1.

Also mono- and dihydroxylated CHN metabolites were tested for affinity for the ER. In general, hydroxylated CHN metabolites showed a higher affinity than the hydroxylated BaP metabolites. 1-OH-CHN, 2-OH-CHN and 3-OH-CHN and 1,2-OH-CHN displaced radiolabeled E2 with EC<sub>50</sub> values ranging from  $2.6 \times 10^{-5}$  to  $6.3 \times 10^{-7}$  M (Table 1). 4-OH-CHN, 5-OH-CHN and 6-OH-CHN did not show any affinity for the ER in binding assays.

### 3.2 Cell proliferation assay (modified E-screen)

To investigate if the binding of the BaP and CHN metabolites to the ER results in a functional response, we performed a proliferation assay using estrogen responsive T47D cells (modified E-screen assay). E2 induced dose-dependent cell proliferation with an EC<sub>50</sub> value of  $11 \pm 4$  pM (mean  $\pm$  SEM; n = 7). Maximal proliferation was induced by 1 nM E2 and this concentration was used as a reference for 100% effect. After 5 days, the cell number increased about 5-fold by this concentration of E2.

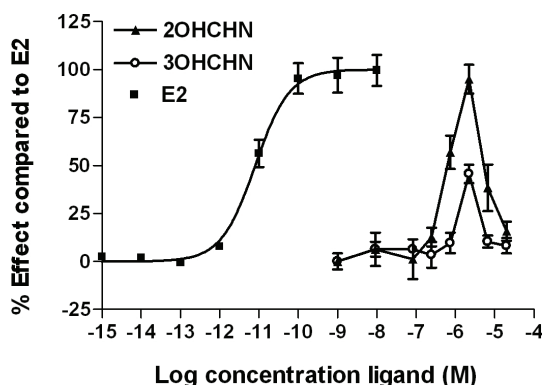


**Figure 4:** Proliferation of T47D cells by E2 (■), 2-OH-CHN (▲) and 3-OH-CHN (○). Cells were pre-incubated with assay-medium for two days, and subsequently exposed to test compounds for 5 days. Shown are representatives of three independent experiments. Each point represents the mean of triplicate incubations  $\pm$  standard error of the mean.

---

None of the BaP metabolites, nor BaP itself induced cell proliferation similar to that observed for E2. However, at concentrations up to 10  $\mu$ M, BaP, 2-OH-BaP, 3-OH-BaP, 8-OH-BaP and 9-OH-BaP induced increases in cell number after 5 days incubation, that ranged from 10 to 40% of the effect observed for E2. At concentrations of 10  $\mu$ M or higher, 2-OH-BaP, 6-OH-BaP, 11-OH-BaP, 12-OH-BaP and 7,8-OH-H<sub>2</sub>BaP decreased the number of cells, when compared to control incubations, indicating toxicity (data not shown). Microscopical observations showed cell detachment and cell disruption at these concentrations. 1-OH-BaP, 4-OH-BaP, 6-OH-BaP, 8-OH-BaP and 9-OH-BaP did not induce nor decrease cell numbers.

At concentrations of 1  $\mu$ M and 30  $\mu$ M, 2-OH-CHN and 3-OH-CHN stimulated proliferation of T47D cells up to 75% and 60 % of the maximal effect of 1 nM E2, respectively (Figure 4). At higher concentrations, no further increase of cell number was observed, probably due to toxicity or other effects of the CHN-metabolites. EC<sub>50</sub> values for 2-OH-CHN and 3-OH-CHN, calculated based on partial sigmoidal dose-response curves, were 1.2  $\mu$ M for 2-OH-CHN and 4.9  $\mu$ M for 3-OH-CHN, respectively (Table 1). CHN, 1-OH-CHN, 4-OH-CHN, 5-OH-CHN, 6-OH-CHN and 1,2-OH-CHN did not exert any effect on proliferation of T47D cells.

### 3.3 ER-Calux assay

#### *Estrogenic effects of BaP and its hydroxylated metabolites in the ER-Calux*

The estrogenic activity of BaP and its hydroxylated metabolites was also investigated using stably transfected T47D cells, expressing luciferase activity upon activation of the ER. Maximal response of E2 was observed at 100 pM and this concentration was used as a reference for 100% effect. An E2 concentration-effect curve was included in triplicate on each plate. The EC<sub>50</sub> value for E2 was 10  $\pm$  1.5 pM (mean  $\pm$  SEM; n=15).

BaP and several hydroxylated metabolites showed estrogenic activity in the following order: 9-OH-BaP > 8-OH-BaP > 3-OH-BaP > 2-OH-BaP > BaP > 7-OH-BaP (Figure 5). EC<sub>50</sub> values ranged from 1 nM to 10  $\mu$ M (Table 1). 1-OH-BaP, 4-OH-BaP, 5-OH-BaP, 6-OH-BaP, 10-OH-BaP, 11-OH-BaP, 12-OH-BaP, 7,8-OH-BaP and 7,8-OH-H<sub>2</sub>BaP did not induce an estrogenic response. 2-OH-BaP and 9-OH-BaP produced greater maximal response of luciferase signalling than E2, i.e. 145% and 170% respectively (Figure 5).

Since the estrogenic effects of BaP in the ER-Calux are likely due to cytochrome P450-mediated metabolism to hydroxylated metabolites, BaP was incubated simultaneously with furafylline (FUR), a selective inhibitor of CYP1A2. The presence of 3  $\mu$ M FUR in the microsomal incubation, however, potentiated estrogenic activity (EC<sub>50</sub>) of BaP (Figure 6): its EC<sub>50</sub> value was reduced from 2.7  $\mu$ M to 60 nM. 3  $\mu$ M FUR alone did not have any effect on luciferase expression in T47D cells (data not shown).

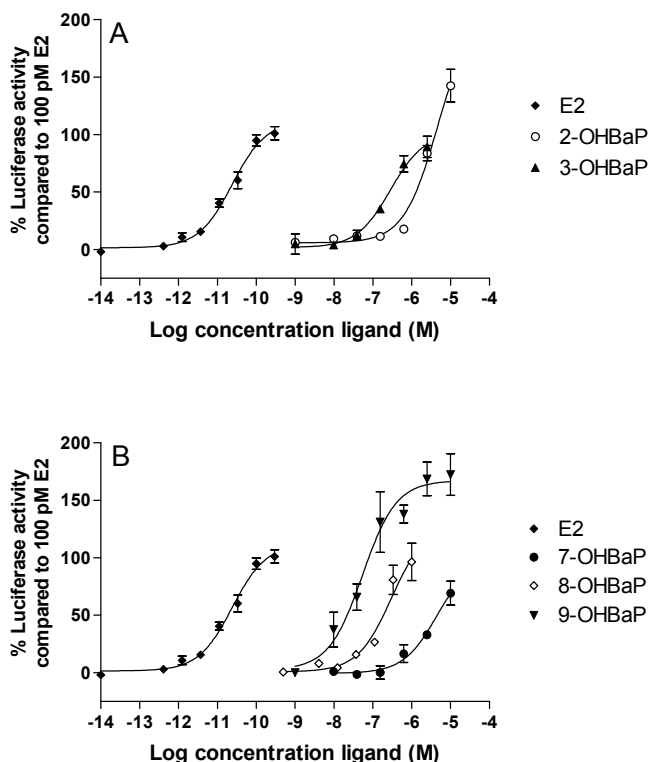


**Figure 5:** Estrogenic activity (induction of luciferase activity) of BaP-metabolites in T47D cells. Cells were pre-incubated with assay-medium for two days, and subsequently exposed for 6 hours to E2 (◆), 2-OH-BaP (○) and 3-OH-BaP (■) (A), and E2 (◆), 7-OH-BaP (●), 8-OH-BaP (◇) and 9-OH-BaP (▼) (B). Shown are representatives of three independent experiments. Each point represents the mean of triplicate incubations  $\pm$  standard error of the mean.

To investigate a possible interaction of aryl hydrocarbon receptor (AhR)-activation and metabolism of BaP in the ER-Calux assay, cells were incubated with BaP and 3',4'-dimethoxyflavone (DMF), a known antagonist of the AhR. Although 10  $\mu$ M DMF decreased E2-response to 90%, it completely inhibited all estrogenic activity of BaP (Figure 6). 10  $\mu$ M DMF alone did not have any effect on luciferase expression in T47D cells (data not shown).

#### *Estrogenic effects of hydroxylated CHN metabolites in the ER-Calux*

CHN and all available metabolites were also tested for estrogenicity in the ER-Calux assay. An estrogenic response was observed for 1-OH-CHN, 2-OH-CHN and 3-OH-CHN. 1-OH-CHN and 3-OH-CHN had similar activities, with  $EC_{50}$  values of 1.7  $\mu$ M and 1.1  $\mu$ M, respectively (Table 1 and Figure 7). 2-OH-CHN showed a higher estrogenic activity ( $EC_{50}$  0.32  $\mu$ M). Its maximal response was much higher than that of E2, i.e. 400% (Figure 7).

Such a 'supramaximal' effect was also observed for 2-OH-BaP and 9-OH-BaP (Figure 5), however for 2-OH-CHN it was even more pronounced. With increasing passages of the T47D cell line, the response by 2-OH-CHN diminished, but a 1.5-fold induction compared to 10 nM E2 was still observed after 6 hours incubation at passage number 25. After 24 hours, the response of 2-OH-CHN was 200-300% compared to E2 (data not shown).

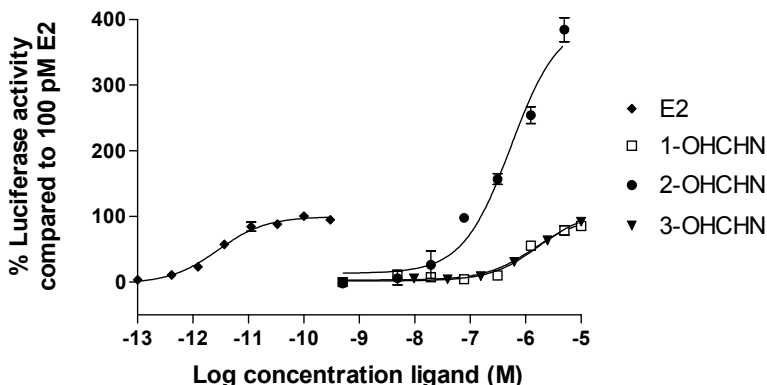


**Figure 6:** Effect of furafylline (FUR) and 3',4'-dimethoxyflavone (DMF) on estrogenic activity (induction of luciferase activity) of BaP in T47D cells. Cells were pre-incubated with assay-medium for two days, and subsequently exposed for 6 hours to E2 (●), BaP (□), BaP with 3 μM FUR (▲), and BaP with 10 μM DMF (◆). The arrow indicates the effects of 3 μM FUR and 10 μM DMF alone. Shown are representatives of three independent experiments. Each point represents the mean of triplicate incubations  $\pm$  standard error of the mean.

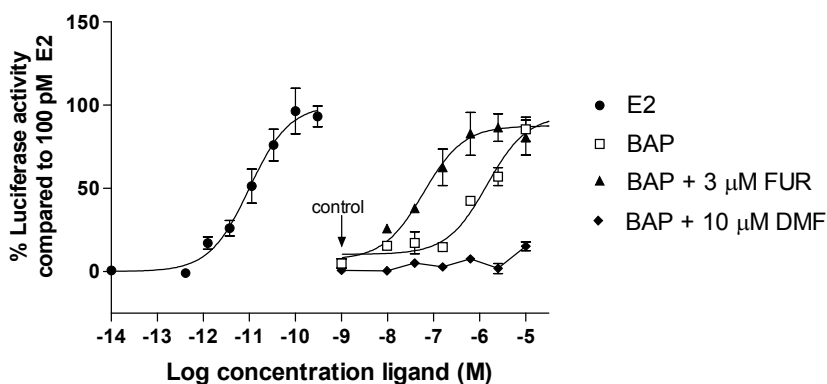


**Figure 7:** Estrogenic activity (induction of luciferase activity) of CHN-metabolites in T47D cells. Cells were pre-incubated with assay-medium for two days, and subsequently exposed for 6 hours to E2 (●), 1-OH-CHN (●), 2-OH-CHN (■), and 3-OH-CHN (□). Shown are representatives of three independent experiments. Each point represents the mean of triplicate incubations  $\pm$  standard error of the mean.

We have investigated whether the supra-maximal effect of 2-OH-CHN was ER-mediated. Co-treatment of 2.5  $\mu$ M 2-OH-CHN with 10 nM of the ER-antagonist ICI187,820 was sufficient to completely block the effects of 100 pM E2 and also the response of 2.5  $\mu$ M 2-OH-CHN in the ER-Calux assay (Figure 8), indicating that the supra-maximal response induced by 2-OH-CHN was entirely ER-mediated.

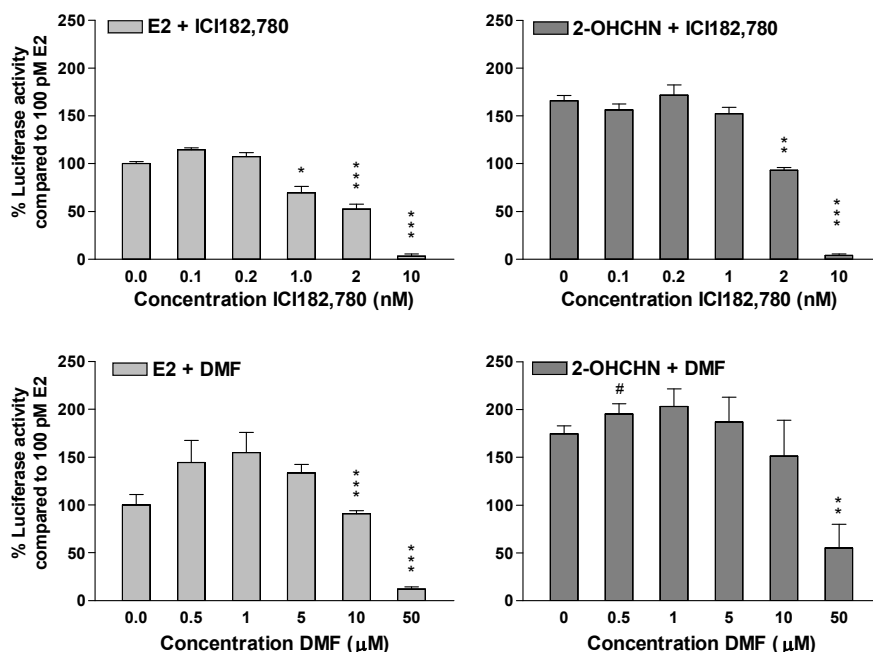


**Figure 8:** Effect of ICI187,820 and 3',4'-dimethoxyflavone (DMF) on estrogenic activity (induction of luciferase activity) in T47D cells. Cells were pre-incubated with assay-medium for two days, and subsequently exposed for 6 hours to 100 pM E2 (left graphs) or 2.5  $\mu$ M 2-OH-CHN (right graphs) alone, and in co-treatment with various concentrations DMF (light gray bars) or ICI187,820 (dark gray bars). Shown are representatives of two independent experiments. Each point represents the mean of triplicate incubations  $\pm$  standard error of the mean. Indicated are effects that were significantly lower than effects in control cells at  $p < 0.05$  (\*),  $p < 0.01$  (\*\*), and  $p < 0.001$  (\*\*\*), and significantly higher than effects in control cells at  $p < 0.05$  (#) (Student's t-test).

Next, we investigated whether the AhR was involved in the supra-maximal response by 2-OH-CHN, by co-incubation with the AhR-antagonist DMF (10  $\mu$ M), a concentration able to completely block the estrogenic effects of BaP, as described earlier this section. DMF only decreased the effect of 2-OH-CHN from 175% to 150%.

The highest concentration tested, 50  $\mu$ M DMF, reduced the effect of 2-OH-CHN to 50% (Figure 8). However, it also reduced the effect of 100 pM E2 to less than 20% of its maximal effect. Hence, DMF was not able to block the supra-maximal effect of 2-OH-CHN,

even at concentrations that significantly interfered with E2 signalling. This suggests that a putative role for the AhR in the increased estrogenic response of 2-OH-CHN can be excluded. Although DMF seemed to diminish the response of E2 at concentrations of 10 and 50  $\mu$ M, it seems to increase the maximal response of E2 and 2-OH-CHN at lower concentrations (Figure 8).

A possible explanation for our data so far may be that 2-OH-CHN, 2-OH-BaP and 9-OH-BaP increase the concentration of ER in the T47D cells. Therefore, an ELISA technique was used to quantify the concentration of ER in T47D cells treated similarly as in the ER-Calux assay. A small but statistically significant increase of ER concentration was observed after 6 hours exposure of the cells to 2.5  $\mu$ M 2-OH-CHN (Figure 9).

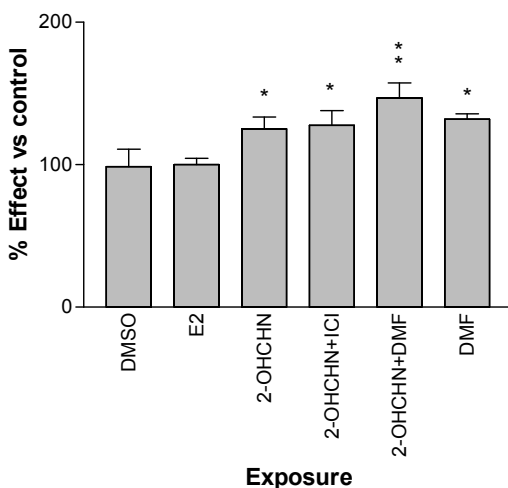


**Figure 9:** Effect of 2-OH-CHN on ER concentration as determined by ELISA. Cells were pre-incubated with assay-medium for two days, and subsequently exposed for 6 hours to DMSO, 100 pM E2, 10  $\mu$ M DMF, 2.5  $\mu$ M 2-OH-CHN, 2.5  $\mu$ M 2-OH-CHN with 10 nM ICI187,820, 2.5  $\mu$ M 2-OH-CHN with 10  $\mu$ M DMF, 2.5  $\mu$ M 2-OH-BAP, 2.5  $\mu$ M 2-OH-BAP with 10 nM ICI187,820 and 2.5  $\mu$ M 2-OH-BAP with 10  $\mu$ M DMF. Shown are representatives of three independent experiments. Each point represents the mean of four incubations  $\pm$  standard error of the mean. Data were considered significantly higher than control cells at  $p < 0.05$  (\*) and  $< 0.01$  (\*\*), and significantly lower than control cells at  $p < 0.01$  (##) (Student's t-test).

Because a large signal was already obtained in control cells that constitutively express the ER, and we had no means to determine what percentage of this signal is specific for the ER, the precise extent of induction of ER concentration by 2-OH-CHN cannot be established from the present ELISA data. Nevertheless, it is clear that 2-OH-CHN has an increasing effect on ER-concentration in these cells (Figure 9). 10  $\mu$ M DMF and 10 nM ICI182,780 could not diminish the increase in ER concentration by 2-OH-CHN.

Interestingly, DMF alone or in combination with 2-OH-CHN, also significantly increased ER-concentration compared to control cells and cells incubated with 2-OH-CHN, respectively (Figure 9).

#### *Estrogenic affinity of mixture of 7 hydroxylated PAH metabolites*

Because very often different hydroxylated metabolites are formed from PAHs and occur in the environment together, a mixture of hydroxylated PAH metabolites was also tested for combined affinity for the ER. A mixture of 7 PAH-metabolites was prepared at equi-effective concentrations (Table 2), i.e. they would all yield the same effect when tested individually. These equi-effective concentrations were based on the  $EC_{50}$  values of the individual PAH-metabolites (Table 1). The mixture of 7 PAH-metabolites clearly showed complete displacement of radiolabeled E2 at high concentrations, resulting in an  $EC_{50}$  value of  $2.9 \times 10^{-6}$  M (Figure 10A). This concentration reflects the total amount of PAH-metabolites present. At this concentration, the calculated effect for each individual compound would be 8%, therefore, based on concentration addition<sup>1</sup>, the predicted effect of the mixture would be 56%, which is in very good agreement with the observed 50% effect (Table 2 and Figure 10B).

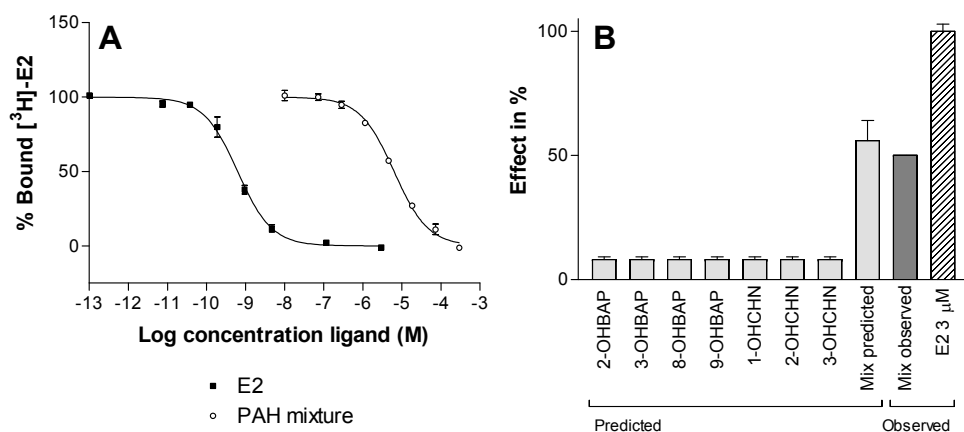


**Figure 10:** **A:** Displacement of [<sup>3</sup>H]-E2 from ER from sheep uterus cytosol by unlabeled E2 (■) and a mixture of equi-effective concentrations of 2-, 3-, 8- and 9-OH-BaP as well as 1-, 2- and 3-OH-CHN (○). The concentration on the x-axis represents the combined total concentration of all metabolites in the mixture. Shown are representatives of two independent experiments. Each point represents the mean of duplicate incubations. The bars indicate the higher and lower values. **B:** Predicted effect of the individual compounds at concentrations as present in the mixture that shows 50% displacement of [<sup>3</sup>H]-E2. Also indicated are the predicted effect of the total mixture (light gray bar), the observed effect (black bar) and the maximal effect of 3 μM E2 (hatched bar). Bars represent higher and lower values. See text for further details.

---

## 4 Discussion

### 4.1 *Formation of estrogenic PAH metabolites by CYP activity and estrogenic properties of metabolites*

As shown by our rat liver microsomal experiments, BaP and CHN metabolism by CYP enzymes in rat liver microsomes leads to the formation of estrogenic metabolites. We did not perform extended structural analysis, but we have shown by HPLC analysis that at least several hydroxylated BaP and CHN metabolites were formed, namely 1-OH-BaP or 6-OH-BaP, 3-OH-BaP, 8-OH-BaP or 9-OH-BaP, 7,8-dihydroxy-BaP, 1-OH-CHN, 3-OH-CHN and 1,2-dihydroxy-CHN. Subsequently, we tested all possible mono-hydroxylated and several dihydroxylated metabolites for estrogenicity in a radioligand binding assay. In general, 3-OH-BaP and 9-OH-BaP are the most estrogenic metabolites of BaP, followed by 8-OH-BaP, 2-OH-BaP and 7-OH-BaP. 3-OH-BaP and 9-OH-BaP are the major products of BaP-metabolism by rat liver CYP enzymes, and have been observed in various species<sup>[53,236]</sup>, but also the 1- and 7-OH-BaP have been identified<sup>[237,238]</sup>. One of the most estrogenic metabolites, 2-OH-BaP however, has never been observed in CYP-mediated metabolism studies with BaP.

Another major metabolite of CYP-mediated BaP bio-activation is 7,8-OH-H<sub>2</sub>BaP. Further oxidation of this metabolite results in the carcinogenic BaP-7,8-dihydrodiol-9,10-diolepoxide (BPDE)<sup>[239]</sup>. 7,8-OH-H<sub>2</sub>BaP did not show any estrogenic activity in our studies, and this is explained by the fact that along with planarity the aromaticity is lost in the ring with the two hydroxyl-groups, both are features required for binding to the ER<sup>[147]</sup>.

Small differences were observed between the results from the ER binding assay and the ER-Calux. The ER-Calux is more sensitive than the binding assay, however, metabolism and toxicity may modify ER-signaling. This may explain why 1-OH-BaP and 10-OH-BaP, although possessing low ER binding affinity, did not show activity in the ER-Calux assay. The di-hydroxylated PAH metabolites were also not active in the ER-Calux, probably due to toxicity of these catechols.

The CHN-metabolites 2-OH-CHN and 1,2-OH-CHN exhibited higher affinity and activity than 1- or 3-OH-CHN. In general, the hydroxylated metabolites of CHN showed higher binding affinities and estrogenic activities than the BaP-metabolites. This may be explained by the presence of an 'extra' aromatic ring in BaP, which may cause some sterical hindrance during binding. Compared to the BaP structure, the CHN molecular skeleton better resembles the E2 structure.

Our present data on the estrogenicity of BaP and CHN metabolites correspond very well with a model in which the hydroxyl groups of the various PAH metabolites may form similar hydrogen bonds with Glu353, Arg394 and His524 of the ER when their skeletons overlap with that of estradiol. These interactions are known to be very important for binding to the ER<sup>[147]</sup>. We have recently confirmed this by molecular dynamics simulations and found that indeed the PAH metabolites bind to the ER $\alpha$  via hydrogen bonding<sup>[149]</sup>. The metabolites, however, only possess one hydroxyl group, and this probably explains their lower affinities compared to E2. Hirose et al.<sup>[220]</sup> very recently published a study on (anti)-estrogenic activities of mono-hydroxylated BaP-metabolites, but reported no EC<sub>50</sub> values. They state that except for 5-OH-BaP, all metabolites exhibit estrogenic affinity for ER $\alpha$  and ER $\beta$ . This is not in accordance with our data. It is also not consistent with the available (Q)SAR data that indicate the importance of the position of the hydroxyl-moieties for interaction with the ER. Probably, 4-, 5-, 6-, 11- and 12-OH-BaP cannot achieve such an interaction.

All assays studied here contain both subtypes of the ER, namely  $\alpha$  and  $\beta$ , although ER $\alpha$  is most abundant and predominantly expressed<sup>[240]</sup>. Theoretically, the presence of two types of receptors may result in a biphasic dose-response curve if the affinities of a ligand for the two receptors are different. This is clearly not true for the ER ligands studied here, because mono-phase curves were obtained. The binding assay was performed with ER from sheep cytosol, while human ER was present in the E-screen and the ER-Calux. Binding affinities observed for many ligands towards sheep ER, such as E2, DES and genistein (van Lipzig, unpublished results), were in excellent correspondence with values for binding to human ER $\alpha$  from literature<sup>[147,241]</sup>. Specific regions in human and sheep ER, responsible for DNA binding, hormone binding, phosphorylation, nuclear localization and transcription activation are highly conserved between mammalian ERs. In particular, sheep ER $\alpha$  DNA binding domain (DBD) shows 100% similarity with human ER $\alpha$ , and the ligand binding domains (LBD) shows 96.8% identity<sup>[242]</sup>. Thus, we conclude that the use of the ER from sheep uterus cytosol is appropriate for correlation with human ER studies.

#### 4.2 ER binding affinity of PAH metabolite mixture: 'concentration addition'

Exposure to PAH occurs by e.g. cigarette smoking, diet, environmental pollution, during daily life as well as by occupation. It involves exposure to many different PAHs and after uptake, also to complex mixtures of their metabolites. We therefore investigated the joint effect of a mixture of low affinity estrogenic mono-hydroxylated PAH metabolites in the current study. Kortenkamp *et al.*<sup>[243]</sup> already showed that for a number of estrogenic compounds, their combined effect could be explained by 'concentration addition'. This

concept is based on similar action of the mixture components, and 'concentration addition' is generally used to explain their joint effect. Here, we show that for a mixture of 7 PAH metabolites with weak estrogenic activities, this concept is also applicable (see<sup>[243]</sup> for a discussion of the concept of concentration addition and independent action). Exposure to the individual components at concentrations as present in a mixture that shows 50% displacement of E2, would theoretically result in only 8.0% displacement of E2 by the individual components of the mixture. The predicted joint effect according to the 'concentration addition' principle would be 56%, very close to the observed 50% effect. The presented results show that mixtures of weakly estrogenic PAH metabolites in fact induce significant estrogenic effects. Hence, while the risk from exposure to individual weak estrogenic compounds seems negligible, combined they may disrupt hormone regulation in humans and wildlife. This is the first study to show such a combination effect for hydroxylated PAH metabolites on the ER.

**Table 2**

Compound	Concentration ( $\mu$ M)	Effect (%)
E2	3.00	100.0
2-OH-BAP	0.33	7.98
3-OH-BAP	0.10	7.98
8-OH-BAP	0.18	7.98
9-OH-BAP	0.98	7.98
1-OH-CHN	2.56	7.98
2-OH-CHN	0.06	7.98
3-OH-CHN	0.39	7.98
Total Mix	4.60	Predicted: 55.9 Observed: 50.0

**Table 2:** Mixture experiment, with corresponding concentrations in the total mixture in  $\mu$ M, the total mixture concentration, the predicted effect of the individual compounds and the total mixture, and the observed effect of the total mixture, expressed as % of the maximal effect of E2.

#### 4.3 Role of CYP enzymes and AhR in the Estrogenicity of BaP

PAHs such as BaP have been found to activate the AhR, a transcription factor that among others, may induce CYP enzymes involved in BaP metabolism<sup>[86,244]</sup> and that may inhibit ER-signaling by receptor down-regulation<sup>[229,230]</sup>. T47D cells used for the ER-Calux assay, also express the AhR,<sup>[230,245]</sup>. Therefore, we investigated if the estrogenic activity of BaP

observed in the ER-Calux assay, is (partially) dependent on BaP-induced AhR activation, and subsequent induction of CYP enzymes.

Firstly, we blocked CYP1A2 activity with a specific inhibitor, furafylline (FUR). FUR increased the estrogenic activity in T47D cells 15-fold. Probably, CYP1A2 is not the only enzyme involved in the bio-activation of BaP into estrogenic metabolites and blocking its activity may lead to an increased activity of BaP by other CYP iso-enzymes, such as CYP1A1 and 1B1<sup>[86]</sup>.

Secondly, we investigated the role of the AhR in the estrogenic activity of BaP, using the AhR-antagonist DMF<sup>[245]</sup>. Although 10  $\mu$ M DMF reduced the effect of E2 by 10%, it completely reduced the estrogenic response of BaP. Hence the estrogenicity of BaP in the ER-Calux assay most likely is due to induction of BaP-metabolising enzymes CYP1A1 and 1B1 by AhR activation. As yet, AhR-agonists were known for their anti-estrogenic activities<sup>[209,229]</sup>. On the other hand, susceptibility to PAHs has been attributed to simultaneous expression of ER and AhR<sup>[246]</sup>. Recently, it has been shown that AhR-agonists induce recruitment of un-liganded ER, invoking estrogenic responses<sup>[247]</sup>. Our present results also indicate that AhR-agonists should not explicitly be regarded as anti-estrogens because they may increase estrogenicity of PAHs by enhancing their metabolism to estrogenic metabolites.

#### 4.4 *Supra-maximal estrogenic activity of 2-OH-CHN in ER-Calux*

In the ER-Calux cells, 2-OH-CHN very remarkably increased maximal luciferase activity up to 400%, compared to the maximal effect of E2. The effect was also observed for 2-OH-BaP and 9-OH-BaP, however much less distinct. The effects were further investigated using 2-OH-CHN, and we showed that it was entirely ER-mediated, since the response was completely blocked by the ER-antagonist ICI182,780. The results from the ELISA experiments show that the supramaximal effect may be due to up-regulation of the ER concentration by 2-OH-CHN. ER mRNA and protein levels have been shown to be regulated by estrogens in T47D cells, although the exact mechanisms are still unclear<sup>[248,249]</sup>.

A possible role of the AhR in this effect was investigated with the AhR-antagonist DMF. 10  $\mu$ M DMF could not block the effects of 2-OH-CHN, although this concentration DMF was sufficiently high to block the AhR in experiments with BaP. At a higher concentration (50  $\mu$ M) DMF partially reduced the estrogenic response. However, this concentration probably is toxic because it dramatically decreased the E2 response. Lower concentrations of DMF (0.5-5  $\mu$ M) even increased luciferase activity, induced by 100 pM E2 or 2.5  $\mu$ M 2-OH-CHN. This may be explained by AhR mediated down-regulation of nuclear ER concentration<sup>[229,230]</sup>, as well as a reduction of ER-dependent transcriptional activity<sup>[250]</sup>. It

---

is presumed that some degree of activation of AhR normally occurs by an endogenous ligand<sup>[251]</sup>. Blockage of the AhR by DMF may, therefore, inhibit constitutive AhR-activation<sup>[252]</sup>, and consequently, AhR-inhibited ER expression is alleviated, resulting in higher ER concentrations or enhanced ER transcriptional activity. This explanation is in good agreement with the results from the ELISA experiments that show ER up-regulation by DMF. Supra-maximal estrogenic responses have been observed before, to some extent for 3-OH-BaP (160%)<sup>[53]</sup>, and resveratrol (400%)<sup>[253]</sup>. In the latter, the authors suggested that the effects may be related to cell types under investigation, and to transcriptional coactivators and corepressors. The supramaximal effect of 2-OH-CHN however, seems (at least partially) rather be due to higher expression of the ER itself.

## 5 Conclusions

Our studies indicate that next to binding to the ER, compounds may be endocrine disruptors via modulation of ER expression (2-OH-CHN), or by inhibiting AhR-mediated pathways (DMF). Furthermore, risk assessment for endocrine disruption by environmentally relevant compounds, such as PAHs, should involve metabolism studies, as well as studies focusing on joint action of combinations of PAH metabolites. Neglecting combination effects and bio-activation through biotransformation may lead to underestimation of health risks of this kind of compounds.

## Acknowledgements

We gratefully acknowledge Dr Freek Ariese, Department of Analytical Chemistry and Applied Spectroscopy, Vrije Universiteit Amsterdam, for providing several pure hydroxylated BaP-metabolites.

## Chapter 3

### Bioactivation of di-brominated biphenyls to estrogenic metabolites by cytochrome P450 activity to Metabolites with Estrogenic Activity and Estrogen Sulfotransferase Inhibition Capacity

Marola M.H. van Lipzig, Jan N.M. Commandeur, Frans J.J. de Kanter, Micaela C. Damsten, Nico P.E. Vermeulen, Evelina Maat, Ed J. Groot, Abraham Brouwer, Monique H.A. Kester, Theo J. Visser and John H.N. Meerman.

Chemical Research in Toxicology, 2005 (18), 1691-700.

---

## ABSTRACT

Exposure of humans and wildlife to xenobiotics, such as halogenated biphenyls, that interfere with the endogenous estrogen balance may lead to endocrine disruption. Such compounds may either mimic or block estradiol's action by agonistic or antagonistic action, respectively. They may also affect endogenous estradiol concentrations by induction or inhibition of enzymes that metabolise estradiol.

In the present study, we demonstrate that estrogenic metabolites of two brominated biphenyls, 2,2'-dibromobiphenyl (2,2'-DBB) and 4,4'-dibromobiphenyl (4,4'-DBB), are formed by rat liver microsomal cytochrome P450 (CYP) activity. Bioactivation of 2,2'-DBB and 4,4'-DBB yielded various mono- and di-hydroxylated bromobiphenyl metabolites which were collected by preparative HPLC and analysed by LC/MS. Several of the metabolites bound to the estrogen receptor (ER), activated the ER and inhibited human estrogen sulfotransferase (hEST). Seven mono-hydroxylated metabolites were positively identified using synthetic mono-hydroxylated reference compounds. These synthetic mono-hydroxylated bromobiphenyls also bound to and activated the ER and inhibited hEST. The highest ER affinity was observed for 4-OH-2,2'-DBB, with an  $EC_{50}$  of 6.6 nM. The highest ER activation was observed for 4-OH-3,4'-DBB ( $EC_{50}$  of 74 nM) while 4-OH-4'-DBB and 4-OH-2,2'-DBB induced a supra-maximal (compared to estradiol) ER activation. The strongest hEST inhibition was found with 4-OH-3,4'-DBB ( $EC_{50}$  of 40 nM).

In conclusion, we show that two di-brominated biphenyls are bioactivated by CYP activity into very potent estrogenic metabolites and inhibitors of hEST. These findings are of vital importance for accurate risk assessment of exposure to environmental contaminants, such as halogenated biphenyls. Neglecting bio-activation through biotransformation will lead to underestimation of health risks of this class of xenobiotics.

## 1 Introduction

Exposure to environmental estrogens has been proposed as a risk factor for disruption of reproductive development and tumorigenesis of humans and wildlife<sup>[4]</sup>. Estrogens play a crucial role in the development, growth and regulation of sexual and reproductive organs and behavior<sup>[2]</sup>. Estrogens act via binding to estrogen receptors (ER), members of the nuclear receptor superfamily, that function as transcription factors to modulate gene expression in a ligand-dependent manner<sup>[142]</sup>. In the nucleus, binding of ligands induces a conformational change of the ER, enabling the receptor to dimerise. The dimer binds to the palindrome estrogen response elements (ERE) in DNA, where it enhances gene transcription leading to e.g. protein synthesis and cell proliferation<sup>[134]</sup>. Two ER isoforms have been identified, ER $\alpha$  and ER $\beta$ , that show different tissue expression and distinct ligand binding properties<sup>[109]</sup>.

In the last decades, a wide variety of structurally diverse environmental compounds have been identified as endocrine disruptors. Among these compounds are natural steroid hormones, pharmaceuticals, industrial chemicals including pesticides, plasticizers, polycyclic aromatic hydrocarbons (PAHs) and polyhalogenated biphenyls (PHBs). PHBs have been used for a variety of industrial purposes, such as organic solvents, pesticides, plasticizers, cutting oils, flame retardants, dielectrics in large volume transformers and capacitors, hydraulic fluids, adhesives and ink<sup>[254]</sup>. Their high chemical stability and low biodegradability seemed valuable, however, these very physical properties resulted in persistence in the environment and ubiquitous bioaccumulation<sup>[255]</sup>. Polybrominated biphenyls (PBBs) were mainly used during the early 1970s as flame retardants (e.g. Firemaster BP-6 and FF-1). They were used at relatively high concentrations in electronic equipment such as computers and television sets, in textiles, cars and in many other applications. Polychlorinated biphenyls (PCBs) and PBBs have been banned from most of above-mentioned applications, but widespread contamination remains a threat for wildlife and humans. This is illustrated by the recent finding that polybrominated biphenyls (PBBs) are present in sperm whales, which normally stay and feed in deep water, indicating that these compounds have reached deep ocean waters<sup>[256]</sup>.

Estrogenic endocrine disruptors may either mimic estradiol's action by agonistic action, or block the ER by antagonizing it. In addition, disturbance of endogenous estradiol concentrations in cells by induction or inhibition of enzymes involved in estrogen (de-)activation may have a significant effect on regular hormone homeostasis. In addition to

---

their ability to bind to the estrogen receptor, it has been shown that some hydroxylated PCB metabolites are very potent inhibitors of human estrogen sulfotransferase (hEST)<sup>[99]</sup>, with higher hEST binding affinities than ER binding affinities. Sulfotransferases are cytosolic phase II biotransformation enzymes, that play an important role in the inactivation of estrogens<sup>[97,98]</sup>. By inhibiting the sulfation of e.g. the endogenous estrogen 17 $\beta$ -estradiol (E2), the hydroxylated PCBs may increase E2 bio-availability in target tissues, thereby exerting an indirect estrogenic effect, which may be more important than their estrogenic activities via the ER<sup>[99]</sup>. Less directly, compounds may also influence receptor concentration, e.g. by altering ER transcription, thereby also disturbing regular hormone balance<sup>[257]</sup>.

Animal studies showed that exposure to PHBs may result, among others, in immunotoxicity, hepatotoxicity and carcinogenicity<sup>[5,258]</sup>. Initially, research focused on the bioaccumulation and toxicity of un-metabolised PHBs. In recent years, the focus has shifted more towards the adverse effects of the metabolites of PHB<sup>[99,259,260]</sup>. Despite their high chemical inertness, PHBs are substrates for various enzymes. Bio-activation mainly occurs via enzymes of the cytochrome P450 (CYP) family. The most important products of CYP-mediated metabolism of PHBs are mono- and di-hydroxy metabolites and dihydrodiols. Further metabolism of the hydroxylated PHBs involves glucuronidation, glutathione conjugation and formation of methylsulfone metabolites<sup>[261]</sup>. Estrogenic effects of PCBs or PCB mixtures (e.g. Aroclor) have been observed *in vitro* in cells<sup>[74]</sup>, and *in vivo*, such as the capacity of increasing uterine wet weight<sup>[1,75-77]</sup>. However, it remains unclear whether estrogenic effects in cells, tissues or whole animals are induced by the parent compounds, which generally show very low affinity for the estrogen receptor, or by metabolites<sup>[1,75,77]</sup>.

Several studies demonstrated the estrogenic properties of hydroxylated PCB metabolites. Non-hydroxylated chlorinated biphenyls showed no affinity for the ER, however, the introduction of a hydroxyl group leads to a strong increase of estrogenic activity of the PHB metabolites<sup>[176,262,263]</sup>. This is in accordance with the structural requirements of an estrogen. The published crystal structures of the ER complexed with the endogenous estrogen 17 $\beta$ -estradiol (E2) and the synthetic hormone DES, have elucidated that ligands bind in a hydrophobic cavity, deeply buried within the receptor. The aromatic ring of E2 occupies the narrow part of binding cavity, while the remainder of the binding cavity is more tolerant for lipophilic substituents, and may accommodate large atoms like chlorine or bromine substituents of the halogenated biphenyls. The hydrogen bonding properties of the hydroxyl groups of E2 contribute significantly to the binding affinity of a ligand. Therefore, a hydroxyl group introduced at an appropriate position by CYP-mediated

metabolism of halogenated biphenyls may play an important role in the formation of estrogenic metabolites.

The toxicology and biological activities of chlorinated biphenyls and their metabolites have been studied to a much larger extent than brominated biphenyls. Due to their structural resemblance, the toxic effects of chlorinated and brominated biphenyls are considered to be quite similar<sup>[264]</sup>. Therefore, we have investigated the CYP catalyzed formation of estrogenic metabolites of two di-brominated biphenyls, namely 2,2'-dibromobiphenyl (2,2'-DBB) and 4,4'-dibromobiphenyl (4,4'-DBB), by rat liver microsomal CYPs. Due to their low degree of halogenation, these compounds are good candidates for CYP mediated metabolism, whereas higher brominated biphenyls are very persistent. Estrogenic activity of metabolites was determined by investigating ER binding affinity and estrogenic activity in the ER-Calux<sup>®</sup> reporter-gene assay. Inhibition of human sulfotransferase activity was also investigated. In addition, we employed a recently published computational linear interaction energy (LIE) model for accurate prediction of absolute ligand binding affinities for binding to the ER $\alpha$ <sup>[149]</sup>. The model was used to predict the binding affinities of four di-hydroxylated bromobiphenyls.

## 2 Methods

### 2.1 Chemicals

17 $\beta$ -Estradiol (E2), 4-hydroxy-4'-bromobiphenyl (4-OH-4'-MBB) and 3'-phosphoadenosine-5'-phosphosulfate (PAPS) were obtained from Sigma Chemical co, (St. Louis, MO, U.S.A). [<sup>3</sup>H]-E2 was obtained from Amersham (Buckinghamshire, UK). NADPH was obtained from AppliChem GmbH (Darmstadt, Germany). 2,2'-DBB was purchased from ICN pharmaceuticals (Costa Mesa, CA, USA) and 4,4'-DBB from Fluka AG (Buchs, Switzerland). Dextran (MW 60.000-90.000) was obtained from Duchefa (Haarlem, the Netherlands). All other chemicals were of analytical grade and purchased from Sigma-Aldrich Co (St Louis, MO, USA).

### 2.2 Microsomal incubation of halogenated biphenyls

Microsomes were prepared from male Wistar rats treated with phenobarbital (PB) or  $\beta$ -naphthoflavone (BNF) as described before<sup>[232]</sup>. 2,2'-DBB was metabolised using PB-induced rat liver microsomes, and 4,4'-DBB was metabolised using BNF-induced rat liver microsomes. Microsomal incubations (10 ml total volume) were performed in 100 mM

---

K<sub>2</sub>HPO<sub>4</sub>/KH<sub>2</sub>PO<sub>4</sub> buffer (pH 7.4), containing 5 mM MgCl<sub>2</sub>, 250 μM halogenated biphenyl, and ca. 1 mg/ml microsomal protein and the reaction was started by addition of NADPH (final concentration 1 mM). After 45 minutes of incubation at 37°C, reactions were terminated by the addition of 10% HClO<sub>4</sub> (10% v/v) and were kept on ice. Incubation mixtures were extracted with 10 ml isopropyl ether which subsequently was evaporated under a stream of nitrogen. Samples were redissolved in 100 μl DMSO, and stored at -20°C with 0.5 mg/ml vitamin C to avoid further oxidation. Controls comprised of incubations without biphenyl, incubations without NADPH and incubations immediately terminated after the start of the reactions.

### 2.3 HPLC analysis of incubation mixtures

Extracts from microsomal incubations of brominated biphenyls were analysed by HPLC (Gilson pumps 303 and 305, manometer 805, dynamic mixer 811C and auto-injector 232 Bio, Gilson, Middleton, WI, USA) using a reversed phase C18-column (Chromspher 5 μM, 100\*3 mm, Varian Chrompack International BV, Middelburg, the Netherlands) and gradient elution. Starting condition was 70% solvent A (90% H<sub>2</sub>O, 10% acetonitrile, 0.1% trifluoroacetic acid) and 30% solvent B (10% H<sub>2</sub>O, 90% acetonitrile, 0.1% trifluoroacetic acid). During the HPLC run, the concentration of solution B was increased. After 10 minutes the gradient contained 60 % solution B, after 20 minutes 100 % solution B and this was continued for 10 minutes. Finally the gradient was brought back to the initial state for 5 minutes before injecting the next sample. The flow rate of the mobile phase was 0.6 ml/min. If needed, fractions were combined, and additionally separated using methanol gradient elution, starting with 90% solvent A (90% H<sub>2</sub>O, 10% methanol) and 10% solvent B (10% H<sub>2</sub>O, 90% acetonitrile, 0.1% trifluoroacetic acid). After 5 minutes the gradient contained 10 % solution B, after 35 minutes 100 % solution B and this was continued for 10 minutes. In both cases, compounds were detected at a wavelength of 254 nm (LC75 spectrophotometer, Perkin-Elmer, Wellesley, MA, USA) and 290 nm (Jasco Ltd, UK, 1575 uv/vis spectrophotometer).

### 2.4 Synthesis of hydroxylated brominated biphenyls

Hydroxylated biphenyls were synthesized according to the method described by Bergman et al with small modifications<sup>[265]</sup>. Four different syntheses were carried out, i.e. a diaryl coupling reactions of 2-bromo-aniline and 2-bromo-anisole, 2-bromo-aniline and 3-bromo-anisole, 4-bromo-aniline and 2-bromo-anisole and of 4-bromo-aniline and 3-bromo-anisole, respectively. Briefly, bromo-aniline (1.0 g) was dissolved in bromo-anisole (5.0 g) at 60°C. The bromo-aniline was diazotized by addition of an excess of 3-methyl butylnitrile (2.0 ml). The temperature was slowly increased to 120°C and kept at this

temperature for 1.5 hours. The unreacted bromo-anisole was removed by vacuum distillation. Demethylation of the components was achieved by addition of boron tribromide in dichloromethane. The crude mixture was extracted and redissolved in 70% methanol for separation by preparative HPLC (see below).

## 2.5 Analysis methods

### *HPLC analysis of synthesized hydroxylated brominated biphenyls*

Hydroxylated dibromobiphenyls were separated by preparative HPLC (Gilson pump 305, manometer 805, dynamic mixer 811C) using a reversed phase C18-column (ChromSpher 5  $\mu$ M, 250 x 10 mm, Varian Chrompack, The Netherlands) and an isocratic elution system with 60% methanol as mobile phase (4.0 ml/min). Compounds were detected at a wavelength of 290 nm (Jasco Ltd, UK, 1575 uv/vis spectrophotometer) and individually collected. After, collection, compounds were analysed for purity by HPLC, GC/MS and NMR. Isolated compounds and corresponding solutions in DMSO displayed light yellow to bright orange colors. Stocks were maintained at -20°C and regularly checked by HPLC for stability.

### *NMR analysis of synthesized hydroxylated brominated biphenyls*

All isolated synthesis products were analysed by  $^1\text{H}$  NMR. H,H-cosy and CH-correlation spectra were also recorded. High-resolution NMR spectra of each compound dissolved in 500  $\mu$ l  $\text{CDCl}_3$  were obtained with a Bruker Avance 400 spectrometer at 27°C (Bruker BioSpin, Rheinstetten, Germany). Acetic acid was used as an internal standard for concentration determination.

### *GC/MS analysis*

GC-MS analyses were performed on a HP 5890 gas chromatograph equipped with a 25 m BPX5 column (0.25 mm i.d., 0.25  $\mu$ m film thickness, SGE, Amstelveen, The Netherlands) coupled to a Hewlett-Packard MSD 5970 mass spectrometer (positive ion source, electron impact ionization, electron energy of 70 eV). Temperatures of the injection port and transfer line were 270 °C. The column temperature was programmed from 40 (5 min) to 270 °C (20°C/min) and kept at 270 °C for 10 min. Full scanning analyses were performed in the range of  $m/z$  150-500. Using these GC-MS conditions, the retention times and mass spectra were recorded for incubation mixtures and reference bromobiphenyls from the synthesis. Before injection, samples were methylated with 2 ml ethereal diazomethane. After overnight derivatization, excess diazomethane was evaporated.

---

### *LC/MS analysis*

The incubation mixtures and the synthesis products were also analysed by HPLC coupled to a mass spectrometer. The chromatic system conditions were similar to the methods described above, i.e. a gradient system was used for the incubation mixtures and an isocratic system was used for the synthesis products. For LC/MS analysis, a reversed phase C18-column (Chromspher 5  $\mu$ M, 100 x 3 mm, Chrompack, the Netherlands) was used in all cases. Mass spectrometric detection was performed with a Finnigan LCQ-DECA mass spectrometer (ThermoQuest, San Jose, CA, USA), operating on the negative ion mode using an APCI interface probe. A potential of 5 kV was applied to the APCI corona discharge. High purity N<sub>2</sub> was used at a flow of 300L/h. Full scanning analysis was performed in the range of  $m/z$  150-650.

## *2.6 Estrogenic activity assays*

### *Competitive ligand binding assay.*

Competitive binding assays were performed as described before<sup>[149]</sup>. Briefly, affinity for the ER was determined using cytosol from homogenised fresh sheep uterus. A mixture of 0.3 nM [<sup>3</sup>H]-E2, uterine cytosolic protein (final concentration 0.5-1 mg/ml) and competing ligand in a total volume of 325  $\mu$ l in TEA-buffer (10 mM TEA, 15  $\mu$ M EDTA, pH 7.4) was incubated for 3 hours at 4°C. Subsequently, unbound radioligand was removed by adsorption for 10 minutes with 0.8%-0.08% charcoal-dextran and centrifugation (10.000 x  $g$ , 10 minutes at 4°C). Aliquots of receptor-bound [<sup>3</sup>H]-E2 were analysed in 4 ml scintillation liquid (HiSafe 3, Perkin Elmer, Wellesley, USA) in a 1900 Tricarb scintillation counter (Packard Instruments, Perkin Elmer). Each experiment, a complete E2 concentration curve was included in duplicate and used to determine 0% and 100% displacement. E2 displaced radiolabeled E2 with an EC<sub>50</sub> value of 0.4  $\pm$  0.05 nM (mean  $\pm$  SEM; n=10). Concentration of DMSO in the assay was always 3%, and this concentration did not alter the binding characteristics of the ER for E2. Experiments were performed at least three times on separate days.

### *Inhibition of sulfotransferase activity.*

Recombinant human estrogen sulfotransferase (hEST) was expressed in *S. typhimurium* as described before<sup>[266]</sup>. Cytosolic preparations from these bacteria were used without further purification. The activity of sulfotransferase 1E1 (hEST) was analysed by measuring the formation of [<sup>3</sup>H]-E2 sulfate after incubation of 1 nM [<sup>3</sup>H]-E2 for 30 minutes at 37°C

with recombinant hEST (0.1 µg/ml) with 50 µl PHB metabolite in a buffer containing 0.1 M sodium phosphate (pH 7.2), 2 mM EDTA and 1 mM dithiothreitol (DTT) in the presence or absence (blanks) of 50 µM PAPS<sup>[99]</sup>. Total volume was 200 µl per incubation. The reactions were stopped by the addition of 0.8 ml ice-cold water, and free [<sup>3</sup>H]-E2 was removed by extraction with 2.5 ml dichloromethane. [<sup>3</sup>H]-E2-Sulfate formation was quantified by liquid scintillation counting of 0.5 ml of the aqueous phase in a scintillation counter (Packard Instruments). Enzymatic sulfation was corrected for background radioactivity measured in the blanks. Inhibition of E2 sulfation by PHB metabolites was investigated by addition of various concentrations of the metabolites to the reaction mixtures. The final DMSO concentration in the assay was 1%. Experiments were performed at least three times on separate days.

#### *ER-Calux® luciferase assay.*

T47D.Luc cells were obtained from BioDetection systems b.v. (BDS, Amsterdam, The Netherlands). The ER-Calux® assay was performed as described before<sup>[184]</sup>. Briefly, cells were plated at a density of 50.000 cells/ml in 100 µl assay medium per well in 96-well plates (Nunclon®, Nalge Europe Limited, Hereford, UK) and allowed to attach overnight. ER-Calux® assay medium contained phenol red-free 1:1 mixture of DMEM and Ham's F12 medium (D/F-, Gibco, Invitrogen, Breda, The Netherlands), supplemented with 0.1 mM non-essential amino acids (NEA), penicillin (50 U/ml)-streptomycin mix (50 µg/ml) and 5% charcoal-dextran stripped fetal bovine serum (CDFBS, Gibco). Medium was renewed the following day and after another 48 hours, cells were exposed to various compounds in triplicate in fresh assay medium. Control incubations and an E2 standard curve were included in triplicate on every plate. E2 induced dose-dependent cell proliferation with an EC<sub>50</sub> value of 11 ± 4 pM (mean ± SEM; n= 7). DMSO concentration was 0.1% (v/v) in all incubations. After 6 hours incubation, cells were lysed and luciferin conversion by luciferase activity was measured in an Anthos Lucy 2 luminometer. Experiments were performed at least three times on different occasions. EC<sub>50</sub> values were calculated using Graphpad Prism 3.0 (GraphPad Software Inc., 2000, San Diego, CA, USA).

## 2.7 Computational details

The prediction of ERα binding affinity was performed as described by van Lipzig et al.<sup>[149]</sup>. Briefly, the crystal structure of the ligand binding domain of the ERα complexed with DES (PDB ID 3ERD)<sup>[144]</sup>, was used to build the protein model using InsightII (Biosym, San Diego, CA, USA). For each ligand, four energy-optimised geometries were obtained covering the broadest range of conformational space of the ligand. Electrostatic potentials were calculated for all conformations using GAMESS at the 6-31G\* level of theory. Molecular

---

dynamics (MD) simulations of all possible orientations of DBB metabolites in the binding cavity of the ER $\alpha$  model were performed using Amber 6.0. Separate MD simulations were performed of ER $\alpha$  bound metabolites in water and unbound metabolites in water. The MD trajectories were used for analysis in the Carnal/Anal module of Amber 6.0 for calculation of energy terms. These were subsequently used in the linear interaction energy (LIE) method was used for prediction of ER $\alpha$  affinity. This approximation relies on the assumption that the  $\Delta G$  depends linearly on changes in the Van der Waals (VDW) and electrostatic (EL) interaction energy ( $E_{\text{interaction}}$ ) of the system<sup>[200,201]</sup> and is described by:

$$\Delta G_{\text{calc}} = (\alpha * E_{\text{interaction}}^{\text{VDW}}) + (\beta * E_{\text{interaction}}^{\text{EL}}).$$

The LIE parameters  $\alpha$  and  $\beta$  were calculated by double regression analysis of the interaction energies obtained from MD simulations, and experimental  $K_d$  values of well-known reference estrogens. We obtained an excellent linear correlation ( $r^2 = 0.94$ ) between experimental and calculated binding energies, with  $K_d$  values ranging from 0.15 mM to 30 pM. ER $\alpha$  affinity of di-hydroxylated brominated biphenyls was subsequently predicted using the parameters  $\alpha=0.823$  and  $\beta=0.21$ .

## 2.8 Statistical analysis

All data were analysed with Graphpad Prism 3.0. Statistical analysis was carried out by Student's *t*-test. P-values  $\leq 0.05$  were considered to indicate a significant difference with control data.

# 3 Results

## 3.1 Microsomal incubations of dibromobiphenyls

2,2'-DBB and 4,4'-DBB were incubated with PB-induced as well as BNF-induced rat liver microsomes. From pilot experiments, which were consistent with results obtained by Mills<sup>[267]</sup>, we learned that planar para-substituted biphenyls, such as 4,4'-DBB, are good substrates for BNF-induced microsomes and not for PB-induced microsomes, whereas non-planar ortho-substituted biphenyls, e.g. 2,2'-DBB, are good substrates for PB-induced microsomes (data not shown). In all further experiments, BNF-induced microsomes were used for metabolism of 4,4'-DBB, and PB-induced microsomes for metabolism of 2,2'-DBB.

In Figure 1, typical HPLC chromatograms ( $\lambda = 290$  nm) of incubation extract of 2,2'-DBB and 4,4'-DBB are shown, illustrating the metabolite profile after 45 minutes incubation at 37°C. No metabolite peaks were formed in incubations terminated after 0 minutes and incubations without NADPH (data not shown).

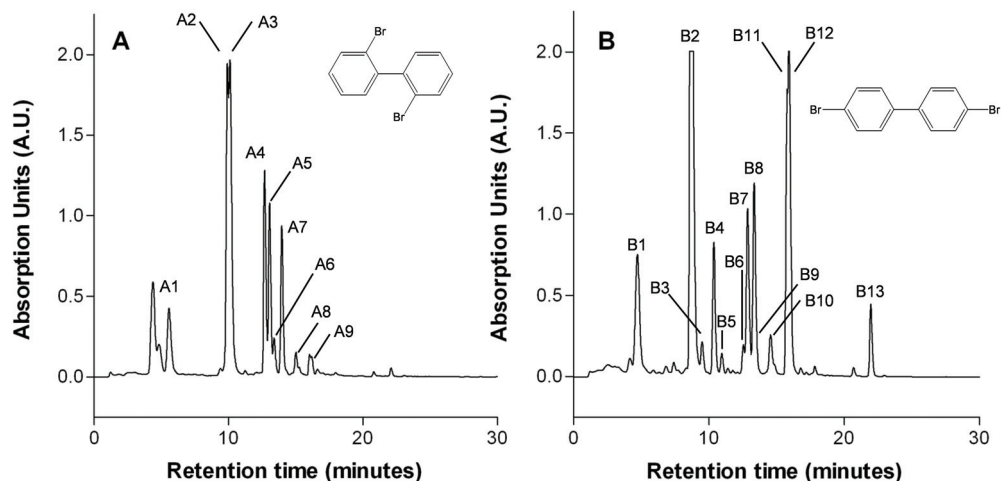


**Figure 1:** Representative HPLC-chromatogram of diisopropyl extracts of 45 minutes incubations of 250  $\mu\text{M}$  DBB with rat liver microsomes. Panel **A** (left) shows the metabolite profile of PB-induced rat liver microsomal incubation of 250  $\mu\text{M}$  2,2'-DBB and Panel **B** (right) shows the results of BNF-induced rat liver microsomal incubation of 250  $\mu\text{M}$  4,4'-DBB. Incubations without NADPH showed similar chromatograms as  $t = 0$  minutes (not shown) and only show parent compound peaks.

### 3.2 Estrogenic affinity of bio-activated 2,2'-DBB and 4,4'-DBB

Bio-activation of 2,2'-DBB and 4,4'-DBB ( $t = 45$  minutes) by the microsomal CYP enzymes leads to a much higher estrogen receptor affinity of the DBBs compared to the control incubations ( $t = 0$  minutes), as shown in Figure 2. The parent compound 2,2'-DBB showed only low ER binding affinity (estimated  $\text{EC}_{50}$  value of 150-250  $\mu\text{M}$ ), while 4,4'-DBB did not show any ER binding affinity at the highest concentration tested (0.3 mM; data not shown).

### 3.3 HPLC analysis and identification of 2,2'-DBB and 4,4'-DBB metabolites

Subsequently, the isopropyl extracts of the CYP incubations of the DBBs were fractionated by HPLC and analysed by LC/MS to investigate which of the products was responsible for the observed increased estrogenic affinity. Therefore 1 ml (equivalent to an initial amount of 2.5  $\mu\text{mol}$  parent compound) was injected. Various metabolites with one or two hydroxylgroups were found, showing the isotope pattern of two bromine atoms (Table 1). From 4,4'-DBB, also hydroxylated metabolites with a single bromine atom were formed.

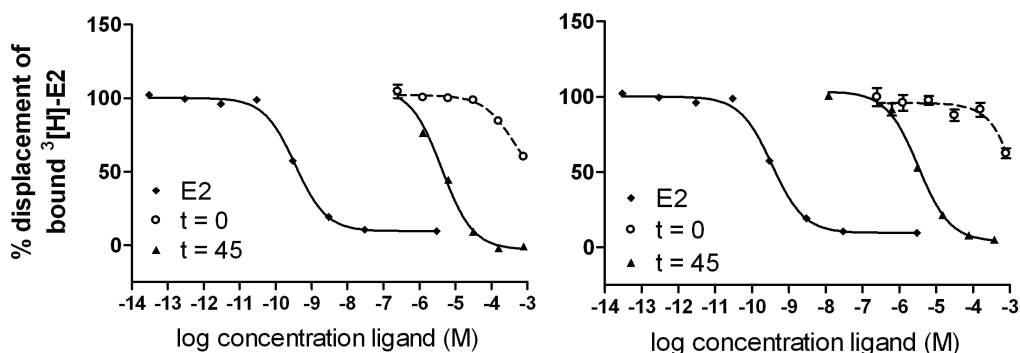
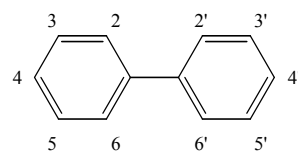


**Figure 2:** Displacement of [<sup>3</sup>H]-E2 from ER from sheep uterus cytosol by unlabeled E2 (◆), control incubations (○), and by 45 minutes incubations of 250 μM 2,2'-DBB (upper panel) and 250 μM 4,4'-DBB (lower panel) with PB and BNF-induced microsomes respectively (▲). The concentration of E2 and parent DBBs is shown in M. Shown is a typical experiment of three independent experiments. Each point represents the mean of triplicate measurements ± standard error of the mean.

Several of the mono-hydroxylated metabolites could be identified by comparison of their retention times with commercially available and synthetic reference compounds. This was followed by spiking of the isopropyl extracts of the CYP incubations with the synthetic compounds and analysis by HPLC. This showed co-elution of the standard mono-hydroxy-compounds indicated in Table 1 with metabolites from the CYP incubations.

Furthermore, LC/MS and GC/MS were performed and retention times and fragmentation patterns of the synthesized reference compounds were compared with peaks in the incubation samples, and their corresponding retention times and fragmentation patterns. LC/MS retention times were unique for all reference compounds. GC/MS and LC/MS analysis yielded unique fragmentation patterns for the methylated hydroxybiphenyls, similarly to chloro- and bromobiphenyl metabolites described in Tulp *et al.* 1977<sup>[268]</sup>. The combined result indicated that seven mono-hydroxy-metabolites could be identified in the incubation samples (Table 2).

**Table 1:** Identification of synthetic hydroxylated dibromobiphenyls by HPLC,  $^1\text{H}$  NMR and GC/MS. NMR signals were assigned using  $^1\text{H}$ ,  $\text{H,H-cosy}$  and  $\text{CH-correlation}$ , as described in the materials section. For the MS mass spectral data; mass to charge ratio of the molecular fragments ( $m/z$ ) and the relative abundance of the number of ions (intensity in %) are shown.



Compound <sup>1</sup>	Method	HPCL	$^1\text{H}$ NMR ( $\text{CDCl}_3$ )	GC	MS
		$R_t$ (min) <sup>a</sup>	$\delta$ in ppm (number of protons, complexity in Hz, position <sup>b</sup> )	$R_t$ (min) <sup>c</sup>	$m/z$ (fragment loss in intensity) <sup>c</sup>
2-OH-4,4'-DBB		22"	7.09 (1H, dd, $^2J=7.5$ , $^3J=1$ , H6), 7.15 (1H, dd, $^2J=8$ , $^3J=1$ , H3), 7.16 (1H, s, H5), 7.35 (2H, tr of d, $^2J=9$ , $^3J=0.5$ , H2', H6'), 7.62 (2H, tr of d, $^2J=9$ , $^3J=0.5$ , H3', H5')	21.13"	342 ( $M^+$ 100), 246/8 (M-Br- $\text{CH}_3$ 53), 182 (M-Br-Br 6), 139 (M-Br-Br- $\text{CH}_3$ -CO 32)
4-OH-2,2'-DBB		13.5"	6.8 (1H, dd, $^2J=8.3$ , $^3J=2.5$ , H5), 7.12 (1H, d, $^2J=8.3$ , H6), 7.19 (1H, d, $^2J=2.5$ , H3), 7.23-7.28 (2H, m, H4', H6'), 7.38 (1H, d of tr, $^2J=7.5$ , $^3J=1.3$ , H5'), 7.67 (1H, dd, $^2J=8.6$ , $^3J=1.5$ , H3')	15.08"	342 ( $M^+$ 100), 261/3 (M-Br-48), 246/8 (M-Br- $\text{CH}_3$ 5), 182 (M-Br-Br 62), 139 (M-Br-Br- $\text{CH}_3$ -CO 92)
6-OH-2,2'-DBB		10.5"	6.96 (1H, dd, $^2J=8$ , $^3J=1$ , H5), 7.19 (1H, tr, $^2J=8$ , H4), 7.26-7.37 (4H, m, H3, H6', H4'), 7.49 (1H, d of tr, $^2J=7.5$ , $^3J=1$ , H5'), 7.75-7.78 (1H, dd, $^2J=2$ , $^3J=1$ , H3')	14.25"	342 ( $M^+$ 42), 261/3 (M-Br-28), 246/8 (M-Br- $\text{CH}_3$ 100), 182 (M-Br-Br 42), 139 (M-Br-Br- $\text{CH}_3$ -CO 57)
3-OH-2,2'-DBB		11"	6.83 (1H, dd, $^2J=7.5$ , $^3J=1.5$ , H5), 7.09 (1H, dd, $^2J=7.5$ , $^3J=1.5$ , H4), 7.1-7.32 (4H, m, H6, H3', H6), 7.39 (1H, d of tr, $^2J=7.5$ , $^3J=1.3$ , H5'), 7.69 (1H, dd, $^2J=8$ , $^3J=1.3$ , H3')	15.13"	342 ( $M^+$ 75), 261/3 (M-Br-100), 246/8 (M-Br- $\text{CH}_3$ 20), 182 (M-Br-Br 35), 139 (M-Br-Br- $\text{CH}_3$ -CO 90)
2-OH-3,2'-DBB		13"	6.90 (1H, tr, $^2J=8.0$ , H5), 7.15 (1H, dd, $^2J=7.5$ , $^3J=1.6$ , H6), 7.25-7.34 (2H, m, H4', H6'), 7.40 (1H, d of tr, $^2J=7.5$ , $^3J=1.3$ , H5'), 7.54 (1H, dd, $^2J=8.0$ , $^3J=1.6$ , H4), 7.71 (1H, dd, $^2J=8.0$ , $^3J=1.3$ , H3')	14.36"	342 ( $M^+$ 45), 261/3 (M-Br-14), 246/8 (M-Br- $\text{CH}_3$ 100), 182 (M-Br-Br 47), 139 (M-Br-Br- $\text{CH}_3$ -CO 43)
3-OH-4,4'-DBB		6"	7.02 (1H, dd, $^2J=8.4$ , $^3J=2.2$ , H6), 7.17 (1H, d, $^3J=2.2$ , H2), 7.55 (3H, t, $^2J=8.2$ , H2', H6'), 7.65 (2H, d, $^2J=8.5$ , H3', H5')	18.04"	342 ( $M^+$ 100), 299 (M- $\text{CH}_3$ -CO 42), 246/8 (M-Br- $\text{CH}_3$ 18), 139 (M-Br-Br- $\text{CH}_3$ -CO 38)
4-OH-3,4'-DBB		6"	7.03 (1H, d, $^2J=8.4$ , H5), 7.51 (1H, dd, $^2J=8.4$ , $^3J=2.1$ , H6), 7.55-7.61 (4H, m, H3', H5', H2', H6'), 7.78 (1H, d of s, $^3J=2.2$ , H2)	18.5"	342 ( $M^+$ 100), 327 (M- $\text{CH}_3$ 64), 299 (M- $\text{CH}_3$ -CO 34), 246/8 (M-Br- $\text{CH}_3$ 18), 139 (M-Br-Br- $\text{CH}_3$ -CO 57)

<sup>1</sup> DBB = dibromobiphenyl, <sup>a</sup> 65% methanol isocratic elution method, <sup>b</sup> Positions of proton as illustrated in figure above Table 1, <sup>c</sup> Procedures are described in the Methods section, analysis was performed in the range of  $m/z$  150-500.

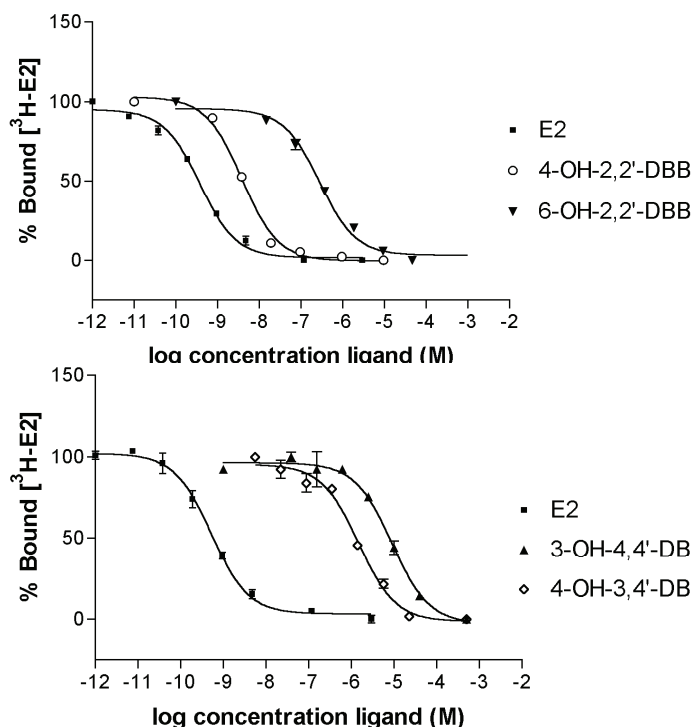


**Figure 3:** Displacement of [<sup>3</sup>H]-E2 from ER from sheep uterus cytosol by purified synthesized hydroxylated brominated biphenyls and E2. Depicted are compounds that displayed affinity for the ER with an EC<sub>50</sub> value of 10<sup>-8</sup> M or lower, i.e. 4-OH-2,2'-DBB (○) and 6-OH-2,2'-DBB (▼) (upper panel) and 3-OH-4,4'-DBB (▲) and 4-OH-3,4'-DBB (◇) (lower panel). Shown are typical experiments of three independent experiments. Each point represents the mean of duplicate incubations, the bars indicate higher and lower values. EC<sub>50</sub> values of all hydroxylated brominated biphenyls tested in the current study are summarised in Table 2.

### 3.4 ER binding of DBB metabolites and synthetic standards

Isolated HPLC fractions of CYP incubations were dissolved in equal volumes (100 µl) DMSO and 10 µl was tested for estrogen receptor binding affinity. Table 2 shows all fractions for which significant ER affinity was measured in the binding assay (> 10% displacement of [<sup>3</sup>H]-E2). For 2,2'-DBB as well as for 4,4'-DBB, fractions containing metabolites with one as well as two hydroxyl groups were found that show binding to the ER. Clearly, introduction of hydroxyl groups in the DBB skeletons strongly increased affinity to the estrogen receptor. This is also shown by the results from the synthetic standards in the ER binding assay: all mono-hydroxylated standards bind to the E2 receptor with EC<sub>50</sub> values ranging from 6.6 nM to 41 µM (Table 2). Binding curves of synthetic standards are presented in Figure 3.

### 3.5 hEST inhibition by DBB metabolites and synthetic standards

Next to binding to the estrogen receptor, the HPLC-purified fractions of CYP incubations were tested for inhibition of hEST activity, as published by Kester et al<sup>[99]</sup>. Parent DBBs were also included in these experiments.

Most fractions inhibited hEST. These fractions include mono-hydroxylated as well di-hydroxylated DBB metabolites. The results of these assays are illustrated in Figure 4 and summarised in Table 2. Also, all mono-hydroxylated DBB synthetic standards inhibited hEST while 2,2'-DBB and 4,4'-DBB themselves did not. EC<sub>50</sub> values varied from 40 nM to 3.1  $\mu$ M (Table 2).

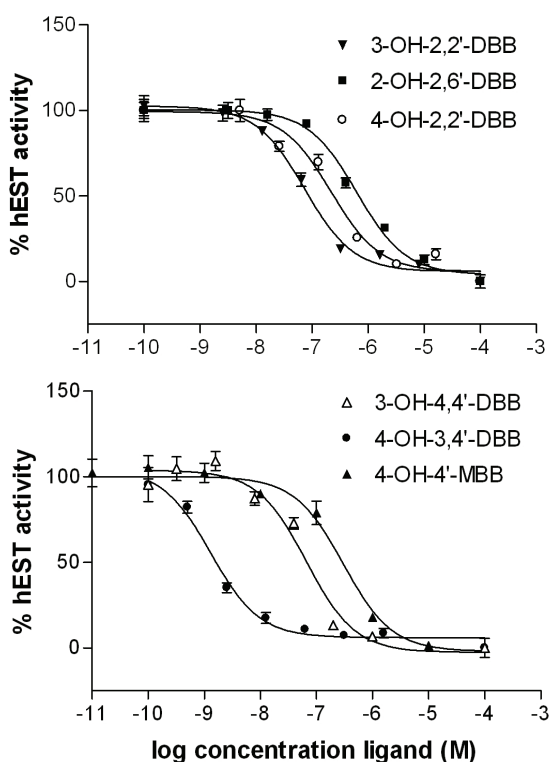


**Figure 4:** Inhibition of formation of [<sup>3</sup>H]-E2 sulfate by human estrogen sulfotransferase (hEST) activity, by synthetic hydroxylated brominated biphenyls. hEST activity was determined by incubation of 1 nM [<sup>3</sup>H]-E2 for 30 minutes at 37°C, in the presence or absence (blanks) of 50  $\mu$ M PAPS<sup>[99]</sup>. Depicted are compounds that displayed affinity for hEST with an EC<sub>50</sub> value of 1  $\mu$ M or lower. Shown are typical experiments of three independent experiments. Each point represents the mean of triplicate incubations  $\pm$  standard error of the mean. EC<sub>50</sub> values of all hydroxylated brominated biphenyls tested in the current study are summarised in Table 2.

### 3.6 Estrogenic activity of synthetic-hydroxylated biphenyls in the ER-Calux® assay.

The transcriptional activity of the synthetic standards was tested in the ER-Calux® reporter gene assay (Figure 5). All synthetic hydroxylated biphenyls induced luciferase activity ( $EC_{50}$  values ranged from 74 to 664 nM (Table 2). Induction of luciferase activity by 6-OH-2,2'-DBB only reached 35% of the maximal effect of E2 (100%) (Figure 5, upper panel). 3-OH-2,2'-DBB and 4-OH-2,2'-DBB showed some toxicity at very high concentrations ( $> 10 \mu\text{M}$ , not shown). Remarkably, 4-OH-4'-MBB and 4-OH-2,2'-DBB induced supra-maximal luciferase activation, respectively 320% and 180% of the maximal response of E2 (Figure 5, lower panel).

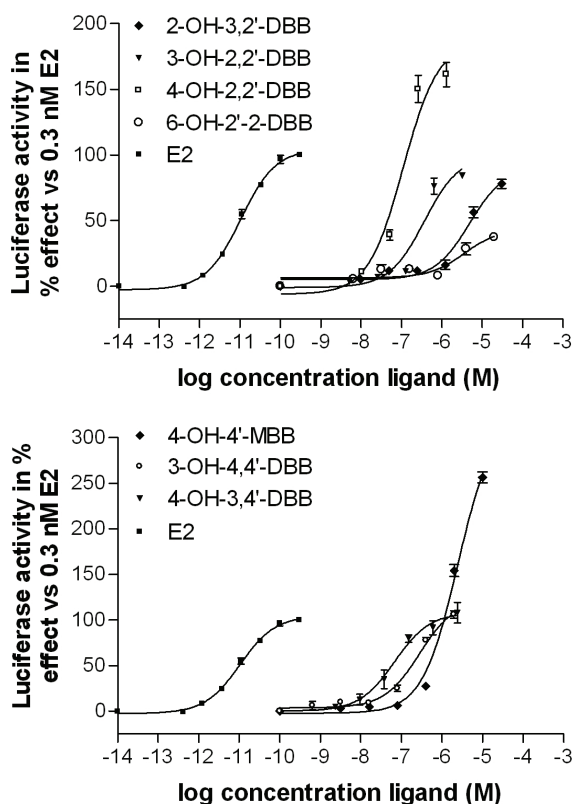


**Figure 5:** Estrogenic activity (induction of luciferase activity) of hydroxylated bromobiphenyls in T47D cells measured in the ER-Calux® assay. Cells were pre-incubated with assay-medium for two days, and subsequently exposed for 6 hours to E2 (■), 2-OH-3,2'-DBB (◆), 3-OH-2,2'-DBB (▼), 4-OH-2,2'-DBB (□) and 6-OH-2,2'-DBB (○) (upper panel) and 4-OH-4'-MBB (◆), 3-OH-4,4'-DBB (○), 4-OH-3,4'-DBB (▼) (lower panel). Shown are representatives of two independent experiments. Each point represents the mean of triplicate incubations  $\pm$  standard error of the mean.

**Table 2**

Metabolite			Estrogenic properties of compound standards						
LC/MS		Identity <sup>a</sup>	ER binding		hEST inhibition		ER-Calux®		
			EC <sub>50</sub> in nM (s.d.)		EC <sub>50</sub> in nM (s.d.)		EC <sub>50</sub> in nM (s.d.)		
2,2'-DBB									
A1 <sup>c</sup>	diBr-mono-OH	n.i.							
A2	diBr-diOH	n.i.							
A3	diBr-diOH	n.i.							
A4	diBr-monoOH	2-OH-3,2'-DBB	10100	(3400)	3120	(1000)	>1000 <sup>b</sup>		
A5	diBr-monoOH	6-OH-2,2'-DBB	196	(64)	1000	(120)	>1000 <sup>b</sup>		
A6	diBr-monoOH	4-OH-2,2'-DBB	6.6	(4)	640	(110)	125	(20)	
A7	diBr-monoOH	3-OH-2,2'-DBB	41800	(6600)	320	(90)	367	(85)	
A8	non-Br metabolite								
A9	non-Br metabolite								
4,4'-DBB									
B1 <sup>c</sup>	mono-Br-diOH	n.i.							
B2	mono-Br-diOH	n.i.							
	+ diBrdiOH	n.i.							
B3	diBr-diOH	n.i.							
B4	diBr-diOH	n.i.							
B5	diBr-diOH	n.i.							
B6	monoBr-monoOH	4-OH-4'-MBB	11400	(4300)	470	(160)	>1000 <sup>b</sup>		
B7	diBr-diOH	n.i.							
B8	non-Br metabolite								
B9	diBr-diOH	n.i.							
B10	diBr-diOH	n.i.							
B11	2x diBr-monoOH	4-OH-3,4'-DBB	1960	(40)	40	(20)	74	25	
		3-OH-4,4'-DBB	3530	(1500)	440	(150)	210	16	
B12	non-Br metabolite								

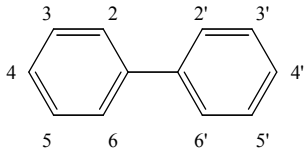
<sup>a</sup> Identification based on co-elution with synthetic standards and identical MS-data. NMR, LC/MS and GC/MS data of the standards are shown in Table 1. <sup>b</sup> EC<sub>50</sub> value was higher than 1000 nM; at this concentration, estrogenic activity was >10% compared to 10<sup>-9</sup> nM E2. <sup>c</sup> All numbered HPLC-fractions showed >10% displacement of [<sup>3</sup>H]-E2 from the receptor compared to 10<sup>-7</sup> nM E2. n.i.: not identified. non-Br metabolite: metabolite without bromo-substituent.

**Table 2:** Identity and estrogenic properties of isolated metabolites after HPLC separation of 45-minute microsomal incubations of 2,2'-DBB (PB-induced microsomes), and 4,4'-DBB (BNF-induced microsomes). Identity of metabolites was based on comparison of retention times and MS data with those of synthetic standards (Table 1). Several metabolites were identified by HPLC and LC/MS. The ER binding affinities, hEST inhibition activities and estrogenic activity by induction of luciferase activity (ER-Calux®) of the corresponding synthesized and purified compounds are shown (EC<sub>50</sub> values in nM).

### 3.7 Prediction of binding affinity by the LIE computational model

ER $\alpha$  binding affinity of four di-hydroxylated brominated biphenyls was calculated using the recently published model for accurate prediction of absolute ligand binding affinities. The optimised LIE parameters  $\alpha=0.823$  and  $\beta=0.21$  were used to calculate the binding affinities of 3,4'-di-OH-2,2'-DBB, 3,4-di-OH-2,2'-DBB, 4,4'-di-OH-2,2'-DBB and 3,3'-di-OH-4,4'-DBB. Interaction energies were obtained from MD simulations of di-hydroxylated brominated bound to the solvated ER $\alpha$  as described in the Methods section. The predicted  $\Delta G_{\text{calc}}$  and  $K_d$  values are presented in Table 3.

**Table 3**

Structure	Metabolite	Calculated $\Delta G$ (LIE)	Predicted EC <sub>50</sub>
		Kcal/mol	$\mu\text{M}$
	3,4'-di-OH-2,2'-DBB	-8.602	0.54
	3,4-di-OH-2,2'-DBB	-7.770	2.2
	4,4'-di-OH-2,2'-DBB	-7.538	3.2
	3,3'-di-OH-4,4'-DBB	-6.399	24.5

**Table 3:** Free energies of binding ( $\Delta G_{\text{calc}}$ ) and predicted ER affinity ( $K_d$ ), of binding of four di-hydroxylated bromobiphenyls to ER $\alpha$ .  $\Delta G_{\text{calc}}$  was calculated using the linear interaction energy (LIE) method (van Lipzig et al, JMC 2004) and is expressed in kcal/mol. LIE parameters used were  $\alpha = 0.82$  and  $\beta = 0.20$ . Predicted  $K_d$  value is expressed in  $\mu\text{M}$ .

## 4 Discussion

In the present study, we investigated the estrogenic properties of hydroxylated metabolites of two brominated biphenyls, 2,2'-DBB and 4,4'-DBB, formed by rat microsomal CYP activity, and their inhibition of hEST, an important enzyme for estradiol metabolism.

CYP mediated metabolism of 2,2'-DBB yielded 2-OH-3,2'-DBB, 3-OH-2,2'-DBB, 4-OH-2,2'-DBB, 6-OH-2,2'-DBB, one unidentified monohydroxy-dibromobiphenyl and two unidentified di-hydroxylated dibromobiphenyls. Based on HPLC analysis with detection at 254 and 290 nm, the most abundant metabolites are 3-OH-2,2'-DBB and 2-OH-3,2'-DBB. Metabolism studies of 2,2'-DBB and 4,4'-DBB were performed before<sup>[267]</sup>, however, no hydroxylated metabolites of 2,2'-DBB were not reported yet. Literature data show that

biotransformation of 2,2'-dichlorobiphenyl (2DCB) by rat CYPs yielded 3-OH-2,2'-DCB, 4-OH-2,2'-DCB and 5-OH-2,2'-DCB, and several dichlorobiphenyldiols<sup>[269]</sup>. Thus rat CYP activity shows some similar characteristics in the metabolism of chlorinated and brominated biphenyls.

CYP mediated biotransformation of 4,4'-DBB yielded mono- and di-hydroxylated mono-bromobiphenyl, and mono- and di-hydroxylated dibromobiphenyls (Table 2). The most abundant metabolites are an unidentified di-hydroxylated dibromobiphenyl, 3-OH-4,4'-DBB and 4-OH-3,4'-DBB, the latter is formed via CYP mediated metabolisms involving an NIH-shift. Earlier rat metabolism studies with 4,4'-DBB also showed formation of 3-OH-4,4'-DBB and 4-OH-3,4'-DBB<sup>[268]</sup>. In the present study, mono-brominated 4-OH-4'-MBB was identified as well. Our findings are in also good agreement with studies examining metabolism of the corresponding chlorinated congener, 4,4'-dichlorobiphenyl (4DCB), using liver CYP enzymes from various species<sup>[270]</sup>. Several di-hydroxylated dichlorobiphenyls were also found in the present study, similar to earlier studies with rat, rabbit and frog CYPs<sup>[271 and references therein]</sup>, however, many of these metabolites remain unidentified.

The observed preferential metabolism of 2,2'-DBB by PB-induced liver microsomes, with induced CYP2B activity, compared to BNF-induced microsomes is explained by the fact that CYP2B mainly binds non-planar compounds, whereas BNF-induced rat liver microsomal CYP, with induced 1A activity, generally favours biotransformation of co-planar compounds, such as 4,4'-DBB. The expression and induction of P450 isoenzymes differs between rat and human. Human CYP1A2 is expressed primarily in liver, and although there is still conflicting evidence for the expression of enzymatically functional CYP1A1 in humans, it is inducible by dioxins and polycyclic aromatic hydrocarbons such as PCB or PBB in many different tissues and cell lines<sup>[272]</sup>. Furthermore, it was recently clearly demonstrated that CYP1A1 is expressed in human liver<sup>[273]</sup>. As for CYP2B, it was demonstrated that the specific human isoform CYP2B6 covers 2-10% of the total human liver P450 content. Furthermore, CYP2B6 is involved in the metabolism of almost 25% of current pharmaceuticals, and the expression of CYP2B6 is strongly induced by compounds such as phenobarbital (PB)<sup>[274]</sup>.

The ER binding data of the synthesized metabolites are in very good agreement with known structural activity relationships of estrogens. The highest affinity was observed for 4-OH-2,2'-DBB, with an EC<sub>50</sub> of 6.6 nM. Visualization of the binding of 2,2'-DBB metabolites to the ER $\alpha$  using a molecular modeling program (Insight II) showed that the two bromines in 4-OH-2,2'-DBB fill the ER binding cavity in a similar manner as the two lipophilic ethyl groups of DES, which are thought to be responsible for its high affinity. At the same time, the hydroxyl group at the 4-position of 4-OH-2,2'-DBB may form hydrogen bonds with

---

Glu353 and Arg394. Together, these features cause 4-OH-2,2'-DBB to be a potent estrogen. Remarkably, 6-OH-2,2'-DBB showed to be a relatively potent estrogen ( $EC_{50}=200$  nM), despite the fact that the hydroxyl group does not seem to be directed towards the hydrogen bonding amino acids in the ER, as mentioned above. It remains unclear why this compound shows a relatively high affinity. The hydroxyl group apparently finds extra Van de Waals or electrostatic interactions in the ER, which are not seen for other estrogens.

Competitive ER binding data such as presented in this study may only reveal whether a compound has a low or high affinity for the ER; it does not tell whether a compound may be an agonist or an antagonist for the receptor. Therefore, we tested the synthetic mono-hydroxylated DBBs in the ER-Calux<sup>®</sup> assay. In this study, ER agonists induce the expression of the enzyme luciferase, while ER antagonists block the receptor and inhibit the expression of this enzyme by estrogenic compounds. The results from the ER-Calux<sup>®</sup> assay clearly show that all the synthetic mono-hydroxylated DBBs are full agonists. Remarkably, 4-OH-4'-MBB and 4-OH-2,2'-DBB induced a supra-maximal luciferase activation, similar to what we have observed for some hydroxylated metabolites of benzo[a]pyrene and chrysene<sup>[46]</sup>. We have shown recently, that this effect seems (at least partially) be due to higher expression of the ER by these hydroxylated metabolites<sup>[46]</sup>.

Beside activation of the ER, inhibition of hEST has been associated with endocrine disruption. It was shown *in vivo*, that normal development of reproductive organs and function of male mice was disrupted due to chronic estrogen stimulation, caused by knocking out estrogen sulfotransferase<sup>[275]</sup>. These data strongly emphasize the significance of hEST inhibition for endocrine disruption, next to ER activation. Therefore, hEST inhibition by PBB metabolites was also investigated in this study. 4-OH-3,4'-DBB showed the strongest potency ( $EC_{50}$ ; 40 nM). 4-OH-2,2'-DBB, 3-OH-2,2'-DBB, 4-OH-3,4'-DBB and 3-OH-4,4'-DBB showed moderate hEST inhibition. Kester et al.<sup>[99]</sup> investigated hEST inhibition of hydroxylated chlorinated biphenyls. They showed that an OH group at a para-position with an ortho chloro-substituent is required for high hEST inhibitory potency. This configuration of an *ortho* chloro-substituent next to a phenolic hydroxyl group is also present in other inhibitors of sulfotransferases and may represent a common 'pharmacophore'<sup>[276,277]</sup>. Also inhibition of hEST by halogenated biphenyls is favoured by coplanar structure. However substitution of a halogen *ortho* to the phenyl-phenyl bond shows no effects on hEST activity. This corresponds well with our observations.

The di-hydroxylated biphenyl metabolites could not be identified due to lack of reference compounds. Also their estrogenic activity could not be tested in the ER-Calux<sup>®</sup> because not enough material could be isolated from the microsomal incubations to allow

experiments with purified compounds. In the experiments testing the estrogenic activities of the collected fractions after microsomal incubation with CYPs, the di-hydroxylated metabolite fractions from both 2,2'-DBB and 4,4'-DBB incubations show higher estrogenic activities than the fractions with mono-hydroxylated biphenyls (Table 2). Therefore, we calculated ER $\alpha$  binding affinities of four hypothetical di-hydroxylated metabolites, using our recently developed computational method for accurate prediction of ER $\alpha$  affinity<sup>[149]</sup>. 3,4-di-hydroxy-2,2'-DBB is equivalent to a di-hydroxylated metabolite of 2DCB identified in the rat<sup>[271]</sup>, and may be a metabolite formed via an epoxide. The other three metabolites, 3,4'-diOH-2,2'-DBB, 4,4'-diOH-2,2'-DBB and 3,3'-diOH-4,4'-DBB result from hydroxylation of both biphenyl rings, and may be secondary metabolites of 4-OH-2,2'-DBB or 3-OH-4,4'-DBB. The predicted affinities of the di-hydroxylated metabolites for the ER $\alpha$  ranged from 0.54 to 25  $\mu$ M (Table 3). These affinities are generally lower than the affinity of their mono-hydroxylated analogs. While two hydroxyl groups at a distance of 10 to 12 Å are found to be important for the high affinity of estrogens such as E2, DES and genistein<sup>[147,149]</sup>, the two hydroxyl groups in the PBB metabolites are at much shorter distance (e.g. the 4-OH and 4'-OH position in biphenyl are at a distance of 9 Å) and thus one of the phenolic hydroxyl groups may not be in reach of His 524 in the ER $\alpha$ . It may even hinder optimal binding.

In conclusion, the contribution of the di-hydroxylated products to the total increase of estrogenic activity by CYP mediated bioactivation is significant but further research is needed to establish their identities and their estrogenic activities.

Generally, risk assessment of environmental estrogens is focused on parent compounds only<sup>[1,74,75]</sup>. The brominated biphenyls 2,2'-DBB and 4,4'-DBB used in the current study, proved to be good models for the investigation of the role of CYP enzymes in bioactivation of environmental contaminants into more estrogenic compounds. Moreover, very potent estrogenic metabolites are formed, some demonstrate up to nanomolar ER affinity or hEST inhibition potency. These findings are of vital importance for accurate risk assessment of exposure to environmental contaminants, such as halogenated biphenyls. Neglecting bio-activation through biotransformation will lead to underestimation of health risks.



## Chapter 4

### Prediction of Ligand Binding Affinity and Orientation of (Xeno)Estrogens to the Estrogen Receptor by Molecular Dynamics Simulations and the Linear Interaction Energy Method

Marola M.H. van Lipzig, Anton M. ter Laak, Aldo Jongejan, Nico P.E. Vermeulen, Mirjam Wamelink, Daan Geerke and John H.N. Meerman.

Journal of Medicinal Chemistry 2004 (47), 1018-30.

---

## ABSTRACT

Exposure to environmental estrogens has been proposed as a risk factor for disruption of reproductive development and tumorigenesis of humans and wildlife<sup>[4]</sup>. In recent years, many structurally diverse environmental compounds have been identified as estrogens. A reliable computational method for calculation determining estrogen receptor (ER) binding affinity is of great value for the prediction of estrogenic activity of such compounds and their metabolites. In the presented study, a computational model was developed for prediction of binding affinities of ligands to the ER $\alpha$  isoform, using MD simulations in combination with the linear interaction energy (LIE) approach.

The linear interaction energy approximation was first described by Åqvist *et al.*<sup>[200]</sup> and relies on the assumption that the binding free energy ( $\Delta G$ ) depends linearly on changes in the Van der Waals and electrostatic energy of the system. In the present study, MD simulations of ligands in the ER $\alpha$  ligand binding domain (LBD)<sup>[144]</sup>, as well as ligands free in water were carried out, using the Amber 6.0 force field (<http://amber.scripps.edu/>)<sup>[278]</sup>. Contrary to previous LIE methods, we took into account every possible orientation of the ligands in the LBD and weighted the contribution of each orientation to the total binding affinity according to a Boltzman distribution. The training set ( $n = 19$ ) contained estradiol (E2), the synthetic estrogens diethylstilbestrol (DES) and 11 $\beta$ -chloro-ethyl-estradiol (E2-Cl), 16 $\alpha$ -E2 (estriol, EST), the phyto-estrogens genistein (GEN), 8-prenyl naringenin (8PN) and zearalenon (ZEA), four derivatives of benz(*a*)anthracene-3,9-diol and eight estrogenic mono-hydroxylated PAH metabolites. We obtained an excellent linear correlation ( $r^2 = 0.94$ ) between experimental (competitive ER binding assay) and calculated binding energies, with  $K_d$  values ranging from 0.15 mM to 30 pM, a 5.000.000-fold difference in binding affinity.

Subsequently, a test set ( $n = 12$ ) was used to examine the predictive value of our model. This set consisted of the synthetic estrogen 5,11-*cis*-diethyl-5,6,11,12-tetrahydrochrysene-2,8-diol (THC), daidzein (DAI), equol (EQU) and apigenin (API), chlordecone (KEP), progesterone (PRG), several mono- and di-hydroxylated PAH metabolites and two brominated biphenyls. The predicted binding affinities of these estrogenic compounds were in very good agreement with the experimental values (average deviation  $0.61 \pm 0.4$  kcal/mol).

In conclusion, our LIE model provides a very good method for prediction of absolute ligand binding affinities, as well as binding orientation of ligands.

## 1 Introduction

Estrogens play a critical role in growth, development and maintenance of a diverse range of tissues. The effects of estrogens are mediated by the estrogen receptor (ER), a ligand-activated transcription factor<sup>[142]</sup>. Binding of agonists induces a conformational change of the ER, enabling the receptor to homodimerise. The dimer is then translocated to the nucleus, where it enhances gene transcription<sup>[134]</sup>. Two ER isoforms have been identified and crystallized, ER $\alpha$  and ER $\beta$ , that show great resemblance in overall structure. Both bind the endogenous estrogen, 17 $\beta$ -estradiol (E2), but show different tissue expression and distinct responses to various agonist and antagonists<sup>[108,109]</sup>. Binding of agonists induces a specific orientation of the helix 12 (H12), thereby closing the narrow binding site and allowing co-regulators to bind<sup>[279]</sup>. Antagonist binding, however, induces a different orientation of H12, preventing alignment over the binding site and transactivation<sup>[134,145]</sup>.

Exposure to environmental estrogens has been proposed as a risk factor for disruption of reproductive development and tumorigenesis of humans and wildlife<sup>[4]</sup>. In recent years, a wide variety of structurally diverse environmental compounds have been identified as estrogens. Among these compounds are natural steroid hormones, pharmaceuticals, industrial chemicals including polychlorinated biphenyls (PCBs), pesticides and polycyclic aromatic hydrocarbons (PAHs). PAHs have been considered a health risk for wild life and humans for a long time<sup>[207,280]</sup>. This is mainly due to their carcinogenic properties, that result from covalent binding to DNA and other macromolecules after bio-activation to reactive metabolites<sup>[281-283]</sup>. However, it has been recently shown that bio-activation of the PAHs benzo[a]pyrene (BaP) and chrysene (CHN) may also lead to the formation of hydroxylated metabolites with estrogenic activity<sup>[53,284]</sup>. Similarly, formation of hydroxylated metabolites with estrogenic activity has also been observed for chlorinated biphenyls<sup>[78,284]</sup> and metabolites of pesticides such as DDT and methoxychlor<sup>[176,177]</sup>.

In light of the large variety of structurally diverse compounds that bind to the ER $\alpha$ , it is of great value to develop a reliable method to predict ER $\alpha$  binding affinity of compounds. For the ER, several approaches to calculate ligand binding affinities have been used over the last decade, ranging from ligand-based comparative molecular field analysis (CoMFA) studies<sup>[191]</sup> to protein-based methods using empirical scoring functions<sup>[192]</sup> and molecular dynamics simulations (MD), using free energy perturbation methods (FEP)<sup>[196]</sup>. However, accurate prediction of binding affinity of novel estrogens remains difficult, not in the least since most of the approaches are limited in their applicability to compounds that have a

common template structure. Furthermore, conclusive prediction of favoured binding orientation is generally ignored in these studies.

A recent method for estimation of binding affinities is the linear interaction energy (LIE) approximation, which was first described and further extended by Åqvist *et al.*<sup>[200-202]</sup>. The LIE model relies on the assumption that the  $\Delta G$  depends linearly on changes in the Van der Waals and electrostatic energy of the system. This is supported by observations that the free energy of solvation on nonpolar moieties often scale linearly with respect to variables characterizing the size of the solute. The concept of the LIE approach is to separately evaluate the electrostatic and Van der Waals interaction energies of the ligand in the bound and free state. For this purpose, two MD simulations are carried out: one with the ligand bound to the (solvated) receptor and one with the unbound ligand in solvent. Subsequently, averages of interaction energies between the ligand and its surroundings are analysed. The calculated binding free energy ( $\Delta G_{calc}$ ) is obtained from the averages as<sup>[201]</sup>:

$$\Delta G_{calc} = \alpha * \Delta E_{INT}^{VDW} + \beta * \Delta E_{INT}^{EL} = \alpha * (E_{INT_{BOUND}}^{VDW} - E_{INT_{FREE}}^{VDW}) + \beta * (E_{INT_{BOUND}}^{EL} - E_{INT_{FREE}}^{EL}) \quad (1)$$

where  $E_{INT}^{VDW}$  denotes the Van der Waals interaction energy and  $E_{INT}^{EL}$  electrostatic interaction energy, of the ligand bound to the receptor (*BOUND*) and the ligand free in solution (*FREE*).

Obtaining suitable values for  $\alpha$  and  $\beta$  has been subject of several investigations described recently. The  $\alpha$  value strongly depends on the system of interest, the force field employed and the computational methods that are applied. A proper  $\alpha$  value must therefore first be determined by comparing calculated and experimentally estimated binding affinities. Originally, the LIE method was introduced with a fixed value of 0.5 for  $\beta$ <sup>[200]</sup>. However, an extensive study on the solvation energy of various series of small substrates with different number of electronegative groups, showed that  $\beta$  significantly differs between substrates that vary in the number of strong electronegative groups. For example,  $\beta$  was shown to decrease with the number of hydroxyl groups<sup>[201]</sup>. This might be due to an overestimation of the force field of electrostatic interactions between these groups and their surroundings, possibly because polarization effects are not properly described by force fields. Therefore, like  $\alpha$ , the value of  $\beta$  also depends on the system under investigation and the force field used. In conclusion, in order to set up a LIE model for the prediction of ligand binding affinities using a particular force field, it is necessary to perform a double regression ( $\alpha$  and  $\beta$ ) analysis of a set of compounds, and their experimental  $\Delta G$  values.

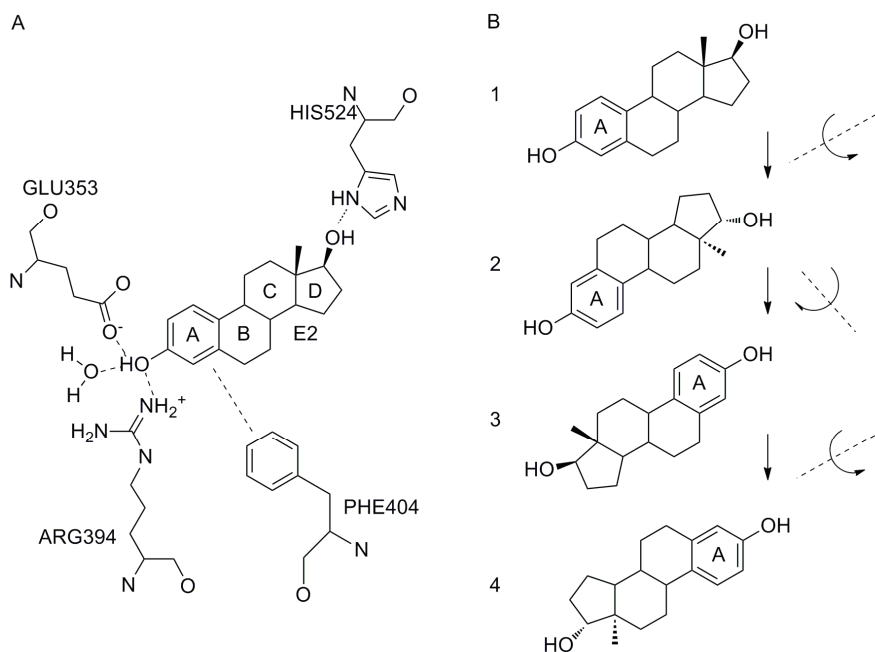


**Figure 1:** **A:** Schematic view of hydrogen bonding and aromatic interactions (dashed lines) between estradiol (E2) and several residues (Glu353, Arg394, His524 and Phe404) of the ER $\alpha$  and a water molecule. E2 is depicted in orientation 1. **B:** The four ligand docking orientations used in the present study, with E2 as an example.

In the present study, MD simulations (100 ps) of receptor-bound ligands as well as ligands free in water were carried out. In addition, to investigate the favoured binding mode, ligands were manually docked in the crystal structure of the ER $\alpha$  LBD in all possible orientations, as illustrated for E2 in Figure 1A and 1B. To calibrate our model, we used the endogenous estrogen E2, the synthetic estrogens diethylstilbestrol (DES) and 11 $\beta$ -chloro-ethyl-estradiol (E2-Cl), the steroid 16 $\alpha$ -E2 (estriol, EST), the phyto-estrogens genistein (GEN), 8-prenyl naringenin (8PN) and zearalenon (ZEA), four derivatives of benz(a)anthracene-3,9-diol and eight estrogenic mono-hydroxylated PAH metabolites (Figure 2A). The binding affinities for the ER $\alpha$  in this training set ( $n = 19$ ) range from 0.15 mM to 30 pM. For the prediction of binding affinities of compounds for the ER $\alpha$ , the synthetic estrogen 5,11-*cis*-diethyl-5,6,11,12-tetrahydrochrysene-2,8-diol (THC), the phyto-estrogens daidzein (DAI), equol (EQU) and apigenin (API), the pesticide chlordecone (kepone, KEP), the endogenous hormone progesterone (PRG), the PAH metabolites 3-hydroxy-benzo[a]pyrene (3-OH-BaP), 3-hydroxy-chrysene (3-OH-CHN), 7,8-dihydroxy-BaP (7,8-diOH-BaP) and 1,2-dihydroxy-CHN (1,2-diOH-CHN) and two brominated biphenyls (2,2'-dibromo-biphenyl, 2DBB, and 4,4'-dibromo-biphenyl, 4DBB) were used as a test set ( $n = 12$ , Figure 2B).

**Figure 2A: Training set**

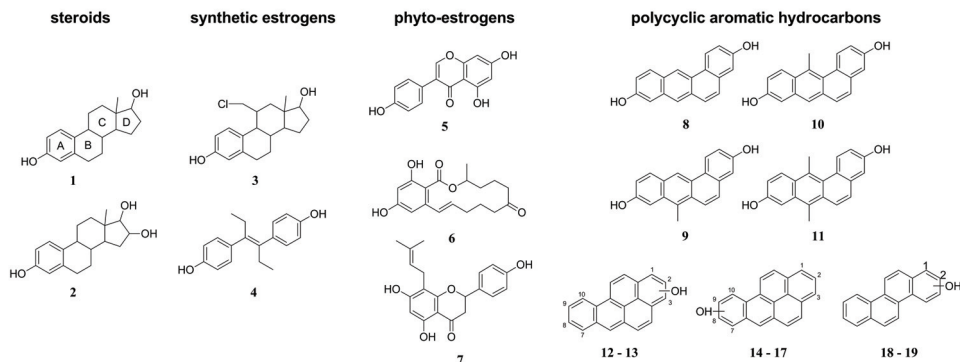


**Figure 2B: Test set**

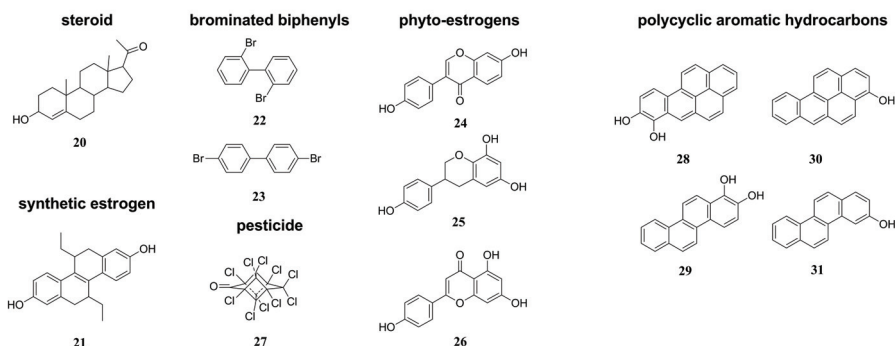


**Figure 2:** Molecular structures and names of estrogenic compounds of the **training set** ( $n = 19$ , Figure 2A) and estrogenic compounds of the **test set** ( $n = 12$ , Figure 2B) used in the present study. Training set: **1**, estradiol (E2); **2**, estradiol (EST); **3**, 11 $\beta$ -chloro-estradiol (E2-Cl); **4**, DES; **5**, genisteine (GEN); **6**, zearalenone (ZEA); **7**, 8-prenyl-naringenin (8PN); **8**, benz[a]anthracene-3,9-diol (BA-diol); **9**, 7-methyl-benz[a]anthracene-3,9-diol (7-MBA-diol); **10**, 12-methyl-benz[a]anthracene-3,9-diol (12-MBA-diol); **11**, 7,12-dimethyl-benz[a]anthracene-3,9-diol (7,12-DMBA-diol); **12-13**, 1- and 2-hydroxy-benzo[a]pyrene (1-OH-BaP, 2-OH-BaP); **14-17**, 7-, 8-, 9- and 10-hydroxy-benzo[a]pyrene (7-OH-BaP, 8-OH-BaP, 9-OH-BaP, 10-OH-BaP); **18-20**, 1- and 2-hydroxy-chrysene (1-OH-CHN, 2-OH-CHN). For benzo[a]pyrene and chrysene derivatives, the numbering indicates the positions of the hydroxyl groups. Test set: **20**, progesterone (PRG); **21**, 5,11-cis-diethyl-5,6,11,12-tetrahydrochrysene-2,8-diol (THC); **22**, 2,2'-dibromo-biphenyl (2DBB); **23**, 4,4'-dibromo-biphenyl (4DBB); **24**, daidzein (DAI); **25**, equol (EQU); **26**, apigenin (API); **27**, kepone (KEP); **28**, 7,8-dihydroxy-benzo[a]pyrene (7,8-diOH-BaP); **29**, 1,2-dihydroxy-chrysene (1,2-diOH-CHN); **30**, 3-hydroxy-benzo[a]pyrene (3-OH-BaP); **31**, 3-hydroxy-chrysene (3-OH-CHN). All structures are shown in orientation 1, as illustrated for E2 in Figure 1B.

## 2 Experimental Methods

### 2.1 Chemicals

<sup>3</sup>[H]-E2 was obtained from Amersham (Buckinghamshire, UK). Dextran (MW 60.000-90.000) was obtained from Duchefa, Haarlem, the Netherlands. 8-Prenylnaringenin was a kind gift from Dr. Fred Stevens, Department of Bioorganic Chemistry, Vrije Universiteit, Amsterdam, The Netherlands<sup>[285]</sup>. Pure hydroxy-benzo[*a*]pyrenes (purity ≥98%) were obtained from the Chemical Carcinogen Reference Standard Repository of the National Cancer Institute (Kansas, USA). Pure hydroxy-chrysenes were kindly provided by Dr. Albrecht Seidel, Biochemical Institute for Environmental Carcinogens, Hamburg, Germany. All other chemicals were purchased from Sigma-Aldrich Co (St Louis, USA).

### 2.2 Competitive ligand binding assay

Competitive binding assays were performed as described before<sup>[185]</sup>. Briefly, compounds were incubated with sheep uterus cytosol and [<sup>3</sup>H]-E2 for 3 hours at 4°C. Receptor-bound [<sup>3</sup>H]-E2 was separated from unbound [<sup>3</sup>H]-E2 by charcoal-dextran absorption and centrifugation and measured in a 1900 Tricarb scintillation counter (Packard Instruments, Perkin Elmer Wellesley, U.S.A.), after the addition of scintillation cocktail (HiSafe 3, Perkin Elmer). The ligand binding affinities ( $K_d$ ) were calculated with Graphpad Prism 3.0 (GraphPad Software Inc., 2000, San Diego, CA). All compounds were tested for binding affinity in our laboratory except for the DMBA-metabolites and 11 $\beta$ -chloro-ethyl-E2 (E2-Cl), for which  $K_d$  values were taken from literature<sup>[150,286]</sup>.

## 3 Computational Details

### 3.1 Ligand parameterisation

For the prediction of ligand binding affinities, docking studies were performed with the various ligands of the training set ( $n=19$ ) and the test set ( $n=12$ ). Selection of the investigated ligands was based on structural diversity and wide range of binding affinities for the ER. Initial structures of the ligands were generated with the xLEaP module of Amber 6.0. Coordinates of crystal structures of ligands were used for E2 (Protein Data Bank (PDB) ID 1ERE), DES (PDB ID 3ERD), GEN (PDB ID 1QKM), ZEA (Cambridge Structural Database, CSD) and THC (PDB ID 1L2J). Subsequently, conformation analysis and subsequent hierarchical clustering were performed using Sybyl 6.7 (Tripos Inc., St Louis,

---

Missouri) to obtain four energy-optimised geometries covering the broadest range of the conformational space of the ligand. Electrostatic potentials were calculated for all conformers using GAMESS (US) at the 6-31G\* level of theory.

In case of E2, EST and ZEA, which consist of a flexible, closed multiple ring system, conformation analyses were performed with Macromodel (Schrödinger, Inc.). In the case of GEN and biphenyls, conformation analysis resulted in one optimal conformation. In these cases, geometry optimisations with several fixed torsions over the rotatable bond between two aromatic rings, were performed with GAMESS at the STO-3G level of theory. Because the hydroxylated metabolites of BaP and CHN are planar, no conformational analysis was performed on the structures of their metabolites, however, two conformations with opposite orientations of the hydroxyl hydrogen in the plane were used for geometry optimisation. For all ligands, the generated optimised structures were used as different conformers in the calculation of electrostatic potentials at the 6-31G\* level of theory. Calculated electrostatic potentials were subsequently applied in the multi-conformational restraint electrostatic potential (RESP) fitting procedure to obtain atomic charges for all compounds<sup>[287]</sup>.

### 3.2 Extra Amber 6.0 ligand parameters

The Amber 6.0 package comprised libraries for all atom types for the amino acids in the LBD of the ER. Most of the atom types used for the ligands were also already parameterised to our satisfaction, except for torsions between non-substituted aromatic and non-aromatic sp<sup>2</sup>-hybridized carbon atoms in DES, GEN, ZEA and two aromatic rings in biphenyls. Their torsional force constants were optimised using an *ab initio* approach. The potential energy surface of rotation over the dihedral as calculated in GAMESS using the STO-3G basis set for geometry optimisations, and the 6-31G\* basis set for energy calculations, compared to the potential energy surface in Amber 6.0 (data not shown) showed that the ideal force constant for the single bond between the two sp<sup>2</sup>-hybridized carbons in Amber should be 4 kcal/mol for GEN, DES and ZEA, and 3 kcal/mol for the biphenyls. Subsequently, these force constants were used in all MD simulations. Optimal bond lengths were based on those found in the crystal structures of GEN and DES, and biphenyls, and set to 1.40 Å and 1.51 Å respectively.

### 3.3 ER $\alpha$ LBD structure

The crystal structure of the LBD (residues Ser 305 to Leu 549) of the ER $\alpha$  complexed with DES (PDB ID 3ERD)<sup>[144]</sup>, was used to build the protein model, and all molecular dynamics simulations were based on this protein structure. Missing side-chains, from surface loops, were modelled using the homology module of InsightII (Biosym, San Diego). The terminal

amino acids were treated as charged. The charges of the ionisable groups were set to correspond to a pH of 7.4, resulting in a net charge of  $-5 e^-$ . Coordinates of six crystallographic water molecules, directly interacting with either the ER residues Glu353, Arg394 or the 3-OH group of DES, were also obtained from the published crystal structure.

### 3.4 Docking of the ligands

Positions of E2 (PDB ID *1ERE*) and DES in the ER LBD from the published crystal structures<sup>[134,144]</sup> were used as templates for the docking of the ligands. Ligands were placed in the binding site of the ER by manual docking, using InsightII. If available, ligand crystal structure coordinates were used, otherwise, low energy conformations obtained by GAMESS were applied. In the direct surroundings of the 'A'-ring of E2, the ER binding site is rather narrow and flat, allowing little variation in the position of the aromatic ring. The remainder of the cavity is tolerant for a variety of hydrophobic groups. In order to calculate the preferred orientation of ligands, E2 was docked in four orientations as depicted in Figure 1B. Subsequently, all ligands were docked in four different orientations, thereby fitting aromatic moieties on the 'A'-ring of E2 in its four orientations. Special care was taken in minimizing overlap between protein and ligand, and when appropriate, in adjusting the orientation of OH-groups in the direction of the interacting amino acid residues, in particular Glu353, Arg394 or His524.

The 12-methyl group in 12-methyl-benz[a]anthracene-diol (12-MBA-diol) and 7,12-dimethyl-benz[a]anthracene-diol (BA-diol) causes these structures to be non-planar, with a dihedral involving the methyl group of  $22^\circ$ . This dihedral was observed in several dimethylbenz[a]anthracene (DMBA) crystal structures (CSD) and was found after geometry minimizations in GAMESS (STO-3G). Since the optimal dihedral may be  $22^\circ$  or  $-22^\circ$  and the transition between these states is unlikely to occur in MD simulations due to the rather high energy barrier (17.0 kcal/mol), we docked both isomers in four orientations, resulting in eight final orientations for each of the two benz[a]anthracenes. Similarly, the large bromo-substituents in the biphenyl structures prohibit complete rotation over the single bond connecting the phenyl rings. Therefore, these compounds were also docked in eight orientations. Due to the large bromo-substituents, some of these orientations, however, experienced severe steric hindrance and these were not included in further studies.

### 3.5 MD simulations of ligands bound to the ER and free ligands in water

The starting structure of each receptor-ligand was solvated in water using the tLEaP module of Amber 6.0. The complex was surrounded by a rectangular box of equilibrated water molecules, based on the TIP3P water model<sup>[288]</sup>. The minimum distance between

---

the complex and the boundaries was 6 Å, resulting in typical box volume sizes of about  $3.0 \times 10^6 \text{ Å}^3$  and contained circa 20,000 atoms including ER and ligand. All calculations were carried out in the Sander module of Amber 6.0, under periodic boundary conditions with a cut-off distance of 10.0 Å.

Subsequently, MD simulations were performed to equilibrate the total volume of the water box for 20 ps. MD runs were performed at constant pressure (1 atm) and constant temperature (300K). During equilibration, positional restraints were applied on the backbone  $C_\alpha$ 's of the ER and the crystal waters in the ER to fix their Cartesian coordinates. After the system had adapted suitable volume and pressure, an energy minimization was carried out for 10 ps, using steepest descent for 0.01 ps, followed by the full conjugate gradient minimization method. The positional restraints remained applied to the backbone  $C_\alpha$ 's and the crystal waters during minimization.

Finally, the minimized structures of the solvated receptor-ligand complexes were used for MD simulations. Binding of the ligands to the ER $\alpha$  was simulated for 100 ps at constant pressure. No restraints were applied during these MD runs. During the first 15 ps, the temperature was raised from 0 to 300K. During the subsequent 35 ps, velocities and coordinates were saved every ps. These trajectory files were used for analysis in the Carnal/Anal module of Amber 6.0 for structural stability and hydrogen bonding, and calculation of the energy terms for the linear interaction energy method.

Simulations of free ligands in water were performed in a similar protocol. Ligands were solvated by surrounding the ligand by a box of water molecules (TIP3P) with a minimum distance between the ligand and the boundaries of 20 Å, resulting in a box volume of about  $1.5 \times 10^6 \text{ Å}^3$  with circa 10,000 atoms. All calculations were carried out under periodic boundary conditions with a cut-off distance of 10.0 Å. Equilibration of the water box (20 ps), minimization (10 ps) and subsequent MD simulations (100 ps) were carried out as described for the receptor-ligand complex. No restraints were applied. Per ligand 50 trajectory files were obtained and the last 35 (constant temperature) were used for analysis.

## 4 Results

### 4.1 Structural analysis of MD simulations

The use of relatively short MD simulations of 100 ps allowed us to investigate many different binding orientations at relatively low computational cost. Because 100 ps is rather short for extensive studies on protein dynamics, equilibration and minimisation were carried out before MD in order to obtain stable receptor-ligand complexes for each ligand in each binding orientation tested, using positional restraints on the  $C_\alpha$ 's of the

backbone. Inspection of the trajectories revealed that secondary and tertiary structure of the receptor-ligand complex remained stable during the 100 ps of the MD simulation with this strategy. The averaged root mean square deviation (rmsd) values of the backbone  $C_\alpha$ 's compared to the initial conformation were found to be stable after the first 30 ps of the MD run for almost all simulations. Rmsd values of the backbone  $C_\alpha$ 's for all MD simulations compared to the DES-bound crystal structure was rather small, i.e.  $1.26 \pm 0.12$  Å. For some of the biphenyl structures, the protein structure was still slightly diverging after 30 ps of simulation ( $\Delta\text{rmsd} > 0.0025$  Å/ps). Extension with 50 ps led to satisfactory stable ( $\Delta\text{rmsd} < 0.001$  Å/ps) and small rmsd values ( $C_\alpha$ 's  $1.14 \pm 0.10$  Å), which were subsequently analysed over the last 85 ps. These results indicate that during 100 to 150 ps of simulation, the ligand-protein complex remained stable, and that substitution of DES by other ligands does not affect the conformation of the protein.

Analysis of the rmsd values of the heavy atoms of several selected amino acid residues of the binding cavity (343, 346, 349, 350, 353, 384, 387, 388, 391, 394, 404, 424, 521, 524, 525) showed even smaller variations: average rmsd =  $0.98 \pm 0.1$  Å. This indicates that the orientation and conformation of the amino acids directly involved in ligand binding was also well-preserved.

## 4.2 Free energy of binding and hydrogen bonding

Variation in the Van der Waals interaction energy ( $E_{INT}^{VDW}$ ) was smaller during the MD runs with an average standard deviation of circa 10% over 35 frames, than the electrostatic interaction energy ( $E_{INT}^{EL}$ ), showing a standard deviation of more than 20%.

Hydrogen bonding during MD simulations between the ligand and the receptor or the surrounding water molecules was analysed with Carnal/Anal (Amber module for Cartesian coordinates analysis). This revealed that next to the 'regular' hydrogen bonds with the residues Glu353, Arg394 and His524 and a water molecule as seen for DES and E2 in the crystal structures, many ligands also interacted by hydrogen bonding with Leu525, Leu391, Gly521 and Met343. Sporadically, a hydrogen bond interaction was found with Ala350, Met388, Leu346, Leu387 and Met421 (data not shown). The occurrence of hydrogen bonds during the last 70 ps of the MD simulation is shown in Table 1. Hydrogen bonding with other residues than Glu353, Arg394 and His524 is summarised by 'other'. For the residues Glu353, Arg394 and His524 and the water molecule, a percentage of more than 100% indicates that more than one hydrogen bond between the ligand and the amino acid is formed during the simulation. This implies a more stable interaction. In most cases, hydrogen bonding with Glu353, Arg394 and His524 was observed for the orientation with the best Amber interaction energy.

**Table 1A**

Ligand	Orientation	Glu353	Arg394	His524	OTHER	WATER	TOTAL
DES	1	102.9	28.6	40.0	17.1	62.9	251.4
	2	-	28.6	5.7	105.7	100.0	240.0
	4	102.9	17.1	91.4	105.7	2.9	320.0
E2	1	114.3	14.3	97.1	11.4	88.6	325.7
	2	100.0	14.3	94.3	88.6	82.9	380.0
	3	100.0	28.6	100.0	100.0	105.7	434.3
	4	100.0	-	97.1	100.0	14.3	311.4
E2-Cl	1	111.4	25.7	97.1	20.0	91.4	345.7
	2	105.7	31.4	100.0	105.7	51.4	394.3
EST	1	117.1	8.6	40.0	45.7	91.4	302.9
	3	97.1	80.0	-	88.6	2.9	268.6
GEN	1	94.3	60.0	-	108.6	65.7	328.6
	2	102.9	31.4	91.4	100.0	77.1	402.9
	3	120.0	31.4	91.4	154.3	57.1	454.3
	4	100.0	8.6	94.3	0.0	91.4	294.3
8PN	1	-	-	2.9	154.3	-	157.1
	4	111.4	-	68.6	17.1	91.4	288.6
ZEA	2	100.0	-	-	-	-	100.0
BA-diol	1	100.0	23.1	73.1	42.3	92.3	330.8
	2	14.3	14.3	100.0	108.6	97.1	334.3
	3	105.7	45.7	51.4	8.6	91.4	302.9
	4	100.0	31.4	97.1	100.0	-	328.6
7-MBA-diol	1	-	2.9	68.6	5.7	108.6	185.7
	2	-	-	45.7	100.0	54.3	200.0
	3	-	14.3	57.1	102.9	51.4	225.7
	4	111.4	31.4	88.6	28.6	85.7	345.7
12-MBA-diol	1	100.0	46.2	-	76.9	69.2	292.3
	2	100.0	11.4	94.3	22.9	-	228.6
	3	103.9	19.2	50.0	0.0	88.5	261.5
	4	71.4	8.6	62.9	31.4	65.7	240.0
	1a	91.4	37.1	94.3	94.3	88.6	405.7
	2a	100.0	25.7	100.0	105.7	-	331.4
	3a	107.7	30.8	96.2	100.0	84.6	419.2
	4a	102.9	-	62.9	2.9	-	168.6
7,12-DMBA-diol	1	108.6	22.9	94.3	17.2	85.7	328.6
	2	100.0	105.7	-	11.4	68.6	285.7
	3	100.0	25.7	34.3	42.9	94.3	297.2
	4	100.0	22.9	94.3	0.0	85.7	302.9
	1a	100.0	17.1	68.6	0.0	74.3	260.0
	2a	105.7	37.1	100.0	91.4	97.1	431.4
	3a	-	11.4	37.1	97.1	34.3	180.0
	4a	8.6	-	51.4	0.0	97.1	157.1

**Table 1B**

Ligand	Orientation	Glu353	Arg394	His524	OTHER	WATER	TOTAL
<b>1-OH-BaP</b>	1	-	-	-	5.7	100.0	105.7
	2	-	-	-	114.3	-	114.3
	3	-	-	91.4	0.0	-	91.4
	4	-	-	-	0.0	97.1	97.1
<b>2-OH-BaP</b>	1	108.6	57.1	-	0.0	60.0	225.7
	2	100.0	8.6	-	0.0	-	108.6
	3	-	-	100.0	0.0	-	100.0
	4	-	-	14.3	31.4	-	45.7
<b>7-OH-BaP</b>	1	-	-	97.1	0.0	-	97.1
	2	-	-	-	11.4	-	11.4
	3	-	-	-	0.0	100.0	100.0
	4	-	-	-	114.3	-	114.3
<b>8-OH-BaP</b>	1	-	-	82.9	0.0	-	82.9
	2	-	-	57.1	2.9	-	60.0
	3	108.6	71.4	-	0.0	94.3	274.3
	4	100.0	2.9	-	0.0	-	102.9
<b>9-OH-BaP</b>	1	-	-	-	0.0	100.0	100.0
	2	-	-	97.1	0.0	-	97.1
	3	-	-	-	100.0	-	100.0
	4	45.7	-	-	0.0	125.7	171.4
<b>10-OH-BaP</b>	1	-	-	-	0.0	-	0.0
	2	-	-	-	2.9	-	2.9
	3	-	-	-	88.6	-	88.6
	4	-	-	-	100.0	-	100.0
<b>1-OH-CHN</b>	1	74.3	2.9	-	0.0	48.6	125.7
	2	100.0	-	-	0.0	-	100.0
	3	-	-	97.1	0.0	-	97.1
	4	-	-	-	14.3	-	14.3
<b>2-OH-CHN</b>	1	100.0	28.6	-	0.0	88.6	217.1
	2	11.4	11.4	-	0.0	102.9	125.7
	3	-	-	85.7	5.7	-	91.4
	4	-	-	11.4	22.9	-	34.3

**Table 1** (left and right pages): Presence of hydrogen bonds, between ligands and the residues Glu353, Arg394, His524 of the ER $\alpha$  LBD or (any) water molecule during 70 ps of MD simulation. The values represent the percentages of the total time of MD simulation that a particular hydrogen bond was present. Hydrogen bonding with other residues of the ER $\alpha$  (i.e. Leu525, Leu391, Gly521, Met343, Ala350, Met388, Leu346, Leu387 and Met421) is summarised by 'other'. The table presents estrogens from the training set with two (or more) hydroxyl groups only. All simulated orientations were analysed. For the residues Glu353, Arg394 and His524 and the water molecule, a percentage of more than 100% indicates that more than one hydrogen bond between the ligand and the amino acid is formed during the simulation. For an explanation of the orientation numbers see Figure 1B.

---

### 4.3 Binding orientations

For each ligand, generally four different orientations were evaluated for binding to the ER $\alpha$ . A good steric complementarity with the binding site was not achieved for all orientations. In some cases certain orientations showed very large overlap and sterical hindrance with the protein atoms, causing these complexes to be unusable for MD simulations. This occurred with certain orientations of DES, ZEA and 8PN. For all successfully docked orientations, MD simulations were performed and the results of their binding properties are presented in Table 2.

In the case of DES and E2, we found that the most favourable orientation in the ER $\alpha$ , i.e. the orientation with the best interaction energy, was matching the orientation found in the crystal structures for both ligands. Interestingly, our studies showed that the energetically favourable orientation of GEN in the ER $\alpha$  (similar to orientation 3 of E2 in Figure 1) is different from its orientation in the crystal structure of ER $\beta$ . This may be related to the fact that GEN is an agonist for ER $\alpha$  but a partial agonist for ER $\beta$ . Moreover, GEN induces an antagonized receptor conformation, by a different alignment of helix 12 than seen for agonists<sup>[145]</sup>.

### 4.4 Linear interaction energy calculations

The experimental binding energies ( $\Delta G_{\text{exp}}$ ) were calculated from the experimentally determined ligand binding affinities ( $K_d$ ) by eq.2, using the gas constant ( $R$ ) and the temperature ( $T$ ):

$$\Delta G_{\text{exp}} = -RT \ln K_d \quad (2)$$

The  $K_d$  values were determined in a radioligand receptor binding assay with sheep uterus cytosol as a source for the ER.

To obtain values for  $\Delta G_{\text{calc}}$ , Van der Waals ( $E_{\text{INT}}^{\text{VDW}}$ ) and electrostatic ( $E_{\text{INT}}^{\text{EL}}$ ) interaction energies between the ligand and its environment were calculated for all trajectory files from the MD simulation. The interaction energy ( $E_{\text{INT}}$ ) between a ligand and its surroundings, i.e. receptor-water (eq. 3a), or water only (eq. 3b), is equal to the difference between the energy of the total system ( $E_T$ ) and the sum of the energy of the individual components of the system: water ( $E_W$ ), receptor ( $E_R$ ) and ligand ( $E_L$ ) for the ligand-receptor complex, or water ( $E_W$ ) and ligand for the free ligand ( $E_L$ ) respectively. Thus, the interaction energies ( $E_{\text{INT}}$ ) are described as follows:

$$E_{\text{INT}_{\text{BOUND}}}^{\text{VDW}} + E_{\text{INT}_{\text{BOUND}}}^{\text{EL}} = (E^{\text{VDW}} + E^{\text{EL}})_{T_{\text{BOUND}}} - (E^{\text{VDW}} + E^{\text{EL}})_W - (E^{\text{VDW}} + E^{\text{EL}})_R - (E^{\text{VDW}} + E^{\text{EL}})_L \quad (3a)$$

$$E_{\text{INT}_{\text{FREE}}}^{\text{VDW}} + E_{\text{INT}_{\text{FREE}}}^{\text{EL}} = (E^{\text{VDW}} + E^{\text{EL}})_{T_{\text{FREE}}} - (E^{\text{VDW}} + E^{\text{EL}})_W - (E^{\text{VDW}} + E^{\text{EL}})_L \quad (3b)$$

Energy terms were calculated in the Sander module of Amber (acronym for Simulated Annealing with NMR-Derived Energy Restraints), by a single-step energy calculation of the total system and all the separate components, under the same conditions as the MD simulations. Energies were averaged over frames taken every 2 ps from the last 70 ps of the trajectory. Subsequently, Amber interaction energies ( $\Delta E_{AMBER}$ ) were calculated for any orientation  $i$  by eq. 4:

$$\Delta E_{AMBER_i} = (E_{INT_{bound,i}}^{VDW} - E_{INT_{free}}^{EL}) + (E_{INT_{bound,i}}^{VDW} - E_{INT_{free}}^{EL}) = E_{INT_i}^{VDW} + E_{INT_i}^{EL} \quad (4)$$

In order to include all orientations of each compound in our model,  $\Delta E_{AMBER}$  values for the different orientations were used for calculation of a Boltzman weight factor ( $p_i$ ) for orientation  $i$  by

$$p_i = \left( e^{-\Delta E_{AMBER_i} / k_B T} \right) / \sum_i \left( e^{-\Delta E_{AMBER_i} / k_B T} \right) \quad (5)$$

where  $k_B$  is the Boltzman constant (kcal/mol/K) and  $T$  the temperature (K). The experimental  $\Delta G_{exp}$  values, the calculated  $\Delta E_{INT}^{VDW}$  and  $\Delta E_{INT}^{EL}$  values and the Boltzman factors (weighing ( $\Delta E_{INT}^{VDW} + \Delta E_{INT}^{EL}$ ) of each individual orientation) were then applied in a double linear regression analysis using the fit function of the XLSTAT tool (XLSTAT4.4, <http://www.xlstat.com>) in Microsoft Excel 2000. Using this tool, the Boltzman weight factors can be used in the double regression analysis. Optimal  $\alpha$  and  $\beta$  values are calculated via eq. 6:

$$\Delta G_{exp} = \alpha * \Delta E_{INT_i}^{VDW} + \beta * \Delta E_{INT_i}^{EL} \quad (6)$$

First, ligands with two or more OH-groups were used for the calculation of  $\alpha$  and  $\beta$  specific for two or more OH-groups. Subsequently, a specific  $\beta$  was calculated for ligands with one OH-group using the previously obtained  $\alpha$ . Applying the optimal values for  $\alpha$  and  $\beta$  to the averaged Van der Waals and electrostatic energy terms in eq. 1,  $\Delta G_{calc_i}$  for each orientation was obtained. The final binding energy ( $\Delta G_{calc}$ ) of a ligand was obtained by summation of the binding energies of each individual orientation multiplied by the Boltzman weight factor ( $p_i$ ):

$$\Delta G_{calc} = \sum (p_i * \Delta G_{calc_i}) \quad (7)$$

**Table 2A:** Ligands of training set with  $\geq 2$  OH-groups

Ligand	Or.	$E^{\text{VDW}}$	$E^{\text{EL}}$	$E^{\text{VDW}}$	$E^{\text{EL}}$	$\Delta E_{\text{AMBER}}$	$p_i$	$p_i * \Delta G_{\text{calc}, i}$	$\Delta G_{\text{calc}}$	$\Delta G_{\text{exp}}$
		<i>receptor-bound</i>		<i>free</i>						
DES	1	-40.44	-23.04	-21.53	-31.51	-10.43	0.27	-3.78		
	2	-38.22	-19.69	-21.53	-31.51	-4.87	0.00	0.00	-12.54	-12.55
	4	-37.32	-26.74	-21.53	-31.51	-11.02	0.73	-8.76		
E2	1	-39.60	-27.12	-23.12	-32.74	-10.86	0.79	-9.78		
	2	-38.36	-27.57	-23.12	-32.74	-10.08	0.21	-2.46	-12.24	-12.40
	3	-37.59	-23.39	-23.12	-32.74	-5.12	0.00	0.00		
	4	-38.76	-19.88	-23.12	-32.74	-2.78	0.00	0.00		
E2-Cl	1	-44.69	-25.64	-26.40	-32.11	-11.83	0.99	-13.66	-13.74	-14.42
	2	-41.30	-26.15	-26.40	-32.11	-8.94	0.01	-0.09		
EST	1	-42.70	-24.23	-23.21	-43.23	-0.49	1.00	-12.23	-12.23	-12.20
	3	-41.31	-18.02	-23.21	-43.23	7.12	0.00	0.00		
GEN	1	-36.12	-25.43	-20.14	-40.22	-1.19	0.00	-0.01		
	2	-31.72	-27.07	-20.14	-40.22	1.58	0.00	0.00	-9.78	-9.39
	3	-34.21	-31.37	-20.14	-40.22	-5.21	0.81	-7.89		
	4	-34.29	-30.44	-20.14	-40.22	-4.36	0.19	-1.87		
8PN	1	-48.51	-9.61	-26.87	-42.03	10.79	0.00	0.00	-10.19	-11.02
	4	-43.83	-23.28	-26.87	-42.03	1.80	1.00	-10.19		
ZEA	2	-44.29	-17.70	-26.27	-35.85	0.12	1.00	-11.19	-11.19	-11.04
BA-diol	1	-38.55	-17.08	-21.66	-34.94	-5.83	0.85	-7.44		
	2	-37.23	-14.19	-21.66	-34.94	-2.42	0.00	-0.02	-8.66	-9.15
	3	-38.77	-13.17	-21.66	-34.94	-2.04	0.00	-0.01		
	4	-38.87	-24.76	-21.66	-34.94	-4.78	0.15	-1.18		
7-MBA-diol	1	-33.84	-28.59	-23.12	-32.88	0.38	0.00	0.00		
	2	-34.25	-24.77	-23.12	-32.88	4.59	0.00	0.00	-11.33	-11.59
	3	-34.54	-24.09	-23.12	-32.88	4.07	0.00	0.00		
	4	-33.20	-28.17	-23.12	-32.88	-7.63	1.00	-11.33		
12-MBA-diol	1	-37.19	-22.58	-21.44	-37.32	-1.01	0.00	-0.01		
	2	-39.34	-23.48	-21.44	-37.32	-4.06	0.11	-1.34		
	3	-38.19	-23.03	-21.44	-37.32	-2.46	0.01	-0.08		
	4	-36.60	-18.64	-21.44	-37.32	3.53	0.00	0.00	-10.42	-9.36
	1a	-36.25	-26.26	-21.44	-37.32	-3.74	0.07	-0.66		
	2a	-36.34	-27.59	-21.44	-37.32	-5.16	0.72	-7.41		
	3a	-35.70	-27.02	-21.44	-37.32	-3.96	0.09	-0.91		
	4a	-37.18	-20.93	-21.44	-37.32	0.66	0.00	0.00		
7,12-DMBA-diol	1	-36.73	-27.00	-24.28	-31.92	-7.53	0.48	-4.46		
	2	-39.83	-23.44	-24.28	-31.92	-7.08	0.23	-2.54		
	3	-39.97	-21.32	-24.28	-31.92	-5.10	0.01	-0.09		
	4	-37.44	-25.56	-24.28	-31.92	-6.80	0.14	-1.36	-9.65	-8.81
	1a	-40.13	-21.41	-24.28	-31.92	-5.35	0.01	-0.14		
	2a	-35.65	-27.28	-24.28	-31.92	-6.73	0.13	-1.07		
	3a	-42.02	-13.03	-24.28	-31.92	1.15	0.00	0.00		
	4a	-39.05	-13.23	-24.28	-31.92	3.92	0.00	0.00		

**Tabel 2B:** Ligands of training set with 1 OH-group

Ligand	Or.	$E^{\text{VDW}}$	$E^{\text{EL}}$	$E^{\text{VDW}}$	$E^{\text{EL}}$	$\Delta E_{\text{AMBER}}$	$p_i$	$p_i * \Delta G_{\text{calc}, i}$	$\Delta G_{\text{calc}}$	$\Delta G_{\text{exp}}$
		<i>receptor-bound</i>		<i>free</i>						
<b>1-OH-BaP</b>	1	-37.02	-14.34	-24.48	-21.28	-5.61	0.99	-7.33	-7.37	-6.58
	2	-37.19	-8.31	-24.48	-21.28	0.25	0.00	0.00		
	3	-36.71	-11.53	-24.48	-21.28	-2.49	0.01	-0.03		
	4	-38.39	-8.43	-24.48	-21.28	-1.07	0.00	0.00		
<b>2-OH-BaP</b>	1	-34.87	-23.40	-24.71	-23.35	-10.20	1.00	-8.38	-8.38	-7.51
	2	-33.93	-17.21	-24.71	-23.35	-3.08	0.00	0.00		
	3	-36.42	-11.83	-24.71	-23.35	-0.19	0.00	0.00		
	4	-39.32	-6.70	-24.71	-23.35	2.05	0.00	0.00		
<b>7-OH-BaP</b>	1	-35.83	-12.39	-24.06	-22.21	-1.95	0.10	-0.54	-6.13	-5.87
	2	-38.21	-5.65	-24.06	-22.21	2.41	0.00	0.00		
	3	-36.14	-13.39	-24.06	-22.21	-3.26	0.90	-5.57		
	4	-38.44	-7.53	-24.06	-22.21	0.31	0.00	-0.01		
<b>8-OH-BaP</b>	1	-35.70	-10.04	-23.44	-22.93	0.63	0.00	0.00	-8.29	-7.85
	2	-37.23	-10.48	-23.44	-22.93	-1.35	0.00	0.00		
	3	-34.25	-21.50	-23.44	-22.93	-9.38	1.00	-8.28		
	4	-36.79	-14.83	-23.44	-22.93	-5.25	0.00	-0.01		
<b>9-OH-BaP</b>	1	-36.31	-9.55	-24.54	-23.03	1.72	0.00	0.00	-6.56	-6.85
	2	-35.91	-11.70	-24.54	-23.03	-0.04	0.01	-0.02		
	3	-37.41	-8.45	-24.54	-23.03	1.72	0.00	0.00		
	4	-37.68	-13.07	-24.54	-23.03	-3.17	0.99	-6.54		
<b>10-OH-BaP</b>	1	-37.76	-3.91	-25.51	-18.95	2.79	0.00	0.00	-6.31	-5.26
	2	-38.06	-5.42	-25.51	-18.95	0.98	0.00	-0.01		
	3	-36.71	-7.57	-25.51	-18.95	0.18	0.01	-0.03		
	4	-38.46	-8.75	-25.51	-18.95	-2.75	0.99	-6.27		
<b>1-OH-CHN</b>	1	-32.45	-17.95	-24.48	-21.28	-4.65	0.36	-1.84	-4.41	-6.09
	2	-29.04	-21.67	-24.48	-21.28	-4.96	0.61	-2.39		
	3	-33.94	-15.06	-24.48	-21.28	-3.25	0.03	-0.18		
	4	-34.69	-5.70	-24.48	-21.28	5.37	0.00	0.00		
<b>2-OH-CHN</b>	1	-33.17	-19.60	-24.71	-23.35	-4.70	1.00	-5.36	-5.36	-8.51
	2	-32.97	-12.03	-24.71	-23.35	3.06	0.00	0.00		
	3	-33.97	-10.44	-24.71	-23.35	3.65	0.00	0.00		
	4	-34.26	-6.46	-24.71	-23.35	7.35	0.00	0.00		

**Table 2:** Overview of the Van der Waals ( $E^{\text{VDW}}$ ) and electrostatic ( $E^{\text{EL}}$ ) interaction energy contributions to the interaction energy ( $\Delta E_{\text{AMBER}}$ ), the calculated ( $\Delta G_{\text{calc}}$ ) and the experimentally ( $\Delta G_{\text{exp}}$ ) derived free energies of binding for binding of 19 ligands to the ER $\alpha$ , in all orientations (Or.) simulated with MD. The  $\Delta G_{\text{exp}}$  values were calculated from  $K_d$  values determined using a sheep uterus cytosol radioligand binding assay. Structures and names of ligands and orientations are given in Figure 2A and Figure 1 respectively. Table 2A presents ligands in the training set with two or more hydroxyl groups, table 2B shows ligands with one hydroxyl group.  $p_i$  denotes the weight factor from the Boltzman distribution based on  $\Delta E_{\text{AMBER}}$ .  $p_i * \Delta G_{\text{calc}, i}$  represents the binding free energy for orientation  $i$  calculated calculated with the LIE method, using a common  $\alpha = 0.82$  and  $\beta_{\text{OH} \geq 2} = 0.20$  (number of OH groups  $\geq 2$ ) or  $\beta_{\text{OH}=1} = 0.43$  (number of OH groups =1). Per ligand, the final  $\Delta G_{\text{calc}}$  equals the sum of  $p_i * \Delta G_{\text{calc}, i}$ . All  $\Delta E$  and  $\Delta G$  values are given in kcal/mol.

---

#### 4.5 Training set

For estrogens with two or more OH-groups the best fitting values were:  $\alpha = 0.82$  and  $\beta_{\text{OH}\geq 2} = 0.20$ . For estrogens with one OH-group, single regression analysis using  $\alpha = 0.82$  yielded a value for  $\beta_{\text{OH}=1}$  of 0.43. When no fixed value for  $\alpha$  was used, double regression analysis yielded optimal values of  $\alpha = 0.84$  and  $\beta_{\text{OH}=1} = 0.46$ . This indicates the LIE method results in similar parameters, independently of the chosen data set. Nevertheless, one value for  $\alpha$  (0.82) was used for all compounds.

Upon correlation of  $\Delta G_{\text{calc}}$  with  $\Delta G_{\text{exp}}$ , a linear correlation coefficient ( $r^2$ ) of 0.94 was obtained (Figure 3) when all orientations of each ligand were taken into account and Boltzman weighting based upon the Amber interaction energy was applied. If the regression analysis was performed also taking all orientations in account, but weighted evenly, the correlation between calculated and experimental  $\Delta G$  values drops ( $r^2 = 0.87$ ). This is to be expected, because there is a large bias due to overestimated influence of less favourable orientations on the regression analysis. When  $\Delta G_{\text{calc}}$  values were calculated based only on the orientation with the best interaction energy of each ligand in the ER, also an excellent correlation was found between calculated  $\Delta G_{\text{calc}}$  value vs. experimental binding energy ( $r^2 = 0.94$ ).

#### 4.6 Prediction

The optimised LIE parameters ( $\alpha = 0.82$ ,  $\beta_{\text{OH}\geq 2} = 0.20$  and  $\beta_{\text{OH}=1} = 0.43$ ) were applied to a test set of compounds with known estrogenic activity, namely THC, API, DAI and EQU and the PAH metabolites 1,2-di-OH-CHN and 7,8-di-OH-BaP, all compounds with two or more OH groups. Two mono-hydroxylated compounds, 3-OH-BaP and 3-OH-CHN, were also investigated. Finally, the binding of four ligands without hydroxyl groups, KEP, 2DBB, 4DBB and PRG, was investigated (see Figure 2B for structures). Interaction energies were obtained from similar MD simulations as described for the other compounds. The results of the interaction energy and  $\Delta G_{\text{calc}}$  calculations are shown in Table 3. The  $\Delta G_{\text{calc},i}$  values were calculated using the optimal  $\alpha$  (0.82) and the two OH-dependent  $\beta$ -values (0.20 and 0.43) obtained by linear regression analysis as described above. For ligands without hydroxyl group, no  $\beta$ -parameter could be optimised, therefore the theoretical value for  $\beta$  was used, i.e.  $\beta_{\text{OH}=0} = 0.5$ . The calculated  $\Delta G$  values are plotted against the experimental  $\Delta G$  values in Figure 3, with the open symbols representing the training set of compounds. The predicted  $\Delta G$  values for these compounds are all in very good agreement with the experimental values (average deviation  $0.61 \pm 0.4$  kcal/mol and linear correlation coefficient between experimental and calculated  $\Delta G$  values,  $r^2 = 0.85$ ,  $n = 10$ ) (Table 3 and Figure 3). THC was originally docked in the ER in 4 orientations, however, analysis of the

MD runs showed that the ethyl moieties of the centro-symmetrical molecule showed a large flexibility such that THC in orientation 1 and 4 adopted the same conformation, as well as orientations 2 and 3. Therefore, the interaction energy values for orientation 1 and 4, and 2 and 3 were averaged. The predicted orientation of binding of THC (orientation 1 and 4) to the ER is identical to the observed binding orientation in the crystal structure published by Shiau *et al*<sup>[289]</sup>. The LIE model predicted very low ER $\alpha$  affinity ( $K_d = 10$  mM) for PRG. However, due to solubility problems, the highest concentration that could be tested in the ER binding assay was 0.3 mM, which showed no significant displacement of radiolabeled estradiol. The LIE model predicted moderate ER $\alpha$  affinity for 4DBB (Table 3), while no affinity was observed *in vitro*. Inspection of the trajectory files showed that the binding cavity is much bigger than the planar 4DBB structure. Calculating interactions with extra vacuum in the binding site may be the reason for the observed high interaction energy. Taking into account extra water molecules in the binding cavity may represent reality better, however, we have not included this in our model.

**Table 3A:** calculated binding energies per orientation

Ligand	Nr. of OH	Or.	$E^{VDW}$ <i>receptor-bound</i>	$E^{EL}$ <i>receptor-bound</i>	$E^{VDW}$ <i>free</i>	$E^{EL}$ <i>free</i>	$\Delta E_{AMBER}$	$p_i$	$\Delta G_{calc, i}$
THC	2	1	-44.23	-22.83	-27.82	-30.23	-9.02	1.00	-12.03
		2	-42.90	-20.12	-27.82	-30.23	-4.97	0.00	-10.38
API	3	1	-35.53	-20.36	-20.30	-37.88	2.30	0.47	-4.26
		2	-36.45	-19.49	-20.30	-37.88	2.23	0.53	-5.05
		3	-36.57	-15.77	-20.30	-37.88	5.84	0.00	-0.01
		4	-35.63	-14.78	-20.30	-37.88	7.77	0.00	0.00
DAI	3	1	-31.47	-22.87	-19.88	-42.34	7.88	0.00	0.00
		2	-30.70	-30.79	-19.88	-42.34	0.72	0.99	-6.54
		3	-31.03	-27.42	-19.88	-42.34	3.77	0.01	-0.04
		4	-31.08	-26.52	-19.88	-42.34	4.62	0.00	-0.01
EQU	2	1	-33.46	-19.62	-20.22	-50.30	17.44	0.00	-0.01
		2	-34.96	-16.27	-20.22	-50.30	19.29	0.00	0.00
		3	-34.89	-21.90	-20.22	-50.30	13.74	0.87	-5.52
		4	-37.05	-18.61	-20.22	-50.30	14.86	0.13	-0.98
1,2-diOH-CHN	2	1	-33.33	-22.78	-23.07	-25.43	-7.61	1.00	-7.91
		2	-37.20	-10.75	-23.07	-25.43	0.55	0.00	0.00
		3	-37.67	-6.60	-23.07	-25.43	4.23	0.00	0.00
		4	-36.10	-9.85	-23.07	-25.43	2.55	0.00	0.00
7,8-diOH-BaP	2	1	-38.68	-17.81	-24.89	-34.22	2.63	0.00	0.00
		2	-36.91	-25.66	-24.89	-34.22	-3.45	1.00	-8.17
		3	-40.57	-15.51	-24.89	-34.22	3.04	0.00	0.00
		4	-35.35	-22.38	-24.89	-34.22	1.39	0.00	0.00
3-OH-BaP	1	1	-37.62	-8.26	-24.06	-21.92	0.09	0.00	0.00
		2	-34.87	-18.07	-24.06	-21.92	-6.97	1.00	-7.27
		3	-36.35	-12.08	-24.06	-21.92	-2.45	0.00	0.00
		4	-38.69	-8.83	-24.06	-21.92	-1.55	0.00	0.00
3-OH-CHN	1	1	-33.99	-20.79	-24.06	-21.92	-8.81	1.00	-7.70
		2	-32.26	-18.20	-24.06	-21.92	-4.49	0.00	0.00
		3	-35.87	-7.58	-24.06	-21.92	2.52	0.00	0.00
		4	-31.27	-15.42	-24.06	-21.92	-0.72	0.00	0.00
KEP	0	1	-40.98	0.12	-28.36	-5.79	-6.71	0.00	-0.02
		2	-42.77	-1.59	-28.36	-5.79	-10.21	1.00	-9.73
2DBB	0	1a	-28.29	-2.23	-20.37	-6.94	-3.22	0.03	-0.13
		1b	-28.22	-1.03	-20.37	-6.94	-1.95	0.00	-0.01
		1c	-28.42	-0.70	-20.37	-6.94	-1.82	0.00	-0.01
		2	-29.40	-3.16	-20.37	-6.94	-5.25	0.96	-5.33
4DBB	0	1a	-32.19	-1.62	-19.78	-5.52	-8.52	0.28	-2.36
		1b	-31.65	-1.69	-19.78	-5.52	-8.04	0.13	-1.00
		1c	-30.91	-1.78	-19.78	-5.52	-7.39	0.04	-0.31
		1d	-32.31	-1.90	-19.78	-5.52	-8.90	0.54	-4.63
PRG	0	1	-49.75	-5.53	-29.54	-27.77	2.03	1.00	-5.52

**Table 3** (left and below): Overview of the Van der Waals ( $E^{\text{VDW}}$ ) and electrostatic ( $E^{\text{EL}}$ ) interaction energy contributions to the interaction energy ( $\Delta E_{\text{AMBER}}$ ) (**Table 3A**), the calculated ( $\Delta G_{\text{calc}}$ ) and the experimentally ( $\Delta G_{\text{exp}}$ ) derived free energies of binding (**Table 3B**) of the test set ( $n = 12$ ) for binding to the ER $\alpha$ , in all orientations (Or.) simulated with MD. The  $\Delta G_{\text{exp}}$  values were calculated from  $K_d$  values determined using a sheep uterus cytosol radioligand binding assay. Structures and names of ligands and orientations are shown in Figure 2B and Figure 1 respectively.  $\Delta G_{\text{calc},i}$  represents the binding free energy for orientation  $i$  calculated with the LIE method, using  $\alpha = 0.82$  and  $\beta_{\text{OH}\geq 2} = 0.20$  (number of OH groups  $\geq 2$ ),  $\beta_{\text{OH}=1} = 0.43$  (number of OH groups =1) or  $\beta_{\text{OH}=0} = 0.5$  (no OH groups). Per ligand, the final  $\Delta G_{\text{calc}}$  equals the sum of  $p_i \cdot \Delta G_{\text{calc},i}$ . All  $\Delta E$  and  $\Delta G$  values are given in kcal/mol.  $K_d$  is expressed in mol/L. No  $\Delta G_{\text{exp}}$  could be obtained for PRG and 4DBB (highest concentration that could be tested was 0.3 mM).

**Table 3B:** Binding energies and affinities per compound

Ligand	$\Delta G_{\text{calc}}$	$\Delta G_{\text{exp}}$	$K_d$	$K_d$
	Predicted	Observed	Predicted	Observed
THC	-12.03	-11.70	$1.7 \cdot 10^{-9}$	$3.0 \cdot 10^{-9}$
API	-9.32	-8.49	$1.6 \cdot 10^{-7}$	$6.6 \cdot 10^{-7}$
DAI	-6.59	-7.18	$1.6 \cdot 10^{-5}$	$5.9 \cdot 10^{-6}$
EQU	-6.52	-6.82	$1.8 \cdot 10^{-5}$	$1.1 \cdot 10^{-5}$
1,2-diOH-CHN	-7.91	-8.31	$1.7 \cdot 10^{-6}$	$8.8 \cdot 10^{-7}$
7,8-diOH-BaP	-8.17	-6.65	$1.1 \cdot 10^{-6}$	$1.4 \cdot 10^{-5}$
3-OH-BaP	-7.27	-8.19	$5.1 \cdot 10^{-6}$	$1.1 \cdot 10^{-6}$
3-OH-CHN	-7.70	-7.41	$2.5 \cdot 10^{-6}$	$4.0 \cdot 10^{-6}$
KEP	-9.75	-8.66	$7.8 \cdot 10^{-8}$	$4.9 \cdot 10^{-7}$
2DBB	-5.49	-5.20	$1.0 \cdot 10^{-4}$	$1.6 \cdot 10^{-4}$
4DBB	-8.30	> -4.8	$9.0 \cdot 10^{-7}$	> $3 \cdot 10^{-4}$
PRG	-5.52	> -4.8	$1.0 \cdot 10^{-4}$	> $3 \cdot 10^{-4}$

---

## 5 Discussion

The primary aim of this study was to develop a MD model for the binding of agonists to the ER, in order to accurately predict binding affinity and preferred binding orientation of (xeno)estrogens with a LIE approach.

### 5.1 *Differences between sheep and human ER $\alpha$*

For binding assays, we used ER from sheep uterus cytosol. Binding affinities observed for many ligands towards sheep ER, such as E2, DES, genistein, 8PN and zearalenon, but also other ligands tested in our laboratory, which are not included in this study, were in excellent correspondence with values for binding to human ER $\alpha$  (hER $\alpha$ ) from literature<sup>[147,241]</sup>. The sheep ER $\alpha$  (sER $\alpha$ ) shows highly conserved identity with ER from other mammalian species. Overall homology with human ER $\alpha$  is 91%. However, all specific regions responsible for DNA binding, hormone binding, phosphorylation, nuclear localization and transcription activation are even more conserved, in particular, the DNA binding domain (DBD) shows 100% similarity with hER, and the ligand binding domain (LBD) shows 96.8% identity. In the LBD of human ER $\alpha$  which was used for the MD simulation studies, twelve amino acids differ with sheep ER $\alpha$  (in helix 1 of hER $\alpha$ : 306, 307, in helix 2: 316, 321, loop: 327, in helix 3: 348, start of helix 5: 371, start of helix 10: 467, in helix 11: 502, 507, 510, and 514)<sup>[242]</sup>. Structural alignment of the LBD sequence of sheep ER $\alpha$  with the crystal structure coordinates of human ER $\alpha$  in InsightII showed that none of these amino acids are directly interacting with any of the ligands tested in the MD simulations. Furthermore, the differences between the interchanged residues are relatively small, i.e. sizes, charges and especially hydrophobic properties of the residues are similar between human and sheep ER $\alpha$ . An exception is the neutral Gln 502 in hER $\alpha$ , which is substituted with a charged Arg residue in sheep ER $\alpha$ , nevertheless, its position is on the outer surface of helix 11 and distant from the binding cavity. Therefore, the differences in the amino acid sequence appear to be of no direct consequence to the observed binding affinities of the tested ligands. Thus, we conclude that the use of the ER from sheep uterus cytosol is appropriate for correlation with human ER $\alpha$  modelling studies.

### 5.2 *Effect of temperature on the K<sub>d</sub>*

The MD simulations of ligand binding to the ER were performed at a temperature of 300K, while *in vitro* binding studies were carried out at 277K (4°C). We did not observe significant differences in ER binding affinity of E2, incubated at room temperature (293K)

compared to incubation at 4°C (data not shown). Ligand binding to wild-type ER is known to be very temperature-independent. Several mutations induce temperature-sensitivity of ligand binding characteristics<sup>[290-292]</sup>, but very few naturally occurring temperature-unstable receptor mutants have been identified<sup>[293]</sup>. In addition,  $\Delta G_{\text{calc}}$  is calculated from experimental  $K_d$  values using equation 2. Consequently, the deviation in  $\Delta G_{\text{calc}}$  using  $T = 277\text{K}$  instead of  $T = 300\text{K}$  would be too small (8%) to be significantly resolved in ER binding studies.

### 5.3 Structural analysis of MD simulations

Evaluation of the MD simulations of the receptor-ligand complexes revealed that the secondary and tertiary structures including helix 12, remained stable during the MD simulation. Rmsd values, Van der Waals and electrostatic interaction energies and temperature were found to be constant over the last 70 ps of the MD runs for all simulations. Examination of the orientation and conformation of the amino acids directly involved in ligand binding showed that the architecture of the binding site was conserved very well during simulation. Hydrogen bond interactions between ligand, Glu353 and Arg394 and stabilizing water molecules showed good correlation with better interaction energy values. The six crystal water molecules swapped places for hydrogen bonding with the ligand and Glu353 and Arg394 during MD simulations. This emphasizes their important role in stabilizing the interactions between Glu353, Arg394 and the bound ligand. Furthermore, hydrogen bonding with these residues contributed more to the interacting energies of ligands, than interaction with His524. This confirms the knowledge that the energy contribution of the interaction of the phenol ring in E2 with the ER is about 1.9 kcal/mol, while the energy contribution of the opposite hydroxyl group is about 0.6 kcal/mol<sup>[147,294]</sup>.

### 5.4 Aromatic interactions

Deviation of the originally perpendicular orientation of the aromatic ring of Phe404 in the E2-ER $\alpha$  complex, resulting in loss of pi-stacking of the interacting phenol of the ligand during the MD simulations, resulted in less favourable interaction energies. Twisting of the Phe404 ring occurred especially in the absence of an aromatic ring, for example in orientations 3 or 4 of E2. Perpendicular pi-stacking conformation of Phe404 and the aromatic moiety of a ligand contributes significantly to the binding energy<sup>[295,296]</sup>. In general, molecular mechanical force fields perform not specifically well in calculating aromatic interactions. However, this particular contribution is apparently estimated quite well using the Amber 6.0 force field, because there was a good correlation between calculated and experimentally determined binding energies.

---

### 5.5 Parameterisation of ligands

In Amber 6.0, no suitable length and torsion parameters were available for a single bond between two sp<sup>2</sup>-hybridized carbon atoms. Therefore, extra Amber parameters were developed in this study. Due to  $\pi$ - $\pi$  interactions over this bond, there is a tendency to adapt a coplanar conformation. However, from experimental studies (e.g. crystal structures) and various computational (DFT and *ab initio*) studies, it is known that in biphenyl, the rings adapt a dihedral of circa 40° due to repulsion of the adjacent H-atoms. *Ab initio* calculations with genistein also showed that its phenolic ring favourably conforms to a non-planar dihedral of 30° with the other rings. After optimisation of the parameters, examination of the newly gained MD trajectories showed more flexibility of the biphenyls and genistein-like molecules, and the torsions over the single bond mainly adapted dihedrals of 40 and 30 degrees respectively.

In general, the solubility of a ligand decreases with reduced flexibility. Consequently, the  $\Delta G$  of binding to macromolecules, such as the ligand binding cavity of the ER, may be bigger for such ligands compared to more flexible ligands, due to a smaller loss of entropy. Concluding, our study shows that taking into account the flexibility of the biphenyl and genistein-like structures led to a more realistic calculation of interaction energies, and more crucially, the final results are in excellent agreement with the theory behind the LIE method.

### 5.6 Linear interaction energy method

One of the main advantages of the LIE method over other computational methods calculating binding affinities, is the fact that the LIE includes a solvent model. Since binding of the ligand to the receptor as well as binding to the solvent is taken into account, the LIE handles the desolvation free energy reasonably well. Initially, the electrostatic part was calculated by an electrostatic linear response approximation (parameter  $\beta$ ), while the Van der Waals contribution (parameter  $\alpha$ ) was calculated by calibration against experimental binding data. Since the latter is dependent on experimental data, it may implicitly take into account other contributions, such as force field errors and systematic entropy terms. However, in recent times, the electrostatic scaling factor ( $\beta$ ) for the electrostatic contributions has been subject of several studies and appeared to be (partially) system dependent. Åqvist and Hansson<sup>[201]</sup> demonstrated that the presence of hydroxyl groups in solvent and solvated compound interfered with the electrostatic linear response. This was mainly attributed to the short-range character of dipolar fields and the existence of hydrogen-bonding in and between the simulated states (solute and solvent in their studies). Marelius *et al.* improved the application of the LIE by applying different values for  $\beta$  for ligands with different polarity<sup>[203]</sup>. They divided compounds in different  $\beta$ -classes:

charged, dipolar without hydroxyl groups, dipolar with one hydroxyl group, dipolar with two hydroxyl groups, dipolar with two or more hydroxyl groups, and with the use of the different  $\beta$ 's, they found good correlation between experimental and calculated binding energies.

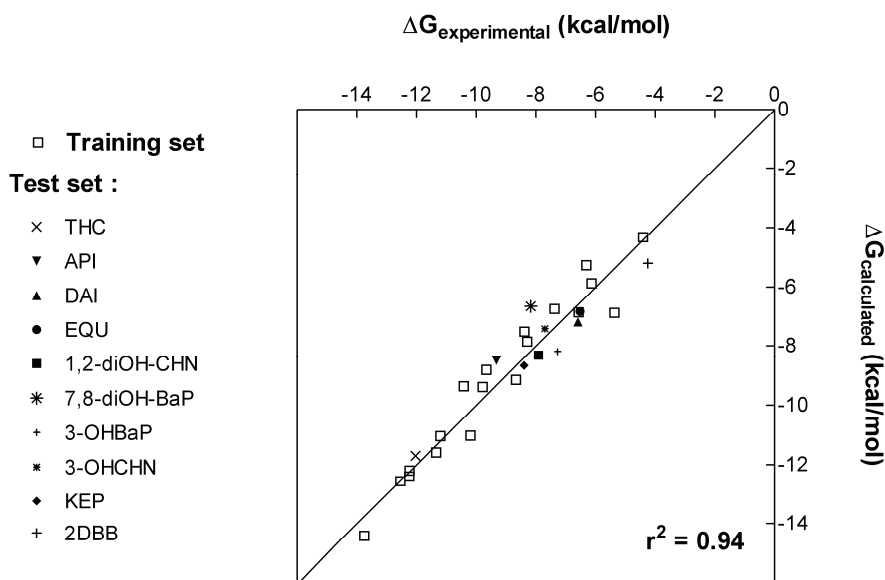


**Figure 3:** Graph presenting the relationship of calculated  $\Delta G$  values ( $\Delta G_{calc}$ ) versus experimentally obtained  $\Delta G$  values ( $\Delta G_{exp}$ ) in kcal/mol for binding energies of the ligands of the training set ( $n = 19$ ), shown by the **open squares**. The straight line represents the line  $\Delta G_{calc} = \Delta G_{exp}$  ( $y = x$ ). The linear correlation coefficient ( $r^2$ ) reflects the deviations of the experimental and calculated values from this line. The **solid symbols** represent the  $\Delta G_{calc}$  versus  $\Delta G_{exp}$  of the ligands in the test set ( $n = 12$ ). Data for PRG and 4DBB are not shown the highest concentration that could be tested was 0.3 mM, which showed no competition with radiolabeled E2. The linear correlation coefficient ( $r^2$ ) for the compounds of the test set is 0.85.

The development of an accurate model for ligand binding to the ER is particularly susceptible for deviations such as described above, since the hydrogen bonds between ER and a ligand provide interactions which are crucial for binding for most ligands, and significantly enhance the binding affinity<sup>[147]</sup>. We simulated the binding to the ER with a training set, consisting of 11 ligands with two or more hydroxyl groups and 10 ligands with only one hydroxyl group. Both groups were large enough and also the binding affinities covered a wide enough range to perform double regression analysis to gain optimal values for  $\alpha$  and  $\beta$ . The results are shown in the correlation graph (Figure 3). The optimal values for ligands with two hydroxyl groups were:  $\alpha = 0.82$  and  $\beta_{OH\geq 2} = 0.20$  ( $n = 11$ ).

---

Subsequently, using  $\alpha = 0.82$ , a specific value of  $\beta_{\text{OH}=1} = 0.43$  was obtained for mono-hydroxylated compounds ( $n = 8$ ).

Four compounds without hydroxyl groups were included in the test set for the LIE method. KEP and 2DBB show moderate and low binding affinity for the ER respectively, and for PRG and 4DBB no affinity could be determined. Using the theoretical value for  $\beta$  (0.5), good estimates were made for the binding affinities for KEP and 2DBB (Table 3). Nevertheless, for ligands without hydroxyl-group it would be ideal to determine an optimal value for  $\beta$  from a larger data set and include these in our model. However, compounds without hydroxyl-group that possess affinity for the ER are scarce.

### 5.7 Different binding orientations

In the currently described LIE method, for each ligand, orientations are included that represent all possibilities. However, molecules will be present in the LBD of a receptor most of the time in the orientation with the best interaction energy. Therefore, the fact that the orientation with the best interaction energy, predicted by our model for DES, E2 and THC, match those found in the crystal structures of ER $\alpha$  LBD complexed with these compounds, indicates the good quality of our model. Nevertheless, other orientations of DES and E2 may also significantly contribute to the total binding affinity.

Another observation from protein X-ray studies is the binding mode of the antagonists ICI 162,780 and ICI 164,384. These ER-antagonists are 7 $\alpha$ -substituted derivatives of E2 and bind with very high affinity to both subtypes of the ER<sup>[108,297]</sup>. Their side chains interact with specific residues, preventing helix 12 to associate with the rest of the LBD. In order to do so, the side chain must protrude from the binding cavity via the 11 $\beta$ -position of the E2 moiety<sup>[134,298]</sup>. Consequently, these molecules must bind in an ‘up-side down’-orientation similar to orientation 2 of E2 in our model, and apparently, the ER hosts this kind of binding. This also supports our hypothesis that E2, and also other compounds, may bind in several orientations.

Remarkably, the most favourable binding orientation of GEN predicted by our model (orientation 3), is distinct from its binding orientation observed in the crystal structure of the ER $\beta$ , which is equivalent to orientation 1 of E2<sup>[145]</sup>. During the MD simulation the perpendicular (T-shaped) aromatic interaction between the Phe404 and the phenolic ring of GEN was distorted, while for orientations 3 and 4 this interaction was stable and this led to higher interaction energies. In our model, with orientation 3 and 4, the flavone portion of GEN occupies the narrow part of the binding cavity, similar to the ‘A’-ring of E2 in orientation 1. The O4 moiety interacts with the Glu353 and Arg394 in the ER and the phenolic ring interacts with His524. In contrast, in the crystal structure of GEN complexed to ER $\beta$ , the phenolic ring occupies the same position as the ‘A’-ring of E2 in orientation 1.

These differences in orientation of GEN in ER $\alpha$  and ER $\beta$  may be related to the fact that GEN is a full agonist for ER $\alpha$  and a partial agonist for ER $\beta$ , inducing an antagonized receptor conformation<sup>[145]</sup>.

Although the architecture of the binding cavity of ER $\beta$  shows great similarity with the binding cavity of ER $\alpha$ , it has been shown that ER $\alpha$  and ER $\beta$  respond differently to agonists and antagonists<sup>[108,109]</sup>. GEN binds with moderate affinity to both ERs, however shows significant higher affinity for the ER $\beta$  (~30-fold)<sup>[109]</sup>. The two amino acid differences between the residues of the binding cavity of ER $\alpha$  and ER $\beta$  may have a direct effect on the observed differences in ligand binding preferences<sup>[108]</sup>. Due to the 'inwards' orientation of its side chain, the methionine at position 336 in ER $\beta$  occupies a larger volume in the binding cavity than the corresponding leucine at position 384 in ER $\alpha$ , possibly favouring another binding orientation of GEN. Also, the side chain of isoleucine 373 in ER $\beta$  occupies more binding cavity space than the corresponding methionine 421 in ER $\alpha$ . Both substitutions are lining the binding cavity at the histidine 524-side of E2, and may have significant effects on the preferred binding modes of GEN and other ligands.

## 6 Conclusions

A computational model was developed for prediction of binding affinities of ligands to the ER $\alpha$  using MD simulations in combination with the linear interaction energy (LIE) approach. We obtained an excellent linear correlation ( $r^2 = 0.94$ ,  $n = 19$ ) between experimental and calculated  $\Delta G$  values for compounds that bind to the ER $\alpha$  with  $K_d$  values ranging from 0.15 mM to 30 pM, a 5.000.000-fold difference in binding affinity. The excellent correlation for the compounds of the training set, which are structurally very diverse, is remarkable. The predictive value of our model is shown by predicting binding affinities of a collection of structurally diverse estrogenic compounds that are in very good agreement with the experimental values: the predicted  $\Delta G$  values for these compounds showed an average deviation of only 0.61 kcal/mol for absolute binding affinities.

An important advantage of the LIE method is the fact that it includes a solvent model and takes into account all possible binding orientations. The LIE approach provides a very good method for predicting of absolute ligand binding affinities, as well as binding orientation of ligands. The presented LIE model is of great value for the prediction of estrogenic activity of compounds such as xeno-estrogens or potential metabolites of estrogens, that are hard to generate or isolate and therefore difficult to test *in vitro*, but may be applied to other systems as well.



## Chapter 5

Prediction of Binding Affinity of Halogenated Biphenyls to  
the Estrogen Receptor by Molecular Dynamics Simulations  
and the Linear Interaction Energy Method

---

## ABSTRACT

Many structurally diverse environmental compounds have been identified as environmental estrogens and are proposed to be a risk factor for reproductive development and tumorigenesis of humans and wildlife, and among them are the polyhalogenated biphenyls (PHB). As yet, focus has been mainly on the estrogenic properties of polychlorinated biphenyls (PCB), however, also brominated biphenyl congeners have shown to exhibit significant estrogenic activities. More important, cytochrome P450-mediated bioactivation of many halogenated biphenyls yields numerous mono- and di-hydroxylated metabolites, which have been shown to be more estrogenic than their parent compounds, and may exhibit up to nanomolar ER $\alpha$  affinity, comparable with the affinity of the endogenous 17 $\beta$ -estradiol (E2).

The use of computational models becomes more and more important in the prediction of ER $\alpha$  affinity for compounds such as these metabolites. In order to further expand our recently published computational LIE model for prediction of ER $\alpha$  binding affinities, molecular dynamics simulations were performed with 22 structurally related brominated and chlorinated biphenyl congeners from literature and from in-house synthesis. Experimental binding affinities (EC<sub>50</sub> values) of 15 newly synthesized hydroxylated brominated biphenyls ranged from 7.0 nM to 41  $\mu$ M. The acquired correlation between the calculated and experimental binding energy ( $\Delta G$ ) values of hydroxylated halogenated biphenyls was good ( $r^2 = 0.74$ ), and the average absolute variation between  $\Delta G_{\text{calc}}$  and  $\Delta G_{\text{exp}}$  was  $0.59 \pm 0.1$  kcal/mol (s.e.m.). We conclude that the LIE method proves again to be a valuable tool for accurate prediction of binding affinities of compounds, such as DHB metabolites, which are hard to generate or isolate, and therefore difficult to test *in vitro*.

## 1 Introduction

Exposure to environmental estrogens has been proposed as a risk factor for disruption of reproductive development and tumorigenesis of humans and wildlife<sup>[4]</sup>. A wide variety of structurally diverse environmental compounds have been identified as endocrine disruptors. Among these compounds are natural steroid hormones, pharmaceuticals, industrial chemicals including pesticides, plasticizers, polycyclic aromatic hydrocarbons (PAHs) and polyhalogenated biphenyls (PHBs). PHBs have been used for a variety of industrial purposes, such as organic solvents, pesticides, plasticizers, cutting oils, flame retardants, dielectrics in large volume transformers and capacitors, hydraulic fluids, adhesives and ink<sup>[254]</sup>. Their high chemical stability and low biodegradability seemed valuable, however, these very physical properties result in persistence in the environment and ubiquitous bioaccumulation<sup>[255]</sup>. PHBs have been banned from most industrial applications, but widespread contamination remains a threat for wild life and humans<sup>[299]</sup>.

The effects of estrogens are mediated by the estrogen receptor (ER), a ligand-activated transcription factor<sup>[142]</sup>. Binding of agonists induces a conformational change of the ER, enabling the receptor to homodimerise. The dimer is then translocated to the nucleus, where it enhances gene transcription<sup>[134]</sup>. Two ER isoforms have been identified and crystallized, ER $\alpha$  and ER $\beta$ , that show great resemblance in overall structure. Both bind the endogenous estrogen, 17 $\beta$ -estradiol (E2), but show different tissue expression and distinct responses to various agonist and antagonists<sup>[108,109]</sup>. Binding of agonists induces a specific orientation of the helix 12, closing the narrow binding site, allowing co-regulators to bind<sup>[279]</sup>. Antagonist binding, however, induces a different orientation of helix 12, preventing alignment over the binding site and transactivation<sup>[134,145]</sup>. Estrogenic endocrine disruptors, such as halogenated biphenyls, may either mimic estradiol's action by agonistic action, or block the ER by antagonizing it.

PHBs are substrates for various enzymes. Bio-activation mainly occurs via enzymes of the cytochrome P450 (CYP) family, yielding mono- and di-hydroxy metabolites and dihydrodiols<sup>[22]</sup>. Further metabolism of the hydroxylated PHBs involves glucuronidation, glutathione conjugation and formation of methylsulfone metabolites<sup>[261]</sup>. In general, chlorinated or brominated biphenyls are not estrogenic, however, we and others have recently shown that various hydroxylated polybrominated biphenyl (PBB) and polychlorinated biphenyl (PCB) metabolites, exhibit very high estrogenic activities<sup>[22,176,262,263]</sup>. Analytical methods such as LC/MS, GC/MS or ECD usually are not

sufficiently sensitive or selective for absolute structural analysis of metabolites present in enzymatic incubations. Considering the large variety of potentially estrogenic PHB metabolites that may be formed by CYP enzyme activity, it is of great value to develop reliable methods to predict ER binding affinity of these compounds. Risk assessment of the endocrine disrupting properties of PHBs is inadequate if the effects of their metabolites are not taken into account<sup>[22,300]</sup>.

We recently presented a computational model for the prediction of estrogenic binding affinities of (xeno-)estrogens to the ER $\alpha$ <sup>[149]</sup>. This model is based on MD simulations in combination with the linear interaction energy (LIE) approach<sup>[200]</sup>, and is validated with compounds that bind to the ER $\alpha$  with EC<sub>50</sub> values ranging from 0.15 mM to 30 pM. The LIE approach provides a very good method for the prediction of absolute ligand binding affinities, as well as binding orientation of ligands. The latter was recently also experimentally confirmed by studying the interaction of hydroxylated PAHs by the use of fluorescence line-narrowing spectroscopy (FLNS)<sup>[301]</sup>.

The LIE method for estimation of binding affinities relies on the assumption that the free energy of binding ( $\Delta G$ ) depends linearly on changes in the Van der Waals and electrostatic energy of the system. This approach separately evaluates the electrostatic and Van der Waals interaction energies of the ligand in the bound and free state. For this purpose, MD simulations of the ligand bound to the (solvated) receptor and the unbound ligand in solvent are carried out. Subsequently, the  $\Delta G$  is obtained from the averaged interaction energies as<sup>[201]</sup>:

$$\Delta G_{calc} = \alpha * \Delta E_{INT}^{VDW} + \beta * \Delta E_{INT}^{EL} = \alpha * (E_{INT_{BOUND}}^{VDW} - E_{INT_{FREE}}^{VDW}) + \beta * (E_{INT_{BOUND}}^{EL} - E_{INT_{FREE}}^{EL}) \quad (1)$$

where  $E_{INT}^{VDW}$  indicates the Van der Waals interaction energy and  $E_{INT}^{EL}$  electrostatic interaction energy, of the ligand bound to the receptor (*BOUND*) and the ligand free in solution (*FREE*). The electrostatic parameter  $\beta$  is calculated by an electrostatic linear response approximation while the Van der Waals parameter  $\alpha$  is calculated by calibration against experimental binding data. Since the latter is dependent on experimental data, it implicitly takes into account other contributions, such as force field errors and systematic entropy terms. Initially, the value of  $\beta$  was theoretically defined to be 0.5<sup>[202]</sup>. However, it was recently demonstrated that also this electrostatic scaling factor can be system dependent<sup>[149,201]</sup>. Especially the hydrogen-bonding between the ligand and its surrounding showed to be of great importance. Our published ER $\alpha$  model included 12 estrogenic compounds, such as estradiol (E2) and DES, and 16 estrogenic hydroxylated PAH metabolites. Double regression analysis yielded one optimal value of  $\alpha = 0.82$  for all compounds, and two optimal values for  $\beta$ . The  $\beta$  value depends on the number of

hydroxyl groups of the compound,  $\beta_{\text{OH}\geq 2}$  is 0.20 for ligands with two hydroxyl groups, and  $\beta_{\text{OH}=1}$  is 0.43 for mono-hydroxylated compounds.

In the present study, we tested our ER $\alpha$  LIE model for the prediction of ER $\alpha$  binding affinities of hydroxylated PHB metabolites. We used 18 halogenated biphenyl metabolites of which experimental binding data were available. For six more halogenated biphenyls without experimental binding affinities predicted with our method. The expanded ER $\alpha$  LIE model may be of great value to risk assessment of compounds such as xeno-estrogens or their potential metabolites, which are hard to generate or isolate, or even unknown and therefore impossible to test *in vitro*.

## 2 Experimental Methods

### 2.1 Chemicals

17 $\beta$ -Estradiol and 4-hydroxy-4'-bromobiphenyl was purchased from Sigma Chemical co. (St. Louis, MO, USA). [ $^3\text{H}$ ]-E2 was obtained from Amersham (Buckinghamshire, UK). 2,2'-DBB was purchased from ICN pharmaceuticals (NY, USA) and 4,4'-DBB from Fluka AG (Buchs, Switzerland). Dextran (MW 60.000-90.000) was obtained from Duchefa, Haarlem, The Netherlands. All other chemicals were of analytical grade and purchased from Sigma-Aldrich Co.

### 2.2 Synthesis of hydroxylated brominated biphenyls

Several hydroxylated biphenyls were synthesized according to the method described by Bergman *et al.* with small modifications<sup>[265]</sup>. Four different syntheses were carried out, i.e. a diaryl coupling reactions of 2-bromo-aniline and 2-bromo-anisole, 2-bromo-aniline and 3-bromo-anisole, 4-bromo-aniline and 2-bromo-anisole and of 4-bromo-aniline and 3-bromo-anisole, respectively (Figure 1). Briefly, bromo-aniline (1.0 g) was dissolved in bromo-anisole (5.0 g) at 60°C. The bromo-aniline was diazotized by addition of an excess of 3-methyl butylnitrile (2.0 ml). The temperature was slowly increased to 120°C and kept at this temperature for 1.5 hours. The unreacted bromo-anisole was removed by vacuum distillation. Subsequently, GC/MS analysis was performed as described below. Demethylation of the components was achieved by addition of boron tribromide in dichloromethane. The crude mixture was extracted and redissolved in 70% methanol for further analysis by HPLC, LC/MS and NMR.

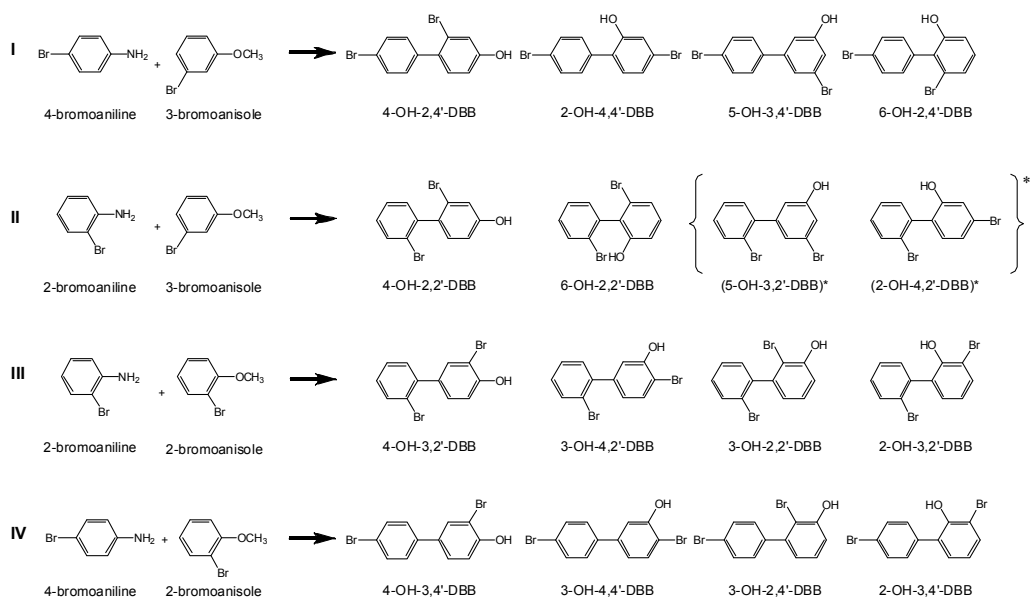


**Figure 1:** Schematic diagram of the four different syntheses performed in the current study (denoted I to IV) and their products, i.e. mono-hydroxylated dibromobiphenyls (DBB). The details are described in the Methods section. Two compounds from synthesis II (\*shown in brackets) were not isolated from the synthesis mixture. All other product were identified, isolated and tested for estrogenic binding affinity as described in the Methods and Results sections.

### 1.1 GC/MS analysis of hydroxylated brominated biphenyls

To verify product formation of the synthesis reactions, GC/MS analyses of the synthesis mixtures were performed on a HP 5890 gas chromatograph equipped with a 25 m BPX5 column (0.25 mm i.d., 0.25  $\mu$ m film thickness, SGE, Amstelveen, The Netherlands) coupled to a Hewlett-Packard MSD 5970 mass spectrometer (positive ion source, electron impact ionization, electron energy of 70 eV). Temperatures of the injection port and transfer line were 270 °C. The column temperature was programmed from 40 (5 min) to 270 °C (20°C/min) and kept at 270 °C for 10 min. Full scanning analyses were performed in the range of  $m/z$  150-500. Before demethylation by boron tribromide, retention times and mass spectra were recorded for the bromobiphenyls synthesis mixtures. The results of the GC/MS measurements are shown in Table 1.

### 1.2 HPLC analysis of hydroxylated brominated biphenyls

Hydroxylated di-bromobiphenyls were subsequently separated by preparative HPLC (Gilson pump 305, manometer 805, dynamic mixer 811C) using a reversed phase C18-column (ChromSpher 5  $\mu$ M, 250 x 10 mm, Varian Chrompack, The Netherlands) and an isocratic elution system with 60% methanol as mobile phase (4.0 ml/min). Compounds were detected at a wavelength of 290 nm (Jasco Ltd, UK, 1575 uv/vis spectrophotometer). After collection, compounds were analysed for purity by HPLC and NMR. Isolated compounds and corresponding solutions in DMSO displayed light yellow to bright orange colors. Stocks were maintained at -20°C and regularly checked by HPLC for stability.

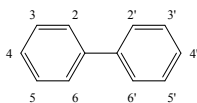
### 1.3 LC/MS analysis of hydroxylated brominated biphenyls

The synthesis products were also analysed by HPLC coupled to a mass spectrometer. The chromatographic system conditions were similar to the methods described above, i.e. a gradient system was used for the incubation mixtures and an isocratic system was used for the synthesis products. For LC/MS analysis, a reversed phase C18-column (ChromSpher 5  $\mu$ M, 100 x 3 mm, Chrompack, the Netherlands) was used in all cases. Mass spectrometric detection was performed with a Finnigan LCQ-DECA mass spectrometer (ThermoQuest, San Jose, CA, USA), operating on the negative ion mode using an APCI interface probe. A potential of 5 kV was applied to the APCI corona discharge. High purity N<sub>2</sub> was used at a flow of 300 L/h. Full scanning analysis was performed in the range of  $m/z$  150-650. The results of the LC/MS measurements are shown in Table 1.

### 1.4 NMR analysis of hydroxylated brominated biphenyls

All isolated synthesis products were analysed by <sup>1</sup>H NMR for structure identification. H<sub>2</sub>O-cosy and CH-correlation spectra were also recorded. High-resolution NMR spectra of each compound dissolved in 500  $\mu$ l CDCl<sub>3</sub> were obtained with a Bruker Avance 400 spectrometer at 27°C (Bruker BioSpin, Rheinstetten, Germany). Ethanol was used as an internal standard for concentration determination. The results of the NMR measurements are shown in Table 1.

Table 1



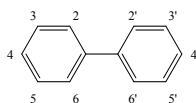
Method	HPLC	<sup>1</sup> H NMR (CDCl <sub>3</sub> )	GC	MS
Synthesis / Products <sup>1</sup>	R <sub>t</sub> (min) <sup>a</sup>	δ in ppm (number of protons, complexity in Hz, position <sup>b</sup> )	R <sub>t</sub> (min)	m/z (fragment loss in % intensity) <sup>c</sup>
I 2-OH-6,4'-DBB	14"	7.68 (2H, tr of d, <sup>2</sup> J=8.9, <sup>3</sup> J=2.4, <sup>3</sup> J=2.0, H3', H5'), 7.25 (3H, m, H3, H2', H6'), 7.15 (1H, tr, <sup>2</sup> J=8.04, H4), 7.96 (1H, dd, <sup>2</sup> J=8.2, <sup>3</sup> J=1.15, H5)	21.13"	342 (M+• 100), 246/8 (M-Br-CH <sub>3</sub> 53) 182 (M-Br-Br 6) 139 (M-Br-Br-CH <sub>3</sub> -CO 32)
4-OH-2,4'-DBB	18"	6.85 (1H, dd, <sup>2</sup> J=8.37, <sup>3</sup> J=2.6, H5), 7.17 (1H, dd, <sup>2</sup> J=8.43, H3), 7.19 (1H, dd, <sup>3</sup> J=2.6, H6), 7.27 (2H, tr of d, <sup>2</sup> J=9.02, <sup>3</sup> J=1.98, <sup>3</sup> J=2.52, H2', H6'), 7.55 (2H, tr of d, <sup>2</sup> J=8.56, <sup>3</sup> J=1.97, <sup>3</sup> J=2.52, H3', H5'),	15.08"	342 (M+• 100), 327 (M-CH <sub>3</sub> 13), 299 (M-CH <sub>3</sub> -CO 17), 246/8 (M-Br-CH <sub>3</sub> 71)
2-OH-4,4'-DBB	22"	7.09 (1H, dd, <sup>2</sup> J=7.5, <sup>3</sup> J=1, H6), 7.15 (1H, dd, <sup>2</sup> J=8, <sup>3</sup> J=1, H3), 7.16 (1H, s, H5), 7.35 (2H, tr of d, <sup>2</sup> J=9, <sup>3</sup> J=0.5, H2', H6'), 7.62 (2H, tr of d, <sup>2</sup> J=9, <sup>3</sup> J=0.5, H3', H5')	14.25"	342 (M+• 100), 246/8 (M-Br-CH <sub>3</sub> 53) 182 (M-Br-Br 6) 139 (M-Br-Br-CH <sub>3</sub> -CO 32)
3-OH-5,4'-DBB	25"	7.00 (3H, m, H2, H4, H6), 7.41 (2H, tr of d, <sup>2</sup> J=8.63, <sup>3</sup> J=2.51, H3', H5'), 7.57 (2H, tr of d, <sup>2</sup> J=8.64, <sup>3</sup> J=2.56, H3)	15.13"	342 (M+• 100) <sup>d</sup>
II 4-OH-2,2'-DBB	13.5"	6.8 (1H, dd, <sup>2</sup> J=8.3, <sup>3</sup> J=2.5, H5), 7.12 (1H, d, <sup>2</sup> J=8.3, H6), 7.19 (1H, d, <sup>2</sup> J=2.5, H3), 7.23-7.28 (2H, m, H4', H6'), 7.38 (1H, d of tr, <sup>2</sup> J=7.5, <sup>3</sup> J=1.3, H5'), 7.67 (1H, dd, <sup>2</sup> J=8.6, <sup>3</sup> J=1.5, H3')	15.08"	342 (M+• 100), 261/3 (M-Br 48), 246/8 (M-Br-CH <sub>3</sub> 5) 182 (M-Br-Br 62) 139 (M-Br-Br-CH <sub>3</sub> -CO 92)
2-OH-6,2'-DBB	10.5"	6.96 (1H, dd, <sup>2</sup> J=8, <sup>3</sup> J=1, H5), 7.19 (1H, tr, <sup>2</sup> J=8, H4), 7.26-7.37 (4H, m, H3, H6', H4'), 7.49 (1H, d of tr, <sup>2</sup> J=7.5, <sup>3</sup> J=1, H5'), 7.75-7.78 (1H, dd, <sup>2</sup> J=2, <sup>3</sup> J=1, H3')	14.25"	342 (M+• 42), 261/3 (M-Br 28), 246/8 (M-Br-CH <sub>3</sub> 100) 182 (M-Br-Br 42) 139 (M-Br-Br-CH <sub>3</sub> -CO 57)

<sup>1</sup> Synthesis numbering according to illustration in Figure 1. DBB = dibromobiphenyl

<sup>a</sup> 65% methanol isocratic elution method, <sup>b</sup> Positions of proton as illustrated in figure in Table 1, <sup>c</sup> Procedures are described in the Methods section, analysis was performed in the range of m/z 150-500, <sup>d</sup> No fragmentation was observed.

**Table 1** (left and right page): Identification of synthetic hydroxylated dibromobiphenyls by HPLC, <sup>1</sup>H NMR and GC/MS. NMR signals were assigned using <sup>1</sup>H, H,H-cosy and CH-correlation, as described in the materials section. For the MS mass spectral data; mass to charge ratio of the molecular fragments (m/z) and the relative abundance of the number of ions (intensity in %) are shown.

Table 1 continued



Method	HPLC	<sup>1</sup> H NMR (CDCl <sub>3</sub> )	GC	MS
Synthesis / Products <sup>1</sup>	R <sub>t</sub> (min) <sup>a</sup>	δ in ppm (number of protons, complexity in Hz, position <sup>b</sup> )	R <sub>t</sub> (min)	m/z (fragment loss in % intensity) <sup>c</sup>
III 3-OH-2,2'-DBB	11"	6.83 (1H, dd, <sup>2</sup> J = 7.5, <sup>3</sup> J = 1.5, H5), 7.09 (1H, dd, <sup>2</sup> J = 7.5, <sup>3</sup> J = 1.5, H4), 7.1-7.32 (4H, m, H6, H3', H6), 7.39 (1H, d of tr, <sup>2</sup> J = 7.5, <sup>3</sup> J = 1.3, H5'), 7.69 (1H, dd, <sup>2</sup> J = 8, <sup>3</sup> J = 1.3, H3')	15.13"	342 (M+• 75), 261/3 (M-Br 100), 246/8 (M-Br-CH <sub>3</sub> 20) 182 (M-Br-Br 35) 139 (M-Br-Br-CH <sub>3</sub> -CO 90)
2-OH-3,2'-DBB	13"	6.90 (1H, tr, <sup>2</sup> J = 8.0, H5), 7.15 (1H, dd, <sup>2</sup> J = 7.5, <sup>3</sup> J = 1.6, H6), 7.25-7.34 (2H, m, H4', H6'), 7.40 (1H, d of tr, <sup>2</sup> J = 7.5, <sup>3</sup> J = 1.3, H5'), 7.54 (1H, dd, <sup>2</sup> J = 8.0, <sup>3</sup> J = 1.6, H4), 7.71 (1H, dd, <sup>2</sup> J = 8.0, <sup>3</sup> J = 1.3, H3')	14.36"	342 (M+• 45), 261/3 (M-Br 14), 246/8 (M-Br-CH <sub>3</sub> 100) 182 (M-Br-Br 47) 139 (M-Br-Br-CH <sub>3</sub> -CO 43)
3-OH-4,2'-DBB	17"	6.80 (1H, dd, <sup>2</sup> J = 8.24, <sup>3</sup> J = 2.1, H6), 7.09 (1H, d, <sup>3</sup> J = 2.1, H2), 7.23 (1H, d of tr, <sup>2</sup> J = 7.96, <sup>3</sup> J = 1.9, H4'), 7.31 (1H, d of tr, <sup>2</sup> J = 7.61, <sup>3</sup> J = 1.9, H2'), 7.37 (1H, d of tr, <sup>2</sup> J = 7.58, <sup>3</sup> J = 1.2, H3'), 7.52 (1H, d, <sup>2</sup> J = 8.23, H5), 7.67 (1H, dd, <sup>2</sup> J = 8.01, <sup>3</sup> J = 1.14, H5')	16.06"	342 (M+• 100), 327 (M-CH <sub>3</sub> 35), 299 (M-CH <sub>3</sub> -CO 35), 246/8 (M-Br-CH <sub>3</sub> 15) 182 (M-Br-Br 10) 139 (M-Br-Br-CH <sub>3</sub> -CO 90)
4-OH-3,2'-DBB	18"	7.09 (1H, d, <sup>2</sup> J = 8.4, H5), 7.21 (1H, d of tr, <sup>2</sup> J = 7.2, <sup>3</sup> J = 2, H1), 7.30 (2H, m, H6, H6'), 7.36 (1H, d of tr, <sup>2</sup> J = 7.5, <sup>3</sup> J = 1.2, H5'), 7.54 (1H, d, <sup>3</sup> J = 2.1, H2), 7.67 (1H, dd, <sup>2</sup> J = 8.0, <sup>3</sup> J = 1.2, H3')	16.37"	342 (M+• 100), 299 (M-CH <sub>3</sub> -CO 40), 246/8 (M-Br-CH <sub>3</sub> 15) 182 (M-Br-Br 15) 139 (M-Br-Br-CH <sub>3</sub> -CO 70)
IV 3-OH-2,4'-DBB	4"	6.77 (1H, dd, <sup>2</sup> J = 7.5, <sup>3</sup> J = 1.35, H6), 6.99 (1H, dd, <sup>2</sup> J = 8.0, <sup>3</sup> J = 1.46, H4), 7.79 (1H, tr, <sup>2</sup> J = 7.79, H5), 7.30 (2H, d, <sup>2</sup> J = 8.37, H2', H6'), 7.60 (2H, d, <sup>2</sup> J = 8.34, H3', H5')	16.68"	342 (M+• 100), 299 (M-CH <sub>3</sub> -CO 38), 246/8 (M-Br-CH <sub>3</sub> 15) 182 (M-Br-Br 10) 139 (M-Br-Br-CH <sub>3</sub> -CO 75)
3-OH-4,4'-DBB	6"	7.02 (1H, dd, <sup>2</sup> J = 8.4, <sup>3</sup> J = 2.2, H6), 7.17 (1H, d, <sup>3</sup> J = 2.2, H2), 7.55 (3H, t, <sup>2</sup> J = 8.2, H2', H6'), 7.65 (2H, d, <sup>2</sup> J = 8.5, H3', H5')	18.03"	342 (M+• 100), 299 (M-CH <sub>3</sub> -CO 42), 246/8 (M-Br-CH <sub>3</sub> 18) 139 (M-Br-Br-CH <sub>3</sub> -CO 38)
4-OH-3,4'-DBB	6"	7.03 (1H, d, <sup>2</sup> J = 8.4, H5), 7.51 (1H, dd, <sup>2</sup> J = 8.4, <sup>3</sup> J = 2.1, H6), 7.55-7.61 (4H, m, H3', H5', H2', H6'), 7.78 (1H, d of s, <sup>3</sup> J = 2.2, H2)	18.5"	342 (M+• 100), 327 (M-CH <sub>3</sub> 64), 299 (M-CH <sub>3</sub> -CO 34), 246/8 (M-Br-CH <sub>3</sub> 18), 139 (M-Br-Br-CH <sub>3</sub> -CO 57)
2-OH-3,4'-DBB	7"	5.80 (1H, m, H5), 6.95 (1H, dd, <sup>2</sup> J = 6.5, <sup>3</sup> J = 1.8, H6), 7.09 (1H, d, <sup>2</sup> J = 6.5, H4), 7.36 (2H, d, <sup>2</sup> J = 8.5, H2', H6'), 7.80 (2H, d, <sup>2</sup> J = 8.1, H3', H5')	15.58"	342 (M+• 60), 299 (M-CH <sub>3</sub> -CO 40), 261/3 (M-Br 5), 246/8 (M-Br-CH <sub>3</sub> 100) 182 (M-Br-Br 15) 139 (M-Br-Br-CH <sub>3</sub> -CO 42)

---

### 1.5 Competitive ligand binding assay

Competitive binding assays were performed as described before<sup>[46]</sup>. Briefly, affinity for the ER was determined using cytosol from homogenised fresh sheep uterus. A mixture of 0.3 nM [<sup>3</sup>H]-E2, uterine cytosolic protein (0.5 mg/ml) and competing ligand in Tris (10 mM)-EDTA (15 µM) buffer (TEA, pH 7.4) was incubated for 3 hours at 4°C. After 10 minutes incubation with 0.8%-0.08% charcoal-dextran slurry at 4°C, unbound radioligand was removed by centrifugation and supernatant was analysed for receptor-bound [<sup>3</sup>H]-E2 in a 1900 Tricarb scintillation counter (Packard Instruments, Perkin Elmer, Wellesley, U.S.A.). Each experiment, a complete E2 concentration curve was included in duplicate and used to determine 0% and 100% displacement. Concentration of DMSO in the assay was always 3%, and this concentration did not alter the binding characteristics of the ER for E2. Experiments were performed at least three times on separate days. Test concentrations up to 1.0 mM of compounds were used to obtain complete sigmoidal competition curves for EC<sub>50</sub> calculation. E2 displaced radiolabeled E2 with an EC<sub>50</sub> value of 0.4 ± 0.05 nM (mean ± SEM; n = 10). The ligand binding affinities (K<sub>d</sub>) were calculated with Graphpad Prism 3.0 (GraphPad Software Inc., 2000, San Diego, CA, USA).

## 3 Computational details

### 3.1 Ligand parameterization

For the prediction of ligand binding affinities, docking studies were performed with the various ligands as described before<sup>[149]</sup>. Briefly, structures of the ligands were generated with the xLEaP module of Amber 6.0. Conformation analysis and subsequent hierarchical clustering were performed using Sybyl 6.7 (Tripos Inc., St Louis, Missouri) to obtain four energy-optimised geometries covering the broadest range of the conformational space of the ligand. Conformation analysis of non-hydroxylated biphenyl resulted in one optimal conformation. In this case, energy optimizations were performed with several fixed torsions (with dihedral angles ( $\phi$ ) of 30, 90 and 130°) over the rotatable bond between the two aromatic rings with GAMESS at the STO-3G level of theory. Electrostatic potentials were calculated for all conformers of all ligands using GAMESS (US) at the 6-31G\* level of theory, and subsequently applied in the multi-conformational restraint electrostatic potential (RESP) fitting procedure to obtain atomic charges<sup>[287]</sup>. Since the Amber 6.0 force field holds no suitable parameters for the torsional force constant of biphenyl, we optimised this force constant using an *ab initio* approach. The ideal force constant for the single bond between two sp<sup>2</sup>-hybridized was 3 kcal/mol<sup>[149]</sup>.

### 3.2 ER $\alpha$ LBD structure

The crystal structure of the LBD (residues Ser 305 to Leu 549) of the ER $\alpha$  complexed with DES (PDB ID 3ERD)<sup>[144]</sup>, was used to build the protein model, and all molecular dynamics simulations were based on this protein structure. Missing side-chains from surface loops were modelled using the homology module of InsightII (Biosym, San Diego). The terminal amino acids were treated as charged. The charges of the ionisable groups were set to correspond to a pH of 7.4, resulting in a net charge of -5e. Coordinates of six crystallographic water molecules, directly interacting with either the ER residues Glu353, Arg394 or the 3-OH group of DES, were also obtained from the published crystal structure.

### 3.3 Docking of the ligands

Positions of E2 (PDB ID 1ERE) and DES in the ER LBD from the published crystal structures<sup>[134,144]</sup> were used as templates for the docking of the ligands. Low energy conformers of the ligands were placed in the binding site of the ER by manual docking, using InsightII. In the initial model, E2 was docked in four orientations as depicted in Figure 2.

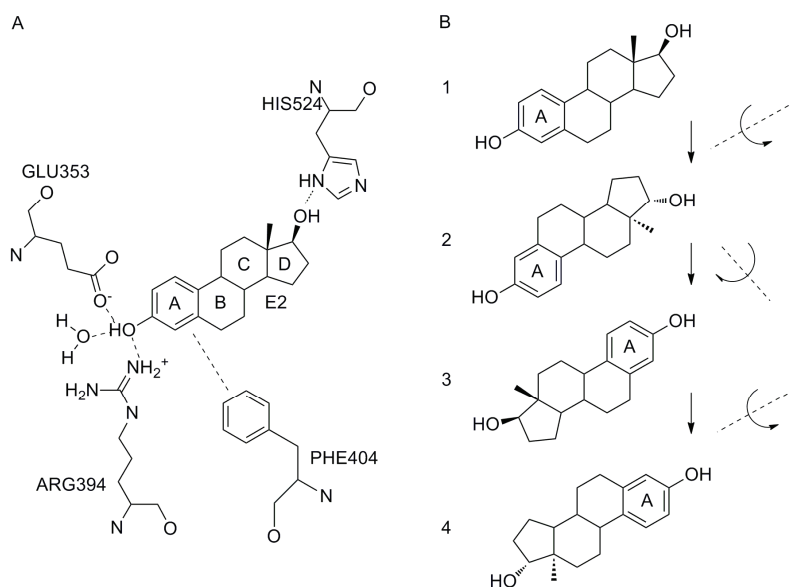


**Figure 2:** Schematic view of the orientation of binding of estrogens to the ER $\alpha$ . Figure 2A shows hydrogen bonding and aromatic interactions (dashed lines) between estradiol (E2) and several residues (Glu353, Arg394, His524 and Phe404) of the ER $\alpha$  and a water molecule, as observed in the published crystal structure<sup>[134]</sup>. E2 is depicted in orientation 1. B: Overview of the four docking orientations used in the present study, with E2 as an example.

---

Subsequently, all ligands were docked, fitting aromatic moieties on the 'A'-ring of E2 in its four orientations. Special care was taken in minimizing overlap between protein and ligand, and when appropriate, in adjusting the orientation of OH-groups in the direction of the interacting amino acid residues, in particular Glu353, Arg394 or His524. Chloro- or bromo-substitution at *ortho*-position(s) in the biphenyl structures prohibits complete rotation over the single bond connecting the phenyl rings. Therefore, two conformations (e.g.  $\phi = 40^\circ$  and  $\phi = -40^\circ$ ) per compound were docked in four orientations each, thus resulting in eight different orientations in the ER $\alpha$  model.

However, corresponding to orientations 3 and 4 in Figure 2, there was only room for one of the halogen substituents, since the binding cavity neighboring the Arg294, Glu353 and Phe404 is very tight. Due to the symmetry of certain ligands, in some cases docking resulted in identical orientations. Occasionally, docked ligands experienced severe sterical hindrance with receptor residues, and these orientations were not included in further studies.

### 3.4 MD simulations of ligands bound to the ER and free ligands in water

MD simulations were performed as described by van Lipzig *et al.*<sup>[149]</sup>. Briefly, the starting structure of each receptor-ligand was solvated in water using the tLEaP module of Amber 6.0. The complex was surrounded by a rectangular box of equilibrated water molecules, based on the TIP3P water model<sup>[288]</sup>, with typical box volume sizes of about  $3.0 \cdot 10^6 \text{ \AA}^3$ . Ligands were also solvated in a water box, with a volume of about  $1.5 \cdot 10^6 \text{ \AA}^3$ . All calculations were carried out in the Sander module of Amber 6.0, under periodic boundary conditions with a cut-off distance of 10.0 Å.

### 3.5 Structural analysis of MD simulations

For each compound, two simulations were carried out, namely one with the biphenyl bound to the (solvated) receptor and one with the biphenyl in solvent. In order to get stable MD runs, equilibration and minimisation were carried out prior to MD simulations, using positional restraints on the C $_{\alpha}$ 's of the backbone. Simulations of the binding of the biphenyls to ER $\alpha$  were carried out for 160 ps. Inspection of the trajectories revealed that secondary and tertiary structure of the receptor-ligand complexes became stable after 60 ps. Rmsd values of the backbone C $_{\alpha}$  atoms did not change anymore over the last 100 ps of the MD simulation ( $\Delta\text{rmsd} < 0.001 \text{ \AA/ps}$ ; rmsd C $_{\alpha}$ 's  $1.14 \pm 0.10 \text{ \AA}$ ). Finally, averages of interaction energies between the ligand and its surroundings were analysed over the last 85 ps (Tables 2 and 3).

### 3.6 Determination of calculated binding affinities ( $\Delta G_{calc}$ ) and prediction of binding affinities

To obtain values for  $\Delta G_{calc}$ , Van der Waals ( $E_{INT}^{VDW}$ ) and electrostatic ( $E_{INT}^{EL}$ ) interaction energies between the ligand and its environment were calculated for all trajectory files from the MD simulation. The interaction energies ( $E_{INT}$ ) of the ligand bound to the solvated receptor ('bound', eq. 2a), or the ligand in water only ('free', eq. 2b), are described as follows:

$$E_{INT_{BOUND}}^{VDW} + E_{INT_{BOUND}}^{EL} = (E^{VDW} + E^{EL})_{T_{BOUND}} - (E^{VDW} + E^{EL})_W - (E^{VDW} + E^{EL})_R - (E^{VDW} + E^{EL})_L \quad (2a)$$

$$E_{INT_{FREE}}^{VDW} + E_{INT_{FREE}}^{EL} = (E^{VDW} + E^{EL})_{T_{FREE}} - (E^{VDW} + E^{EL})_W - (E^{VDW} + E^{EL})_L \quad (2b)$$

where  $E_T$  denotes the energy of the total system,  $E_W$  the energy of the water molecules,  $E_R$  represents the receptor energy, and  $E_L$  the ligand energy. The separate Van der Waals (VDW) and electrostatic (EL) interaction energy terms were calculated in the Sander module of Amber, by a single-step energy calculation of the total system and all the separate components, under the same conditions as the MD simulations. Energies were averaged over frames taken every 2 ps from the last 85 ps of the trajectory. Subsequently, Amber interaction energies ( $\Delta E_{AMBER}$ ) were calculated for any orientation  $i$  by eq. 3:

$$\Delta E_{AMBER_i} = (E_{INT_{bound,i}}^{VDW} - E_{INT_{free}}^{EL}) + (E_{INT_{bound,i}}^{VDW} - E_{INT_{free}}^{EL}) = E_{INT_i}^{VDW} + E_{INT_i}^{EL} \quad (3)$$

Similar to our published model<sup>[149]</sup>,  $\Delta E_{AMBER}$  of all orientations of each compound were used to calculate their contribution to the total interaction energy, using a Boltzmann weight factor ( $p_i$ ) for orientation  $i$  by

$$p_i = \left( e^{-\Delta E_{AMBER_i} / k_B T} \right) / \sum_i \left( e^{-\Delta E_{AMBER_i} / k_B T} \right) \quad (4)$$

where  $k_B$  is the Boltzmann constant (kcal/mol/K) and  $T$  the temperature (K).

Subsequently,  $\Delta G_{calc,i}$  values were calculated using the  $\alpha$  and  $\beta$  values obtained from our previously published LIE model:  $\alpha = 0.82$  and  $\beta_{OH \geq 2} = 0.20$  for ligands with two hydroxyl groups,  $\alpha = 0.82$  and  $\beta_{OH=1} = 0.43$  for mono-hydroxylated compounds and  $\alpha = 0.82$  and  $\beta_{no\ OH} = 0.5$  for non-hydroxylated compounds<sup>[149]</sup>. The final binding energy ( $\Delta G_{calc}$ ) of each ligand was obtained by summation of the binding energies of each individual orientation multiplied by the Boltzmann weight factor ( $p_i$ ):

$$\Delta G_{calc} = \sum (p_i * \Delta G_{calc,i}) \quad (5)$$

---

### 3.7 Data analysis

Double linear regression analysis was performed using the XLSTAT tool (XLSTAT4.4, <http://www.xlstat.com>) in Microsoft Excel 2000. Statistical analysis was carried out by Student's *t*-test using Graphpad Prism 4.0 software. P-values  $\leq 0.05$  were considered to indicate a significant difference with control data.

## 4 Results and Discussion

### 4.1 Aim of the study

Our computational ER $\alpha$  LIE model was tested for the prediction of ER $\alpha$  binding affinities of hydroxylated PHB metabolites. Molecular dynamics simulations were performed with 22 structurally related compounds. The experimental binding energies ( $\Delta G_{\text{exp}}$ ) were calculated from the experimentally determined ligand binding affinities ( $K_d$ ). The results are summarised in Table 2.

Experimentally determined binding affinities ( $EC_{50}$  values) of the hydroxylated brominated biphenyls ranged from 7.0 nM to 41  $\mu\text{M}$ . Although brominated biphenyls have been found to be persistent environmental contaminants, and exposure to brominated biphenyls has been suggested to be a risk factor in endocrine disruption<sup>[302]</sup>, the estrogen receptor binding affinities of individual hydroxylated bromobiphenyls have not been published as yet, in contrast to the binding affinities of hydroxylated chlorinated biphenyl congeners or hydroxylated brominated diphenyl ethers<sup>[23,241,263]</sup>. We conclude that substitution at the *ortho*-position(s) improves estrogenic binding affinity over *para*-substituted halogenation, and two substituents increase ER $\alpha$  binding affinities even more than one. Our studies comprise mostly biphenyls with two bromo-substituents, still, in all cases the double *ortho*-substituted biphenyls show the highest ER $\alpha$  affinity. These observations have also been made when studying (hydroxylated) chlorinated biphenyls<sup>[262,263,303]</sup>. *Para*-hydroxylation enhanced binding affinity significantly in all cases, when compared to hydroxylation at the *meta*-position, which adds still more estrogenic binding affinity than *ortho*-hydroxylation. One exception to this is the 6-OH-2',2-DBB, which shows a remarkable high binding affinity.

From earlier studies with PCBs it was concluded that biphenyls with an unhindered 4-hydroxyl-group show better ER $\alpha$  binding affinity than when flanked by one or two neighboring chloro substituents. This is also in good agreement with our observations, for example when comparing 4-OH-2,2'-DBB ( $EC_{50}$  0.007  $\mu\text{M}$ ) with 4-OH-3,2'-DBB ( $EC_{50}$  1.45  $\mu\text{M}$ ), and 4-OH-2,4'-DBB ( $EC_{50}$  0.086  $\mu\text{M}$ ) with 4-OH-3,4'-DBB ( $EC_{50}$  1.96  $\mu\text{M}$ ).

As for the parent compounds used in the present study, 2,2'-DBB showed very weak ER-affinity (170  $\mu\text{M}$ ), and 4,4'-DBB and 2,2'-DCB did not compete significantly with radiolabeled estradiol for binding to the ER (Table 2). The latter is explained by the fact that bromine atoms are bigger than chlorine atoms, and also more lipophilic, which in the case of the ER $\alpha$  apparently results in a better interaction with the receptor.

Several of the hydroxylated metabolites used in the present study have been tested *in vitro* in the stable estrogen receptor-mediated chemical-activated luciferase gene expression (ER-Calux<sup>®</sup>) assay<sup>[184]</sup>, i.e. 2-OH-3,2'-DBB, 3-OH-2,2'-DBB, 4-OH-2,2'-DBB, 6-OH-2,2'-DBB, 4-OH-4'-MBB, 3-OH-4,4'-DBB and 4-OH-3,4'-DBB. All these metabolites showed to be agonists<sup>[22]</sup>.

#### 4.2 Correlation calculated versus predicted $\Delta G$ values

The predicted  $\Delta G$  values are in good agreement with the experimental values (average deviation  $1.22 \pm 1.4$  kcal/mol). The results are summarised in Table 3. Figure 3A shows the graphical correlation between predicted and observed  $\Delta G$  values ( $r^2 = 0.74$ ). Figure 3B shows the correlation ( $r^2 = 0.76$ ) between predicted and observed  $\Delta G$  values of the DHB dataset, extended with nine compounds from the test set from the previously published model (four phytoestrogens and five hydroxylated PAHs).

A few observations are worth mentioning: Two of the synthesized biphenyls were predicted to have very different binding properties from those observed. In the receptor binding study, 6-OH-2,2'-DBB showed a high ER binding affinity of 0.196  $\mu\text{M}$ , however, the predicted EC<sub>50</sub> value however was very low ( $\Delta G = -5.4$ ,  $K_d = 109$   $\mu\text{M}$ ), about the same as the non-hydroxylated parent compound. However, it is not likely that its hydroxyl on the 6'-position enhances binding affinity through interaction(s) with the important hydrogen bonding partners, Glu353, Arg394 or His524. since this is nearly impossible because both biphenyl rings clash with the ER protein when the hydroxyl is orientated towards Glu353 and Arg394 or towards His524. Possibly, as a result of the position of the OH group and three substituents at the *ortho* positions, the lipophilic or electronic properties are very different from all other compounds used, and in that case, the LIE method may yet be inadequate to accurately correct for this particular detail. Other explanations may be that 6-OH-2,2'-DBB binds as a partial agonist or even a partial antagonist (this could be supported by the fact that 6-OH-2,2'-DBB only partially induced ER-mediated luciferase activity in the ER-Calux<sup>®</sup> assay, as shown in our previous study<sup>[22]</sup>). Or, exotically, two molecules bind at the same time. Maybe, 6-OH-2,2'-DBB has other unexplained allosteric effects on the ER $\alpha$  which explain the high observed binding affinity, however, we were not able to include extra experimental or *in silico* work on any of these possibilities.

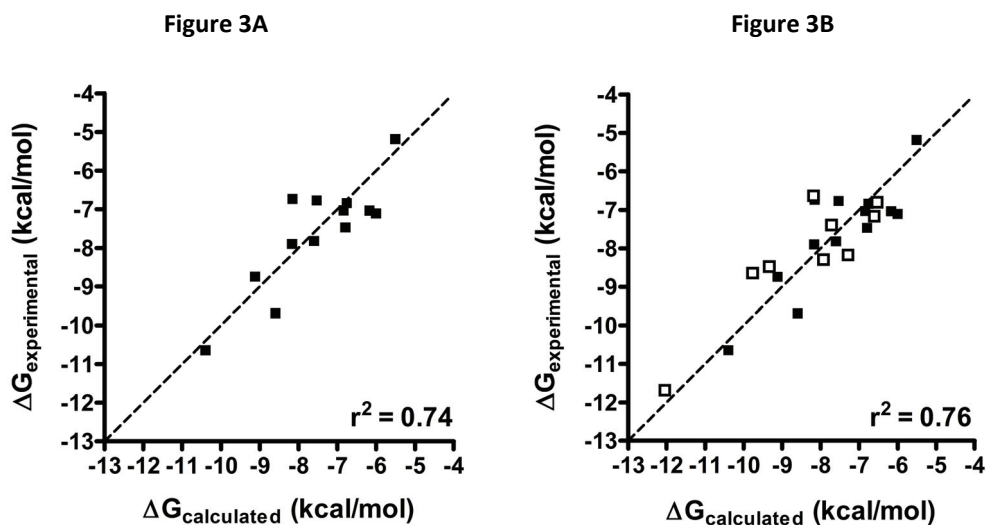


**Figure 3:** Graphs presenting the relationship of predicted  $\Delta G$  values ( $\Delta G_{\text{calculated}}$ ) versus experimentally obtained  $\Delta G$  values ( $\Delta G_{\text{experimental}}$ ) in kcal/mol. **A**, binding energies of the ligands of the DHB set alone ( $n=13$ , solid squares). **B**, binding energies of the DHB set (solid squares), extended with the test set from the previously published LIE model ( $n=22$ , open squares). The straight line represents the line  $\Delta G_{\text{calc}} = \Delta G_{\text{exp}}$  ( $y = x$ ). The linear correlation coefficient ( $r^2$ ) reflects the deviations of the experimental and calculated values from this line.

The predicted binding affinity of 3-OH-4,2'-DBB was much higher than the observed affinity in the binding assay. *In silico*, we observed that this compound interacts via an extra hydrogen bond contact with Leu346 in the ER $\alpha$ , causing extra interaction energy, as shown in Table 4, which may explain the calculated high binding affinity. However, we have not been able to explain the lower observed experimental binding affinity.

**Table 2** (right page): Binding affinities and structures of hydroxylated bromobiphenyls, chlorinated and non-hydroxylated biphenyls used in the current study. <sup>a</sup>MBB: monobromo biphenyl, DBB: dibromo biphenyl, MBB: monochloro biphenyl, DCB: dichloro biphenyl, TCB: tetrachloro biphenyl, <sup>b</sup>recalculated from relative binding affinity (compared to E2) to EC<sub>50</sub> for sheep, <sup>c</sup>Experimental values (mouse) adapted from literature<sup>[263]</sup>, <sup>d</sup>Experimental values (mouse) adapted from literature<sup>[241]</sup>, <sup>e</sup>Experimental values (rat) adapted from literature<sup>[304]</sup>, <sup>f</sup>Experimental values (human) adapted from literature<sup>[305]</sup>, <sup>g</sup>No affinity observed, tested up to 0.3 mM.

**Table 2**

	Compound <sup>a</sup>	Structure	EC <sub>50</sub> (s.e.m.) in $\mu$ M	
<i>Brominated biphenyls</i>	4-OH-2,2'-DBB		0.007	(0.002)
	4-OH-2,4'-DBB		0.086	(0.005)
	6-OH-2,2'-DBB		0.196	(0.06)
	3-OH-2,2'-DBB		0.418	(0.07)
	4-OH-3,2'-DBB		1.45	(0.16)
	3-OH-2,4'-DBB		1.71	(1.20)
	4-OH-3,4'-DBB		1.96	(0.04)
	3-OH-4,4'-DBB		3.53	(1.5)
	6-OH-2,4'-DBB		6.49	(1.5)
	2-OH-4,4'-DBB		7.3	(2.1)
	5-OH-3,4'-DBB		7.4	(1.5)
	2-OH-3,2'-DBB		10.1	(3.4)
	4-OH-4'-MBB		11.4	(4.3)
	2-OH-3,4'-DBB		12.2	(3.8)
	3-OH-4,2'-DBB		41.1	(7.2)
<i>Chlorinated biphenyls</i>	4-OH-2,4,6-DCB		0.0039 <sup>c</sup> /0.0017 <sup>d</sup>	
	4',4'-di-OH-2- MCB		0.0084 <sup>c</sup> /0.0041 <sup>d</sup>	
	4,4'-di-OH-3,3',5,5'-TCB		165 <sup>e</sup> /1.26 <sup>c</sup> /0.70 <sup>d</sup>	
	4-OH-2,2',6,6'-TCB		0.19 <sup>f</sup>	
<i>Non-hydroxylated biphenyls</i>	2,2'-DBB		173 (102)	
	4,4'-DBB		>300 <sup>g</sup>	
	2,2'-DCB		>300 <sup>g</sup>	

<i>Table 3A</i>	Or.	$\Delta E^{\text{VDW}}$	$\Delta E^{\text{EL}}$	$\Delta E^{\text{VDW}}$	$\Delta E^{\text{EL}}$	$\Delta E_{\text{AMBER}}$	$p_i$	$\Delta G_{\text{calc. } i}$	$\Delta G_{\text{calc}}$	$\Delta G_{\text{exp}}$
Ligand		Receptor-bound		Solvated					Predicted	Observed
2,4'-DBB	1	-30.70	-2.96	-20.68	-5.94	-7.04	0.56	-6.76	-6.59	n.d.
	2	-30.03	-3.44	-20.68	-5.94	-6.85	0.41	-6.45		
	3	-28.70	-2.74	-20.68	-5.94	-4.82	0.01	-5.00		
	4	-30.33	-1.37	-20.68	-5.94	-5.08	0.02	-5.66		
2,2'-DBB	1	-29.40	-3.16	-20.37	-6.94	-5.25	0.96	-5.55	-5.49	-5.16
	2	-28.29	-2.23	-20.37	-6.94	-3.22	0.03	-4.17		
	3	-28.22	-1.03	-20.37	-6.94	-1.95	0.00	-3.51		
	2a	-28.42	-0.70	-20.37	-6.94	-1.82	0.00	-3.51		
2,2'-DCB	1	-28.53	-2.99	-18.95	-7.10	-5.46	0.97	-5.83	-6.39	n.d.
	2	-27.26	-1.14	-18.95	-7.10	-2.34	0.01	-3.86		
	3	-26.95	-2.29	-18.95	-7.10	-3.18	0.02	-4.17		
	4	-26.17	-1.73	-18.95	-7.10	-1.84	0.00	-3.25		
4,4'-DBB	2a	-27.11	-3.20	-18.95	-7.10	-4.25	0.13	-4.76	-8.30	n.d.
	1	-32.19	-1.62	-19.78	-5.52	-8.52	0.28	-8.27		
	2	-31.65	-1.69	-19.78	-5.52	-8.04	0.13	-7.86		
	3	-30.91	-1.78	-19.78	-5.52	-7.39	0.04	-7.29		
3,4'-DBB	4	-32.31	-1.90	-19.78	-5.52	-8.90	0.54	-8.50	-9.52	n.d.
	1	-31.66	-1.34	-18.33	-4.94	-9.73	0.09	-9.18		
	2	-30.73	-2.00	-18.33	-4.94	-9.45	0.06	-8.73		
	3	-31.19	-2.18	-18.33	-4.94	-10.09	0.17	-9.20		
4-OH-2,2'-DBB	4	-31.51	-2.67	-18.33	-4.94	-10.91	0.68	-9.72	-10.38	-10.65
	1	-28.87	-17.70	-17.40	-17.10	-12.07	0.07	-9.71		
	1a	-28.92	-19.22	-17.40	-17.10	-13.64	0.93	-10.43		
	2	-29.84	-12.83	-17.40	-17.10	-8.17	0.00	-8.34		
4-OH-2,4'-DBB	2a	-29.36	-12.36	-17.40	-17.10	-7.22	0.00	-7.73	-8.58	-9.70
	3	-30.56	-8.30	-17.40	-17.10	-4.37	0.00	-6.92		
	4	-28.50	-8.62	-17.40	-17.10	-2.62	0.00	-5.36		
	1	-29.36	-18.72	-19.60	-17.50	-10.98	1.00	-8.58		
6-OH-2,2'-DBB	2	-29.66	-14.04	-19.60	-17.50	-6.60	0.00	-6.74	-5.44	-9.21
	3	-31.33	-3.11	-19.60	-17.50	2.66	0.00	-3.24		
	4	-32.02	-7.87	-19.60	-17.50	-2.79	0.00	-5.94		
	1	-29.89	-7.79	-19.08	-17.78	-0.82	0.03	-4.45		
3-OH-2,2'-DBB	1a	-30.24	-9.48	-19.08	-17.78	-2.86	0.96	-5.49	-9.11	-8.76
	2	-27.37	-8.83	-19.08	-17.78	0.66	0.00	-2.84		
	2a	-29.90	-2.71	-19.08	-17.78	4.24	0.00	-2.19		
	3	-30.24	-6.00	-19.08	-17.78	0.62	0.00	-3.94		
4-OH-3,2'-DBB	4	-30.79	-2.55	-19.08	-17.78	3.52	0.00	-2.85	-6.47	-8.01
	1	-29.43	-14.69	-16.40	-18.60	-9.12	0.06	-8.98		
	1a	-30.30	-6.46	-16.40	-18.60	-1.76	0.00	-6.03		
	2	-30.80	-6.72	-16.40	-18.60	-2.52	0.00	-6.56		
3-OH-2,4'-DBB	2a	-27.81	-17.97	-16.40	-18.60	-10.78	0.94	-9.11	-8.15	-7.91
	3	-27.90	-6.83	-16.40	-18.60	0.27	0.00	-4.22		
	4	-28.45	-10.28	-16.40	-18.60	-3.72	0.00	-6.21		
	1	-30.45	-6.83	-19.56	-18.57	0.85	0.00	-3.73		
4-OH-3,4'-DBB	2	-31.06	-11.86	-19.56	-18.57	-4.79	1.00	-6.48	-7.58	-7.84
	3	-30.71	-6.39	-19.56	-18.57	1.03	0.00	-3.75		
	4	-29.59	-3.75	-19.56	-18.57	4.80	0.00	-1.64		
	1	-29.74	-16.19	-17.67	-20.04	-8.22	0.26	-8.22		
3-OH-4,4'-DBB	2	-28.78	-17.76	-17.67	-20.04	-8.83	0.74	-8.13	-6.78	-7.48
	3	-32.00	-7.43	-17.67	-20.04	-1.71	0.00	-6.17		
	4	-30.98	-8.25	-17.67	-20.04	-1.51	0.00	-5.70		
	1	-29.42	-11.67	-18.53	-16.81	-5.74	0.11	-6.67		
3-OH-4,4'-DBB	2	-30.68	-11.64	-18.53	-16.81	-6.98	0.89	-7.70	-6.78	-7.48
	3	-33.46	-3.68	-18.53	-16.81	-1.81	0.00	-6.44		
	4	-31.54	-4.20	-18.53	-16.81	-0.41	0.00	-5.09		
	1	-34.02	-3.21	-22.23	-9.06	-5.94	0.76	-7.10		
3-OH-4,4'-DBB	2	-31.00	-5.15	-22.23	-9.06	-4.87	0.13	-5.48	-6.78	-7.48
	3	-33.44	-1.44	-22.23	-9.06	-3.60	0.01	-5.84		
	4	-32.76	-3.23	-22.23	-9.06	-4.70	0.10	-6.07		

<i>Table 3A continued</i>	Or.	$\Delta E^{\text{VDW}}$	$\Delta E^{\text{EL}}$	$\Delta E^{\text{VDW}}$	$\Delta E^{\text{EL}}$	$\Delta E_{\text{AMBER}}$	$p_i$	$\Delta G_{\text{calc. } i}$	$\Delta G_{\text{calc}}$	$\Delta G_{\text{exp}}$
Ligand		Receptor-bound		Solvated					Predicted	Observed
6-OH-2,4'-DBB	1	-30.77	-8.46	-19.55	-17.76	-1.91	0.04	-5.08	-5.99	-7.12
	2	-30.98	-10.16	-19.55	-17.76	-3.83	0.96	-6.02		
	3	-29.99	-5.15	-19.55	-17.76	2.17	0.00	-2.97		
	4	-33.45	-3.20	-19.55	-17.76	0.67	0.00	-4.95		
2-OH-4,4'-DBB	1	-32.24	-8.11	-21.46	-14.20	-4.70	0.99	-6.16	-6.16	-7.05
	2	-33.58	-3.18	-21.46	-14.20	-1.11	0.00	-5.07		
	3	-33.91	-2.89	-21.46	-14.20	-1.14	0.00	-5.21		
	4	-32.47	-2.04	-21.46	-14.20	1.15	0.00	-3.65		
5-OH-3,4'-DBB	1	-31.72	-5.45	-20.26	-18.22	1.31	0.00	-3.74	-6.82	-7.04
	2	-32.42	-7.34	-20.26	-18.22	-1.29	0.00	-5.17		
	3	-33.92	-4.10	-20.26	-18.22	0.46	0.00	-4.95		
	4	-32.70	-10.56	-20.26	-18.22	-4.78	1.00	-6.83		
2-OH-3,2'-DBB	1	-33.44	-2.99	-20.95	-10.71	-4.77	0.93	-6.84	-6.74	-6.86
	2	-32.35	-2.33	-20.95	-10.71	-3.02	0.05	-5.65		
	3	-31.33	-2.73	-20.95	-10.71	-2.40	0.02	-4.99		
	4	-29.60	-3.66	-20.95	-10.71	-1.60	0.00	-3.98		
4-OH-4'-MBB	1	-27.23	-17.35	-18.50	-16.60	-9.48	1.00	-7.52	-7.52	-6.78
	3	-30.42	-5.98	-18.50	-16.60	-1.30	0.00	-5.08		
2-OH-3,4'-DBB	1	-31.99	-3.04	-20.80	-9.02	-5.21	0.02	-6.54	-8.14	-6.75
	2	-33.58	-3.80	-20.80	-9.02	-7.56	0.97	-8.20		
	3	-33.17	-1.61	-20.80	-9.02	-4.95	0.01	-6.88		
	4	-32.47	-1.57	-20.80	-9.02	-4.22	0.00	-6.28		
3-OH-4,2'-DBB	1	-32.91	-6.94	-20.71	-9.47	-9.66	0.04	-8.91	-10.01	-6.02
	1a	-33.85	-7.81	-20.71	-9.47	-11.48	0.94	-10.07		
	2	-32.63	-3.17	-20.71	-9.47	-5.61	0.00	-7.00		
	2a	-33.18	-5.89	-20.71	-9.47	-8.88	0.01	-8.66		
	3	-30.81	-3.70	-20.71	-9.47	-4.33	0.00	-5.74		
	4	-30.68	-5.46	-20.71	-9.47	-5.95	0.00	-6.42		
4'-OH-2,4,6-DCB	1a	-30.53	-17.93	-20.34	-15.53	-12.59	0.96	-9.46	-9.43	-10.36
	2a	-31.73	-12.97	-20.34	-15.53	-8.83	0.00	-8.24		
	2	-30.42	-16.04	-20.34	-15.53	-10.59	0.03	-8.53		
	3	-31.67	-7.33	-20.34	-15.53	-3.13	0.00	-5.67		
	4	-30.00	-8.15	-20.34	-15.53	-2.27	0.00	-4.66		
	1a	-31.29	-16.87	-20.15	-16.15	-11.86	0.00	-9.49		
4-OH-2,2',6,6'-Tetra-CB	2a	-31.55	-14.24	-20.15	-16.15	-9.50	0.00	-8.54	-11.44	-9.21
	2	-31.43	-20.98	-20.15	-16.15	-16.12	1.00	-11.44		
	3	-31.51	-10.24	-20.15	-16.15	-5.46	0.00	-6.73		
	4	-32.19	-10.48	-20.15	-16.15	-6.38	0.00	-7.39		
	1a	-28.06	-15.74	-16.84	-27.60	0.64	0.00	-6.85		
	2a	-26.57	-17.98	-16.84	-27.60	-0.12	0.00	-6.08		
4,4'-diOH-2-MCB	2	-27.54	-16.52	-16.84	-27.60	0.39	0.00	-6.58	-7.13	-9.89
	3	-26.35	-17.54	-16.84	-27.60	0.55	0.00	-5.81		
	4	-26.93	-21.72	-16.84	-27.60	-4.22	1.00	-7.13		
	1a	-34.62	-8.68	-24.21	-18.49	-0.60	0.00	-6.60		
	2a	-33.52	-13.77	-24.21	-18.49	-4.59	0.54	-6.72		
	2	-34.24	-12.78	-24.21	-18.49	-4.32	0.35	-7.12		
4,4'-diOH-3,3',5,5'-Tetra-CB	3	-33.79	-9.76	-24.21	-18.49	-0.85	0.00	-6.13	-6.90	-7.25
	4	-34.55	-11.78	-24.21	-18.49	-3.63	0.11	-7.17		

**Table 3A** (left and right pages): Interaction energies and  $\Delta G$  values (predicted and observed) of brominated biphenyls. Complete legend: see Table 3B.

**Table 3B**

Ligand	Or.	$\Delta E^{\text{VDW}}$	$\Delta E^{\text{EL}}$	$\Delta E^{\text{VDW}}$	$\Delta E^{\text{EL}}$	$\Delta E_{\text{AMBER}}$	$p_i$	$\Delta G_{\text{calc. } i}$	$\Delta G_{\text{calc}}$	$\Delta G_{\text{exp}}$
		Receptor-bound		Solvated				Predicted Observed		
4-OH-2,2'-DCB	1	-28.16	-16.42	-17.91	-18.15	-8.52	0.17	-1.29	-8.00	n.d.
	1a	-28.17	-17.37	-17.91	-18.15	-9.47	0.82	-6.65		
	2	-26.54	-16.36	-17.91	-18.15	-6.83	0.01	-0.06		
	2a	-27.29	-13.61	-17.91	-18.15	-4.84	0.00	0.00		
	3	-30.07	-9.26	-17.91	-18.15	-3.27	0.00	0.00		
	4	-26.43	-8.47	-17.91	-18.15	1.16	0.00	0.00		
3-OH-2,2'-DCB	1	-27.62	-13.32	-16.48	-19.83	-4.63	0.01	-0.04	-7.60	n.d.
	1a	-28.34	-9.38	-16.48	-19.83	-1.42	0.00	0.00		
	2	-27.56	-16.38	-16.48	-19.83	-7.63	0.87	-6.58		
	2a	-28.98	-7.61	-16.48	-19.83	-0.28	0.00	0.00		
	3	-28.20	-6.54	-16.48	-19.83	1.57	0.00	0.00		
	4	-29.40	-13.39	-16.48	-19.83	-6.49	0.13	-0.99		
6-OH-2,2'-DCB	1	-28.97	-6.61	-17.35	-17.47	-0.76	0.02	-0.11	-5.75	n.d.
	1a	-29.40	-8.37	-17.35	-17.47	-2.95	0.88	-5.18		
	2	-29.08	-7.26	-17.35	-17.47	-1.52	0.08	-0.41		
	2a	-29.50	-3.37	-17.35	-17.47	1.95	0.00	0.00		
	3	-29.44	-3.01	-17.35	-17.47	2.37	0.00	0.00		
	4	-27.15	-8.10	-17.35	-17.47	-0.43	0.01	-0.05		

**Table 3:** Overview of the van der Waals ( $\Delta E^{\text{VDW}}$ ) and electrostatic ( $\Delta E^{\text{EL}}$ ) interaction energy contributions to the interaction energy ( $\Delta E_{\text{AMBER}}$ ), and the calculated ( $\Delta G_{\text{calc}}$ ) and experimentally ( $\Delta G_{\text{exp}}$ ) derived free energies of binding (in kcal/mol) of a series of halogenated biphenyls to the ER $\alpha$  ligand-binding domain (LBD), docked in different orientations (1-4 and 1a-4a, see Computational Details section for explanation) into the ER $\alpha$  (receptor-bound), and the free ligands in water (solvated). The table also presents the Boltzmann weight factor  $p_i$  for each orientation.

**Table 3A** (page before) shows all non-hydroxylated and hydroxylated brominated biphenyls tested in the present study, and four hydroxylated chlorinated biphenyls, from which experimental values were adapted from literature.

**Table 3B** (above) shows the interaction energy contributions of three chlorinated biphenyls, from which no experimental values are available.

Finally, the predicted  $\Delta G$ s of the chlorinated biphenyl congeners 4',4'-diOH-2-MCB, 4,4'-diOH-3,3',5,5'-TCB and 4-OH-2,2',6,6'-TCB, from which experimental ER binding affinities were adapted from literature<sup>[241,263]</sup>, showed some discrepancies with the  $\Delta G$  values. This may be caused by the fact that their binding affinities were measured in other systems, i.e. human, mouse and rat. Sheep and mouse ER $\alpha$  differ only by a few amino acid residues

from human ER $\alpha$ , however, the interchanged Asn527 in mouse (Ser in human) is neighboring His524 and may provide extra interactions in the binding cavity, resulting in distinctive binding affinities.

The number of halogens present in the molecule may also affect the outcome of the LIE calculation for binding to the ER $\alpha$ . Unfortunately, our database is too small to consistently test this possibility.

### 4.3 Structure activity relationship

The set of bromobiphenyls studied in this investigation shows that the ER $\alpha$  hosts binding of biphenyls, preferably halogenated at the *ortho*-positions (i.e. at positions 2 or 2'). An *ortho*-substituent increases the binding affinity to ER $\alpha$ , as is clear for example from the increase in  $\Delta G_{\text{calc}}$  observed for 4-OH-4'-MBB to 4-OH-2,4'-DBB, namely  $\Delta G_{\text{calc}} = -7.5$  kcal/mol and  $-8.6$  kcal/mol respectively. Secondly, two halogens are favoured over one, and one halogen is favoured over no substituent at all. This suggestion is very plausible, given the fact that the two lipophilic ethyl groups of the synthetic hormone DES bind the ER $\alpha$  cavity similarly to the lipophilic halogen substituents, and these are thought to account for its high affinity. A hydroxyl group at the 4-position of the biphenyl is evidently preferred for binding compared to the 2- or 3-position. This was expected, since at the *para*-position, it may form hydrogen bonds with Glu353 and Arg394, as do E2 and DES. Hydroxyl-groups at the 2- or 3-positions are also known to interact with these amino acids, however, these interactions are weaker<sup>[147]</sup>. The lack of an extra hydroxyl group in the biphenyl, which, in the case of E2 and DES interacts with His524, accounts for the generally lower binding affinities measured for biphenyl congeners, however, the two *ortho*-halogens seem to enhance binding significantly.

Based on our results, the brominated biphenyls bind the ER $\alpha$  better than the chlorinated biphenyls: The  $\Delta G_{\text{calc}}$  of 4-OH-2,2'-DBB and 3-OH-2,2'-DBB are  $-10.4$  and  $-9.1$  kcal/mol, respectively, against  $-8.0$  and  $-7.6$  kcal/mol for 4-OH-2,2'-DCB and 3-OH-2,2'-DCB. This difference is probably due to the fact that the bromines are larger and more lipophilic than the chlorines. As a result, biphenyls with bromo substituents display more favourable  $\Delta E^{\text{VDW}}$  values (see Table 3). Brominated biphenyls show a higher complementarity of the bromo substituents with lipophilic pockets available in the binding pocket.

From this and earlier studies, it can be concluded that the cavity hosts preferably biphenyls with *ortho*-substituted halogen(s). Kuiper *et al.*<sup>[109]</sup> showed with chlorinated biphenyls that there is also room for a third lipophilic substituent at the non-phenolic *para*-position of, e.g., 4-OH-2,2'-DBB. The relatively high binding affinity of 4-OH-2,4'-DBB ( $\Delta G_{\text{calc}} = -8.6$  kcal/mol) confirms that a halogen at the *para*-position also enhances affinity for the ER $\alpha$ .

---

## 5 Conclusions

In order to further expand our computational ER $\alpha$  LIE model for prediction of binding affinities, molecular dynamics simulations were performed with 22 structurally related hydroxylated biphenyls. The average variation between  $\Delta G_{\text{calc}}$  and  $\Delta G_{\text{exp}}$  was  $1.16 \pm 0.26$  kcal/mol (s.e.m.), which is acceptable for the predictive value of the LIE model. Since the ER binding affinities taken from literature vary strongly between different publications, these data were not included further in the correlation calculation or correlation graph. As we have shown for environmental estrogens in an earlier study, the LIE method provides again a great tool for the prediction of absolute ligand binding affinities, as well as binding orientation of ligands. It was well possible that the LIE method we described earlier, needed extra adjustment for the application on biphenyl metabolites. For example, Almlof *et al.* incorporated an additional parameter, which was found to depend on the hydrophobicity of the binding site to gain better results<sup>[306]</sup>. In our case, addition of other parameters did not improve our data. In fact, the original LIE parameters obtained by the large diverse dataset we already had, proved to be very suitable for the halogenated biphenyls. From the current study, we can conclude that the LIE method provides to be a useful tool for the prediction of approximate binding affinities of this class of environmental contaminants.

When combining the results of the current study with the test set of the earlier model, we observe again a good overall correlation between predicted and experimental  $\Delta G$  values, and the correlation (i.e. slope and intercept) did not significantly differ from the bromo-biphenyl-only set (Figure 3). This confirms that the LIE approach is a very stable and reliable method. A great variety of structurally different molecules can be assessed. A very important advantage is that putative estrogenic compounds such as metabolites of environmental contaminants such as halogenated biphenyls, which are hard difficult to test *in vitro*, can be investigated. This method may therefore be of great value to comprehensive risk assessment of these kind of hazardous compounds in stead of investigating parent compounds alone.

**Table 4** (right page): Overview of important hydrogen bond interactions of hydroxylated halogenated biphenyls to amino acid residues of the ER $\alpha$ . Shown are the percentages of hydrogen bonds formed between the ligand and the amino acid residues Glu353, Arg394, His524 and a (crystal) water. Three other important hydrogen bond interactions are also listed: Gly521, Leu346 and Leu387. A percentage of more than 100% indicates that more than one hydrogen bond between the ligand and the amino acid is formed during the simulation.

Ligand	Or.	Glu 353	Arg 394	His 524	Wat	Gly 521	Leu 346	Leu 391
4-OH- 2,2'-DBB	1 1a 2 2a 3 4	100 105	5 14					
					40 100 100			
				88 6		91		
4-OH- 2,4'-DBB	1 2 3 4	98 91			84 8			
						3 47		
6-OH- 2,2'-DBB	1 1a 2 2a 3 4			40 91			88 99	
							76	
3-OH- 2,2'-DBB	1 1a 2 2a 3 4				100 82			5 83
							83	
		100		8 97		55		
4-OH- 3,2'-DBB	1 2 3 4		4		86		88	
				8		92		
3-OH- 2,4'-DBB	1 2 3 4	40 100			110			
						94 99		
4-OH- 3,4'-DBB	1 2 3 4	99						
					80			100
						28		
3-OH- 4,4'-DBB	1 2 3 4	2					8	
					85			8
						2 50		
6-OH- 2,4'-DBB	1 2 3 4						100	
								100
Ligand	Or.	Glu 353	Arg 394	His 524	Wat	Gly 521	Leu 346	Leu 391
2-OH- 4,4'-DBB	1 2 3 4						99 28 15	
5-OH- 3,4'-DBB	1 2 3 4							100 70
				88				
2-OH- 3,2'-DBB	1 2 3 4						42 48	
4-OH- 4'-MBB	1 3	109 12			60		49	
			3					
2-OH- 3,4'-DBB	1 2 3 4						23 65	
3-OH- 4,2'-DBB	1 1a 2 2a 3 4						92 70	
								66 16
					56			
						64		
4'-OH- 2,4,6-DCB	1a 2 2a 3 4 1a	84 100	8 16		30 68			12
			2		98			
				94 98				
		76						22
4-OH-2,2',6,6'- Tetra-CB	2 2a 3 4 1a	100			4 100			
				98 98				
			8		100			
4,4'-diOH-2- MCB	2 2a 3 4 1a			82	62 100			82
					56	100	96	22
		72	2	24		48		8
				60	2			24
4,4'-diOH-3,3', 5,5'-Tetra-CB	2 2a 3 4	98 80	8 6				86	
				16 64	94			14



## Chapter 6

The chemical interaction between the estrogen receptor  
and monohydroxybenzo[*a*]pyrene derivatives  
studied by fluorescence line-narrowing spectroscopy

Arjen N. Bader, Maarten M. van Dongen, Marola M.H. van Lipzig, Jeroen Kool, John H.N.  
Meerman, Freek Ariese en Cees Gooijer.

Chemical Research in Toxicology, 2005 (18), 1405-12.

---

## ABSTRACT

A novel approach is presented for studying the chemical interaction between receptor binding sites and ligands. Mono-hydroxylated poly-aromatic compounds were found to be environment sensitive ligands when applying a special mode of fluorescence: fluorescence line-narrowing spectroscopy (FLNS). With this technique, solvent dependencies and ligand-receptor interactions can be studied in great detail, due to the high spectral resolution and the fact that at cryogenic temperatures (4K), no solvent reorientation effects are complicating the interpretation. The FLN spectrum of a ligand bound to the receptor is compared to its spectra in solvent mixtures that mimic the functionalities present within the receptor's binding site. It is shown that for the well-known estrogen receptor (ER), the orientations of two xeno-estrogenic ligands 3- and 9-hydroxybenzo[*a*]pyrene (3- and 9-OH-BaP) can be determined. The FLN results clearly indicate that an H-bond accepted by His524 plays a major role in the binding of these ligands to the ER. Furthermore, the spectra indicated  $\pi$ - $\pi$  stacking aromatic interaction for 9-OH-BaP with Phe404. These results are in line with molecular modelling studies published earlier.

## 1 Introduction

Exposure to environmental estrogens or xeno-estrogens has been proposed to be a risk factor, associated with disruption of reproductive development and tumorigenesis in humans and wildlife<sup>[4]</sup>. Endogenous estrogens play a crucial role in the development, growth and regulation of sexual and reproductive organs and behaviour of mammals<sup>[2]</sup>. They act via binding to estrogen receptors (ER), members of the nuclear receptor superfamily that function as transcription factors to modulate gene expression in a ligand-dependent manner<sup>[142]</sup>. In the nucleus, binding of ligands induces a conformational change of the ER, enabling the receptor to dimerise. The dimer binds to the palindrome estrogen response elements (ERE) in DNA, where it enhances gene transcription leading to e.g. protein synthesis and cell proliferation<sup>[134]</sup>. Two ER isoforms have been identified, ER $\alpha$  and ER $\beta$ , that show different tissue expression and distinct ligand binding properties<sup>[109]</sup>. In the present study, the attention is confined to ER $\alpha$ .

Polycyclic aromatic hydrocarbons (PAHs) form a class of well-known environmental pollutants. Many different PAHs are formed during incomplete combustion of organic material: they can be found in e.g. (cigarette) smoke, exhausts, and burned meat. After uptake in the body, PAHs are metabolised in various ways, resulting in a large variety of oxygenated compounds, some of which are known to be potentially toxic or carcinogenic. An example of such a PAH is benzo[a]pyrene (BaP). In addition to its carcinogenicity and cytotoxicity, BaP also possesses endocrine activity. BaP's structural resemblance with the endogenous estrogen 17 $\beta$ -estradiol (E2) (see Figure 1) has been the objective of several studies<sup>[209,216,218]</sup>. BaP was reported to exhibit estrogenic activity in several cellular systems *in vitro*<sup>[53,54,219,220]</sup>, but no ER-affinity of BaP was found in radioligand binding assays. Recently, it was shown that the estrogenic effect of BaP in T47D breast cancer cells is due to the formation of BaP metabolites<sup>[46]</sup>. For several mono-hydroxylated BaPs (OH-BaPs), including 2-OH-, 3-OH-, 8-OH- and 9-OH-BaP, low-affinity estrogenic activity was reported<sup>[46]</sup>. Despite these relatively low affinities for the individual OH-BaPs, the estrogenic properties of BaP may still be relevant. It should be realised that *in vivo* always a mixture of various metabolites are formed after exposure to PAHs. It was recently shown that a mixture of OH-BaPs induces significant estrogenic responses, much higher than expected<sup>[46]</sup>.

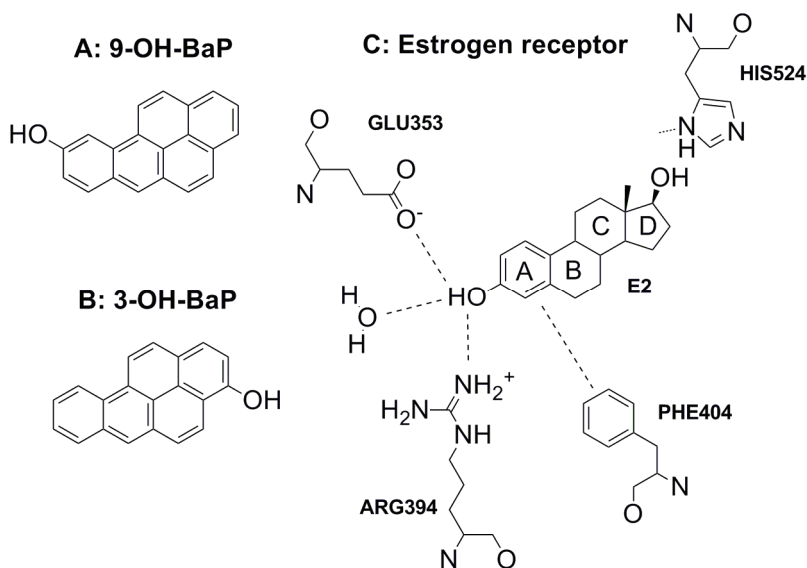


**Figure 1:** The molecular structure of 9-OH-BaP (A), 3-OH-BaP (B), and Estradiol (E2) located in the estrogen receptor (ER) binding pocket (C). The amino acids shown are involved in the binding of E2 to the ER.

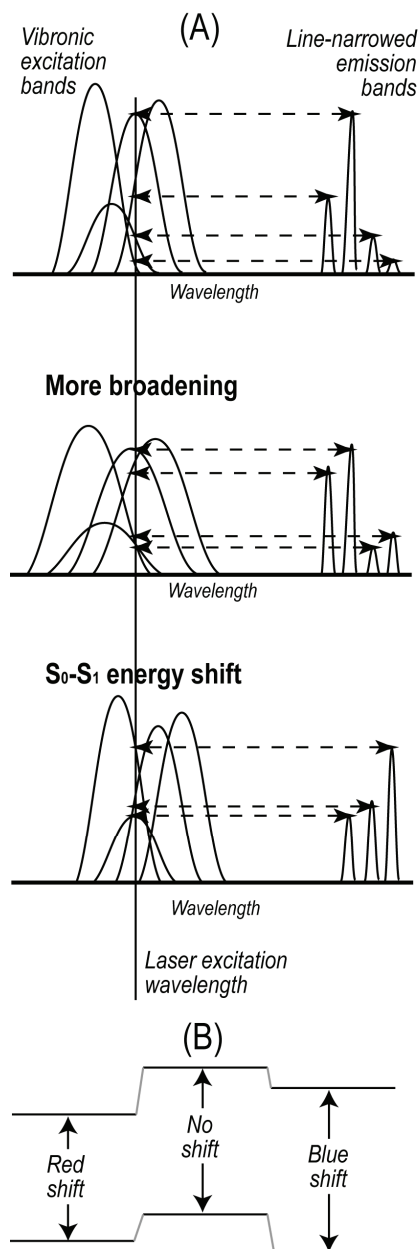
Although for E2 (and also for estrogens such as DES and THC) the binding orientation in the ER is known from crystallographic data (see Figure 1 for E2)<sup>[134,145,289]</sup>, it is very hard to predict binding orientations (and binding affinities) of ligands such as the OH-BaPs dealt with in the present study. Recently, a computational model was published, predicting binding orientation and affinity for many (xeno)estrogens, including estrogenic OH-BaP-metabolites<sup>[149]</sup>. The shape and planarity of an OH-BaP molecule is quite similar to that of E2. The main difference, however, is that an OH-BaP possesses only one hydroxy-group whereas E2 has two. This implies that the orientation of the hydroxyl group of OH-BaPs in the ER may be either towards Glu353 and Arg394, or towards His524 (left hand or right hand side in Figure 1, respectively). Unfortunately, experimental data supporting the one or the other orientation are difficult to obtain. Here, we present a novel methodology that may provide such information, i.e., a special mode of molecular fluorescence known as fluorescence line-narrowing spectroscopy (FLNS). Recently it was shown that FLNS is appropriate for investigating in detail the interaction of adducts and metabolites of BaP with their corresponding antibodies<sup>[307]</sup>.

Briefly, FLNS is a technique in which high-resolution fluorescence spectra are obtained by freezing a liquid sample to below 10 K and applying selective laser excitation<sup>[308,309]</sup>. FLNS can be successfully applied to (substituted) PAHs, even in solvent systems like aqueous buffers. The only restriction to the solvent is that upon cooling it should form an amorphous rather than a (poly) crystalline matrix. Under such conditions the

inhomogeneous broadening of the spectral bands is still significant: each individual analyte molecule is embedded in a particular surrounding of solvent molecules, thus experiencing its own particular interaction. Of course in the rigid, frozen matrix these interactions do not change in time, at least not during the fluorescence lifetime. The crucial feature of FLNS is that by using laser excitation, only those analyte molecules with a transition energy between the ground state  $S_0$  and the first electronically excited state  $S_1$  exactly matching the wavelength of the laser will be excited, and as a result only those selected solute molecules will emit fluorescence. This explains why narrow lines in emission are obtained<sup>[308,309]</sup>. If the laser wavelength is somewhat shorter so that vibrations of the  $S_1$  state are excited, the FLN emission pattern usually becomes more complicated. This is illustrated in Figure 2A, where four  $S_1$  vibrations are simultaneously excited. After excitation, non-radiative relaxation of the molecule to the associated  $S_{1,0}$  level takes place, followed by light emission. As a result four line-narrowed bands (also known as zero phonon lines, ZPLs) are observed in the emission spectrum. The photon energy differences between these lines and the laser line correspond to the excited state vibrations.

For the present purposes it is of main importance to note that the shape of the emission pattern is strongly influenced by solute-solvent interaction. This is schematically illustrated in Figure 2A where four vibrations are considered. For ease of comparison the intensities of the four ZPLs are labelled A/B/C/D and the intensity of the strongest ZPL is arbitrarily set equal to 10). This results in an intensity ratio of 4/10/2/1 in the upper spectrum in this figure. When the vibronic excitation bands are broadened, as in the middle spectrum of Figure 2A, the ratio becomes 8/10/2/3. This means that an enhancement of the relative intensity of the ZPLs at both edges of the multiplet origin band, i.e., band A and D, can be attributed to an increase of the inhomogeneous broadening. In other words, there is a larger variety in interaction energies with the solvent. When the vibronic excitation bands shift to lower energy (to the red), as is the case in the lower spectrum in Figure 2A, the ratio becomes 0/5/6/10. This implies that an increase in the relative intensity of the ZPLs on the right hand side in the multiplet origin band, i.e., bands C and D, is indicative for a red shift in the excitation spectrum. Obviously the opposite is true in case of decreased inhomogeneous broadening and a blue shift, respectively. To summarise, the qualitative analysis of Figure 2 illustrates how minor solvatochromic shifts and minor changes in inhomogeneous broadening that are hardly observable in conventional, broadbanded fluorescence spectroscopy can be sensitively monitored in FLNS using the relative intensities of the ZPLs. In other words, FLNS will be an appropriate technique to probe the local environment of the solute<sup>[307]</sup>.

**Figure 2:** Solvent dependencies in FLN spectra. (A) Schematic of a limited number of excitation and emission bands in a low temperature amorphous matrix. More broadening of the vibronic bands in excitation or a shift in  $S_1$ - $S_0$  energy results in a change in the relative intensities of the ZPLs in emission. (B) Schematic to show the effect of solute/solvent interaction on the  $S_0$ - $S_1$  energy difference. The  $S_1$  can be less or more stabilised than the  $S_0$  state, resulting in a blue or red shift, respectively.



It should be realized that Figure 2A gives only a simplified picture in which exclusively ZPLs are shown in the FLN spectrum while other, complicating, spectral features are ignored. In practice, in most cases a strong broad background is observed, red shifted compared to the ZPLs. This background is composed of phonon side bands (PSBs)<sup>[308,309]</sup>. PSBs are due to electron phonon coupling, i.e., coupling of electronic transitions with lattice vibrations of the solvent matrix. The relative intensities of the ZPLs compared to the PSBs decreases with the strength of the interaction between solute and matrix; therefore PSBs are not only complicating the spectra but in principle they provide substantial information as well.

In a previous study, devoted to the interaction between antigens and their corresponding antibodies<sup>[307]</sup>, the approach followed was to record the FLN spectra of the fluorophore in a variety of solvent mixtures selected for their different solvation behaviour. By comparing the spectrum of the fluorophore bound to its antibody to this set of reference spectra, the dominating chemical interaction between antigen and antibody could be established. In the present study, a similar approach is chosen to investigate the binding of 3-OH-BaP and 9-OH-BaP to the ER. These two compounds were selected because they show a clear solvent dependency in their FLN spectra. Unlike the antibodies in the previous

study, the crystal structure of the ER is known. This makes the selection of the solvent mixtures straightforward: they are chosen such that the functionalities in the binding site are mimicked as much as possible. The ligands, however, have an affinity for the ER that is lower than that of E2. This indicates that in case of OH-BaPs only part of the functionalities in the binding pocket is used. Our main goal is to determine experimentally which functionalities are important for the binding and thus determine the orientations of the two OH-BaPs inside the ER binding pocket. The results can be verified by using the molecular modelling data published recently<sup>[149]</sup>. Furthermore, such an investigation will help in further exploration of the FLNS approach for studying protein/ligand interactions, a method that may become relevant in determining ligand orientation, especially in situations where protein crystal structures are lacking.

## 2 Experimental methods

### 2.1 Chemicals

The solvents glycerol and triethylamine were obtained from Aldrich (Seelze, Germany). Acetone, methylcyclohexane, n-butyl alcohol, were obtained from Baker (Deventer, The Netherlands), toluene from Fisher (Loughborough, UK). 3- and 9-hydroxybenzo[a]pyrene were obtained from NCI-MRI (Kansas City, MO, USA) and 17 $\beta$ -estradiol from Sigma Chemical Co. (St. Louis, USA). L(+)-Ascorbic acid (Baker) was added to prevent the monohydroxybenzo[a]pyrene derivatives from further oxidation.

### 2.2 Expression of ER $\alpha$ protein

The estrogen receptor- $\alpha$  LBD (ER; a kind gift of Dr Marc Ruff; Laboratoire de Biologie et Génomique Structurales 1, IGBMC, Illkirch, France) was expressed in *e-coli* according to Eiler et al [19], but without estradiol in the medium. The cells were pelleted at 4600 rpm for 60 min. and the pellet was subsequently suspended in 50 ml 10 mM monosodium hydrogen phosphate buffer (pH 7.4; adjusted by KOH) containing 150 mM NaCl. The cells were again pelleted at 4000 rpm for 15 min. and the pellet was suspended in 50 ml of the same buffer. This washing step was repeated two more times. After the last washing step, the pelleted cells were suspended in 25 ml of the same buffer. Purification of the ER $\alpha$  was performed by use of three french press cycles (700 bar) and ultrasonic sound (microtip, 30% duty cycle output 7, 10 cycles) to break up the cells and finally ultracentrifugation (100.000 g) for one hour to obtain the soluble receptor in the supernatant. The receptor concentration was estimated by determining the B<sub>max</sub> value. The soluble receptor (concentration of approximately 1  $\mu$ M) stock solution was stored at -80°C.

---

### 2.3 *Receptor binding experiments*

1-10  $\mu\text{M}$  solutions of OH-BaP in various solvents were measured. The solutions of ER-bound compound were made by diluting a 100  $\mu\text{M}$  OH-BaP stock solution in ethanol 10 times with 1  $\mu\text{M}$  ER in 10 mM Tris EDTA buffer, followed by incubation for one hour at 4°C. The bound OH-BaP fraction was separated from the unbound fraction as follows: after incubation, the unbound OH-BaP was retained by a charcoal (0.1%) column packed with dextran (0.01%) in Tris EDTA buffer (pH 7.5). The purified samples were directly cooled on ice to avoid re-establishing of the equilibrium between bound and unbound ligand. As a control experiment, an excess of E2 was added to a solution of ER and OH-BaP. Because of the strong affinity differences, the receptor binding sites will become exclusively occupied by the high-affinity ligand E2 and therefore all OH-BaP molecules will be displaced and subsequently adsorb to the charcoal in the column. For both 3-OH-BaP and 9-OH-BaP no fluorescence emission in the column effluent (ER/E2 complex solution) was observed, indicating that the charcoal purification is fully effective in removing unbound OH-BaP and that in our FLNS study we are exclusively dealing with OH-BaP/ER complexes. Binding of 3-OH-BaP or 9-OH-BaP was further checked by recording FLN spectra in Gly/Buf both in the presence and absence of ER (see below).

Four quartz tubes at a time were placed in a home-made sample holder mounted to the top of the cold head of a closed-cycle 4K liquid helium refrigerator (SRDK-205 Cryocooler, Janis Research Company, Wilmington, MA, USA). The excitation source was a XeCl excimer laser (Lambda Physik LPX 110i, Göttingen, Germany) pumping a dye laser (Lambda Physik, LPD 3002). The excimer laser was operated at 10 Hz, producing 10 ns 50 mJ pulses. Using PBBO as a dye, a tuneable output in the 386-420 nm range was obtained. The four samples could be measured separately by moving the cold head at an angle of 45° with respect to both the excitation beam and collection optics. Fluorescence emission was collected with a 3-cm F/1.2 quartz lens at a 90° angle to the excitation beam, focused by a 10-cm F/4 quartz lens on the entrance slit of a Spex 1877 0.6-m triple monochromator (Edison, NJ, USA) and detected with an intensified CCD camera (iStar DH720-25U-03, Andor instruments, Belfast, Northern Ireland) operated in the gated mode to reject stray and scattered light. The spectral resolution of the emission spectrum was 0.1 nm.

### 3 Results

As mentioned in the introduction, the main topic dealt with in the present study is the orientation of the OH-BaP hydroxy-group in the receptor. Since the affinity of the parent compound benzo[*a*]pyrene to the ER is much lower than the affinities of its monohydroxy-derivatives, most probably H-bonding interaction plays an important role<sup>[147]</sup>. Such interactions dominate the ER-E2 complex, as visualised in Figure 1C: with the two amino acids situated on the left hand side, an H-bonding network can be formed: the COO<sup>-</sup>-group of Glu353 accepts an H-bond from the ligand, whereas the NH<sub>2</sub><sup>+</sup>-group of Arg394 donates an H-bond to the ligand. On the right hand side, the imidazole ring of His524 is present, a group known to act exclusively as an H-bond acceptor. Of course contrary to E2, in OH-BaPs only one OH-group is available so that in principle two opposite orientations are possible. Furthermore, besides H-bonding also  $\pi$ - $\pi$  interaction might play a role. In view of the configuration depicted in Figure 1C, such an interaction of OH-BaP with Phe404 being located below the aromatic ring in E2 will be conceivable.

It should be noted that both H-bonding and  $\pi$ - $\pi$  interaction will strongly influence the shape of the FLN spectrum, whereas obviously effects caused by reorientation of solvent molecules (Stokes shift) are excluded in 4K matrices. These two types of ligand/receptor interaction will be mimicked using various solvent combinations.

The solvent combinations used to study both the OH-BaP/ER complexes are shown in Table 1. Four categories can be distinguished: (1) reference solvent, (2) H-bonding solvents, (3)  $\pi$ - $\pi$  interacting solvents, and (4) combinations of the latter two. The reference solvent, methylcyclohexane (MCH), is nonpolar and nonprotic and will therefore show minimal interactions. MCH yields amorphous matrices under cryogenic conditions, unlike some of the other solvents that had to be included in this study. For these solvents mixtures with MCH were used (solvent/MCH = 10/90 v/v). Such an approach also allows using combinations of solvents from the different categories (solvent1/solvent2/MCH = 10/10/80 v/v/v). Another selection criterion was that miscibility with MCH should not be a problem; no phase separation should occur, even under low temperature conditions. Additionally, the solubility of the OH-BaPs concerned was not a problem at the concentrations dealt with.

**Table 1**

		9-OH-BaP					3-OH-BaP			
Interaction	Solvent	A	B	C	D	E	A	B	C	D
<b>Estrogen Receptor</b>										
- ER present	ER in Gly/Buf	2	2	7	6	10	0	1	4	10
- ER absent	Gly/Buf	10	3	3	0	0	6	10	6	8
<b>Hydrophobic interaction</b>										
- reference	MCH	1	2	10	6	2	1	10	8	6
<b>H-bonding interaction</b>										
- with Glu and Arg	+ BuOH	3	2	10	5	2	1	7	8	10
- with His	+ TEA	2	1	10	10	8	1	2	7	10
<b><math>\pi</math>-<math>\pi</math> interaction</b>										
- with Phe	+ Tol.	1	2	10	7	6	2	10	8	10
- with C=O	+ Ace.	4	6	10	6	4	4	10	7	5
<b>Both H-bonding and <math>\pi</math>-<math>\pi</math></b>										
- with Phe and Glu&Arg	+ Tol. + BuOH	2	2	10	6	2	1	4	8	10
- with C=O and Glu&Arg	+ Ace. + BuOH	2	3	10	6	3	1	5	7	10
- with Phe and His	+ Tol. + TEA	2	2	9	9	10	0	3	10	8
- with C=O and His	+ Ace. + TEA	5	2	7	8	10	0	4	10	8

**Table 1:** Relative intensities of the multiplet origin ZPLs (A) 840 cm<sup>-1</sup>, (B) 980 cm<sup>-1</sup>, (C) 1050 cm<sup>-1</sup>, (D) 1177 cm<sup>-1</sup> and (E) 1328 cm<sup>-1</sup> in the FLN spectrum of 9-OH-BaP (see Figure 4), and of the multiplet origin ZPLs (A) 1075 cm<sup>-1</sup>, (B) 1175 cm<sup>-1</sup>, (C) 1325 cm<sup>-1</sup> and (D) 1395 cm<sup>-1</sup> in the FLN spectrum of 3-OH-BaP (see Figure 6). For Gly/Buf, three other strong blue shifted bands are observed (at 770, 857 and 960 cm<sup>-1</sup>, with relative intensities 4, 10 and 6, respectively).

To study the role of H-bonding, two solvents were added to MCH, i.e., 1-butanol (BuOH) and triethylamine (TEA). The interaction with the H-bonding network of Glu353 and Arg394 (see Figure 1C), is mimicked using BuOH. This solvent can both donate and accept an H-bond<sup>[310]</sup>. In view of the miscibility conditions with MCH, alcohols with a shorter alkyl chain could not be used. The interaction with His524 is mimicked by TEA, a solvent known to have exclusively H-bond accepting properties similar to the imidazole ring of this amino acid<sup>[310]</sup>. To mimic the aromatic interaction due to Phe404, toluene (Tol.) was used. It should, however, be realised that  $\pi$ -electron interaction can also be due to other functionalities present in the ER such as carbonyl groups. Therefore also acetone (Ace.) was used as a solvent. Finally, in the ER, H-bonding and  $\pi$ - $\pi$  interaction can play a role simultaneously. Therefore, the four possible combinations of these two categories of solvents were included as well.

The estrogen receptor itself was dissolved in 50% buffer and 50% glycerol (Gly/Buf), the latter solvent being added to ensure the formation of an amorphous matrix under

cryogenic conditions, a basic requirement to obtain FLN spectra. Since the affinity of the ER to the two OH-BaPs considered is relatively weak<sup>[46]</sup>, a clean-up step was involved to remove the unbound fraction as described in the Experimental Section.

## 2.4 9-OH-BaP

The FLN spectra of 9-OH-BaP bound to the ER and dissolved in the abovementioned solvent combinations are shown in Figure 3. First, it should be noted that the spectrum of 9-OH-BaP bound to the ER differs strongly from its spectrum in Gly/Buf, confirming complete binding of 9-OH-BaP to the ER. Furthermore, significant differences for other spectra are observed. Already from the shapes of the baselines some information can be inferred. In the spectrum of 9-OH-BaP bound to the ER, weak ZPLs located on a strong red-shifted and broad baseline are observed. Since the observed background is intense, the electron-phonon coupling will be strong. Similar features are observed for 9-OH-BaP in the presence of TEA (H-bond accepting interaction), toluene (aromatic  $\pi$ -electron interaction) and acetone (carbonyl  $\pi$ -electron interaction), but the degree of electron phonon coupling is much stronger in the presence of acetone or TEA than in the presence of the other solvents.

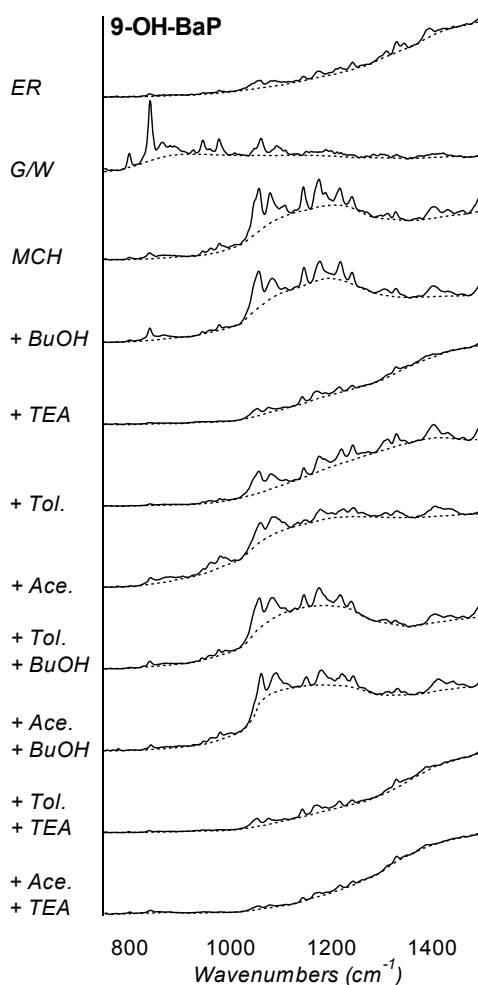
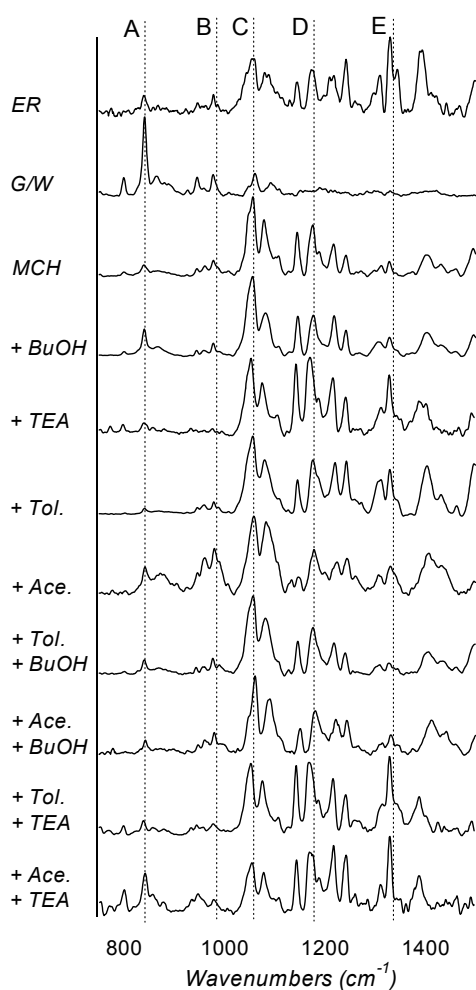


**Figure 3:** Normalised FLN spectra of 9-hydroxybenzo[a]pyrene in various solvents (or solvent combinations) and bound to the estrogen receptor. On the x-axis the energy difference with respect to the excitation wavelength in wavenumbers is used. The excitation wavelength was 403 nm.

In order to distinguish the ZPLs from the baseline, the concentration of acetone had to be lowered to 0.1% and the concentration of TEA to 0.01% (these are the concentrations used to record the spectra in Figure 3). It should be noted that the shapes of the baseline in the presence of acetone differs from the ones in toluene or TEA. The baselines observed for the latter two are similar to the one of 9-OH-BaP bound to the ER, whereas for acetone it is much less red-shifted. Also the combination of TEA and toluene or acetone yields spectral baselines similar to that of the ER. Baseline subtraction is an appropriate way to better visualize the relative intensities of the ZPLs (see Figure 4)<sup>[307,311]</sup>. Across the 0-0



region, five main bands were selected to monitor solute/solvent interaction: (A) 840  $\text{cm}^{-1}$ , (B) 980  $\text{cm}^{-1}$ , (C) 1055  $\text{cm}^{-1}$ , (D) 1175  $\text{cm}^{-1}$  and (E) 1330  $\text{cm}^{-1}$ , corresponding to vibrations in the  $S_1$  excited state. The intensity ratios of these bands observed in various solvents are listed in Table 1. In Gly/Buf, the intensity ratio is 10/3/3/0/0. When the ER is present, this ratio changes dramatically to 2/2/7/6/10, which proves that 9-OH-BaP is bound to the ER. MCH (reference spectrum) provides an intensity ratio of 1/2/10/6/2. In the presence of BuOH (both H-bond accepting and donating interaction) it changes to 3/2/10/5/2, i.e., a minor blue shift is observed. Conversely, in the presence of TEA (H-bond accepting interaction only) the intensity ratio becomes 2/1/10/10/8, i.e., a red shift with respect to MCH is observed. Considering  $\pi$ -electron interaction, the intensity ratio in the presence of toluene becomes 1/1/10/7/6 (red shift), whereas in the presence of acetone the ratio becomes 4/6/10/6/4 (more broadening, no significant shift).

**Figure 4:** Normalised FLN spectra of 9-hydroxybenzo[a]pyrene after baseline correction in various solvents (or solvent combinations) and bound to the estrogen receptor (the uncorrected spectra are shown in Figure 3). The relative intensities of bands (A), (B), (C), (D) and (E) are given in Table 1.

When solvent mixtures are measured in which both BuOH and  $\pi$ -electron containing molecules are present, the FLN spectra are rather similar to those recorded in absence of the latter. There is only a minor change in going from BuOH (3/2/10/5/2) to BuOH-toluene (2/2/10/6/2) and BuOH-acetone (2/3/10/6/3). It is, however, not very likely that in such solvent mixtures 9-OH-BaP will exclusively interact with 1-butanol, and not with toluene or acetone at all. Probably, the effect of BuOH on the spectrum is much stronger than the effect of  $\pi$ - $\pi$  interaction. As mentioned earlier, both the presence of TEA and toluene results in a red shift. In BuOH-toluene this effect is even stronger: the intensity ratio becomes 2/2/9/9/10. If TEA and acetone are combined, the ratio becomes 5/2/7/8/10 indicating more broadening and a red-shift as well (note that band A is relatively strong).

## 2.5 3-OH-BaP

The FLN spectra of 3-OH-BaP bound to the ER and dissolved in the abovementioned solvent combinations are shown in Figure 5. Similar to the results obtained for 9-OH-BaP, the ER and the Gly/Buf spectrum are strongly different, indicating complete binding of 3-OH-BaP to the ER. Also for the baselines the trend is similar: in the spectrum of 3-OH-BaP bound to the ER low intensity ZPLs are seen, located on a strong red-shifted broad baseline. Also for 3-OH-BaP the degree of electron-phonon coupling is high, both in the presence of acetone (carbonyl  $\pi$ -electron interaction) and in the presence of TEA (H-bond accepting interaction); again the concentration had to be lowered to 0.1 % and 0.01% respectively to be able to distinguish the ZPLs above the broad background. In contrast with the results obtained for 9-OH-BaP, in the presence of toluene (aromatic  $\pi$ -electron interaction) no strong red-shifted baseline was observed. Considering the shapes of the baselines, the spectrum of 3-OH-BaP bound to the ER is most similar to the spectra recorded in the presence of TEA (both with and without an additional  $\pi$ -electron containing solvent).

The baseline-subtracted spectra of 3-OH-BaP are shown in Figure 6. Four main bands were monitored: (A) 1075  $\text{cm}^{-1}$ , (B) 1175  $\text{cm}^{-1}$ , (C) 1325  $\text{cm}^{-1}$  and (D) 1395  $\text{cm}^{-1}$ ; their relative intensities are shown in Table 1. In Gly/Buf, the intensity ratio is 6/10/6/8. Three additional ZPLs were found at the blue edge of the Gly/Buf spectrum at 770, 857 and 960  $\text{cm}^{-1}$  (with relative intensities 4, 10 and 6, respectively); since these bands did not show up in the other spectra they are not included in Figures 5 and 6 and Table 1. In the presence of the ER, the ratio becomes 0/1/4/10, confirming that 3-OH-BaP is fully bound to the ER. In the reference spectrum (MCH) the intensity ratio is 1/10/8/6. In the presence of BuOH (both H-bond donating and accepting interaction) it changes to 1/7/8/10, while in the presence of TEA (H-bond accepting interaction only) it becomes 1/2/7/10. Apparently, both H-bonding solvents cause a red shift (in the presence of TEA this red shift is much

more pronounced); conversely, for Gly/Buf the shift is to the blue. Considering  $\pi$ -electron interaction, the intensity ratio in the presence of toluene becomes 2/10/8/10 (red shift), whereas in the presence of acetone the ratio becomes 4/10/7/5 (minor blue shift). As regards solvent mixtures with both H-bonding and  $\pi$ -electron containing molecules, the combination of BuOH and one of the  $\pi$ -electron containing solvents results in a red shift in

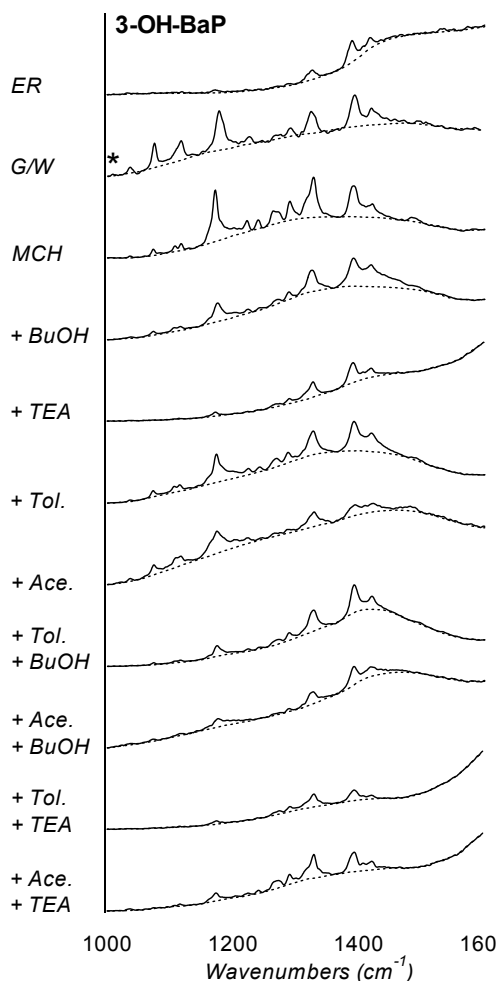


**Figure 5:** Normalised FLN spectra of 3-hydroxybenzo[a]pyrene in various solvents (or solvent combinations) and bound to the estrogen receptor. On the x-axis the energy difference with respect to the excitation wavelength in wavenumbers is used. The excitation wavelength was 410 nm. The star indicates that in the 700-1000  $\text{cm}^{-1}$  range three additional major bands are observed.

the 3-OH-BaP spectrum, i.e., the intensity ratios become 1/4/8/10 (in the presence of BuOH and toluene) and 1/5/7/10 (in the presence of BuOH and acetone). In the presence of TEA and toluene the intensity ratio becomes 0/3/10/8, and in the presence of TEA and acetone 0/4/10/8. Apparently, the latter two solvent combinations cause a less pronounced red shift; for TEA the intensity of red edge band D is higher when  $\pi$ -electron containing solvents are not present.

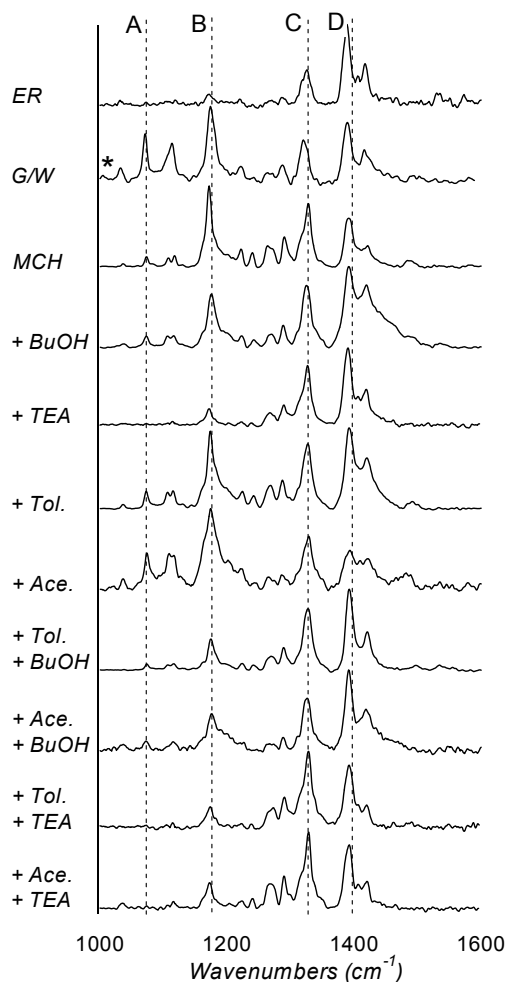


**Figure 6:** Normalised FLN spectra of 3-hydroxybenzo[a]pyrene after baseline correction in various solvent (or solvent combinations) and bound to the estrogen receptor (the uncorrected spectra are shown in Figure 5). The relative intensities of bands (A), (B), (C) and (D) are given in Table 1. The star indicates that three other strong blue shifted bands are observed (at 770, 857 and 960  $\text{cm}^{-1}$ ); these bands are not observed in the other spectra.

---

## 4 Discussion

The results presented above clearly show that the FLN spectra of 3- and 9-OH-BaP are strongly solvent dependent. Considering H-bonding, even a distinction between donating and accepting properties can be made. These solvent characteristics can be quantified using the Kamlet-Taft parameters for solvatochromic properties<sup>[310]</sup>. According to these parameters, a solvatochromic shift caused by TEA, and similarly by the imidazole moiety of His524, is exclusively due to its H-bond accepting capabilities<sup>[310]</sup>. In the spectra of both 3- and 9-OH-BaP, the presence of TEA results in a red shift. Conversely, solvatochromic shifts in aqueous solution and glycerol are predominantly due to the H-bond donating properties of these solvents<sup>[310]</sup>. In the spectra of both 3- and 9-OH-BaP in Gly/Buf, a blue shift is observed. The influence of BuOH is less easily predictable because it has both H-bond donating and accepting properties<sup>[310]</sup>. For 9-OH-BaP, BuOH causes a minor blue shift compared to the spectrum in MCH. For 3-OH-BaP, the opposite is observed: the presence of BuOH results in a red shift. These opposite shifts can be conceived as follows. Solute/solvent interaction always causes a stabilisation of the  $S_0$  state. Whether a blue or red shift is observed, depends on the extent of stabilisation in the  $S_1$  state: more stabilisation in the  $S_1$  state than in the  $S_0$  state will result in a red shift, in the opposite case a blue shift is observed (see Figure 2B). The amount of stabilisation in these states not only depends on the solvent dealt with; it is also influenced by changes in the solute's properties upon excitation. For example, a change in acidity will influence the impact of H-bonding interaction. Such changes in acidity might play a role in the solvent dependency in the spectra of 3- and 9-OH-BaP.

As regards  $\pi$ - $\pi$  interactions, fortunately carbonyl  $\pi$ -electrons and aromatic  $\pi$ -electrons induce significant differences in the FLN spectra so that their influences can be readily established. Also strong red-shifted baselines due to electron phonon coupling are observed, indicating  $\pi$ - $\pi$ -stacking solute/solvent interaction<sup>[307,311]</sup>. This holds for 9-OH-BaP in the presence of toluene where strong electron phonon coupling is observed. For 3-OH-BaP this coupling is only weak. Nonetheless it should be concluded that 3-OH-BaP and toluene do interact significantly since the spectra in toluene and MCH are strongly different (see Figure 6). Most probably, this solute/solvent combination is not interacting in a  $\pi$ - $\pi$  stacking manner; a T-shape conformation of 3-OH-BaP and toluene is more likely. For 9-OH-BaP and toluene, the strong electron phonon coupling does indicate  $\pi$ - $\pi$  stacking interaction. Because the aromatic ring of phenylalanine is similar to toluene (a benzene ring with an alkyl substituent), the Phe404 group in the ER is expected to behave similarly.

A systematic comparison of the FLN spectra (before and after baseline subtraction) in different solvent combinations leads to the following conclusions. For 9-OH-BaP, the spectrum in the presence of TEA and toluene shows the most similarities, but the baseline of the ER spectrum cannot be assigned to either TEA or toluene alone. Nevertheless, the relative intensities of the ZPLs indicate that both an aromatic  $\pi$ -electron moiety and an H-bond accepting group are present in the ER binding site; when only TEA or toluene is present, band E is significantly lower than in the presence of both these two solvents. This suggests that in the ER complex, 9-OH-BaP interacts with an H-bond acceptor, i.e., the imidazole moiety of His524. Furthermore, it is expected that 9-OH-BaP will interact with a toluene-like moiety in the ER, i.e. Phe404, in a  $\pi$ - $\pi$  stacking manner.

From a similar visual inspection of the 3-OH-BaP spectra the following conclusions can be drawn. The spectrum in the ER complex is most similar to the one in the presence of TEA. When besides TEA also  $\pi$ -electron containing solvents are present, the intensity of band D becomes lower compared to band C. Therefore, the orientation of Phe404 in the ER binding pocket can not be predicted; if there is substantial interaction between 3-OH-BaP and the Phe404 side group, it will most likely be in a T-shape conformation. Considering H-bonds, 3-OH-BaP is bound to the ER by interacting with an H-bond acceptor, i.e., the imidazole moiety of His524.

For both 3- and 9-OH-BaP, the orientation in the ER is remarkably different from what is expected based on the studies with E2. For this estrogen, the contributions of the two H-bonds to the total receptor/ligand binding energy have been estimated, showing that the participation of E2's phenolic OH-group in the H-bonding network with Glu353 and Arg394 contributes to a larger extent than the H-bond donated to the His524 does<sup>[134]</sup>. This cannot be simply generalized and applied to other ligands as well. For both mono-hydroxylated BaPs studied here, our results strongly suggest that H-bonding with His524 is the predominant interaction.

The observed H-bonding of the two solutes in the ER that occurs with His524 is in line with molecular modelling data<sup>[149]</sup>. Although molecular modelling and forcefield parameters are particularly suitable for the simulations and calculations of protein/ligand interactions, they do not describe  $\pi$ - $\pi$  interaction very well. However, the molecular modelling data described by Van Lipzig *et al*<sup>[149]</sup> predicted interaction with Phe404. This is confirmed by the FLNS data. Interestingly, the FLNS data indicate whether  $\pi$ - $\pi$  stacking (as for 9-OH-BaP) or a T-shape conformation (as for 3-OH-BaP) should be expected.

---

Thanks to its unique features, FLNS can become a useful tool in ligand/receptor studies. Especially when the functional groups in a receptor binding pocket can be mimicked, as is the case for His and Phe, very useful information can be obtained. Further exploration of this technique is needed because still little is known about the solvent dependency in FLN spectra.

# Chapter 7

Epilogue

---

## 1 Conclusions and perspectives

This thesis describes the results of studies with environmental contaminants, which are bioactivated into (more) estrogenic compounds through metabolism by cytochrome P450 enzymes (CYP). At the time the research of this thesis started, the focus on endocrine disrupting compounds (EDC) was mainly on the biological activity of parent compounds, and only very few studies were including the possibility of their metabolites being responsible for the effects by EDCs. In fact, certain chemicals such as polycyclic aromatic hydrocarbons (PAHs) and polyhalogenated biphenyls (PHBs) were qualified to be estrogenic or otherwise endocrine active, however, as we and others have shown, the parent compounds have no affinity for the estrogen receptor (ER) at all, and very likely, the effects observed have been the result of bioactivation and the formation of biologically active metabolites.

The main aim of the research described in this thesis was to investigate if bioactivation of environmental contaminants may lead to increased estrogenic activity, an understanding that may aid to a more accurate and complete risk assessment, regarding endocrine disrupting potencies of compounds.

We used the estrogen receptor and estrogen signalling as our endocrine target, and CYP activity as bioactivator c.q. metabolite generator. At the start of this research, the crystal structure of the ligand binding domain of the ER $\alpha$  isomer had just been released, and while getting to know the ER $\alpha$  receptor in detail by *in silico* modelling, we targeted it as well experimentally, using *in vitro* samples containing suspect estrogenic compounds. ER $\alpha$  binding and activation of estrogens, xenoestrogens, hydroxylated metabolites and metabolite mixtures from microsomal incubations with environmental contaminants were studied, in order to gain a better understanding of how to deal correctly with bioactivation in endocrine disruption.

Once the significance of EDCs was acknowledged, and EDCs were considered to be a potential threat instead of just a popular phase in science, EDCs were thought to act primarily through nuclear hormone receptors, by inappropriate stimulation or blocking hormone receptors such as ER, AR, TR etcetera. Nowadays, it is widely accepted that that endocrine disruption may occur via many different mechanisms, such as interference with hormone receptor signalling, disturbance of hormone synthesis, storage and clearance, affecting receptor expression levels and even dysregulation of brain function and sexual behaviour. In this last epilogue chapter, an overview, conclusions and some perspectives of the studies presented in this thesis are described.

The introductory **Chapter 1** describes the different manners by which endocrine disruption may affect wildlife, and humans, with emphasis on functions of the estrogen receptor and disruption of estrogen receptor signalling by environmental estrogens. Several notorious environmental estrogens are highlighted, and an overview of the damage they may cause and possible mechanisms of action is provided as well. Also, different *in vitro* assays to test estrogenic properties are described, several of which have been used throughout the research described in this thesis.

The focus of our research has been the ER $\alpha$ , and therefore, an extended description of the physical properties of the ER $\alpha$  is given. The ER $\alpha$  features different conformations, induced by a wide range of ligands. These may be agonists, antagonists, partial agonists or selective estrogen receptor modulators. Their binding modes are accompanied by association of co-regulators, and together these associates govern signalling stimulation or inhibition. Thus, understanding receptor activation or inhibition is not as simple as it seems, and hence, disturbance by EDC isn't either.

The main aim of this thesis was to investigate whether bioactivation of known environmental contaminants, could lead to the formation of more estrogenic metabolites. We focused on the bioactivation of hydrophobic PCBs and PAHs by CYP enzymes and their ER $\alpha$  binding properties. At the time our research started, studies on bioactivation of environmental contaminants with respect to increased estrogenicity were rare. PAHs and PHB were well-known pollutants, which accumulate in lipophilic environment, and they are extensively biotransformed by the CYP enzyme family, e.g. by humans or animals. Therefore, we tested *in vitro* whether CYP enzyme activity would bioactivate PAHs or PHBs into more estrogenic compounds. In **Chapter 2** is described, how their metabolites were formed and isolated from microsomal incubations with benzo[a]pyrene (BaP) and chrysene (CHN). Metabolites were indentified and tested *in vitro* for affinity and activity in estrogen assays (i.e. radioligand binding assay and T47D cell-based ER-Calux<sup>(R)</sup> reporter gene assay). The parent compounds did not exhibit estrogen receptor binding affinity while in the ER-Calux assay, estrogenic activity was observed. The complete microsomal incubation mixture, containing all metabolites formed, was tested for estrogenic activity. The mixture was separated by liquid chromatography, the LC-isolated fractions were tested for estrogenic activity and many fractions showed to exhibit estrogenic activity. Subsequently, synthetical hydroxylated metabolites of BaP and CHN were tested and several of the hydroxylated metabolites showed to be ER $\alpha$  ligands. ER-mediated activation of transcription in the cell-based ER $\alpha$  assay by these metabolites was also shown. Most metabolites were weak estrogens, however, some mono-hydroxylated metabolites exhibited high ER $\alpha$  affinities (micromolar to nanomolar range). The ER-Calux cells also

---

express CYP enzyme activity, so we investigated the role of CYP in the formation of estrogenic metabolites in these cells as well. Similarly to what we observed in the microsome experiments, the parent PAHs, like BaP, produced an ER-mediated estrogenic response. This response could be reduced by inhibition of the aryl hydrocarbon receptor (AhR). CYP activity is induced by ligand binding activation of the AhR. By blocking the AhR with DMF, a specific AhR antagonist, CYP activity diminished and the estrogenic response by BaP was reduced as well, indicating that the AhR-mediated induced CYP activity was responsible for the estrogenic signals, probably by generating estrogenic metabolites.

Finally, we also tested the joint estrogenic affinity of a mixture of 7 synthetical PAH metabolites. The mixture contained *equi-equivalent* amounts of the compounds, i.e. each compounds alone was dosed to exert only 8% of the maximal effect of reference compound estradiol (E2). Together, they induced about 50% of the maximal E2, a significant estrogenic effect. This was in agreement with the expected response, which could be predicted by the concept of *concentration-addition*, which is explained in detail in Chapter 2.

Thus, while the risk from exposure to individually weak estrogenic compounds may seem negligible, combined they may disrupt hormone regulation in humans and wildlife to a larger extent than anticipated on the basis of the parent compounds. A ruling EDC controversy nowadays concerns the issue of low-dose effects, since there is a large gap between the EDC concentrations released through spills or in contaminated areas and the low EDC concentrations humans are exposed to daily. However, if one fails to test biotransformation-increased potencies and the joint effects of combined exposure, the impact of EDCs will be underestimated.

Next to PAHs, PHBs constitute a well-known class of environmental compounds, and they are also known for their potency to disrupt endocrine systems, via blockage of several nuclear receptors (ER, AR, TR). In **Chapter 3**, we demonstrated that mono-hydroxylated metabolites of 4,4'-DBB and 2,2'-DBB, for our purpose model PBBs, are formed by CYP activity. In addition to effective binding to and activation of the ER, they are potent inhibitors of hEST, the human estrogen sulfotransferase as well. In this manner, these metabolites may disrupt endocrine systems of estrogen signalling and homeostasis in multiple manners. In Chapter 3, we describe the identification of different hydroxylated 4,4'-DBB and 2,2'-DBB metabolites. Mono-hydroxylated metabolites were identified, purified, and tested. The presence of di-hydroxylated biphenyl metabolites was also confirmed by LC/MS, and the corresponding fractions showed evidence of ER $\alpha$  affinity. Their exact molecular structures could not be identified due to lack of reference compounds. Therefore, as an alternative, we decided to use newly developed computational models to predict ER $\alpha$  binding affinity (see Chapter 4) of four di-

hydroxylated PBBs. The predicted affinities of the di-hydroxylated metabolites for the ER $\alpha$  were generally lower than the affinity of their mono-hydroxylated analogs, nevertheless, the contribution of the di-hydroxylated products to the total increase of estrogenic activity by CYP mediated bioactivation was found to be significant.

While studying the formation of estrogenic metabolites of the PAHs and PBBs, it became clear that in our hands at that time, isolation and testing of individual metabolites was not always feasible. Therefore, we felt the need to develop a predictive *in silico* model for the binding of ligands to the ER. In **Chapter 4** it is described how the crystal structure of the ER $\alpha$  ligand binding domain was used to develop a model for the accurate prediction of binding affinities of ER $\alpha$ -agonists. *In silico* modeling of the ER $\alpha$  was then still in its infancy, and we applied molecular dynamics (MD) simulations and the linear interaction energy (LIE) method. The LIE methods separately consider the Van der Waals and the electrostatic interactions between a ligand and the receptor. In addition, it incorporates a solvent model, that is, the receptor-bound state as well as the unbound, water-solvated state of the ligand are simulated and analysed. From both simulations, the binding energies ( $\Delta G$ ) are determined and eventually, the affinity ( $K_d$ ) between the ligand and the ER is calculated. To build the *in silico* model, we simulated the binding to the ER $\alpha$  with a training set, consisting of 21 ligands, covering a wide range in binding affinities, tested in our own ER $\alpha$  binding assay (Chapters 2 to 5). The LIE method is based on the linear response assumption for electrostatics together with Van der Waals contributions, calibrated against experimental binding data. As expected, the electrostatic contribution turned out to be strongly influenced by the number of hydroxylgroups of the ligand, and the LIE approach scientifically supports incorporation of this observation, which is further explained and motivated in chapter 4. Furthermore, per ligand, all possible binding orientations (no clashes or structure distortions) were considered and simulated. The final model provided an excellent linear correlation ( $r^2 = 0.94$ ) between experimental and calculated affinities, for structurally diverse compounds, that bind to the ER $\alpha$  with  $K_d$  values ranging from 0.15 mM to 30 pM. Subsequently, a training set of (xeno)estrogens with known estrogen receptor binding affinity, with a variety of structural properties and different number of hydroxyl groups was tested and the predicted affinities for these compounds were all in very good agreement with the experimental values. The predicted  $\Delta G$  values for these compounds showed an average deviation of only 0.61 kcal/mol for absolute binding affinities.

In **Chapter 5** is described how the computational ER $\alpha$  LIE model (see chapter 4) was employed for the prediction of ER $\alpha$  binding affinities of hydroxylated PHB metabolites. Molecular dynamics simulations were performed with 22 structurally related compounds.

---

The experimental binding energies ( $\Delta G_{\text{exp}}$ ) were calculated from the experimentally determined ligand binding affinities of the PHB metabolites, ranging from 7.0 nM to 41  $\mu$ M. The predicted  $\Delta G$  values are in good agreement with the experimental values: the average variation between calculated ( $\Delta G_{\text{calc}}$ ) and experimental ( $\Delta G_{\text{exp}}$ ) binding affinities was  $1.16 \pm 0.26$  kcal/mol (correlation:  $r^2 = 0.74$  between predicted and observed  $\Delta G$  values), which is acceptable for the LIE method. The initial LIE parameters, obtained by the diverse dataset of (xeno)estrogens of the model, proved to be very suitable for the halogenated biphenyls. The LIE method provided again to be a useful tool for the prediction of approximate binding affinities of this class of environmental contaminants, as well as binding orientation of these ligands. The study shows that the ER $\alpha$  hosts binding of biphenyls, preferably halogenated at the *ortho*-positions. From analysis of our observations it was concluded that *ortho*-substituent increased the binding affinity to ER $\alpha$ , two halogens are favoured over one, and one halogen is favoured over no substituent at all. As expected, a hydroxyl group at the 4-position of the biphenyl is preferred for binding compared to the 2- or 3-position. Ortho-halogens enhance binding of the biphenyls more significantly than para-substituted halogens, and brominated biphenyls exhibit higher binding affinity for ER $\alpha$  than chlorinated biphenyls. The larger bromines are more lipophilic than chlorines, and it was confirmed by analysis of the Van der Waals interactions that they interact with the ER $\alpha$  binding cavity more efficiently than chlorines.

The supportive contribution of computational models in understanding mechanisms of action is well-acknowledged and widely applied, however, still hesitation exists regarding the predictive value of e.g. *in silico* protein models. Acceptance of a computational model still requires verification by experimental data. At the time our computational ER $\alpha$  model was released, there were no easy methods available to accurately determine a ligand's binding orientation in a receptor, except by crystallography. In **Chapter 6**, the verification of the binding orientation of two hydroxylated metabolites of BaP to ER $\alpha$ , 3-OH-BaP and 9-OH-BaP, identified from our earlier studies, was investigated by fluorescence line-narrowing (FLN) spectroscopy. FLN spectroscopy is a technique in which high-resolution fluorescence spectra are obtained by freezing a liquid sample to below 10 K and applying selective laser excitation in order to obtain detailed information on interactions between molecules under investigation. In our case, estrogen receptor-bound and solvent-bound states were compared in order to gain insight in binding characteristics, such as binding orientation. From the available estrogenic PAH metabolites 3-OH-BaP and 9-OH-BaP (identified in Chapter 2) were selected, because of their higher natural abundance. FLN spectroscopy spectra of the two compounds were recorded in various solvent mixtures, and compared with the spectrum obtained for the ER $\alpha$ -bound ligand, and it was concluded that both 9-OH-BaP and 3-OH-BaP bind to the ER $\alpha$ . Furthermore, the

phenols of 9-OH-BaP and 3-OH-BaP both predominantly interact with a H-bond acceptor, His524. This was also confirmed by the measurement of two different aromatic interactions ( $\pi$ - $\pi$ ). The interaction was well-detectable for bound 9-OH-BaP and indicating perpendicular  $\pi$ - $\pi$  stacking interaction, but not as distinct for 3-OH-BaP, and suggestive of a more flexible, T-shaped interaction. The observed hydrogen bonding of the two metabolites with His524 of ER $\alpha$  agrees with the results from the *in silico* model from Chapters 4 and 5. Although molecular modelling and forcefield parameters are particularly suitable for the simulations and calculations of protein/ligand interactions, they do not describe  $\pi$ - $\pi$  interaction very well, interestingly, the FLN spectroscopy data indicate whether  $\pi$ - $\pi$  stacking (as for 9-OH-BaP) or a T-shape conformation (as for 3-OH-BaP) should be expected. The favoured binding orientation as detected by FLN spectroscopy supported the *in silico* predictions and fortified the predictive value of the LIE model. In current risk assessment of chemicals and also possibly endocrine disruptors, the challenge is to move from an evaluation model that requires extensive hazard testing in animals, to one, which hypothesis and risk driven in a scientific and convincing manner (Figure 1).

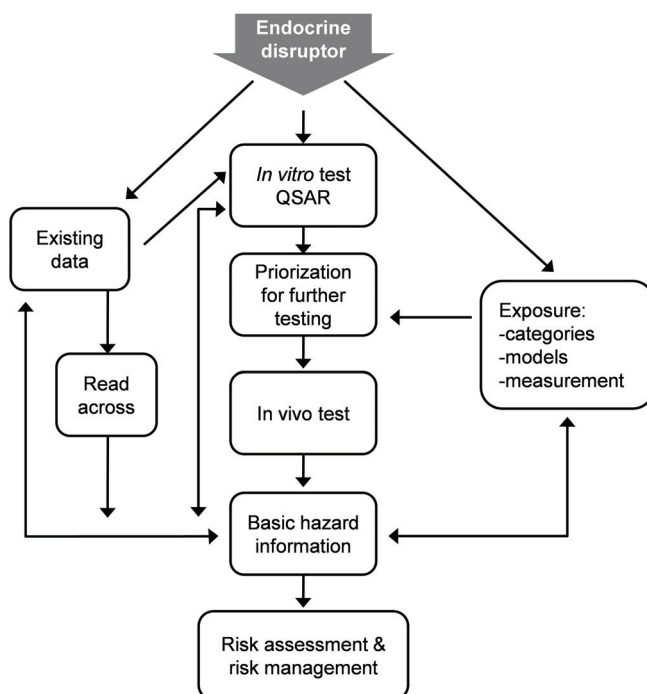


**Figure 1** : Flow chart depicting the principles of efficient environmental risk assessment

---

Ideally, *in vitro* and *in silico* approaches can be used to identify the most relevant *in vivo* information. The combination of the newest experimental *in vitro* techniques and *in silico* modeling provides promising synergy in exposure and risk assessment, and should really reduce the number of *in vivo* studies when evaluating chemical hazards. The work described in the current thesis contributes to achieve success with this challenge.

## 2 Epilogue

Paradoxically, the most important *fact* in research in the field of EDC is the *questioned* relevance. Numerous studies have shown that many different xenobiotic compounds can interfere with endocrine systems of humans and animals. Furthermore, a wide range of studies showed that EDCs are present in the environment, and that humans and animals are daily exposed to them. Concentration of EDCs have been detected in humans and animals and are correlated to higher incidence of a wide range of adverse endocrine health problems.

The missing link is conclusive mechanistic evidence between daily EDC exposure, and a positive association with adverse endocrine health effects. In laboratory settings, in cells or in animals, or after accidentally high exposures (e.g. environmental spills), EDCs have undoubtedly shown to be a risk factor for many reproductive irregularities and increased cancer incidence. However, there is a large gap between the concentration found or used in the pre-conceived circumstances, and the concentration humans are exposed during domestic or occupational life, and although it has been shown that EDC may exert their effects at even at extremely low doses, the question still remains, whether the concentrations EDCs humans are exposed to in daily life are sufficient to induce adverse health effects.

Currently, it is still difficult to show hard evidence for a correlation between actual exposure and increased disease. On the other hand, the lack of this association is clearly not good enough evidenced either, to convince EDC-critical scientists, that exposure to EDCs is *not* relevant for the suggested risks. Different aspects affect the overall endocrine burden in humans. Biomagnifications in e.g. consumable fish, or bioaccumulations in humans yield higher concentrations and thus extra (local) bioavailability than expected, when based on concentrations found in the environment. Biotransformation should also be considered. We and others have shown that EDCs may well be bioactivated and products formed have higher endocrine disrupting activities than the parent compounds. In this light, the aspect of mixture exposure also plays an important role. Individuals and populations are exposed to dynamic concentrations of chemicals, and exposure to EDC unquestionably concerns exposure to mixtures of compounds, targeting multiple

pathways in the endocrine system. Cumulative exposure may add to the endocrine burden as well. Research has shown that specifically fetuses and new-born babies are much more vulnerable to pollutants than adults, especially to endocrine active compounds. Hence, the concentrations of EDCs sufficient to interfere with normal development may be very low. Endocrine disruptors not only induce adverse effects on those exposed directly (including *in utero*), but also on the offspring of exposed individuals, as was demonstrated by the use of DES in the 70's.

In light of this all, we feel it is still extremely important to gather as much information as possible on the endocrine disrupting properties of chemicals. Effort should be put in the (further) development of assays and *in vitro*, *in vivo* and *in silico* predictive models, e.g. to accurately translate between computational and experimental models of mechanism of action or between animal and human exposure (Figure 2).

The experiments and models we have used in this thesis, form some foundation to what different kind of features of EDC we should consider, and why. We presented pioneering studies illustrating that the aspect of bioactivation by CYP enzyme activity and the consequences is one important factor that should be taken into account. When the research described in this thesis was started, the aspect of chemical bioactivation into (more) estrogenic compounds was relatively novel. Several others have reproduced our work since, and have shown that estrogenic metabolites are formed *in vitro* and *in vivo*, and are responsible for endocrine disruptive effects. Different target pathways should be investigated or screened, since estrogen effects have been demonstrated to be cellular context-dependent. Good examples of efficient screening approaches are the high resolution screening methods that have been developed in our lab<sup>[100,101,181,312-314]</sup>, which allow the on-line biotransformation of chemicals and drugs, and directly coupled, their metabolites are screened for any chosen endocrine target, such as a nuclear receptor or sulfotransferase. They allow fast metabolite formation, identification and subsequent bioactivity screening and can be used for many combinations of bioreactor and endocrine target.

Very importantly, it would be a great leap forward if assays were to be developed that give better insight in possible additive, synergizing or counter-acting properties of different EDCs. Exposure generally involves compound mixtures, or cumulative exposure. Biologically active compounds in mixtures, according to the concept of concentration addition, will induce significant effects whereas individually they would not elicit a detectable response. Cumulative effects are a more complex matter and adequate testing is not yet available. Research has shown, that prenatal or neonatal exposure to EDCs also significantly increases adverse health and reproductive effects. Thus new approaches should be developed which concern chemical-chemical interactions, i.e. how will (mixtures of) compounds influence the actions of endocrine disruptors, and vice versa. Of course it

will still be extremely difficult to predict how genes, life stage, life style and disease will affect endocrine disruptors effects.

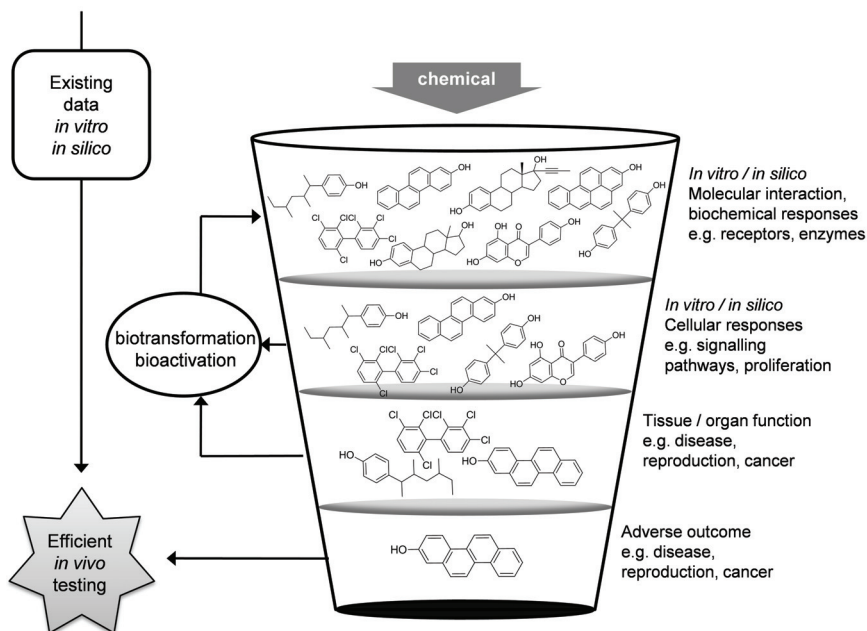


**Figure 2:** more efficient and focused animal in vivo testing by increase use of improved in vitro and in silico testing.

More testing will reveal more details and provide more insight in when, how, and how much risk is increased upon EDC exposure. Also, the ability to adequately predict effects of compounds can be of great help. Especially when metabolites are considered which are hard to generate. As we have shown, the ER $\alpha$  proved to be an excellent model for the development of a quantitative model for agonists. Now, since more crystal structures are available, this could be feasible for many more endocrine targets. As a challenge, simultaneously modeling the active sites of biotransformation enzymes with endocrine target proteins, such as nuclear receptors, could be integrated in one predictive model as well. Current knowledge provides sufficient computational tools, e.g. automated docking procedures, to combine prediction of biotransformation by enzymes and interaction with mechanistic pathways such as estrogen receptor binding. Studying protein-protein interactions e.g. using molecular dynamics can be a great instrument in studying conformation changes defining selective receptor agonism and antagonism.

In the mean time one should at least try and prevent as much exposure as possible for the very vulnerable populations at risk, i.e. pregnant women, breastfeeding women, and unborn and newborn babies.

## Conclusions

The studies performed in the current thesis have provided pioneering insight in the way xenoestrogens and importantly, their metabolites may disrupt several pathways of estrogen function and estrogen receptor signaling. Biotransformation of the xenobiotic compounds BaP, CHN, 2,2'-DBB and 4,4'-DBB by Cytochrome P450 enzymes *in vitro* generated hydroxylated products, which were more estrogenic than their parent compounds. Several of the metabolites showed to interfere with classical ER-mediated responses by binding to the ER $\alpha$ . PAHs and PHBs are also known to be genotoxic, and activation of ER signaling might contribute to their carcinogenicity in tissues at risk for hormonal cancer, such as breast epithelium. Several of the halogenated biphenyl metabolites also inhibited human estrogen sulfotransferase, thereby interfering with normal estrogen homeostasis, another target pathway of endocrine disrupting compounds. Many of the metabolites could be identified and isolated, and most of them exhibited weak estrogenic properties, however, several of the products exhibited up to very high affinity for the ER $\alpha$  of hEST. Despite their sometimes low individual affinities and biological effects, the compounds induced a significant response, when tested as a mixture. Risk assessment doesn't take into account the cumulative effect of different substances, and people are not exposed to just one chemical at a time, but to an assortment of chemicals, many of which have the potential to interfere with hormone functions. The results described in the first half of this thesis, i.e. the estrogenic effects of biotransformation and the mixture effect, emphasize the need for alternative adequate testing strategies, and to search for methods to investigate endocrine disruption beyond the single compound focus.

In the second half of the thesis, an optimised linear interaction energy model (LIE) is described to accurately predict ligand binding affinity of ER $\alpha$  agonists, and we have applied this model successfully to PAH and PHB metabolites. We show, with ER $\alpha$  as a model protein, that *in silico* modeling indeed may provide great predictive value.

In conclusion, this thesis demonstrates that the bioactivation of xenobiotics by cytochrome P450 enzymes may lead to the formation of estrogenic metabolites. *In silico* modeling of the ER $\alpha$  ligand binding domain has enabled us to adequately predict ER $\alpha$  binding affinity, as well as preferred ligand binding orientation, of a wide variety of

---

structurally diverse (xeno)estrogens. We foresee that *in silico* modeling of any endocrine targets (e.g. androgen receptor, thyroid receptor) may be used in combination with biotransformation, e.g. specific CYP active site mapping and automated docking approaches, in order to simultaneously predict metabolite formation, structure, and biological functionality towards a chosen target, and this may be a great tool in the improvement of future risk assessment.

# Abbreviations

AhR	aryl hydrocarbon receptor
BaP	benzo[ <i>a</i> ]pyrene
BNF	$\beta$ -naphthoflavone
CDFBS	charcoal-dextran stripped FBS
CHN	chrysene
CYP	cytochrome P450
CSD	crystal structure database
DBB	dibromobiphenyl
DCB	dichlorobiphenyl
DES	diethylstilbestrol
DMBA	7,12-dimethylbenza[ <i>a</i> ]anthracene
DMEM	Dulbecco's modified Eagle medium
DMF	3',4'-dimethoxyflavone
E2	17 $\beta$ -estradiol
EDC	endocrine disrupting compound
ER	estrogen receptor
FBS	foetal bovine serum
FLN	fluorescence line-narrowing
FUR	furaflavone
hEST	human estrogen sulfotransferase
HPLC	high performance liquid chromatography
LIE	linear interaction energy
MBB	monobromobiphenyl
MD	molecular dynamics
MCH	methylcyclohexane
MS	mass spectroscopy
NEA	non-essential amino acids
PAH	polycyclic aromatic hydrocarbon
PAPS	3'-phosphoadenosine-5'-phosphosulfate
PBB	polybrominated biphenyl
PCB	polychlorinated biphenyl
PHB	polyhalogenated biphenyl
RBA	relative binding affinity
RESP	restraint electrostatic potential
rmsd	root mean square deviation
SRB	sulforhodamine B
TCA	trichloroacetic acid
TEA	triethylamine
TMB	3,3',5,5'-tetramethylbenzidine



# References

- [1] Arcaro, K. F.; Yi, L.; Seegal, R. F.; Vakharia, D. D.; Yang, Y.; Spink, D. C.; Brosch, K.; Gierthy, J. F. 2,2',6,6'-Tetrachlorobiphenyl is estrogenic in vitro and in vivo. *J Cell Biochem* **1999**, *72*, 94-102.
- [2] Danzo, B. J. Environmental xenobiotics may disrupt normal endocrine function by interfering with the binding of physiological ligands to steroid receptors and binding proteins. *Environ Health Perspect* **1997**, *105*, 294-301.
- [3] Gray, L. J.; Parks, L.; Lambright, C.; Orlando, E.; Guillette, L. J. The effects of endocrine-disrupting chemicals on the reproduction and development of wildlife. *Endocrine Disruptors in the Environment*; Springer-Verlag: Heidelberg, 2002; pp 209-248.
- [4] McLachlan, J. A.; Korach, K. S.; Newbold, R. R.; Degen, G. H. Diethylstilbestrol and other estrogens in the environment. *Fundam Appl Toxicol* **1984**, *4*, 686-691.
- [5] Safe, S. H. Polychlorinated biphenyls (PCBs): environmental impact, biochemical and toxic responses, and implications for risk assessment. *Crit Rev Toxicol* **1994**, *24*, 87-149.
- [6] Fusani, L.; Della Seta, D.; Dessi-Fulgheri, F.; Farabollini, F. Altered reproductive success in rat pairs after environmental-like exposure to xenoestrogen. *Proc Biol Sci* **2007**, *274*, 1631-1636.
- [7] Tyler, C. R.; Jobling, S.; Sumpter, J. P. Endocrine disruption in wildlife: a critical review of the evidence. *Crit Rev Toxicol* **1998**, *28*, 319-361.
- [8] Sonnenschein, C.; Soto, A. M. An updated review of environmental estrogen and androgen mimics and antagonists. *J Steroid Biochem Mol Biol* **1998**, *65*, 143-150.
- [9] Hatch, E. E.; Palmer, J. R.; Titus-Ernstoff, L.; Noller, K. L.; Kaufman, R. H.; Mittendorf, R.; Robboy, S. J.; Hyer, M.; Cowan, C. M.; Adam, E.; Colton, T.; Hartge, P.; Hoover, R. N. Cancer risk in women exposed to diethylstilbestrol in utero. *Jama* **1998**, *280*, 630-634.
- [10] Baccarelli, A.; Pesatori, A. C.; Masten, S. A.; Patterson, D. G., Jr.; Needham, L. L.; Mocarelli, P.; Caporaso, N. E.; Consonni, D.; Grassman, J. A.; Bertazzi, P. A.; Landi, M. T. Aryl-hydrocarbon receptor-dependent pathway and toxic effects of TCDD in humans: a population-based study in Seveso, Italy. *Toxicol Lett* **2004**, *149*, 287-293.
- [11] Warner, M.; Eskenazi, B.; Mocarelli, P.; Gerthoux, P. M.; Samuels, S.; Needham, L.; Patterson, D.; Brambilla, P. Serum dioxin concentrations and breast cancer risk in the Seveso Women's Health Study. *Environ Health Perspect* **2002**, *110*, 625-628.
- [12] Aoki, Y. Polychlorinated biphenyls, polychlorinated dibenzo-p-dioxins, and polychlorinated dibenzofurans as endocrine disrupters--what we have learned from Yusho disease. *Environ Res* **2001**, *86*, 2-11.
- [13] Li, D.; Zhou, Z.; Qing, D.; He, Y.; Wu, T.; Miao, M.; Wang, J.; Weng, X.; Ferber, J. R.; Herrinton, L. J.; Zhu, Q.; Gao, E.; Checkoway, H.; Yuan, W. Occupational exposure to bisphenol-A (BPA) and the risk of self-reported male sexual dysfunction. *Hum Reprod* **2010**, *25*, 519-527.
- [14] IEH Chemicals purported to be endocrine disrupters: A compilation of published lists (Web report W20); MRC Institute for Environment and Health: Leicester, UK, 2005.
- [15] Jensen, E.; Jacobson, H. Basic guides to the mechanism of estrogen action. *Recent Prog Horm Res* **1962**, *18*, 387-414.

- 
- [16] Klip, H.; Verloop, J.; van Gool, J. D.; Koster, M. E.; Burger, C. W.; van Leeuwen, F. E. Hypospadias in sons of women exposed to diethylstilbestrol in utero: a cohort study. *Lancet* **2002**, *359*, 1102-1107.
- [17] Heaton, S. N.; Bursian, S. J.; Giesy, J. P.; Tillitt, D. E.; Render, J. A.; Jones, P. D.; Verbrugge, D. A.; Kubiak, T. J.; Aulerich, R. J. Dietary exposure of mink to carp from Saginaw Bay, Michigan. 1. Effects on reproduction and survival, and the potential risks to wild mink populations. *Arch Environ Contam Toxicol* **1995**, *28*, 334-343.
- [18] Aulerich, R. J.; Ringer, R. K. Current status of PCB toxicity to mink, and effect on their reproduction. *Arch Environ Contam Toxicol* **1977**, *6*, 279-292.
- [19] Hsu, S. T.; Ma, C. I.; Hsu, S. K.; Wu, S. S.; Hsu, N. H.; Yeh, C. C.; Wu, S. B. Discovery and epidemiology of PCB poisoning in Taiwan: a four-year followup. *Environ Health Perspect* **1985**, *59*, 5-10.
- [20] Fangstrom, B.; Athanasiadou, M.; Grandjean, P.; Weihe, P.; Bergman, A. Hydroxylated PCB metabolites and PCBs in serum from pregnant Faroese women. *Environ Health Perspect* **2002**, *110*, 895-899.
- [21] Meerts, I. A.; Hoving, S.; van den Berg, J. H.; Weijers, B. M.; Swarts, H. J.; van der Beek, E. M.; Bergman, A.; Koeman, J. H.; Brouwer, A. Effects of in utero exposure to 4-hydroxy-2,3,3',4',5-pentachlorobiphenyl (4-OH-CB107) on developmental landmarks, steroid hormone levels, and female estrous cyclicity in rats. *Toxicol Sci* **2004**, *82*, 259-267.
- [22] van Lipzig, M. M.; Commandeur, J. N.; de Kanter, F. J.; Damsten, M. C.; Vermeulen, N. P.; Maat, E.; Groot, E. J.; Brouwer, A.; Kester, M. H.; Visser, T. J.; Meerman, J. H. Bioactivation of Dibrominated Biphenyls by Cytochrome P450 Activity to Metabolites with Estrogenic Activity and Estrogen Sulfotransferase Inhibition Capacity. *Chem Res Toxicol* **2005**, *18*, 1691-1700.
- [23] Meerts, I. A.; Letcher, R. J.; Hoving, S.; Marsh, G.; Bergman, A.; Lemmen, J. G.; van der Burg, B.; Brouwer, A. In vitro estrogenicity of polybrominated diphenyl ethers, hydroxylated PDBEs, and polybrominated bisphenol A compounds. *Environ Health Perspect* **2001**, *109*, 399-407.
- [24] Harley, K. G.; Marks, A. R.; Chevrier, J.; Bradman, A.; Sjodin, A.; Eskenazi, B. PBDE concentrations in women's serum and fecundability. *Environ Health Perspect* **2010**, *118*, 699-704.
- [25] Eskenazi, B.; Mocarelli, P.; Warner, M.; Chee, W. Y.; Gerthoux, P. M.; Samuels, S.; Needham, L. L.; Patterson, D. G., Jr. Maternal serum dioxin levels and birth outcomes in women of Seveso, Italy. *Environ Health Perspect* **2003**, *111*, 947-953.
- [26] Guillette, L. J., Jr.; Gross, T. S.; Masson, G. R.; Matter, J. M.; Percival, H. F.; Woodward, A. R. Developmental abnormalities of the gonad and abnormal sex hormone concentrations in juvenile alligators from contaminated and control lakes in Florida. *Environ Health Perspect* **1994**, *102*, 680-688.
- [27] Rubin, B. S.; Soto, A. M. Bisphenol A: Perinatal exposure and body weight. *Mol Cell Endocrinol* **2009**, *304*, 55-62.
- [28] Kashiwagi, K.; Furuno, N.; Kitamura, S.; Ohta, S.; Sugihara, K.; Utsumi, K.; Hanada, H.; Taniguchi, K.; Suzuki, K.; Kashiwagi, A. Disruption of Thyroid Hormone Function by Environmental Pollutants. *Journal of Health Science* **2009**, *55*, 147-160.

- [29] Lewis, R. G.; Fortune, C. R.; Blanchard, F. T.; Camann, D. E. Movement and deposition of two organophosphorus pesticides within a residence after interior and exterior applications. *J Air Waste Manag Assoc* **2001**, *51*, 339-351.
- [30] Lu, C.; Toepel, K.; Irish, R.; Fenske, R. A.; Barr, D. B.; Bravo, R. Organic diets significantly lower children's dietary exposure to organophosphorus pesticides. *Environ Health Perspect* **2006**, *114*, 260-263.
- [31] Butte, W.; Heinzow, B. Pollutants in house dust as indicators of indoor contamination. *Rev Environ Contam Toxicol* **2002**, *175*, 1-46.
- [32] Rogan, W. J.; Ragan, N. B. Some evidence of effects of environmental chemicals on the endocrine system in children. *Int J Hyg Environ Health* **2007**, *210*, 659-667.
- [33] Brody, J. G.; Moysich, K. B.; Humblet, O.; Attfield, K. R.; Beehler, G. P.; Rudel, R. A. Environmental pollutants and breast cancer: epidemiologic studies. *Cancer* **2007**, *109*, 2667-2711.
- [34] Cohn, B. A.; Wolff, M. S.; Cirillo, P. M.; Sholtz, R. I. DDT and breast cancer in young women: new data on the significance of age at exposure. *Environ Health Perspect* **2007**, *115*, 1406-1414.
- [35] Kilburn, K. H.; Thornton, J. C. Protracted neurotoxicity from chlordane sprayed to kill termites. *Environ Health Perspect* **1995**, *103*, 690-694.
- [36] Go, V.; Garey, J.; Wolff, M. S.; Pogo, B. G. Estrogenic potential of certain pyrethroid compounds in the MCF-7 human breast carcinoma cell line. *Environ Health Perspect* **1999**, *107*, 173-177.
- [37] Garey, J.; Wolff, M. S. Estrogenic and antiprogestagenic activities of pyrethroid insecticides. *Biochem Biophys Res Commun* **1998**, *251*, 855-859.
- [38] Meeker, J. D.; Barr, D. B.; Hauser, R. Thyroid hormones in relation to urinary metabolites of non-persistent insecticides in men of reproductive age. *Reprod Toxicol* **2006**, *22*, 437-442.
- [39] Jeong, S. H.; Kim, B. Y.; Kang, H. G.; Ku, H. O.; Cho, J. H. Effect of chlorpyrifos-methyl on steroid and thyroid hormones in rat F0- and F1-generations. *Toxicology* **2006**, *220*, 189-202.
- [40] Rauh, V. A.; Garfinkel, R.; Perera, F. P.; Andrews, H. F.; Hoepner, L.; Barr, D. B.; Whitehead, R.; Tang, D.; Whyatt, R. W. Impact of prenatal chlorpyrifos exposure on neurodevelopment in the first 3 years of life among inner-city children. *Pediatrics* **2006**, *118*, e1845-1859.
- [41] Rudel, R. A.; Perovich, L. J. Endocrine disrupting chemicals in indoor and outdoor air. *Atmos Environ* **2009**, *43*, 170-181.
- [42] Heudorf, U.; Mersch-Sundermann, V.; Angerer, J. Phthalates: toxicology and exposure. *Int J Hyg Environ Health* **2007**, *210*, 623-634.
- [43] Henley, D. V.; Korach, K. S. Endocrine-disrupting chemicals use distinct mechanisms of action to modulate endocrine system function. *Endocrinology* **2006**, *147*, S25-32.
- [44] Swan, S. H.; Main, K. M.; Liu, F.; Stewart, S. L.; Kruse, R. L.; Calafat, A. M.; Mao, C. S.; Redmon, J. B.; Ternand, C. L.; Sullivan, S.; Teague, J. L. Decrease in anogenital distance among male infants with prenatal phthalate exposure. *Environ Health Perspect* **2005**, *113*, 1056-1061.
- [45] Soto, A. M.; Sonnenschein, C.; Chung, K. L.; Fernandez, M. F.; Olea, N.; Serrano, F. O. The E-SCREEN assay as a tool to identify estrogens: an update on estrogenic environmental pollutants. *Environ. Health Perspect.* **1995**, *103 Suppl 7*, 113-122.

- 
- [46] van Lipzig, M. M. H.; Vermeulen, N. P. E.; Gusinu, R.; Legler, J.; Frank, H.; Seidel, A.; Meerman, J. H. N. Formation of estrogenic metabolites of benzo[a]pyrene and chrysene by cytochrome P450 activity and their combined and supra-maximal estrogenic activity. *Environmental Toxicology and Pharmacology* **2005**, *19*, 41-55.
- [47] Rajapakse, N.; Silva, E.; Kortenkamp, A. Combining xenoestrogens at levels below individual no-observed-effect concentrations dramatically enhances steroid hormone action. *Environ Health Perspect* **2002**, *110*, 917-921.
- [48] Payne, J.; Scholze, M.; Kortenkamp, A. Mixtures of four organochlorines enhance human breast cancer cell proliferation. *Environ Health Perspect* **2001**, *109*, 391-397.
- [49] Colborn, T.; Dumanoski, D.; Myers, J. P. *Our Stolen Future*; Penguin Books: New York, 1996.
- [50] Cohn, B. A.; Cirillo, P. M.; Wolff, M. S.; Schwingl, P. J.; Cohen, R. D.; Sholtz, R. I.; Ferrara, A.; Christianson, R. E.; van den Berg, B. J.; Siiteri, P. K. DDT and DDE exposure in mothers and time to pregnancy in daughters. *Lancet* **2003**, *361*, 2205-2206.
- [51] Rubin, M. M. Antenatal exposure to DES: lessons learned...future concerns. *Obstet Gynecol Surv* **2007**, *62*, 548-555.
- [52] Steinberg, R. M.; Juenger, T. E.; Gore, A. C. The effects of prenatal PCBs on adult female paced mating reproductive behaviors in rats. *Horm Behav* **2007**, *51*, 364-372.
- [53] Charles, G. D.; Bartels, M. J.; Zacharewski, T. R.; Gollapudi, B. B.; Freshour, N. L.; Carney, E. W. Activity of benzo[a]pyrene and its hydroxylated metabolites in an estrogen receptor-alpha reporter gene assay. *Toxicol Sci* **2000**, *55*, 320-326.
- [54] Fertuck, K. C.; Matthews, J. B.; Zacharewski, T. R. Hydroxylated benzo[a]pyrene metabolites are responsible for in vitro estrogen receptor-mediated gene expression induced by benzo[a]pyrene, but do not elicit uterotrophic effects in vivo. *Toxicol Sci* **2001**, *59*, 231-240.
- [55] Pliskova, M.; Vondracek, J.; Canton, R. F.; Nera, J.; Kocan, A.; Petrik, J.; Trnovec, T.; Sanderson, T.; van den Berg, M.; Machala, M. Impact of polychlorinated biphenyls contamination on estrogenic activity in human male serum. *Environ Health Perspect* **2005**, *113*, 1277-1284.
- [56] Vandenberg, L. N.; Maffini, M. V.; Sonnenschein, C.; Rubin, B. S.; Soto, A. M. Bisphenol-A and the Great Divide: A Review of Controversies in the Field of Endocrine Disruption. *Endocr Rev* **2009**.
- [57] Helferich, W. G.; Andrade, J. E.; Hoagland, M. S. Phytoestrogens and breast cancer: a complex story. *Inflammopharmacology* **2008**, *16*, 219-226.
- [58] Liehr, J. G. 4-hydroxylation of oestrogens as a marker for mammary tumours. *Biochem Soc Trans* **1999**, *27*, 318-323.
- [59] Newbold, R. R.; Padilla-Banks, E.; Snyder, R. J.; Phillips, T. M.; Jefferson, W. N. Developmental exposure to endocrine disruptors and the obesity epidemic. *Reprod Toxicol* **2007**, *23*, 290-296.
- [60] Strom, B. L.; Schinnar, R.; Ziegler, E. E.; Barnhart, K. T.; Sammel, M. D.; Macones, G. A.; Stallings, V. A.; Drulis, J. M.; Nelson, S. E.; Hanson, S. A. Exposure to soy-based formula in infancy and endocrinological and reproductive outcomes in young adulthood. *Jama* **2001**, *286*, 807-814.

- 
- [61] Stettler, N.; Stallings, V. A.; Troxel, A. B.; Zhao, J.; Schinnar, R.; Nelson, S. E.; Ziegler, E. E.; Strom, B. L. Weight gain in the first week of life and overweight in adulthood: a cohort study of European American subjects fed infant formula. *Circulation* **2005**, *111*, 1897-1903.
- [62] Kyselova, V.; Peknicova, J.; Boubelik, M.; Buckiova, D. Body and organ weight, sperm acrosomal status and reproduction after genistein and diethylstilbestrol treatment of CD1 mice in a multigenerational study. *Theriogenology* **2004**, *61*, 1307-1325.
- [63] Naaz, A.; Yellayi, S.; Zakroczymski, M. A.; Bunick, D.; Doerge, D. R.; Lubahn, D. B.; Helferich, W. G.; Cooke, P. S. The soy isoflavone genistein decreases adipose deposition in mice. *Endocrinology* **2003**, *144*, 3315-3320.
- [64] Kim, H. K.; Nelson-Dooley, C.; Della-Fera, M. A.; Yang, J. Y.; Zhang, W.; Duan, J.; Hartzell, D. L.; Hamrick, M. W.; Baile, C. A. Genistein decreases food intake, body weight, and fat pad weight and causes adipose tissue apoptosis in ovariectomized female mice. *J Nutr* **2006**, *136*, 409-414.
- [65] Goodman-Gruen, D.; Kritz-Silverstein, D. Usual dietary isoflavone intake and body composition in postmenopausal women. *Menopause* **2003**, *10*, 427-432.
- [66] Hagmar, L. Polychlorinated biphenyls and thyroid status in humans: a review. *Thyroid* **2003**, *13*, 1021-1028.
- [67] Winneke, G.; Walkowiak, J.; Lilienthal, H. PCB-induced neurodevelopmental toxicity in human infants and its potential mediation by endocrine dysfunction. *Toxicology* **2002**, *181-182*, 161-165.
- [68] Kouki, T.; Okamoto, M.; Wada, S.; Kishitake, M.; Yamanouchi, K. Suppressive effect of neonatal treatment with a phytoestrogen, coumestrol, on lordosis and estrous cycle in female rats. *Brain Res Bull* **2005**, *64*, 449-454.
- [69] Kim, J. H.; Stansbury, K. H.; Walker, N. J.; Trush, M. A.; Strickland, P. T.; Sutter, T. R. Metabolism of benzo[a]pyrene and benzo[a]pyrene-7,8-diol by human cytochrome P450 1B1. *Carcinogenesis* **1998**, *19*, 1847-1853.
- [70] Cavalieri, E. L.; Higginbotham, S.; RamaKrishna, N. V.; Devanesan, P. D.; Todorovic, R.; Rogan, E. G.; Salmasi, S. Comparative dose-response tumorigenicity studies of dibenzo[alpha,l]pyrene versus 7,12-dimethylbenz[alpha]anthracene, benzo[alpha]pyrene and two dibenzo[alpha,l]pyrene dihydrodiols in mouse skin and rat mammary gland. *Carcinogenesis* **1991**, *12*, 1939-1944.
- [71] Bauer, E.; Guo, Z.; Ueng, Y. F.; Bell, L. C.; Zeldin, D.; Guengerich, F. P. Oxidation of benzo[a]pyrene by recombinant human cytochrome P450 enzymes. *Chem Res Toxicol* **1995**, *8*, 136-142.
- [72] Gonzalez, F. J.; Crespi, C. L.; Gelboin, H. V. DNA-expressed human cytochrome P450s: a new age of molecular toxicology and human risk assessment. *Mutat Res* **1991**, *247*, 113-127.
- [73] Kholkute, S. D.; Rodriguez, J.; Dukelow, W. R. The effects of polybrominated biphenyls and perchlorinated terphenyls on in vitro fertilization in the mouse. *Arch Environ Contam Toxicol* **1994**, *26*, 208-211.
- [74] Jansen, H. T.; Cooke, P. S.; Porcelli, J.; Liu, T. C.; Hansen, L. G. Estrogenic and antiestrogenic actions of PCBs in the female rat: in vitro and in vivo studies. *Reprod Toxicol* **1993**, *7*, 237-248.

- 
- [75] Nesaretnam, K.; Corcoran, D.; Dils, R. R.; Darbre, P. 3,4,3',4'-Tetrachlorobiphenyl acts as an estrogen in vitro and in vivo. *Mol Endocrinol* **1996**, *10*, 923-936.
- [76] Gellert, R. J. Uterotrophic activity of polychlorinated biphenyls (PCB) and induction of precocious reproductive aging in neonatally treated female rats. *Environ Res* **1978**, *16*, 123-130.
- [77] Fielden, M. R.; Chen, I.; Chittim, B.; Safe, S. H.; Zacharewski, T. R. Examination of the estrogenicity of 2,4,6,2',6'-pentachlorobiphenyl (PCB 104), its hydroxylated metabolite 2,4,6,2',6'-pentachloro-4-biphenylol (HO-PCB 104), and a further chlorinated derivative, 2,4,6,2',4',6'-hexachlorobiphenyl (PCB 155). *Environ Health Perspect* **1997**, *105*, 1238-1248.
- [78] Kramer, V. J.; Giesy, J. P. Specific binding of hydroxylated polychlorinated biphenyl metabolites and other substances to bovine calf uterine estrogen receptor: structure-binding relationships. *Sci. Total Environ.* **1999**, *233*, 141-161.
- [79] Coecke, S.; Ahr, H.; Blaauboer, B. J.; Bremer, S.; Casati, S.; Castell, J.; Combes, R.; Corvi, R.; Crespi, C. L.; Cunningham, M. L.; Elaut, G.; Eletti, B.; Freidig, A.; Gennari, A.; Gherzi-Egea, J. F.; Guillouzo, A.; Hartung, T.; Hoet, P.; Ingelman-Sundberg, M.; Munn, S.; Janssens, W.; Ladstetter, B.; Leahy, D.; Long, A.; Meneguz, A.; Monshouwer, M.; Morath, S.; Nagelkerke, F.; Pelkonen, O.; Ponti, J.; Prieto, P.; Richert, L.; Sabbioni, E.; Schaack, B.; Steiling, W.; Testai, E.; Vericat, J. A.; Worth, A. Metabolism: a bottleneck in in vitro toxicological test development. The report and recommendations of ECVAM workshop 54. *Altern Lab Anim* **2006**, *34*, 49-84.
- [80] Song, R.; He, Y.; Murphy, M. B.; Yeung, L. W.; Yu, R. M.; Lam, M. H.; Lam, P. K.; Hecker, M.; Giesy, J. P.; Wu, R. S.; Zhang, W.; Sheng, G.; Fu, J. Effects of fifteen PBDE metabolites, DE71, DE79 and TBBPA on steroidogenesis in the H295R cell line. *Chemosphere* **2008**, *71*, 1888-1894.
- [81] Hamers, T.; Kamstra, J. H.; Sonneveld, E.; Murk, A. J.; Visser, T. J.; Van Velzen, M. J.; Brouwer, A.; Bergman, A. Biotransformation of brominated flame retardants into potentially endocrine-disrupting metabolites, with special attention to 2,2',4,4'-tetrabromodiphenyl ether (BDE-47). *Mol Nutr Food Res* **2008**, *52*, 284-298.
- [82] Capellino, S.; Montagna, P.; Villaggio, B.; Soldano, S.; Straub, R. H.; Cutolo, M. Hydroxylated estrogen metabolites influence the proliferation of cultured human monocytes: possible role in synovial tissue hyperplasia. *Clin Exp Rheumatol* **2008**, *26*, 903-909.
- [83] Qiu, X.; Mercado-Feliciano, M.; Bigsby, R. M.; Hites, R. A. Measurement of polybrominated diphenyl ethers and metabolites in mouse plasma after exposure to a commercial pentabromodiphenyl ether mixture. *Environ Health Perspect* **2007**, *115*, 1052-1058.
- [84] Ptak, A.; Ludewig, G.; Robertson, L.; Lehmler, H. J.; Gregoraszczyk, E. L. In vitro exposure of porcine prepubertal follicles to 4-chlorobiphenyl (PCB3) and its hydroxylated metabolites: effects on sex hormone levels and aromatase activity. *Toxicol Lett* **2006**, *164*, 113-122.
- [85] Mercado-Feliciano, M.; Bigsby, R. M. Hydroxylated metabolites of the polybrominated diphenyl ether mixture DE-71 are weak estrogen receptor-alpha ligands. *Environ Health Perspect* **2008**, *116*, 1315-1321.
- [86] Spink, D. C.; Katz, B. H.; Hussain, M. M.; Spink, B. C.; Wu, S. J.; Liu, N.; Pause, R.; Kaminsky, L. S. Induction of CYP1A1 and CYP1B1 in T-47D human breast cancer cells by benzo[a]pyrene is diminished by arsenite. *Drug Metab Dispos* **2002**, *30*, 262-269.

- [87] Ambrosone, C. B.; Freudenheim, J. L.; Graham, S.; Marshall, J. R.; Vena, J. E.; Brasure, J. R.; Laughlin, R.; Nemoto, T.; Michalek, A. M.; Harrington, A.; et al. Cytochrome P4501A1 and glutathione S-transferase (M1) genetic polymorphisms and postmenopausal breast cancer risk. *Cancer Res* **1995**, *55*, 3483-3485.
- [88] Mikhailova, O. N.; Gulyaeva, L. F.; Prudnikov, A. V.; Gerasimov, A. V.; Krasilnikov, S. E. Estrogen-metabolizing gene polymorphisms in the assessment of female hormone-dependent cancer risk. *Pharmacogenomics J* **2006**, *6*, 189-193.
- [89] Hefler, L. A.; Grimm, C.; Bentz, E. K.; Reinthaller, A.; Heinze, G.; Tempfer, C. B. A model for predicting age at menopause in white women. *Fertil Steril* **2006**, *85*, 451-454.
- [90] Shelby, M. D.; Newbold, R. R.; Tully, D. B.; Chae, K.; Davis, V. L. Assessing environmental chemicals for estrogenicity using a combination of in vitro and in vivo assays. *Environ Health Perspect* **1996**, *104*, 1296-1300.
- [91] Miller, W. L. Molecular biology of steroid hormone synthesis. *Endocr Rev* **1988**, *9*, 295-318.
- [92] Sanderson, J. T. The steroid hormone biosynthesis pathway as a target for endocrine-disrupting chemicals. *Toxicol Sci* **2006**, *94*, 3-21.
- [93] You, L. Steroid hormone biotransformation and xenobiotic induction of hepatic steroid metabolizing enzymes. *Chem Biol Interact* **2004**, *147*, 233-246.
- [94] Birnbaum, L. S.; Fenton, S. E. Cancer and developmental exposure to endocrine disruptors. *Environ Health Perspect* **2003**, *111*, 389-394.
- [95] Harris, R. M.; Kirk, C. J.; Waring, R. H. Non-genomic effects of endocrine disruptors: inhibition of estrogen sulfotransferase by phenols and chlorinated phenols. *Mol Cell Endocrinol* **2005**, *244*, 72-74.
- [96] Waring, R. H.; Ayers, S.; Gescher, A. J.; Glatt, H. R.; Meinel, W.; Jarratt, P.; Kirk, C. J.; Pettitt, T.; Rea, D.; Harris, R. M. Phytoestrogens and xenoestrogens: the contribution of diet and environment to endocrine disruption. *J Steroid Biochem Mol Biol* **2008**, *108*, 213-220.
- [97] Zheng, W.; Xie, D.; Cerhan, J. R.; Sellers, T. A.; Wen, W.; Folsom, A. R. Sulfotransferase 1A1 polymorphism, endogenous estrogen exposure, well-done meat intake, and breast cancer risk. *Cancer Epidemiol Biomarkers Prev* **2001**, *10*, 89-94.
- [98] Glatt, H. Sulfation and sulfotransferases 4: bioactivation of mutagens via sulfation. *Faseb J* **1997**, *11*, 314-321.
- [99] Kester, M. H.; Bulduk, S.; Tibboel, D.; Meinel, W.; Glatt, H.; Falany, C. N.; Coughtrie, M. W.; Bergman, A.; Safe, S. H.; Kuiper, G. G.; Schuur, A. G.; Brouwer, A.; Visser, T. J. Potent inhibition of estrogen sulfotransferase by hydroxylated PCB metabolites: a novel pathway explaining the estrogenic activity of PCBs. *Endocrinology* **2000**, *141*, 1897-1900.
- [100] Reinen, J.; Kool, J.; Vermeulen, N. P. Reversed-phase liquid chromatography coupled on-line to estrogen receptor bioaffinity detection based on fluorescence polarization. *Anal Bioanal Chem* **2008**, *390*, 1987-1998.
- [101] Reinen, J.; Vriese, E.; Glatt, H.; Vermeulen, N. P. Development and validation of a fluorescence HPLC-based screening assay for inhibition of human estrogen sulfotransferase. *Anal Biochem* **2006**, *357*, 85-92.
- [102] Spiegelman, B. M.; Heinrich, R. Biological control through regulated transcriptional coactivators. *Cell* **2004**, *119*, 157-167.

- 
- [103] Margueron, R.; Duong, V.; Bonnet, S.; Escande, A.; Vignon, F.; Balaguer, P.; Cavailles, V. Histone deacetylase inhibition and estrogen receptor alpha levels modulate the transcriptional activity of partial antiestrogens. *J Mol Endocrinol* **2004**, *32*, 583-594.
- [104] Rosenfeld, M. G.; Lunyak, V. V.; Glass, C. K. Sensors and signals: a coactivator/corepressor/epigenetic code for integrating signal-dependent programs of transcriptional response. *Genes Dev* **2006**, *20*, 1405-1428.
- [105] O'Malley, B. The Year in Basic Science: nuclear receptors and coregulators. *Mol Endocrinol* **2008**, *22*, 2751-2758.
- [106] Koike, S.; Sakai, M.; Muramatsu, M. Molecular cloning and characterization of rat estrogen receptor cDNA. *Nucleic Acids Res* **1987**, *15*, 2499-2513.
- [107] Kuiper, G. G.; Enmark, E.; Peltö-Huikko, M.; Nilsson, S.; Gustafsson, J. A. Cloning of a novel receptor expressed in rat prostate and ovary. *Proc Natl Acad Sci U S A* **1996**, *93*, 5925-5930.
- [108] Barkhem, T.; Carlsson, B.; Nilsson, Y.; Enmark, E.; Gustafsson, J.; Nilsson, S. Differential response of estrogen receptor alpha and estrogen receptor beta to partial estrogen agonists/antagonists. *Mol. Pharmacol.* **1998**, *54*, 105-112.
- [109] Kuiper, G. G.; Carlsson, B.; Grandien, K.; Enmark, E.; Haggblad, J.; Nilsson, S.; Gustafsson, J. A. Comparison of the ligand binding specificity and transcript tissue distribution of estrogen receptors alpha and beta. *Endocrinology* **1997**, *138*, 863-870.
- [110] Pettersson, K.; Grandien, K.; Kuiper, G. G.; Gustafsson, J. A. Mouse estrogen receptor beta forms estrogen response element-binding heterodimers with estrogen receptor alpha. *Mol Endocrinol* **1997**, *11*, 1486-1496.
- [111] Matthews, J.; Gustafsson, J. A. Estrogen signaling: a subtle balance between ER alpha and ER beta. *Mol Interv* **2003**, *3*, 281-292.
- [112] Chang, E. C.; Frasor, J.; Komm, B.; Katzenellenbogen, B. S. Impact of estrogen receptor beta on gene networks regulated by estrogen receptor alpha in breast cancer cells. *Endocrinology* **2006**, *147*, 4831-4842.
- [113] Vivar, O. I.; Zhao, X.; Saunier, E. F.; Griffin, C.; Mayba, O. S.; Tagliaferri, M.; Cohen, I.; Speed, T. P.; Leitman, D. C. Estrogen receptor [beta] binds to and regulates three distinct classes of target genes. *J Biol Chem* **2010**.
- [114] Kushner, P. J.; Agard, D. A.; Greene, G. L.; Scanlan, T. S.; Shiau, A. K.; Uht, R. M.; Webb, P. Estrogen receptor pathways to AP-1. *J Steroid Biochem Mol Biol* **2000**, *74*, 311-317.
- [115] Saville, B.; Wormke, M.; Wang, F.; Nguyen, T.; Enmark, E.; Kuiper, G.; Gustafsson, J. A.; Safe, S. Ligand-, cell-, and estrogen receptor subtype (alpha/beta)-dependent activation at GC-rich (Sp1) promoter elements. *J Biol Chem* **2000**, *275*, 5379-5387.
- [116] Stein, B.; Yang, M. X. Repression of the interleukin-6 promoter by estrogen receptor is mediated by NF-kappa B and C/EBP beta. *Mol Cell Biol* **1995**, *15*, 4971-4979.
- [117] Liu, M. M.; Albanese, C.; Anderson, C. M.; Hilty, K.; Webb, P.; Uht, R. M.; Price, R. H., Jr.; Pestell, R. G.; Kushner, P. J. Opposing action of estrogen receptors alpha and beta on cyclin D1 gene expression. *J Biol Chem* **2002**, *277*, 24353-24360.
- [118] Bruning, J. C.; Lingohr, P.; Gillette, J.; Hanstein, B.; Avci, H.; Krone, W.; Müller-Wieland, D.; Kotzka, J. Estrogen receptor-alpha and Sp1 interact in the induction of the low density lipoprotein-receptor. *J Steroid Biochem Mol Biol* **2003**, *86*, 113-121.

- [119] Razandi, M.; Pedram, A.; Greene, G. L.; Levin, E. R. Cell membrane and nuclear estrogen receptors (ERs) originate from a single transcript: studies of ERalpha and ERbeta expressed in Chinese hamster ovary cells. *Mol Endocrinol* **1999**, *13*, 307-319.
- [120] Song, R. X.; Zhang, Z.; Santen, R. J. Estrogen rapid action via protein complex formation involving ERalpha and Src. *Trends Endocrinol Metab* **2005**, *16*, 347-353.
- [121] Thomas, P.; Pang, Y.; Filardo, E. J.; Dong, J. Identity of an estrogen membrane receptor coupled to a G protein in human breast cancer cells. *Endocrinology* **2005**, *146*, 624-632.
- [122] Thomas, P.; Dong, J. Binding and activation of the seven-transmembrane estrogen receptor GPR30 by environmental estrogens: A potential novel mechanism of endocrine disruption. *J Steroid Biochem Mol Biol* **2006**.
- [123] Langer, G.; Bader, B.; Meoli, L.; Isensee, J.; Delbeck, M.; Noppinger, P. R.; Otto, C. A critical review of fundamental controversies in the field of GPR30 research. *Steroids* **2010**, *75*, 603-610.
- [124] Otto, C.; Fuchs, I.; Kauselmann, G.; Kern, H.; Zevnik, B.; Andreassen, P.; Schwarz, G.; Altmann, H.; Klewer, M.; Schoor, M.; Vonk, R.; Fritzscheier, K. H. GPR30 does not mediate estrogenic responses in reproductive organs in mice. *Biol Reprod* **2009**, *80*, 34-41.
- [125] Otto, C.; Rohde-Schulz, B.; Schwarz, G.; Fuchs, I.; Klewer, M.; Brittain, D.; Langer, G.; Bader, B.; Prella, K.; Nubbemeyer, R.; Fritzscheier, K. H. G protein-coupled receptor 30 localizes to the endoplasmic reticulum and is not activated by estradiol. *Endocrinology* **2008**, *149*, 4846-4856.
- [126] Pedram, A.; Razandi, M.; Levin, E. R. Nature of functional estrogen receptors at the plasma membrane. *Mol Endocrinol* **2006**, *20*, 1996-2009.
- [127] Funakoshi, T.; Yanai, A.; Shinoda, K.; Kawano, M. M.; Mizukami, Y. G protein-coupled receptor 30 is an estrogen receptor in the plasma membrane. *Biochem Biophys Res Commun* **2006**, *346*, 904-910.
- [128] Cheshenko, K.; Pakdel, F.; Segner, H.; Kah, O.; Eggen, R. I. Interference of endocrine disrupting chemicals with aromatase CYP19 expression or activity, and consequences for reproduction of teleost fish. *Gen Comp Endocrinol* **2008**, *155*, 31-62.
- [129] Palace, V. P.; Pleskach, K.; Halldorson, T.; Danell, R.; Wautier, K.; Evans, B.; Alaei, M.; Marvin, C.; Tomy, G. T. Biotransformation enzymes and thyroid axis disruption in juvenile rainbow trout (*Oncorhynchus mykiss*) exposed to hexabromocyclododecane diastereoisomers. *Environ Sci Technol* **2008**, *42*, 1967-1972.
- [130] Gehm, B. D.; McAndrews, J. M.; Jordan, V. C.; Jameson, J. L. EGF activates highly selective estrogen-responsive reporter plasmids by an ER-independent pathway. *Mol Cell Endocrinol* **2000**, *159*, 53-62.
- [131] Bunone, G.; Briand, P. A.; Miksicek, R. J.; Picard, D. Activation of the unliganded estrogen receptor by EGF involves the MAP kinase pathway and direct phosphorylation. *Embo J* **1996**, *15*, 2174-2183.
- [132] Kato, S.; Endoh, H.; Masuhiro, Y.; Kitamoto, T.; Uchiyama, S.; Sasaki, H.; Masushige, S.; Gotoh, Y.; Nishida, E.; Kawashima, H.; Metzger, D.; Chambon, P. Activation of the estrogen receptor through phosphorylation by mitogen-activated protein kinase. *Science* **1995**, *270*, 1491-1494.
- [133] Smith, C. L.; O'Malley, B. W. Coregulator function: a key to understanding tissue specificity of selective receptor modulators. *Endocr Rev* **2004**, *25*, 45-71.

- 
- [134] Brzozowski, A. M.; Pike, A. C.; Dauter, Z.; Hubbard, R. E.; Bonn, T.; Engstrom, O.; Ohman, L.; Greene, G. L.; Gustafsson, J. A.; Carlquist, M. Molecular basis of agonism and antagonism in the oestrogen receptor. *Nature* **1997**, *389*, 753-758.
- [135] Zhou, G.; Cummings, R.; Li, Y.; Mitra, S.; Wilkinson, H. A.; Elbrecht, A.; Hermes, J. D.; Schaeffer, J. M.; Smith, R. G.; Moller, D. E. Nuclear receptors have distinct affinities for coactivators: characterization by fluorescence resonance energy transfer. *Mol Endocrinol* **1998**, *12*, 1594-1604.
- [136] McNerney, E. M.; Katzenellenbogen, B. S. Different regions in activation function-1 of the human estrogen receptor required for antiestrogen- and estradiol-dependent transcription activation. *J Biol Chem* **1996**, *271*, 24172-24178.
- [137] Kumar, R.; Thompson, E. B. The structure of the nuclear hormone receptors. *Steroids* **1999**, *64*, 310-319.
- [138] Kumar, R.; Volk, D. E.; Li, J.; Lee, J. C.; Gorenstein, D. G.; Thompson, E. B. TATA box binding protein induces structure in the recombinant glucocorticoid receptor AF1 domain. *Proc Natl Acad Sci U S A* **2004**, *101*, 16425-16430.
- [139] Watson, C. S.; Bulayeva, N. N.; Wozniak, A. L.; Alyea, R. A. Xenoestrogens are potent activators of nongenomic estrogenic responses. *Steroids* **2007**, *72*, 124-134.
- [140] Thomas, P.; Dressing, G.; Pang, Y.; Berg, H.; Tubbs, C.; Benninghoff, A.; Doughty, K. Progesterin, estrogen and androgen G-protein coupled receptors in fish gonads. *Steroids* **2006**, *71*, 310-316.
- [141] Safe, S.; Kim, K. Non-classical genomic estrogen receptor (ER)/specificity protein and ER/activating protein-1 signaling pathways. *J Mol Endocrinol* **2008**, *41*, 263-275.
- [142] Evans, R. M. The steroid and thyroid hormone receptor superfamily. *Science* **1988**, *240*, 889-895.
- [143] Bourguet, W.; Ruff, M.; Chambon, P.; Gronemeyer, H.; Moras, D. Crystal structure of the ligand-binding domain of the human nuclear receptor RXR- $\alpha$ . *Nature* **1995**, *375*, 377-382.
- [144] Shiau, A. K.; Barstad, D.; Loria, P. M.; Cheng, L.; Kushner, P. J.; Agard, D. A.; Greene, G. L. The structural basis of estrogen receptor/coactivator recognition and the antagonism of this interaction by tamoxifen. *Cell* **1998**, *95*, 927-937.
- [145] Pike, A. C.; Brzozowski, A. M.; Hubbard, R. E.; Bonn, T.; Thorsell, A. G.; Engstrom, O.; Ljunggren, J.; Gustafsson, J. A.; Carlquist, M. Structure of the ligand-binding domain of oestrogen receptor beta in the presence of a partial agonist and a full antagonist. *Embo J* **1999**, *18*, 4608-4618.
- [146] Vajdos, F. F.; Hoth, L. R.; Geoghegan, K. F.; Simons, S. P.; LeMotte, P. K.; Danley, D. E.; Ammirati, M. J.; Pandit, J. The 2.0 Å crystal structure of the ER $\alpha$  ligand-binding domain complexed with lasofoxifene. *Protein Sci* **2007**, *16*, 897-905.
- [147] Anstead, G. M.; Carlson, K. E.; Katzenellenbogen, J. A. The estradiol pharmacophore: ligand structure-estrogen receptor binding affinity relationships and a model for the receptor binding site. *Steroids* **1997**, *62*, 268-303.
- [148] McDevitt, R. E.; Malamas, M. S.; Manas, E. S.; Unwalla, R. J.; Xu, Z. B.; Miller, C. P.; Harris, H. A. Estrogen receptor ligands: design and synthesis of new 2-arylidene-1-ones. *Bioorg Med Chem Lett* **2005**, *15*, 3137-3142.

- [149] van Lipzig, M. M.; ter Laak, A. M.; Jongejan, A.; Vermeulen, N. P.; Wamelink, M.; Geerke, D.; Meerman, J. H. Prediction of ligand binding affinity and orientation of xenoestrogens to the estrogen receptor by molecular dynamics simulations and the linear interaction energy method. *J Med Chem* **2004**, *47*, 1018-1030.
- [150] Bindal, R. D.; Carlson, K. E.; Reiner, G. C.; Katzenellenbogen, J. A. 11 beta-chloromethyl-[3H]estradiol-17 beta: a very high affinity, reversible ligand for the estrogen receptor. *J. Steroid. Biochem.* **1987**, *28*, 361-370.
- [151] Pike, A. C.; Brzozowski, A. M.; Hubbard, R. E. A structural biologist's view of the oestrogen receptor. *J Steroid Biochem Mol Biol* **2000**, *74*, 261-268.
- [152] Onate, S. A.; Tsai, S. Y.; Tsai, M. J.; O'Malley, B. W. Sequence and characterization of a coactivator for the steroid hormone receptor superfamily. *Science* **1995**, *270*, 1354-1357.
- [153] Onate, S. A.; Boonyaratanakornkit, V.; Spencer, T. E.; Tsai, S. Y.; Tsai, M. J.; Edwards, D. P.; O'Malley, B. W. The steroid receptor coactivator-1 contains multiple receptor interacting and activation domains that cooperatively enhance the activation function 1 (AF1) and AF2 domains of steroid receptors. *J Biol Chem* **1998**, *273*, 12101-12108.
- [154] Wong, S. P.; Li, J.; Shen, P.; Gong, Y.; Yap, S. P.; Yong, E. L. Ultrasensitive cell-based bioassay for the measurement of global estrogenic activity of flavonoid mixtures revealing additive, restrictive, and enhanced actions in binary and higher order combinations. *Assay Drug Dev Technol* **2007**, *5*, 355-362.
- [155] Cassidy, A.; Albertazzi, P.; Lise Nielsen, I.; Hall, W.; Williamson, G.; Tetens, I.; Atkins, S.; Cross, H.; Manios, Y.; Wolk, A.; Steiner, C.; Branca, F. Critical review of health effects of soyabean phyto-oestrogens in post-menopausal women. *Proc Nutr Soc* **2006**, *65*, 76-92.
- [156] Morabito, N.; Crisafulli, A.; Vergara, C.; Gaudio, A.; Lasco, A.; Frisina, N.; D'Anna, R.; Corrado, F.; Pizzoleo, M. A.; Cincotta, M.; Altavilla, D.; Lentile, R.; Squadrito, F. Effects of genistein and hormone-replacement therapy on bone loss in early postmenopausal women: a randomized double-blind placebo-controlled study. *J Bone Miner Res* **2002**, *17*, 1904-1912.
- [157] Nestel, P. J.; Yamashita, T.; Sasahara, T.; Pomeroy, S.; Dart, A.; Komesaroff, P.; Owen, A.; Abbey, M. Soy isoflavones improve systemic arterial compliance but not plasma lipids in menopausal and perimenopausal women. *Arterioscler Thromb Vasc Biol* **1997**, *17*, 3392-3398.
- [158] Adlercreutz, H. Western diet and Western diseases: some hormonal and biochemical mechanisms and associations. *Scand J Clin Lab Invest Suppl* **1990**, *201*, 3-23.
- [159] Brzezinski, A.; Debi, A. Phytoestrogens: the "natural" selective estrogen receptor modulators? *Eur J Obstet Gynecol Reprod Biol* **1999**, *85*, 47-51.
- [160] Maggiolini, M.; Bonofiglio, D.; Marsico, S.; Panno, M. L.; Cenni, B.; Picard, D.; Ando, S. Estrogen receptor alpha mediates the proliferative but not the cytotoxic dose-dependent effects of two major phytoestrogens on human breast cancer cells. *Mol Pharmacol* **2001**, *60*, 595-602.
- [161] Barnes, S.; Grubbs, C.; Setchell, K. D.; Carlson, J. Soybeans inhibit mammary tumors in models of breast cancer. *Prog Clin Biol Res* **1990**, *347*, 239-253.
- [162] Iwasaki, M.; Inoue, M.; Otani, T.; Sasazuki, S.; Kurahashi, N.; Miura, T.; Yamamoto, S.; Tsugane, S. Plasma isoflavone level and subsequent risk of breast cancer among Japanese

- 
- women: a nested case-control study from the Japan Public Health Center-based prospective study group. *J Clin Oncol* **2008**, *26*, 1677-1683.
- [163] Hoffman, R. Potent inhibition of breast cancer cell lines by the isoflavonoid kievitone: comparison with genistein. *Biochem Biophys Res Commun* **1995**, *211*, 600-606.
- [164] Akiyama, T.; Ishida, J.; Nakagawa, S.; Ogawara, H.; Watanabe, S.; Itoh, N.; Shibuya, M.; Fukami, Y. Genistein, a specific inhibitor of tyrosine-specific protein kinases. *J Biol Chem* **1987**, *262*, 5592-5595.
- [165] Nguyen, T. T.; Tran, E.; Nguyen, T. H.; Do, P. T.; Huynh, T. H.; Huynh, H. The role of activated MEK-ERK pathway in quercetin-induced growth inhibition and apoptosis in A549 lung cancer cells. *Carcinogenesis* **2004**, *25*, 647-659.
- [166] Rice, S.; Whitehead, S. A. Phytoestrogens and breast cancer--promoters or protectors? *Endocr Relat Cancer* **2006**, *13*, 995-1015.
- [167] McDonnell, D. P. The Molecular Pharmacology of SERMs. *Trends Endocrinol Metab* **1999**, *10*, 301-311.
- [168] Wu, X.; Hawse, J. R.; Subramaniam, M.; Goetz, M. P.; Ingle, J. N.; Spelsberg, T. C. The tamoxifen metabolite, endoxifen, is a potent antiestrogen that targets estrogen receptor alpha for degradation in breast cancer cells. *Cancer Res* **2009**, *69*, 1722-1727.
- [169] Shang, Y.; Brown, M. Molecular determinants for the tissue specificity of SERMs. *Science* **2002**, *295*, 2465-2468.
- [170] Manas, E. S.; Xu, Z. B.; Unwalla, R. J.; Somers, W. S. Understanding the selectivity of genistein for human estrogen receptor-beta using X-ray crystallography and computational methods. *Structure (Camb)* **2004**, *12*, 2197-2207.
- [171] Howell, A.; DeFriend, D.; Robertson, J.; Blamey, R.; Walton, P. Response to a specific antioestrogen (ICI 182780) in tamoxifen-resistant breast cancer. *Lancet* **1995**, *345*, 29-30.
- [172] Lykkesfeldt, A. E.; Madsen, M. W.; Briand, P. Altered expression of estrogen-regulated genes in a tamoxifen-resistant and ICI 164,384 and ICI 182,780 sensitive human breast cancer cell line, MCF-7/TAMR-1. *Cancer Res* **1994**, *54*, 1587-1595.
- [173] Wu, Y. L.; Yang, X.; Ren, Z.; McDonnell, D. P.; Norris, J. D.; Willson, T. M.; Greene, G. L. Structural basis for an unexpected mode of SERM-mediated ER antagonism. *Mol Cell* **2005**, *18*, 413-424.
- [174] Kieser, K. J.; Kim, D. W.; Carlson, K. E.; Katzenellenbogen, B. S.; Katzenellenbogen, J. A. Characterization of the pharmacophore properties of novel selective estrogen receptor downregulators (SERDs). *J Med Chem* **2010**, *53*, 3320-3329.
- [175] Johnston, S. R. Endocrinology and hormone therapy in breast cancer: selective oestrogen receptor modulators and downregulators for breast cancer - have they lost their way? *Breast Cancer Res* **2005**, *7*, 119-130.
- [176] Garner, C. E.; Jefferson, W. N.; Burka, L. T.; Matthews, H. B.; Newbold, R. R. In vitro estrogenicity of the catechol metabolites of selected polychlorinated biphenyls. *Toxicol Appl Pharmacol* **1999**, *154*, 188-197.
- [177] You, L.; Casanova, M.; Bartolucci, E. J.; Fryczynski, M. W.; Dorman, D. C.; Everitt, J. I.; Gaido, K. W.; Ross, S. M.; Heck Hd, H. Combined effects of dietary phytoestrogen and synthetic endocrine-active compound on reproductive development in Sprague-Dawley rats: genistein and methoxychlor. *Toxicol. Sci.* **2002**, *66*, 91-104.

- [178] Yang, R. S. H. *Toxicology of Chemical Mixtures: Case Studies, Mechanisms, and Novel Approaches*; Academic Press: London, 1994.
- [179] Lin, L. L.; Janz, D. M. Effects of binary mixtures of xenoestrogens on gonadal development and reproduction in zebrafish. *Aquat Toxicol* **2006**, *80*, 382-395.
- [180] Kortenkamp, A. Low dose mixture effects of endocrine disrupters: implications for risk assessment and epidemiology. *Int J Androl* **2008**, *31*, 233-240.
- [181] Van Liempd, S. M.; Kool, J.; Meerman, J. H.; Irth, H.; Vermeulen, N. P. Metabolic profiling of endocrine-disrupting compounds by on-line cytochrome p450 bioreaction coupled to on-line receptor affinity screening. *Chem Res Toxicol* **2007**, *20*, 1825-1832.
- [182] Casals-Casas, C.; Feige, J. N.; Desvergne, B. Interference of pollutants with PPARs: endocrine disruption meets metabolism. *Int J Obes (Lond)* **2008**, *32 Suppl 6*, S53-61.
- [183] von Angerer, E.; Prekajac, J. Benzo[a]carbazole derivatives. Synthesis, estrogen receptor binding affinities, and mammary tumor inhibiting activity. *J Med Chem* **1986**, *29*, 380-386.
- [184] Legler, J.; van den Brink, C. E.; Brouwer, A.; Murk, A. J.; van der Saag, P. T.; Vethaak, A. D.; van der Burg, B. Development of a stably transfected estrogen receptor-mediated luciferase reporter gene assay in the human T47D breast cancer cell line. *Toxicol Sci* **1999**, *48*, 55-66.
- [185] Murk, A. J.; Legler, J.; van Lipzig, M. M.; Meerman, J. H.; Belfroid, A. C.; Spenkelink, A.; van der Burg, B.; Rijs, G. B.; Vethaak, D. Detection of estrogenic potency in wastewater and surface water with three in vitro bioassays. *Environ Toxicol Chem* **2002**, *21*, 16-23.
- [186] Sumbayev, V. V.; Jensen, J. K.; Hansen, J. A.; Andreasen, P. A. Novel modes of oestrogen receptor agonism and antagonism by hydroxylated and chlorinated biphenyls, revealed by conformation-specific peptide recognition patterns. *Mol Cell Endocrinol* **2008**, *287*, 30-39.
- [187] Sumbayev, V. V.; Bonefeld-Jorgensen, E. C.; Wind, T.; Andreasen, P. A. A novel pesticide-induced conformational state of the oestrogen receptor ligand-binding domain, detected by conformation-specific peptide binding. *FEBS Lett* **2005**, *579*, 541-548.
- [188] Zwart, W.; Griekspoor, A.; Rondaij, M.; Verwoerd, D.; Neeffjes, J.; Michalides, R. Classification of anti-estrogens according to intramolecular FRET effects on phospho-mutants of estrogen receptor alpha. *Mol Cancer Ther* **2007**, *6*, 1526-1533.
- [189] Sumpter, J. P.; Jobling, S. Vitellogenesis as a biomarker for estrogenic contamination of the aquatic environment. *Environ Health Perspect* **1995**, *103 Suppl 7*, 173-178.
- [190] Legler, J.; Zeinstra, L. M.; Schuitemaker, F.; Lanser, P. H.; Bogerd, J.; Brouwer, A.; Vethaak, A. D.; De Voogt, P.; Murk, A. J.; Van der Burg, B. Comparison of in vivo and in vitro reporter gene assays for short-term screening of estrogenic activity. *Environ Sci Technol* **2002**, *36*, 4410-4415.
- [191] Tong, W.; Perkins, R.; Xing, L.; Welsh, W. J.; Sheehan, D. M. QSAR models for binding of estrogenic compounds to estrogen receptor alpha and beta subtypes. *Endocrinology* **1997**, *138*, 4022-4025.
- [192] Bissantz, C.; Folkers, G.; Rognan, D. Protein-based virtual screening of chemical databases. 1. Evaluation of different docking/scoring combinations. *J. Med. Chem.* **2000**, *43*, 4759-4767.
- [193] Marchand-Geneste, N.; Cazaunau, M.; Carpy, A. J.; Laguerre, M.; Porcher, J. M.; Devillers, J. Homology model of the rainbow trout estrogen receptor (rtERalpha) and docking of endocrine disrupting chemicals (EDCs). *SAR QSAR Environ Res* **2006**, *17*, 93-105.

- 
- [194] Nose, T.; Shimohigashi, Y. A docking modelling rationally predicts strong binding of bisphenol A to estrogen-related receptor gamma. *Protein Pept Lett* **2008**, *15*, 290-296.
- [195] Celik, L.; Lund, J. D.; Schiott, B. Exploring Interactions of Endocrine-Disrupting Compounds with Different Conformations of the Human Estrogen Receptor alpha Ligand Binding Domain: A Molecular Docking Study. *Chem Res Toxicol* **2008**.
- [196] Oostenbrink, B. C.; Pitera, J. W.; van Lipzig, M. M.; Meerman, J. H.; van Gunsteren, W. F. Simulations of the estrogen receptor ligand-binding domain: affinity of natural ligands and xenoestrogens. *J. Med. Chem.* **2000**, *43*, 4594-4605.
- [197] Sonoda, M. T.; Martinez, L.; Webb, P.; Skaf, M. S.; Polikarpov, I. Ligand dissociation from estrogen receptor is mediated by receptor dimerization: evidence from molecular dynamics simulations. *Mol Endocrinol* **2008**, *22*, 1565-1578.
- [198] Zeng, J.; Li, W.; Zhao, Y.; Liu, G.; Tang, Y.; Jiang, H. Insights into ligand selectivity in estrogen receptor isoforms: molecular dynamics simulations and binding free energy calculations. *J Phys Chem B* **2008**, *112*, 2719-2726.
- [199] Manas, E. S.; Unwalla, R. J.; Xu, Z. B.; Malamas, M. S.; Miller, C. P.; Harris, H. A.; Hsiao, C.; Akopian, T.; Hum, W. T.; Malakian, K.; Wolfrom, S.; Bapat, A.; Bhat, R. A.; Stahl, M. L.; Somers, W. S.; Alvarez, J. C. Structure-based design of estrogen receptor-beta selective ligands. *J Am Chem Soc* **2004**, *126*, 15106-15119.
- [200] Åqvist, J.; Medina, C.; Samuelsson, J. E. A new method for predicting binding affinity in computer-aided drug design. *Protein Eng.* **1994**, *7*, 385-391.
- [201] Åqvist, J.; Hansson, T. On the validity of electrostatic linear response in polar solvents. *Journal of Physical Chemistry* **1996**, *100*, 9512-9521.
- [202] Hansson, T.; Marelus, J.; Åqvist, J. Ligand binding affinity prediction by linear interaction energy methods. *J. Comput. Aided Mol. Des.* **1998**, *12*, 27-35.
- [203] Marelus, J.; Hansson, T.; Åqvist, J. Calculation of ligand binding free energies from molecular dynamics simulations. *International Journal of Quantum Chemistry* **1998**, *69*, 77-88.
- [204] Stjernschantz, E.; Marelus, J.; Medina, C.; Jacobsson, M.; Vermeulen, N. P.; Oostenbrink, C. Are automated molecular dynamics simulations and binding free energy calculations realistic tools in lead optimization? An evaluation of the linear interaction energy (LIE) method. *J Chem Inf Model* **2006**, *46*, 1972-1983.
- [205] de Amorim, H. L.; Caceres, R. A.; Netz, P. A. Linear interaction energy (LIE) method in lead discovery and optimization. *Curr Drug Targets* **2008**, *9*, 1100-1105.
- [206] Cheek, A. O.; Vonier, P. M.; Oberdorster, E.; Burow, B. C.; McLachlan, J. A. Environmental signaling: a biological context for endocrine disruption. *Environ Health Perspect* **1998**, *106 Suppl 1*, 5-10.
- [207] Oost, R. v. d.; Beyer, J.; Vermeulen, N. P. E. Fish biomarkers and environmental risk assessment: a review. *Environmental Toxicology and Applied Pharmacology* **2003**, *in press*.
- [208] Ariese, F.; Ernst, W. H. O.; Sijm, D. T. H. M. Natural and synthetic organic compounds in the environment - a symposium report. *Environmental Toxicology and Pharmacology* **2001**, *10*, 65-80.
- [209] Santodonato, J. Review of the estrogenic and antiestrogenic activity of polycyclic aromatic hydrocarbons: relationship to carcinogenicity. *Chemosphere* **1997**, *34*, 835-848.

- [210] Bhat, H. K.; Vadgama, J. V.; Loya, T. Critical role of oxidative stress in estrogen-induced carcinogenesis. *AACR 93rd Annual meeting*: San Francisco, 2002.
- [211] Li, J. J.; Hou, X.; Bentel, J.; Yazlovitskaya, E. M.; Li, S. A. Prevention of estrogen carcinogenesis in the hamster kidney by ethinylestradiol: some unique properties of a synthetic estrogen. *Carcinogenesis* **1998**, *19*, 471-477.
- [212] Tsutsui, T.; Barrett, J. C. Neoplastic transformation of cultured mammalian cells by estrogens and estrogenlike chemicals. *Environ Health Perspect* **1997**, *105 Suppl 3*, 619-624.
- [213] Morreal, C. E.; Schneider, S. L.; Sinha, D. K.; Bronstein, R. E. Estrogenic properties of 3,9-dihydroxy-7,12-dimethylbenzo[a]anthracene in rats. *J Natl Cancer Inst* **1979**, *62*, 1585-1588.
- [214] Hecht, S. S.; el-Bayoumy, K.; Rivenson, A.; Amin, S. Potent mammary carcinogenicity in female CD rats of a fjord region diol-epoxide of benzo[c]phenanthrene compared to a bay region diol-epoxide of benzo[a]pyrene. *Cancer Res* **1994**, *54*, 21-24.
- [215] Sylvester, P. W.; Aylsworth, C. F.; Van Vugt, D. A.; Meites, J. Effects of alterations in early hormonal environment on development and hormone dependency of carcinogen-induced mammary tumors in rats. *Cancer Res* **1983**, *43*, 5342-5346.
- [216] Cook, J. W.; Dodds, E. C.; Hewett, C. L.; Lawson, W. The oestrogenic activity of some condensed-ring compounds in relation to their other biological activities. *Proc. R. Soc. B.* **1934**, *114*, 272-286.
- [217] Cook, J. W.; Dodds, E. C.; Hewett, C. L. A Synthetic Oestrus-Exciting Compound. *Nature* **1933**, *14*.
- [218] Yang, N. C.; Castro, A. J.; Lewis, M.; Wong, T. W. Polynuclear aromatic hydrocarbons, steroids and carcinogenesis. *Science* **1961**, *134*, 386-387.
- [219] Fertuck, K. C.; Kumar, S.; Sikka, H. C.; Matthews, J. B.; Zacharewski, T. R. Interaction of PAH-related compounds with the alpha and beta isoforms of the estrogen receptor. *Toxicol Lett* **2001**, *121*, 167-177.
- [220] Hirose, T.; Morito, K.; Kizu, R.; Toriba, A.; Hayakawa, K.; Ogawa, S.; Inoue, S.; Muramatsu, M.; Masamune, Y. Estrogenic/antiestrogenic activities of benzo[a]pyrene monohydroxy derivatives. *JOURNAL OF HEALTH SCIENCE* **2001**, *47*, 552-558.
- [221] Adams, J. B.; Phillips, N. S.; Young, C. E. Formation of glucuronides of estradiol-17 beta by human mammary cancer cells. *J Steroid Biochem* **1989**, *33*, 1023-1025.
- [222] Angus, W. G.; Larsen, M. C.; Jefcoate, C. R. Expression of CYP1A1 and CYP1B1 depends on cell-specific factors in human breast cancer cell lines: role of estrogen receptor status. *Carcinogenesis* **1999**, *20*, 947-955.
- [223] Spink, B. C.; Katz, B. H.; Hussain, M. M.; Pang, S.; Connor, S. P.; Aldous, K. M.; Gierthy, J. F.; Spink, D. C. SULT1A1 catalyzes 2-methoxyestradiol sulfonation in MCF-7 breast cancer cells. *Carcinogenesis* **2000**, *21*, 1947-1957.
- [224] Grimmer, G. Analysis of automobile exhaust condensates. *IARC Sci Publ* **1977**, 29-39.
- [225] Jacob, J.; Grimmer, G.; Raab, G.; Emura, M.; Riebe, M.; Mohr, U. Comparison of chrysene metabolism in epithelial human bronchial and Syrian hamster lung cells. *Cancer Lett* **1987**, *38*, 171-180.
- [226] Ruddock, P. J.; Bird, D. J.; McCalley, D. V. Bile metabolites of polycyclic aromatic hydrocarbons in three species of fish from the Severn Estuary. *Ecotoxicol Environ Saf* **2002**, *51*, 97-105.

- 
- [227] Levin, W.; Wood, A. W.; Chang, R. L.; Yagi, H.; Mah, H. D.; Jerina, D. M.; Conney, A. H. Evidence for bay region activation of chrysene 1,2-dihydrodiol to an ultimate carcinogen. *Cancer Res* **1978**, *38*, 1831-1834.
- [228] Tran, D. Q.; Ide, C. F.; McLachlan, J. A.; Arnold, S. F. The anti-estrogenic activity of selected polynuclear aromatic hydrocarbons in yeast expressing human estrogen receptor. *Biochem Biophys Res Commun* **1996**, *229*, 101-108.
- [229] Tian, Y.; Ke, S.; Thomas, T.; Meeker, R. J.; Gallo, M. A. Transcriptional suppression of estrogen receptor gene expression by 2,3,7,8-tetrachlorodibenzo-p-dioxin (TCDD). *J Steroid Biochem Mol Biol* **1998**, *67*, 17-24.
- [230] Wormke, M.; Stoner, M.; Saville, B.; Safe, S. Crosstalk between estrogen receptor alpha and the aryl hydrocarbon receptor in breast cancer cells involves unidirectional activation of proteasomes. *FEBS Lett* **2000**, *478*, 109-112.
- [231] Arcaro, K. F.; O'Keefe, P. W.; Yang, Y.; Clayton, W.; Gierthy, J. F. Antiestrogenicity of environmental polycyclic aromatic hydrocarbons in human breast cancer cells. *Toxicology* **1999**, *133*, 115-127.
- [232] Bessems, J. G.; Te Koppele, J. M.; Van Dijk, P. A.; Van Stee, L. L.; Commandeur, J. N.; Vermeulen, N. P. Rat liver microsomal cytochrome P450-dependent oxidation of 3,5-disubstituted analogues of paracetamol. *Xenobiotica* **1996**, *26*, 647-666.
- [233] Backhaus, T.; Scholze, M.; Grimme, L. H. The single substance and mixture toxicity of quinolones to the bioluminescent bacterium *Vibrio fischeri*. *Aquatic Toxicol* **2000**, *49*, 49-61.
- [234] Altenburger, R.; Bodeker, W.; Faust, M.; Grimme, L. H. Evaluation of the isobologram method for the assessment of mixtures of chemicals. Combination effect studies with pesticides in algal biotests. *Ecotoxicol Environ Saf* **1990**, *20*, 98-114.
- [235] Skehan, P.; Storeng, R.; Scudiero, D.; Monks, A.; McMahon, J.; Vistica, D.; Warren, J. T.; Bokesch, H.; Kenney, S.; Boyd, M. R. New colorimetric cytotoxicity assay for anticancer-drug screening. *J Natl Cancer Inst* **1990**, *82*, 1107-1112.
- [236] Thirman, M. J.; Albrecht, J. H.; Krueger, M. A.; Erickson, R. R.; Cherwitz, D. L.; Park, S. S.; Gelboin, H. V.; Holtzman, J. L. Induction of cytochrome CYP1A1 and formation of toxic metabolites of benzo[a]pyrene by rat aorta: a possible role in atherogenesis. *Proc Natl Acad Sci U S A* **1994**, *91*, 5397-5401.
- [237] Aspry, K. E.; Bjeldanes, L. F. Effects of dietary broccoli and butylated hydroxyanisole on liver-mediated metabolism of benzo[a]pyrene. *Food Chem Toxicol* **1983**, *21*, 133-142.
- [238] Gmur, D. J.; Varanasi, U. Characterization of benzo[a]pyrene metabolites isolated from muscle, liver, and bile of a juvenile flatfish. *Carcinogenesis* **1982**, *3*, 1397-1403.
- [239] Pelkonen, O.; Nebert, D. W. Metabolism of polycyclic aromatic hydrocarbons: etiologic role in carcinogenesis. *Pharmacol Rev* **1982**, *34*, 189-222.
- [240] Vladusic, E. A.; Hornby, A. E.; Guerra-Vladusic, F. K.; Lakins, J.; Lupu, R. Expression and regulation of estrogen receptor beta in human breast tumors and cell lines. *Oncol Rep* **2000**, *7*, 157-167.
- [241] Waller, C. L.; Oprea, T. I.; Chae, K.; Park, H. K.; Korach, K. S.; Laws, S. C.; Wiese, T. E.; Kelce, W. R.; Gray, L. E., Jr. Ligand-based identification of environmental estrogens. *Chem. Res. Toxicol.* **1996**, *9*, 1240-1248.

- [242] Madigou, T.; Tiffocche, C.; Lazennec, G.; Pelletier, J.; Thieulant, M. L. The sheep estrogen receptor: cloning and regulation of expression in the hypothalamo-pituitary axis. *Mol Cell Endocrinol* **1996**, *121*, 153-163.
- [243] Kortenkamp, A.; Altenburger, R. Approaches to assessing combination effects of oestrogenic environmental pollutants. *Sci Total Environ* **1999**, *233*, 131-140.
- [244] Shimada, T.; Hayes, C. L.; Yamazaki, H.; Amin, S.; Hecht, S. S.; Guengerich, F. P.; Sutter, T. R. Activation of chemically diverse procarcinogens by human cytochrome P-450 1B1. *Cancer Res* **1996**, *56*, 2979-2984.
- [245] Lee, J. E.; Safe, S. 3',4'-dimethoxyflavone as an aryl hydrocarbon receptor antagonist in human breast cancer cells. *Toxicol Sci* **2000**, *58*, 235-242.
- [246] Safe, S.; Krishnan, V. Chlorinated hydrocarbons: estrogens and antiestrogens. *Toxicol Lett* **1995**, *82-83*, 731-736.
- [247] Ohtake, F.; Takeyama, K.; Matsumoto, T.; Kitagawa, H.; Yamamoto, Y.; Nohara, K.; Tohyama, C.; Krust, A.; Mimura, J.; Chambon, P.; Yanagisawa, J.; Fujii-Kuriyama, Y.; Kato, S. Modulation of oestrogen receptor signalling by association with the activated dioxin receptor. *Nature* **2003**, *423*, 545-550.
- [248] Alarid, E. T.; Bakopoulos, N.; Solodin, N. Proteasome-mediated proteolysis of estrogen receptor: a novel component in autologous down-regulation. *Mol Endocrinol* **1999**, *13*, 1522-1534.
- [249] Pink, J. J.; Jordan, V. C. Models of estrogen receptor regulation by estrogens and antiestrogens in breast cancer cell lines. *Cancer Res* **1996**, *56*, 2321-2330.
- [250] Kharat, I.; Saatcioglu, F. Antiestrogenic effects of 2,3,7,8-tetrachlorodibenzo-p-dioxin are mediated by direct transcriptional interference with the liganded estrogen receptor. Cross-talk between aryl hydrocarbon- and estrogen-mediated signaling. *J Biol Chem* **1996**, *271*, 10533-10537.
- [251] Denison, M.; Pandini, A.; Nagy, S.; Baldwin, E.; Bonati, L. Ligand binding and activation of the Ah receptor. *Chem Biol Interact* **2002**, *141*, 3.
- [252] Chang, C. Y.; Puga, A. Constitutive activation of the aromatic hydrocarbon receptor. *Mol Cell Biol* **1998**, *18*, 525-535.
- [253] Gehm, B. D.; McAndrews, J. M.; Chien, P. Y.; Jameson, J. L. Resveratrol, a polyphenolic compound found in grapes and wine, is an agonist for the estrogen receptor. *Proc Natl Acad Sci U S A* **1997**, *94*, 14138-14143.
- [254] Hardy, M. L. A comparison of the properties of the major commercial PBDPO/PBDE product to those of major PBB and PCB products. *Chemosphere* **2002**, *46*, 717-728.
- [255] WHO *Polybrominated biphenyls*; IPCS: Geneva, 1994.
- [256] de Boer, J.; Wester, P. G.; Klamer, H. J.; Lewis, W. E.; Boon, J. P. Do flame retardants threaten ocean life? *Nature* **1998**, *394*, 28-29.
- [257] Martin, M. B.; Angeloni, S. V.; Garcia-Morales, P.; Sholler, P. F.; Castro-Galache, M. D.; Ferragut, J. A.; Saceda, M. Regulation of estrogen receptor- $\alpha$  expression in MCF-7 cells by taxol. *J Endocrinol* **2004**, *180*, 487-496.
- [258] Silberhorn, E. M.; Glauert, H. P.; Robertson, L. W. Carcinogenicity of polyhalogenated biphenyls: PCBs and PBBs. *Crit Rev Toxicol* **1990**, *20*, 440-496.

- 
- [259] Vakharia, D. D.; Gierthy, J. F. Use of a combined human liver microsome-estrogen receptor binding assay to assess potential estrogen modulating activity of PCB metabolites. *Toxicol Lett* **2000**, *114*, 55-65.
- [260] Moore, M.; Mustain, M.; Daniel, K.; Chen, I.; Safe, S.; Zacharewski, T.; Gillesby, B.; Joyeux, A.; Balaguer, P. Antiestrogenic activity of hydroxylated polychlorinated biphenyl congeners identified in human serum. *Toxicol Appl Pharmacol* **1997**, *142*, 160-168.
- [261] Letcher, R. J.; Lemmen, J. G.; van der Burg, B.; Brouwer, A.; Bergman, A.; Giesy, J. P.; van den Berg, M. In vitro antiestrogenic effects of aryl methyl sulfone metabolites of polychlorinated biphenyls and 2,2-bis(4-chlorophenyl)-1,1-dichloroethene on 17 $\beta$ -estradiol-induced gene expression in several bioassay systems. *Toxicol Sci* **2002**, *69*, 362-372.
- [262] Connor, K.; Ramamoorthy, K.; Moore, M.; Mustain, M.; Chen, I.; Safe, S.; Zacharewski, T.; Gillesby, B.; Joyeux, A.; Balaguer, P. Hydroxylated polychlorinated biphenyls (PCBs) as estrogens and antiestrogens: structure-activity relationships. *Toxicol Appl Pharmacol* **1997**, *145*, 111-123.
- [263] Korach, K. S.; Sarver, P.; Chae, K.; McLachlan, J. A.; McKinney, J. D. Estrogen receptor-binding activity of polychlorinated hydroxybiphenyls: conformationally restricted structural probes. *Mol Pharmacol* **1988**, *33*, 120-126.
- [264] Andres, J.; Lambert, I.; Robertson, L.; Bandiera, S.; Sawyer, T.; Lovering, S.; Safe, S. The comparative biologic and toxic potencies of polychlorinated biphenyls and polybrominated biphenyls. *Toxicol Appl Pharmacol* **1983**, *70*, 204-215.
- [265] Bergman, A.; Klasson, W. E.; Kuroki, H.; Nilsson, A. Synthesis and Mass-Spectrometry of Some Methoxylated Pcb. *Chemosphere* **1995**, *30*, 1921-1938.
- [266] Hagen, M.; Pabel, U.; Landsiedel, R.; Bartsch, I.; Falany, C. N.; Glatt, H. Expression of human estrogen sulfotransferase in Salmonella typhimurium: differences between hHST and hEST in the enantioselective activation of 1-hydroxyethylpyrene to a mutagen. *Chem Biol Interact* **1998**, *109*, 249-253.
- [267] Mills RA, M. C., Dannan GA, Guengerich FP, Aust SD. Studies on the structure-activity relationships for the metabolism of polybrominated biphenyls by rat liver microsomes. *Toxicol Appl Pharmacol*. **1985**, *78*, 96-104.
- [268] Tulp MT, O. K., Hutzinger O. Identification of hydroxyhalobiphenyls as their methyl ethers by gas chromatography mass spectrometry. *Biomed Mass Spectrom* **1977**, *4*, 310-316.
- [269] Kaminsky, L. S.; Kennedy, M. W.; Adams, S. M.; Guengerich, F. P. Metabolism of dichlorobiphenyls by highly purified isozymes of rat liver cytochrome P-450. *Biochemistry* **1981**, *20*, 7379-7384.
- [270] Schnellmann, R. G.; Volp, R. F.; Putnam, C. W.; Sipes, I. G. The hydroxylation, dechlorination, and glucuronidation of 4,4'-dichlorobiphenyl (4-DCB) by human hepatic microsomes. *Biochem Pharmacol* **1984**, *33*, 3503-3509.
- [271] Sundstrom, G.; Hutzinger, O.; Safe, S. The metabolism of chlorobiphenyls: A review. *Chemosphere* **1976**, *5*, 267-298.
- [272] Kimura, S.; Gonzalez, F. J.; Nebert, D. W. Tissue-specific expression of the mouse dioxin-inducible P(1)450 and P(3)450 genes: differential transcriptional activation and mRNA stability in liver and extrahepatic tissues. *Mol Cell Biol* **1986**, *6*, 1471-1477.

- [273] Stiborova, M.; Martinek, V.; Rydlova, H.; Koblas, T.; Hodek, P. Expression of cytochrome P450 1A1 and its contribution to oxidation of a potential human carcinogen 1-phenylazo-2-naphthol (Sudan I) in human livers. *Cancer Lett* **2005**, *220*, 145-154.
- [274] Rencurel, F.; Stenhouse, A.; Hawley, S. A.; Friedberg, T.; Hardie, D. G.; Sutherland, C.; Wolf, C. R. AMP-activated protein kinase mediates phenobarbital induction of CYP2B gene expression in hepatocytes and a newly derived human hepatoma cell line. *J Biol Chem* **2005**, *280*, 4367-4373.
- [275] Qian, Y. M.; Sun, X. J.; Tong, M. H.; Li, X. P.; Richa, J.; Song, W. C. Targeted disruption of the mouse estrogen sulfotransferase gene reveals a role of estrogen metabolism in intracrine and paracrine estrogen regulation. *Endocrinology* **2001**, *142*, 5342-5350.
- [276] Koster, H.; Halsema, I.; Scholtens, E.; Meerman, J. H.; Pang, K. S.; Mulder, G. J. Selective inhibition of sulfate conjugation in the rat: pharmacokinetics and characterization of the inhibitory effect of 2,6-dichloro-4-nitrophenol. *Biochem Pharmacol* **1982**, *31*, 1919-1924.
- [277] Meerman, J. H.; Sterenborg, H. M.; Mulder, G. J. Use of pentachlorophenol as long-term inhibitor of sulfation of phenols and hydroxamic acids in the rat in vivo. *Biochem Pharmacol* **1983**, *32*, 1587-1593.
- [278] Case, D. A.; Pearlman, D. A.; Caldwell, J. W.; III, T. E. C.; Wang, J.; Ross, W. S.; Simmerling, C.; Darden, T.; Merz, K. M.; Stanton, R. V.; Cheng, A.; Vincent, J. J.; Crowley, M.; Tsui, V.; Gohlke, H.; Radmer, R.; Duan, Y.; Pitera, J.; Massova, I.; Seibel, G. L.; Singh, U. C.; Weiner, P.; Kollman, P. A. Amber is the collective name for a suite of programs that allow users to carry out molecular dynamics simulations, particularly on biomolecules. **1999**.
- [279] Torchia, J.; Rose, D. W.; Inostroza, J.; Kamei, Y.; Westin, S.; Glass, C. K.; Rosenfeld, M. G. The transcriptional co-activator p/CIP binds CBP and mediates nuclear-receptor function. *Nature* **1997**, *387*, 677-684.
- [280] IARC Benzo[a]pyrene. *IARC Monographs on the Evaluation of the carcinogenic Risk of Chemicals to Man*; International Agency for Research on Cancer: Lyon, France, 1973; pp 91-136.
- [281] Alexandrov, K.; Cascorbi, I.; Rojas, M.; Bouvier, G.; Kriek, E.; Bartsch, H. CYP1A1 and GSTM1 genotypes affect benzo[a]pyrene DNA adducts in smokers' lung: comparison with aromatic/hydrophobic adduct formation. *Carcinogenesis* **2002**, *23*, 1969-1977.
- [282] Melendez-Colon, V. J.; Luch, A.; Seidel, A.; Baird, W. M. Cancer initiation by polycyclic aromatic hydrocarbons results from formation of stable DNA adducts rather than apurinic sites. *Carcinogenesis* **1999**, *20*, 1885-1891.
- [283] Weinstein, I. B.; Jeffrey, A. M.; Jennette, K. W.; Blobstein, S. H.; Harvey, R. G.; Harris, C.; Autrup, H.; Kasai, H.; Nakanishi, K. Benzo(a)pyrene diol epoxides as intermediates in nucleic acid binding in vitro and in vivo. *Science* **1976**, *193*, 592-595.
- [284] van Lipzig, M. M. H.; Vermeulen, N. P. E.; Meerman, J. H. N. unpublished results.
- [285] Milligan, S. R.; Kalita, J. C.; Pocock, V.; Van De Kauter, V.; Stevens, J. F.; Deinzer, M. L.; Rong, H.; De Keukeleire, D. The endocrine activities of 8-prenylnaringenin and related hop (*Humulus lupulus* L.) flavonoids. *J. Clin. Endocrinol. Metab.* **2000**, *85*, 4912-4915.
- [286] Morreal, C. E.; Sinha, D. K.; Schneider, S. L.; Bronstein, R. E.; Dawidzik, J. Antiestrogenic properties of substituted benz[a]anthracene-3,9-diols. *J. Med. Chem.* **1982**, *25*, 323-326.

- 
- [287] Bayly, C. I.; Cieplak, P.; Cornell, W. D.; Kollman, P. A. A Well-Behaved Electrostatic Potential Based Method Using Charge Restraints for Deriving Atomic Charges - the Resp Model. *Journal of Physical Chemistry* **1993**, *97*, 10269-10280.
- [288] Jorgensen, W. L.; Chandraskhar, J.; Madura, J. D.; Impey, R. W.; Klein, M. L. Comparison of simple potential functions for simulating liquid water. *J. Chem. Phys.* **1983**, *79*, 926-935.
- [289] Shiau, A. K.; Barstad, D.; Radek, J. T.; Meyers, M. J.; Nettles, K. W.; Katzenellenbogen, B. S.; Katzenellenbogen, J. A.; Agard, D. A.; Greene, G. L. Structural characterization of a subtype-selective ligand reveals a novel mode of estrogen receptor antagonism. *Nat. Struct. Biol.* **2002**, *9*, 359-364.
- [290] Reese, J. C.; Katzenellenbogen, B. S. Characterization of a temperature-sensitive mutation in the hormone binding domain of the human estrogen receptor. Studies in cell extracts and intact cells and their implications for hormone-dependent transcriptional activation. *J. Biol. Chem.* **1992**, *267*, 9868-9873.
- [291] Pike, J. W.; Dokoh, S.; Haussler, M. R.; Liberman, U. A.; Marx, S. J.; Eil, C. Vitamin D3--resistant fibroblasts have immunoassayable 1,25-dihydroxyvitamin D3 receptors. *Science* **1984**, *224*, 879-881.
- [292] Northrop, J. P.; Gametchu, B.; Harrison, R. W.; Ringold, G. M. Characterization of wild type and mutant glucocorticoid receptors from rat hepatoma and mouse lymphoma cells. *J. Biol. Chem.* **1985**, *260*, 6398-6403.
- [293] Tora, L.; Mullick, A.; Metzger, D.; Ponglikitmongkol, M.; Park, I.; Chambon, P. The cloned human oestrogen receptor contains a mutation which alters its hormone binding properties. *Embo J.* **1989**, *8*, 1981-1986.
- [294] Fanchenko, N. D.; Sturchak, S. V.; Shchedrina, R. N.; Pivnitsky, K. K.; Novikov, E. A.; Ishkov, V. L. The specificity of the human uterine receptor. *Acta Endocrinol. (Copenh.)* **1979**, *90*, 167-175.
- [295] Tsuzuki, S.; Honda, K.; Azumi, R. Model chemistry calculations of thiophene dimer interactions: origin of pi-stacking. *Journal of the American Chemical Society* **2002**, *124*, 12200-12209.
- [296] Jaffe, R.; Smith, G. A quantum chemistry study of benzene dimer. *Journal of Chemical Physics* **1996**, *105*, 2780-2788.
- [297] Kuiper, G. G.; Lemmen, J. G.; Carlsson, B.; Corton, J. C.; Safe, S. H.; van der Saag, P. T.; van der Burg, B.; Gustafsson, J. A. Interaction of estrogenic chemicals and phytoestrogens with estrogen receptor beta. *Endocrinology* **1998**, *139*, 4252-4263.
- [298] Pike, A. C.; Brzozowski, A. M.; Walton, J.; Hubbard, R. E.; Thorsell, A. G.; Li, Y. L.; Gustafsson, J. A.; Carlquist, M. Structural insights into the mode of action of a pure antiestrogen. *Structure (Camb)* **2001**, *9*, 145-153.
- [299] Davis, J. A.; May, M. D.; Greenfield, B. K.; Fairey, R.; Roberts, C.; Ichikawa, G.; Stoelting, M. S.; Becker, J. S.; Tjeerdema, R. S. Contaminant concentrations in sport fish from San Francisco Bay, 1997. *Mar Pollut Bull* **2002**, *44*, 1117-1129.
- [300] Silva, E.; Rajapakse, N.; Kortenkamp, A. Something from "nothing"--eight weak estrogenic chemicals combined at concentrations below NOECs produce significant mixture effects. *Environ Sci Technol* **2002**, *36*, 1751-1756.
- [301] Bader, A. N.; van Dongen, M. M.; van Lipzig, M. M.; Kool, J.; Meerman, J. H.; Ariese, F.; Goolijer, C. The chemical interaction between the estrogen receptor and

- monohydroxybenzo[a]pyrene derivatives studied by fluorescence line-narrowing spectroscopy. *Chem Res Toxicol* **2005**, *18*, 1405-1412.
- [302] Various, A. Chemosphere issue on brominated compounds in the environment. *Chemosphere* **2002**, *46*, 579-728.
- [303] Lesuisse, D.; Albert, E.; Bouchoux, F.; Cerede, E.; Lefrancois, J. M.; Levif, M. O.; Tessier, S.; Tric, B.; Teutsch, G. Biphenyls as surrogates of the steroidal backbone. Part 1: synthesis and estrogen receptor affinity of an original series of polysubstituted biphenyls. *Bioorg Med Chem Lett* **2001**, *11*, 1709-1712.
- [304] Blair, R. M.; Fang, H.; Branham, W. S.; Hass, B. S.; Dial, S. L.; Moland, C. L.; Tong, W.; Shi, L.; Perkins, R.; Sheehan, D. M. The estrogen receptor relative binding affinities of 188 natural and xenochemicals: structural diversity of ligands. *Toxicol Sci* **2000**, *54*, 138-153.
- [305] Matthews, J.; Zacharewski, T. Differential binding affinities of PCBs, HO-PCBs, and aroclors with recombinant human, rainbow trout (*Onchorhynchus mykiss*), and green anole (*Anolis carolinensis*) estrogen receptors, using a semi-high throughput competitive binding assay. *Toxicol Sci* **2000**, *53*, 326-339.
- [306] Almlof, M.; Brandsdal, B. O.; Aqvist, J. Binding affinity prediction with different force fields: examination of the linear interaction energy method. *J Comput Chem* **2004**, *25*, 1242-1254.
- [307] Bader, A. N.; Grubor, N. M.; Ariese, F.; Gooijer, C.; Jankowiak, R.; Small, G. J. Probing the interaction of benzo[a]pyrene adducts and metabolites with monoclonal antibodies using fluorescence line-narrowing spectroscopy. *Anal Chem* **2004**, *76*, 761-766.
- [308] Jankowiak, R. In "Shpol'skii Spectroscopy and Other Site-Selection Methods"; Wiley & Sons: New York, 2000; pp 235-271.
- [309] Jankowiak, R.; Small, G. J. Fluorescence line-narrowing spectroscopy in the study of chemical carcinogenesis. *Anal Chem* **1989**, *61*, 1023A-1024A, 1026A-1029A, 1031A-1103.
- [310] Kamlet, M. J.; Abboud, J. L. M.; Abraham, M. H.; Taft, R. W. Linear solvation energy relationships. 23. A comprehensive collection of the solvatochromic parameters,  $\rho^*$ ,  $\alpha$ , and  $\beta$ , and some methods for simplifying the generalized solvatochromic equation. *J. Org.Chem.* **1983**, *48*, 2877-2887.
- [311] Suh, M.; Ariese, F.; Small, G. J.; Jankowiak, R.; Liu, T. M.; Geacintov, N. E. Conformational studies of the (+)-trans, (-)-trans, (+)-cis, and (-)-cis adducts of anti-benzo[a]pyrene diolepoxide to N2-dG in duplex oligonucleotides using polyacrylamide gel electrophoresis and low-temperature fluorescence spectroscopy. *Biophys Chem* **1995**, *56*, 281-296.
- [312] Kool, J.; van Liempd, S. M.; Harmsen, S.; Beckman, J.; van Elswijk, D.; Commandeur, J. N.; Irth, H.; Vermeulen, N. P. Cytochrome P450 bio-affinity detection coupled to gradient HPLC: on-line screening of affinities to cytochrome P4501A2 and 2D6. *J Chromatogr B Analyt Technol Biomed Life Sci* **2007**, *858*, 49-58.
- [313] Kool, J.; Ramautar, R.; van Liempd, S. M.; Beckman, J.; de Kanter, F. J.; Meerman, J. H.; Schenk, T.; Irth, H.; Commandeur, J. N.; Vermeulen, N. P. Rapid on-line profiling of estrogen receptor binding metabolites of tamoxifen. *J Med Chem* **2006**, *49*, 3287-3292.
- [314] van Liempd, S. M.; Kool, J.; Niessen, W. M.; van Elswijk, D. E.; Irth, H.; Vermeulen, N. P. On-line Formation, Separation, and Estrogen Receptor Affinity Screening of Cytochrome P450-Derived Metabolites of Selective Estrogen Receptor Modulators. *Drug Metab Dispos* **2006**, *34*, 1640-1649.



# Nederlandse Samenvatting

De estrogeenreceptor, milieu-estrogenen en de rol van  
cytochroom P450 in bioactivatie

---

## DE ESTROGEENRECEPTOR, MILIEU-ESTROGENEN, EN DE ROL VAN CYTOCHROOM P450 IN BIOACTIVATIE.

Het onderzoek dat in dit proefschrift wordt beschreven, handelt over de biotransformatie en de bio-activatie van milieucontaminanten met estrogene activiteit, waardoor zij kunnen worden omgezet in endocriene disruptors (ED), stoffen met een hormoon-verstorende werking. Een hormoonverstorende stof wordt gedefinieerd als een lichaamsvreemde stof, die het endocriene systeem van mens of dier kan ontregelen. Het endocriene systeem regelt via hormonen processen als de geslachtsontwikkeling, stofwisseling, groei, homeostase, gedrag en ionenhuishouding. Hormonen zijn signaalstoffen die heel specifiek gen expressie in een cel sturen door te binden aan receptoren, zoals bijvoorbeeld de estrogeen receptor (ER). Zoogdieren, vogels, reptielen, amfibieën en vissen hebben allen een vergelijkbaar hormoonsysteem. Milieucontaminanten kunnen deze hormoonhuishouding op verschillende manieren verstoren. De verstoring van de estrogene hormoon huishouding wordt uitgebreid beschreven in **Hoofdstuk 1**, de algemene introductie. Interferentie vindt bijvoorbeeld plaats als stoffen zelf hormoonactiviteit vertonen, moleculaire structuren zijn dan vaak gelijkend aan het lichaamseigen hormoon, en kunnen zodoende aan een hormoonreceptor binden. De receptor kan hierdoor extra worden geactiveerd, de stof werkt dan als agonist. De receptor kan ook sub-optimaal worden geactiveerd door een stof die werkt als partiële agonist of selectieve receptor modulator of helemaal worden geblokkeerd door een antagonist. In in alle gevallen zullen afwijkende signalen worden afgeven. Endocriene disruptors kunnen ook de productie of afbraak van de lichaamseigen hormonen beïnvloeden door de werking van betrokken enzymen te verstoren.

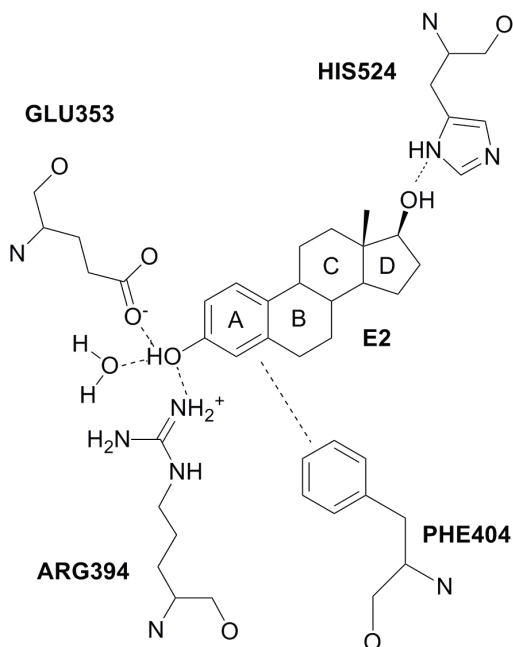
De afgelopen decennia is in de wetenschap uitvoerig aangetoond dat op veel verschillende plaatsen op aarde afwijkingen zijn waargenomen bij dieren en mensen. Afwijkingen zoals abnormale geslachtsorganen, veranderde sexe-ratio's bij het nageslacht, vervrouwelijking, steriliteit, borst- en prostaatkanker, worden in verband gebracht met de aanwezigheid van milieuverontreinigende stoffen. Deze stoffen zijn veelal in het milieu terecht gekomen door de toenemende industrialisering van de westerse samenleving. Het gaat om allerlei stoffen die zeer breed worden toegepast in producten zoals geneesmiddelen, zonnebrand crèmes, verf en kleurstoffen, brandvertragers, speelgoed, voedselverpakkingen, bestrijdingsmiddelen, schoonmaakmiddelen, oplosmiddelen, weekmakers en allerlei andere industriële chemicaliën. Veel van de bestrijdingsmiddelen en industrieel geproduceerde stoffen die op grote schaal werden gebruikt halverwege de vorige eeuw, bleken slecht afbreekbaar, waardoor zij zich ophoopten in de voedselketen. De negatieve effecten op de reguliere hormoonhuishouding werden pas veel later bekend. Inmiddels is

het publieke bewustzijn veel groter, het milieubeleid is aangescherpt en de concentraties in het milieu zijn gedaald ten opzichte van toen. (Nieuwe) stoffen worden tegenwoordig beter getest, maar het is nog erg moeilijk om in te schatten wat nu precies het risico is van de huidige blootstelling aan hormoonverstorende stoffen. Hormonen zelf zijn vaak al actief in heel lage concentraties, endocriene systemen zijn namelijk erg gevoelig, dus lage concentraties milieucontaminanten kunnen al voor problemen zorgen. Een belangrijk punt van discussie is het grote verschil tussen de concentraties stoffen die gebruikt worden in laboratoria, en de concentraties van stoffen die worden gevonden in ons milieu. Echter, het blijft van het grootste belang zoveel mogelijk informatie te vergaren over de biologische activiteit van endocriene disruptors, zoals alle mogelijke werkingsmechanismen (doelwit) waarop stoffen kunnen aangrijpen en het niveau van blootstelling. Wat onder andere is gebleken uit de resultaten beschreven in de verschillende hoofdstukken van dit proefschrift, is het belang van het in kaart brengen van de biologische activiteiten en de consequenties van het ontstaan van (actieve) metabolieten van milieucontaminanten (dus niet alleen de uitgangsverbindingen onderzoeken), en het belang van adequaat inschatten van de effecten van blootstelling aan mengsels van stoffen.

In **hoofdstuk 2** wordt de bioactivatie van specifieke groepen milieucontaminanten besproken, te weten de polycyclische koolwaterstoffen (PAK) en de poly-gehalogeneerde biphenylen (PHB). Deze stoffen zijn vooral bekend om hun genotoxische activiteit, welk ontstaat nadat zij in het lichaam door cytochrome P450 enzymen (CYP) worden gemetaboliseerd. Echter door deze biotransformatie ontstaan ook stoffen met verhoogde estrogene activiteit. Metabolieten welke *in vitro* werden gevormd zijn geïdentificeerd, en getest op receptor binding en receptor activatie. Sommige metabolieten zijn ook geteste op interferentie van humaan estrogeen sulfotransferase (hEST) functie. hEST is betrokken bij de endogene estrogeen homeostase (metabolisme), en heeft daardoor indirect effect op estrogene activiteit. De resultaten hiervan zijn beschreven in **hoofdstuk 3**. Veel van de gevonden PAK en PHB metabolieten blijken estrogen actief te zijn in één of allebei de geteste estrogene signaalroutes (ER en hEST). De affiniteiten van enkele metabolieten waren net zo hoog (nanomolair) als die van 17 $\beta$ -estradiol, het endogene estrogeen. Bovendien zijn de gecombineerde effecten van een mix van PAKs en PHBs met zwakke estrogene activiteit getest, en deze bleken significant hoger te zijn dan de activiteiten van de individueel geteste stoffen. De geringe individuele estrogene activiteit van deze stoffen zou als verwaarloosbaar kunnen worden gezien, echter gezamenlijk induceren deze metabolieten wel degelijk een estrogeen effect in onze testen. Hieruit blijkt maar weer hoe belangrijk het is, om naast de afzonderlijk biologische activiteiten van hormoon-

verstoorders ook het gedrag van deze stoffen in mengsels te onderzoeken, in het bijzonder wanneer het betrekking heeft op blootstellingen aan lage concentraties.

Naast *in vitro* laboratoriumwerk is tijdens het promotie onderzoek ook gebruik gemaakt van *in silico* werkwijzen. Hierbij is op de computer, met behulp van geavanceerde software, een eiwit model gemaakt van het ligand bindingsdomein van de humane estrogeen receptor  $\alpha$ . (hER $\alpha$ ). Het moleculaire eiwitmodel is gebaseerd op de gepubliceerde kristalstructuur van de receptor, en de interactie tussen ligand en de receptor is berekend op basis van de lineaire interactie energie (LIE) benadering. Deze gaat uit van een lineair verband tussen de vrije bindingsenergie (receptor affiniteit) en veranderingen in Van der Waals en elektrostatische energie van een systeem. De Van der Waals (o.a. aromatische interacties) en elektrostatische energieën (zoals waterstofbruggen) worden berekend met behulp van moleculaire dynamica (MD), waarbij het ligand-receptor complex in evenwicht is. Figuur 1 laat zien hoe estradiol (E2) via beide soorten interacties gebonden is in de ER $\alpha$  bindingsgroeve.



**Figuur 1:** E2 (estradiol) bindt via waterstof bruggen en aromatische interacties aan aminozuren van ER $\alpha$ .

Gedurende MD simulaties worden zowel het ligand-receptor complex in water (gebonden staat) en het ligand in water (ongebonden staat) gevolgd, en het verschil tussen de twee toestanden blijkt zeer goed te correleren met de receptor affiniteit van de onderzochte stoffen. De details van het opzetten van het eiwit model, de uitwerking van de LIE, de parameterisering van de MD simulaties en de resultaten staan beschreven in **hoofdstuk 4**. Door een grote dataset aan stoffen met uiteenlopende estrogene activiteit te gebruiken, is het model zeer geschikt gebleken om nauwkeurig de bindingsaffiniteit en bindingsoriëntatie van mogelijk estrogene stoffen te voorspellen. De dataset bestaat uit o.a. natuurlijke hormonen, geneesmiddelen, fytoestrogenen en bestrijdingsmiddelen, waarvan *in vitro* de affiniteit voor de receptor is bepaald. Aansluitend zijn uit onze metabolismestudies geïdentificeerde en ongeïdentificeerde PAK en PHB metabolieten in het *in silico* model getest, en de affiniteit voor de ER $\alpha$  van een reeks van metabolieten is voorspeld. De resultaten hiervan staan beschreven in **hoofdstuk 5**.

Om de bindingsorientaties, welke door het model worden voorspeld, te toetsen, is gebruik gemaakt van hoge resolutie fluorescentie spectroscopie (fluorescence line-narrowing, FLN). Het onderzoek dat hiervoor is uitgevoerd staat beschreven in **hoofdstuk 6**. Met deze techniek kan onderzocht worden wat de voorkeursbindingsorientatie is van auto-fluorescente stoffen, zoals in ons geval gehydroxyleerde PAK metabolieten. Deze binden via waterstofbruggen aan de ER $\alpha$ , en met FLN kan precies bepaald worden of dit via H-donor dan wel H-acceptor gebeurt, en of er al dan niet aromatische interacties zijn, welke duiden op een specifieke bindingsoriëntatie. De voorspellingen komen goed overeen met de voorkeurspositie die het LIE model heeft voorspeld, en onderbouwen hiermee de voorspellende waarde van het LIE model.

Het proefschrift wordt afgesloten met **hoofdstuk 7**, een epiloog, waarin de resultaten nog eens tegen een algemener licht worden gehouden. Op basis van het onderzoek, beschreven in het proefschrift, moet geconcludeerd worden, dat het risico van blootstelling aan estrogenen onderschat zal worden, als niet voldoende rekening wordt gehouden met de bioactivatie van de uitgangsstof, en als geen rekening wordt gehouden met gecombineerde blootstellingseffecten. Deze eigenschappen kunnen goed in kaart worden gebracht met gebruikmaking van *in vitro* en *in silico* modellen, zoals beschreven in dit proefschrift.

---

## Nawoord

*“I am glad I did it, partly because it was well worth it,  
and chiefly because I shall never have to do it again”*

Mark Twain  
(1835-1910)



# Dank

De oplossing van deze woordzoeker is een wijze les en een bewezen feit, van toepassing op dit proefschrift. De puzzel is, net als het proefschrift, gevormd door vele lieve mensen; familie, vrienden, collega's, vakbroeders en -zusters en studenten. Zonder hun hulp was het me nooit gelukt! Ik dank hen en iedereen die ik ben vergeten, voor hun expertise, inzichten, vertrouwen en de aanhoudende interesse, het enthousiasme, de hoop, de vriendschap en natuurlijk de liefde, want dankzij al deze ingrediënten is dit proefschrift toch nog tot stand gekomen en daar ben ik bijzonder blij om!

D	D	C	E	E	C	A	M	A	N	N	O	H	F	M	L	O	A	N	E
U	L	K	L	H	D	A	I	A	E	D	R	R	I	E	J	N	I	T	T
Y	K	O	R	A	R	U	A	L	L	C	E	C	I	W	E	E	K	H	T
O	R	I	R	I	U	I	E	A	H	E	A	H	C	A	L	E	S	I	E
D	S	R	E	E	T	D	N	R	K	E	C	M	I	O	L	L	A	J	I
N	A	K	A	S	G	A	I	T	L	I	N	A	J	L	E	R	S	S	L
J	E	A	A	H	J	S	C	A	M		R	R	Y		P	A		A	U
R	E	B	N	E	T		N	R	A		A	C	Y	A	M	M	E	N	J
S	E	R	O	A			A	E	R	M	K	E	O	I	N	N	E	D	O
S	A	T	O	E	K		R	T	T	E		L	R	E	I	U	S	R	C
		B	E	E	S	E	F	E	I	N	A	J	J	T	Q	J	T	E	I
R	O	S	W	I	N	T	E	P	J		A	R	R	I	I	N		A	N
H	E	T	T	Y	P		H	S	N	M	A	A	N	G	O	A		S	
		F	H	T	E	B	S	E	I	L	M	O	A	D	N	A	L	O	J
	A	T	I	L	L	A	H		R	R	M	F		I	E	K	F	A	A
	D	E	N	N	I	S		T	E	D	N	E	L	O	E	K	I	E	D
U	O	N	I	M	N		K	N	I	O	N	E	N	A	J	R	E	P	L
S	U	M	S	A	R	E	A	R	T	D	V	A	S	N	A	R	F		A
J	O	H	N	U	E	T	J	N	A	E	U	O	C	M	E	R			I
	O	E	H	T	O		A			M		J	B	O	R	N	O	T	T

AFKE  
BAS  
ED  
GEROLD  
JENNIFER  
LAURA  
MARK  
MINOU  
PERJAN  
ROB  
TNO

ALDO  
CAL  
ESTHER  
GIJS  
JEROEN  
LIESBETH  
MARLEEN  
MIRJAM  
PETER  
SASKIA  
TOEJA

ANDRE  
CHRIS  
EVELINA  
HARRY  
JOHN  
LOEKIE  
MARTIJN  
MONIQUE  
PIETER  
SEBASTIAAN  
TON

ANDREAS  
CHRISTA  
FEE  
HENRY  
JOLANDA  
LYCKE  
MARTINE  
NICO  
RASMUS  
TEUN

ANTON  
CLAUDIA  
FRANCINE  
HETTY  
JUDITH  
MARCEL  
MIA  
OKKE  
REMCO  
THEO

ARJEN  
DAAN  
FRANS  
JAN  
JULIETTE  
MARIEKE  
MICAELA  
OSWIN  
RENATO  
THIJS

ATILLA  
DENNIS  
FREEK  
JELLE  
KEES  
MARJOLEIN  
MICHIEL  
PAOLA  
RNC  
TIALDA

Oplossing: \_\_\_\_\_



---

## Publications

**van Lipzig M.M.H.**, Commandeur J.N.M., de Kanter F.J., Damsten M.C., Vermeulen N.P.E., Maat E., Groot E.J., Brouwer A., Kester M.H., Visser T.J., Meerman J.H.N., Bioactivation of dibrominated biphenyls by cytochrome P450 activity to metabolites with estrogenic activity and estrogen sulfotransferase inhibition capacity. *Chem Res Toxicol.* **2005** Nov;18(11):1691-700.

**van Lipzig, M.M.H.**; Vermeulen, N.P.E.; Gusinu, R.; Legler, J.; Frank, H.; Seidel, A.; Meerman, J.H.N., Formation of estrogenic metabolites of benzo[a]pyrene and chrysene by cytochrome P450 activity and their combined and supra-maximal estrogenic activity. *Environmental Toxicology and Pharmacology* **2005**, 19, 41-55.

Bader A.N., van Dongen M.M., **van Lipzig M.M.H.**, Kool J., Meerman J.H.N., Ariese F., Gooijer C., The chemical interaction between the estrogen receptor and monohydroxybenzo[a]pyrene derivatives studied by fluorescence line-narrowing spectroscopy. *Chem Res Toxicol.* **2005** Sep;18(9):1405-12.

**van Lipzig M.M.H.**, ter Laak A.M., Jongejan A., Vermeulen N.P.E., Wamelink M., Geerke D., Meerman J.H.N., Prediction of ligand binding affinity and orientation of xenoestrogens to the estrogen receptor by molecular dynamics simulations and the linear interaction energy method. *J Med Chem.* **2004** Feb 12;47(4):1018-30.

### *Related publications*

Murk A.J., Legler J., **van Lipzig M.M.H.**, Meerman J.H.N., Belfroid A.C., Spenkelink A., van der Burg B., Rijs G.B., Vethaak D., Detection of estrogenic potency in wastewater and surface water with three in vitro bioassays. *Environ Toxicol Chem.* **2002** Jan;21(1):16-23.

Oostenbrink B.C., Pitera J.W., **van Lipzig M.M.H.**, Meerman J.H.N., van Gunsteren W.F., Simulations of the estrogen receptor ligand-binding domain: affinity of natural ligands and xenoestrogens. *J Med Chem.* **2000** Nov 30;43(24):4594-605.

### *Other*

van Iersel M.L., van Lipzig M.M.H., Rietjens I.M., Vervoort J., van Bladeren P.J., GSTP1-1 stereospecifically catalyzes glutathione conjugation of ethacrynic acid. *FEBS Lett.* **1998** Dec 11;441(1):153-7.

---

# Curriculum Vitae

Marola van Lipzig werd op 18 oktober 1972 geboren in Delft. In 1991 behaalde zij het gymnasium diploma aan het Strabrecht College te Geldrop. Van 1991 tot 1997 studeerde zij Milieuhygiëne aan Wageningen University & Research Centre (WUR). Tijdens de doctoraalfase werkte zij in de afstudeerrichtingen Toxicologie (WUR), Gezondheidsleer en Epidemiologie (WUR in samenwerking met Gezondheidsrisiko Analyse en Toxicologie aan de Universiteit Maastricht) en liep zij een stage Toxicologie en Moleculaire Biologie in het Biomedical Research Centre van het Ninewells Hospital in Dundee, Schotland. Na het afronden van de studie werd zij als assistent in opleiding (AiO) aangesteld aan de Faculteit Exacte Wetenschappen aan de Vrije Universiteit in Amsterdam. Op de afdeling Farmacochemie, sectie Moleculaire Toxicologie, legde zij zich van 1998 tot 2003 toe op de *in vitro* en *in silico* bioactivatie van xenoestrogenen, en de resultaten van dat onderzoek zijn beschreven in het voor u liggende proefschrift. Van 2003-2005 was zij aan de VU actief als Post-doc onderzoeker Computational Chemistry, sectie Moleculaire Toxicologie, en werkte aan bioactivatie van (kandidaat)medicijnen. Aansluitend volgde een Post-doc positie bij de sectie Medicinal Chemistry aan de VU van 2005 tot 2007, welke gericht was op de karakterisatie van chemokine receptoren. Beide projecten werden uitgevoerd in samenwerking met het toenmalige N.V. Organon te Oss. Sinds 2007 is zij werkzaam als Study Director Biomarkers bij TNO Kwaliteit van Leven, te Zeist.